ProQuest LLC.
789 East Eisenhower Parkway
P.O. Box 1346
Ann Arbor, MI 48106 – 1346

THE FORMATION OF NON-METALLIC INCLUSIONS DURING STEELMAKING

A thesis submitted to the Council for National Academic Awards in application for the degree of

Doctor of Philosophy

in

THE SHEFFIELD POLYTECHNIC

by

Peter Edward Waudby, M.Sc., A.R.I.C.

October, 1973

The author is Senior Investigator in the Steelmaking Section at the Research and Development Department, Special Steels Division of the British Steel Corporation, Swinden Laboratories, Moorgate, Rotherham.

The Formation of Non-Metallic Inclusions During Steelmaking

The work was carried out at Swinden Laboratories and also at various melting shops within the Special Steels Division of the British Steel Corporation. It formed part of an extensive and continuing programme of work on non-metallic inclusions and a thesis based on earlier laboratory deoxidation experiments carried out between 1967 and 1970 was successfully submitted for the degree of Master of Science in the University of Sheffield in December, 1970.

The present thesis is based on a series of steelmaking trials aimed at improving steel cleanness and carried out during the period May, 1970 to June, 1973 under the supervision of Dr. D. Engledow and Mr. T. J. J. Smith. During this period, regular tutorials were held at the Sheffield Polytechnic to discuss the progress of the work and the following conferences/seminars were attended:-

(i) B.I.S.R.A. Conference, "Clean Steel", held at Scarborough, October, 1970*

(ii) Seminar in Process Metallurgy held at Imperial College, London, April, 1973

(iii) International Symposium on Metallurgical Chemistry - Applications in Ferrous Metallurgy, held at Sheffield University, July, 1971*

(iv) "Non-Metallic Inclusions in Steel - Their Occurrence and Effects". Series of Seminars held at Sheffield Polytechnic, 1973*

* Paper presented

The results obtained in this programme of work and the theories developed are, to the best of my knowledge, original except where reference is made to other authors. No part of this thesis has been submitted for degrees at any other college or university.

P. E. Waudby

October, 1973

ACKNOWLEDGEMENTS

I would like to record my thanks to Dr. K. J. Irvine, Head of Research, and Dr. A. Nicholson, Process Research Manager, Swinden Laboratories for permission to submit this thesis.

It is with great pleasure that I acknowledge the help and suggestions of:-

(i) Mr. T. J. J. Smith, Department of Metallurgy, Sheffield Polytechnic

(ii) Dr. D. Engledow, Steelmaking Section, Swinden Laboratories

(iii) Dr. F. B. Pickering, Department of Metallurgy, Sheffield Polytechnic

(iv) Dr. W. J. M. Salter, Metallurgical Department, Stocksbridge and Tinsley Park Works

I am also indebted to other staff members for their practical help:-

(i) Metallographic Section

(ii) Analytical Chemistry Section

(iii) Reprographic Section

Finally, I should also like to thank Mrs. B. Bonser for typing the manuscript.

SUMMARY

A comprehensive review of the literature on deoxidation and inclusion formation has been carried out, including the results of both laboratory experiments and full scale plant trials. The main areas for discussion have been:-

(i) Nucleation of inclusions
(ii) Growth and elimination of inclusions
(iii) Effect of steelmaking variables on inclusion formation
(iv) Reoxidation of steel
(v) Steel-refractory interactions

The experimental work has comprised a number of planned investigations into the types of oxide inclusions present at various stages during the steelmaking, tapping and teeming of several qualities of steel made by basic electric arc and open-hearth processes. A series of trials aimed at improving steel cleanness have been carried out and it has been possible to study the effects of numerous process variables during steelmaking on the nature of the non-metallic inclusions in the liquid metal.

It has been shown that despite a bath of steel being relatively free from inclusions prior to tapping, the entrainment of exogenous material (e.g. slag, reoxidation and refractory erosion products) during tapping and teeming can result in quality problems and/or reduced yield. Ladle refractory erosion is a major source of inclusions, particularly in higher manganese steels, and the practice of slag-metal mixing during tapping to effect desulphurisation has been shown to lead to slag-based inclusions in the ingot.

The formation of alumina agglomerates in 25 t slab ingots of carbon-manganese-niobium steel has been studied. A steelmaking practice aimed at reducing the incidence of these agglomerates and improving ductility has been developed involving among other things, a full aluminium deoxidation practice, 70% Al_2O_3 ladle refractories and argon shrouding of the teeming stream.

An attempt has been made to account for the changes in the types of oxide inclusions throughout the steelmaking of each trial cast. Finally, brief consideration has been given to possible methods of further improving steel cleanness.

CONTENTS

CONTENTS (continued)

SECTION 1 - INTRODUCTION

Steelmaking processes involve removing large amounts of dissolved impurity elements from molten iron. Most of the impurities are removed by oxidation reactions, which are promoted by introducing oxygen into the melt from highly oxidising slags or gases.

As the concentration of oxidisable elements is lowered, the activity of oxygen increases until at the end of the oxidation period, a low carbon melt can contain up to 0.15% dissolved oxygen. In the case of killed steels this must be lowered so that the subsequent solidification in the mould proceeds without evolution of carbon monoxide resulting from the carbon-oxygen reaction. Otherwise the carbon monoxide bubbles would cause the remaining liquid to effervesce in the mould and produce a steel with a high degree of porosity. This deoxidation process can be conducted in normal steelmaking practice by diffusion deoxidation under reducing slags, and/or by precipitation deoxidation by the addition of elements which have a greater affinity for oxygen than carbon at the temperature of molten steel. Precipitation deoxidation leads to the formation of solid or liquid reaction products which are sparingly soluble in the liquid steel and which tend to separate because of their physical properties.

At any given time during the steelmaking process the total oxygen content of the molten metal is comprised of the oxygen dissolved in the liquid steel, which is largely determined by the carbon, manganese, silicon and other elements in the steel, and the oxide inclusions which are in suspension in the bath. In high carbon steels, particularly in the presence of manganese and silicon, the dissolved oxygen is usually quite low, but there can nevertheless be an appreciable amount of non-metallic material in the melt, either from deoxidation, or from reoxidation, slag entrainment and refractory erosion which take place during the steelmaking, tapping

and teeming processes. Whilst there is a continual tendency for these non-metallic inclusions to float out of the melt, the rate of removal depends upon the type of inclusion which is present. Moreover, there is frequently a continual renewal of the inclusions by the entrapment of slag, erosion products and reoxidation products.

Whilst every precaution is taken during steelmaking to eliminate oxide inclusions, some of them invariably find their way into the ingot, in which a proportion of them are entrapped during solidification. These entrapped oxide inclusions can be the cause of dangerous defects and frequently result in the rejection of the material because of poor quality. The type, shape, size, amount and distribution of the inclusions can markedly affect the useful properties of the steel. In practice, for example, there are many cases in which, in spite of the same composition, heat treatment, and structural condition of the steel, large differences can occur in certain properties such as ductility, toughness, workability and also corrosion resistance. Numerous studies in the literature deal with the detrimental effects of inclusions on the physical and mechanical properties of steel, and for these reasons the steelmaker tries to keep the content of oxide impurities in steel to a minimum.

In order to improve the quality of the steel by eliminating inclusions as far as possible, it is first necessary to know at which stage in the steelmaking, tapping and teeming processes the inclusions are formed, and if possible their origin. It was with this objective that the work which is described in this thesis was carried out.

SECTION 2 - LITERATURE REVIEW

2.1 CLASSIFICATION OF INCLUSIONS

Deoxidation may occur when the deoxidant is added to the melt and this results in the formation of primary deoxidation products. Deoxidation may also occur during cooling of both the liquid and solid steel at decreasing temperature, due to the action of the alloying elements in the liquid and solid steel and to the decreasing solubility of oxygen. This results in the formation of secondary deoxidation products. The primary deoxidation products have a greater opportunity for escape from the steel than those which form by the secondary process on a falling temperature scale. In the solidified steel, those inclusions which were formed by the deoxidation reactions are usually a result of both primary and secondary processes[1].

Non-metallic inclusions can also be divided into two other groups, those of indigenous origin and those of exogenous origin[2]. The former group contains inclusions occurring as a result of chemical reactions taking place in molten or solidifying steel, whereas the latter group contains those resulting from mechanical entrainment of slags, refractories or other materials with which the molten steel comes in contact. Adopting Sims' definition[3], indigenous inclusions are those that precipitate as a result of chemical reactions in the steel. They consist principally of oxides and sulphides and the reactions which form them may be induced either by additions to the steel or simply by changes in solubility during the cooling and freezing of the steel. Exogenous inclusions occur in great variety, but for the most part are readily distinguishable from indigenous inclusions. Characteristic features of exogenous inclusions include a generally larger size, sporadic occurrence, preferred location in ingot or casting, irregular shape and complex structure. They usually occur as oxides, a result of the compositions of potential exogenous materials

such as slags and refractories.

Although the above division of inclusions provides a natural starting point for a discussion of their origin and formation, this division is an oversimplification. It is a common phenomenon for instance, that indigenous precipitation can occur on exogenous nuclei during the whole of the steelmaking process. Many inclusions, therefore, continuously change their composition in the steel melt and even in the solid steel[4].

2.2 THERMODYNAMICS OF DEOXIDATION

2.2.1 Deoxidation Equilibria

Numerous studies in the literature deal with the thermodynamics of deoxidation reactions and comprehensive reviews of past work on steelmaking equilibria have been published[5-9].

Deoxidation equilibria relating to the most common deoxidants used in steelmaking are summarised in Fig. 2.1 as a log-log plot of the concentration of oxygen in solution in liquid iron against that of the added elements[10,11]. In all cases, the oxygen and the alloying elements in solution are in equilibrium with the appropriate gas, liquid or solid oxide phase at 1600°C, e.g., 1 atm. CO, pure B_2O_3, pure Al_2O_3, etc. The curves for Mn, Si and C are from compiled data. The curves for Cr, V, B, Ti and Al are based on recent work by Fruehan using an oxygen galvanic cell[12].

In a general form, the solubility of a deoxidation product, M_xO_y, resulting from the reaction of a deoxidant, M, with oxygen in liquid iron is represented by:-

$$M_xO_y = x\underline{M} + y\underline{O} \qquad \text{eqn. (2.1)}$$

for which, at a given temperature, the equilibrium constant is:-

$$K = \frac{h_M^x \cdot h_O^y}{a_{M_xO_y}} \qquad \text{eqn. (2.2)}$$

in which 'h' represents the Henrian activity (dilute wt. % solution) and 'a' the Raoultian activity (pure oxide) at equilibrium. The composition of the oxide phase in

equilibrium with the melt depends on the temperature and alloy composition. For example, at the univariant point at 1600°C, iron containing about 3% Cr* coexists in equilibrium with chromite, $FeO.Cr_2O_3$ and chromic oxide, Cr_2O_3. Below 3% Cr, chromite is the equilibrium oxide phase and above 3% Cr, chromic oxide is formed as the equilibrium phase. The points marked on the curves give compositions corresponding to the three-phase univariants at which two oxide phases are in equilibrium with the melt. The curves intersecting at these points should have different slopes. However, the data are not accurate enough to reveal changes in the slopes of the curves at the univariant points.

With the exception of (FeMn)O, all other solid deoxidation products have essentially stoichiometric compositions. In such cases, the activity of the oxide is unity by definition.

Since, in general, the deoxidants added to steel are present in dilute solution, the solute activities are given by:-

$$h_M = f_M \cdot [\% M] \quad \text{.. .. ..} \quad \text{eqn. (2.3)}$$

$$h_O = f_O \cdot [\% O] \quad \text{.. .. ..} \quad \text{eqn. (2.4)}$$

where f_M and f_O are the Henrian activity coefficients of the deoxidant and oxygen respectively. At infinitely dilute solution, $h_M = [\% M]$ and $h_O = [\% O]$ in the metal. Substituting equations (2.3) and (2.4) into equation (2.2) and taking $a_{M_xO_y} = 1$ gives:-

$$K = [\% M]^x \cdot [\% O]^y \cdot f_M^x \cdot f_O^y \quad \text{.. .. ..} \quad \text{eqn. (2.5)}$$

where f_M and f_O approach 1 as $[\% M] \longrightarrow 0$ $f_O \to 1$ as $[\% M] \to 0$?)

It can be seen from Fig. 2.1 that in several systems, the solubility of oxygen initially decreases with increasing content of the deoxidant. Further increase in the concentration of the deoxidant then leads to an increase in the oxygen solubility. The resulting minimum points are caused by changes in the activity coefficients,

---

* Unless stated otherwise, all compositions, deoxidant additions, etc. are given as wt. %

f_M and f_O, with [% M]. In the systems under consideration, as the concentration of the deoxidising element increases, so does its activity. However, the deoxidising element also decreases the activity coefficient of oxygen. The net result is that a minimum may occur in the oxygen solubility. The general trend is that the minimum oxygen content decreases as the stability of the deoxidation product increases. In addition, the concentration of the deoxidising element at which the minimum occurs, decreases with increasing stability of the oxide.

Using the above data, the temperature dependence of the equilibrium constant K in equation (2.5) is given in Table 2.1 for several deoxidants[10]. Reliable equilibrium constants for deoxidation by boron, vanadium and titanium are only available at 1600°C. In deoxidation with titanium, 'TiO' is formed at titanium contents above about 5%. At lower titanium contents, several oxides have been observed[13], e.g. $FeO.TiO_2$ (liquid), TiO_2, Ti_2O_3 and Ti_3O_5. However, below 0.3% Ti, the solubility product at 1600°C can be presented satisfactorily by $\left[h_{Ti}\right] . \left[h_O\right]^2$, although TiO_2 may not necessarily be the equilibrium oxide phase.

2.2.2 Effect of Alloying Elements on the Activity Coefficient of Oxygen

The additions of most deoxidants to steel decrease the activity coefficient of oxygen. The effect of various elements on the activity coefficient of oxygen is presented in Fig. 2.2 as a plot of $\log f_O^j$ versus wt. % j. The results for aluminium, titanium, boron, vanadium and chromium were recently obtained by Fruehan[12] using a galvanic cell to measure the activity of oxygen. The results for the other elements were obtained using conventional gas equilibrium techniques and have been compiled by Elliott et al[7].

For most low alloy steels, a convenient method of describing the effect of an alloying element, j, on the activity coefficient of oxygen is by the interaction

coefficient, e_o^j, defined as:-

$$e_o^j = \frac{d(\log f_O)}{d(\text{wt. \% j})} \Bigg|_{[\% j] \rightarrow 0} \quad .. \quad .. \quad .. \quad \text{eqn. (2.6)}$$

This is equivalent to the slopes of the lines in Fig. 2.2 at extreme dilution. It is emphasised that the interaction coefficient can only be used in the limiting case of low concentration of the alloying element. A list of the interaction coefficients is given in Table 2.2 together with the composition limits for which equation (2.6) is a reasonable approximation[11]. As a general rule, the more stable the oxide of the alloying element, the greater is the negative value of the interaction coefficient.

2.2.3 Silicon-Manganese Deoxidation

Silicon and manganese are the most widely used deoxidants added to steel in the furnace and/or in the ladle. Although deoxidation by silicon is more effective than that by manganese, simultaneous deoxidation by these two elements gives a much lower residual oxygen in solution. This fact was first demonstrated by Korber and Oelsen[14] in their study of the silicon and manganese reactions in liquid iron-slag systems. Hilty and Crafts[15] examined deoxidation by Si-Mn in alumina crucibles under an argon atmosphere. They found that the oxygen equilibrium for a certain silicon content decreased strongly with increasing manganese content, but no explanation was given. Bell[16] reviewed much of the early work on Si-Mn deoxidation and concluded that manganese increases the deoxidising power of silicon, but not to the extent reported by Hilty and Crafts. It appears likely that the FeO-MnO-SiO_2 slags used by Hilty and Crafts picked up Al_2O_3 from the crucible, and their melts then equilibrated with FeO-MnO-SiO_2-Al_2O_3 slags[6]. Samples of the slags were not obtained, however, and no investigation of the inclusions was made. It is not possible, therefore, to directly confirm this effect. In a later investigation, Bell[17] studied the effect of manganese on the silicon-oxygen equilibrium in liquid iron at 1550°C, and his results are shown graphically in Fig. 2.3.

Walsh and Ramachandran[18] used the results of Hilty and Crafts and explained the lower oxygen equilibrium by the fact that the deoxidation product was a manganese silicate having a silica activity, a_{SiO_2}, less than 1. They calculated an expression for a_{SiO_2} as a function of temperature, h_{Mn} and h_{Si}:-

$$\log a_{SiO_2} = 6.85 + \frac{12\,700}{T} - 0.5 \log \frac{h_{Mn}}{h_{Si}} \quad .. \quad .. \quad .. \quad \text{eqn. (2.7)}$$

On the basis of this data, however, the activity of silica becomes unity at Mn:Si activity ratios less than 1.7, whilst on the basis of Bell's data, the Mn:Si ratio must be less than 4 to give silica of unit activity. This discrepancy is probably due to the effect of alumina in the experiments of Hilty and Crafts, mentioned previously.

Kojima and Sano[19] also studied the effect of manganese on the equilibrium between silicon and oxygen in the presence of a silica-saturated slag. They found a decreasing oxygen content with increasing manganese content which they attributed to the fact that manganese increases the activity coefficient of silicon. They established the interaction coefficient, e_{Si}^{Mn}, as 0.281 in the interval 1550-1650°C for manganese contents up to 1.2%.

Turkdogan[10,20] calculated the equilibrium reaction data for Si-Mn deoxidation in the following manner. When steel is deoxidised by manganese, the reaction product is a liquid or solid solution of 'FeO' and MnO which form essentially ideal solutions. Representing the reaction by:-

$$\underline{Mn} + FeO\ (s, l) = Fe(l) + MnO\ (s, l) \quad .. \quad .. \quad .. \quad .. \quad \text{eqn. (2.8)}$$

then for the ideal solid and liquid solutions of 'FeO' and MnO,

$$K_{Mn} = \frac{N_{MnO}}{N_{FeO} \cdot [\%\ Mn]} \quad .. \quad .. \quad .. \quad .. \quad .. \quad \text{eqn. (2.9)}$$

where N is the mole fraction. The temperature dependence of K_{Mn} for the liquid and

solid oxides is given by

$$\log K_{Mn} \text{ (liquid oxide)} = \frac{6440}{T} - 2.95 \quad \text{.. .. .. eqn. (2.10)}$$

$$\log K_{Mn} \text{ (solid oxide)} = \frac{6945}{T} - 2.95 \quad \text{.. .. .. eqn. (2.11)}$$

The composition of the deoxidation product in equilibrium with a particular manganese concentration in liquid iron calculated from these equations is plotted in Fig. 2.4 for three different temperatures. The corresponding deoxidation equilibrium is shown in Fig. 2.5.

For silicon deoxidation, it is generally agreed that in silica-saturated melts containing less than about 3% Si, the deoxidation product $[\%\ Si] \cdot [\%\ O]^2$ is essentially independent of the silicon content. With increasing silicon content, f_{Si} increases and f_O decreases such that $[\%\ Si] \cdot [\%\ O]^2$ remains essentially constant for silicon contents less than about 3%. The silicon-oxygen equilibrium for various temperatures is shown in Fig. 2.6.

For Si-Mn deoxidation, Turkdogan[20] assumed that the products formed are essentially manganese silicates containing little iron oxide. The equilibrium conditions for this dual deoxidation reaction were then obtained from the sum of the individual deoxidation reactions for manganese and silicon to give:-

$$\underline{Si} + 2\ MnO = 2\ \underline{Mn} + SiO_2 \quad \text{.. .. .. .. eqn. (2.12)}$$

for which

$$K_{Si-Mn} = \frac{[\%\ Mn]^2}{[\%\ Si]} \cdot \frac{a_{SiO_2}}{(a_{MnO})^2} \quad \text{.. .. .. .. eqn. (2.13)}$$

$$\log K_{Si-Mn} = \frac{1510}{T} + 1.27 \quad \text{.. .. .. .. eqn. (2.14)}$$

where a_{SiO_2} and a_{MnO} are Raoultian activities of oxides in the molten manganese silicate deoxidation product relative to pure solid oxides. The oxygen content of iron in equilibrium with the deoxidation product (essentially pure manganese silicate) at

known concentrations of silicon and manganese is given in Fig. 2.7 for 1600°C. The effectiveness of manganese in boosting the deoxidising power of silicon decreases with increasing silicon content.

The amount of Si-Mn deoxidant to be added to achieve a specified level of deoxidation can be readily calculated from the above equilibrium data. Such calculations, of course, only apply to the idealised case of 100% efficiency of the deoxidant and the establishment of equilibrium. An example is given in Fig. 2.8 for deoxidation at 1650°C of steel containing initially 0.1% oxygen. The top scale on the abscissa is the total amount of silicon added to achieve the particular residuals in equilibrium with the deoxidation product formed. The total manganese added is about 0.08% higher than the residual concentration shown in Fig. 2.8.

It follows from equation (2.13) that above a critical ratio, $[\%\ Si]/[\%\ Mn]^2$, for a given temperature, solid silica forms as the deoxidation product. The critical silicon and manganese contents of iron in equilibrium with silica-saturated manganese silicate melts are given in Fig. 2.9 for several temperatures. If, for any particular temperature, the composition of the metal lies above the curve, manganese does not participate in the deoxidation reaction and solid silica is formed instead. In the region below the curve, the deoxidation product is a molten manganese silicate, the composition of which is determined by the ratio $[\%\ Si]/[\%\ Mn]^2$ in the metal.

2.2.4 Aluminium Deoxidation

The deoxidation of steel melts by aluminium has been studied in detail by many workers[15, 21-28] and it is well known that values of the equilibrium constant $[\%\ Al]^2 \cdot [\%\ O]^3$ obtained by different investigators for aluminium and oxygen in liquid iron vary from about 10^{-9} to about 10^{-14} at 1600°C. This discrepancy has been much discussed and Repetylo et al[29] have confirmed that the variation results chiefly from the presence of alumina suspensions. It was shown that if liquid metal with aluminium and oxygen contents corresponding to point S in Fig. 2.10 was held in

a crucible and all oxygen ingress was prevented, the metal composition gradually approached the equilibrium curve of Gokcen and Chipman[30]. After 10 min, more than 80% of the initial oxygen content had been converted to alumina and, if the test was continued, residual oxygen contents ranging from 0.006 - 0.002% were obtained. The lowest value obtained for the equilibrium constant $[\%\,Al]^2 \cdot [\%\,O]^3$ was 5.10^{-13} (compared to 3.10^{-9} initially).

With longer holding times of 20 min or more, it was impossible to reach the oxygen equilibrium value of 0.001% corresponding to an equilibrium constant of 10^{-14}. This was probably caused by a suspension of very fine alumina particles remaining in the liquid metal even after 20 min.

Experiments made with the same apparatus in an oxygen-bearing atmosphere with successive aluminium additions to the liquid metal gave total aluminium and oxygen values in the scatter range of Hilty and Crafts' curve[15], Fig. 2.10. In view of the extreme rapidity of reaction between aluminium and oxygen, these high values indicate continuous formation of alumina inclusions in the liquid metal. According to Pomey and Trentini[31], this type of experiment clearly shows the difficulties involved in obtaining low oxide inclusion contents during melting and casting in air.

2.3 KINETICS OF DEOXIDATION

Some of the first studies on the development of deoxidation reactions with time and the mechanics involved in the formation and separation of inclusions were carried out by Plöckinger and Wahlster[32,33]. As Fig. 2.11 shows, these authors distinguished between dissolved oxygen and oxygen combined with inclusions. The development of these two constituents during the course of the operation shows the essential characteristics of the mechanism of precipitation deoxidation, i.e. rapid decrease of dissolved oxygen associated with the formation of numerous deoxidation products, together with delayed and slower decrease of total oxygen corresponding to the elimination of the deoxidation products.

The validity of this mechanism has been confirmed by more recent studies in which the dissolved oxygen was measured and recorded against time, either directly by the use of an electrochemical cell[34], or indirectly by the radioactive tracing of secondary inclusions[35].

A more explicit understanding of the deoxidation process has led to a subdivision of the overall operation into a certain number of component stages[36]:-

(i) solution of the deoxidant in the metal

(ii) nucleation of the deoxidation products

(iii) growth of the nuclei

(iv) elimination of the inclusions

In practice, these stages overlap to a large extent and there are other phenomena such as reoxidation which complicate the process. Bearing in mind the complexity of the problems involved, these four stages will be examined separately so as to indicate the effect of each one on the rate of deoxidation.

2.3.1 Solution of Deoxidant

Although this first stage can be easily followed during controlled laboratory experiments in terms of diffusion theory, the same stage becomes much more complex to follow during deoxidation on an industrial scale. For instance, when deoxidation and alloying are carried out during tapping into the ladle, account must be taken of the following factors:-

(i) tapping may take a long time (~10 min) and is accompanied by fairly intensive stirring owing to the impact of the metal stream

(ii) additions of deoxidants are usually large

(iii) deoxidation is usually carried out by several elements being added separately.

All these conditions involve a transitional period during which the primary deoxidation products appear in a random manner and have variable compositions.

The kinetic character of deoxidant solution has been described by A. M. Levin[37] who showed that the addition of a deoxidising element, even below its equilibrium content, causes precipitation of oxides through progressive solution.

The significance of the solution stage on the subsequent deoxidation stages has been indicated by the following observations:-

(i) on a macroscopic scale, a certain heterogeneity of alloying elements is always observed; on a microscopic scale it can be much greater. This is confirmed, for example, by accidental brittle fractures owing to abnormally high local concentrations of an alloying element such as manganese. As there are delays in homogenisation of alloying elements, then it will probably be the same for deoxidising elements.

(ii) in the case of deoxidation by aluminium, Olette et al[34] showed that the method of introducing the addition influences the kinetics of deoxidation, Fig. 2.12. They explained the slower decrease in dissolved oxygen with a solid addition by the delay caused in the solution and homogenisation of the aluminium as a result of a layer of fine alumina particles on the surface of the deoxidant inhibiting diffusion of the aluminium into the melt. This observation is in agreement with the hypothesis formulated by Chipman[38] in 1962 regarding the formation of stabilising films at the interface between regions with a high concentration of oxygen. A stabilising film of galaxite, $MnO.Al_2O_3$, has been observed in a sample taken from an induction furnace shortly after the addition of an Fe-Al-Mn alloy[36]. It was found by microanalysis that the ratio of internal manganese : external manganese was as high as 1.8 : 1.

These few observations indicate that the solution and homogenous distribution of the deoxidant is a stage which is not instantaneous and is, therefore, liable to cause a delay in the overall deoxidation process. The steelmaker has certain means of influencing this stage such as by variation of tapping temperature, composition and size of solid deoxidants, and stirring in the ladle. However, whilst there is scope for seeking the most favourable conditions, it is nevertheless believed that this stage is not the most decisive one for the success of the overall deoxidation process.

2.3.2 Nucleation of Deoxidation Products

At first sight, the question of nucleation processes in the formation of deoxidation products seems to be only of academic interest. Although the formation of oxides in liquid iron involves the formation of new phases, and the nucleation process is therefore decisive, it has never been observed, for example, that the formation of alumina on adding aluminium to an iron-oxygen melt fails to occur as a result of nucleation inhibition. It might be concluded from this that the efficiency of deoxidation is related much more to the removal of inclusions once they have formed. This is not the case, however, and it is now known that nucleation processes can exert an important influence on the practical course of deoxidation.

Two nucleation mechanisms are possible, namely homogeneous nucleation which takes place in the mass without the assistance of impurities, and heterogeneous nucleation which takes place with the aid of a substrate. In order to understand the deoxidation process better, it is necessary to know which of these two mechanisms is responsible for the formation of inclusions, what the connection is between the nucleation stage and the later stages of growth and flotation, and finally, what practical means, if any, there are for the steelmaker to influence this stage.

The theoretical approach to the problem has been made principally for homogeneous nucleation. According to the classical nucleation theories of Becker,

Volmer and Weber, the energy required to form a spherical embryo of radius r is:-

$$E = 4\pi r^2\sigma + \frac{4}{3}\pi r^3 \frac{\Delta G}{v} \qquad \text{eqn. (2.15)}$$

where σ is the interfacial energy between the precipitate and the molten metal, ΔG is the chemical free-energy change accompanying the formation of the precipitate and v is the molar volume of the precipitate. The free-energy change resulting when a mole of the second phase is formed is ΔG, and for the formation of a deoxidation product M_xO_y from the reaction of a deoxidant M with oxygen in liquid iron

$$\Delta G = -RT.\ln \frac{\left(h_M^x . h_O^x\right)_{act.}}{\left(h_M^x . h_O^x\right)_{eq.}} \qquad \text{eqn. (2.16)}$$

$$= -RT.\ln\frac{K'}{K} \qquad \text{eqn. (2.17)}$$

where K is the equilibrium solubility product, K' is the corresponding product for the actual components in supersaturated solution and K'/K is termed the super-saturation ratio. The work necessary to form the second phase is largest at a critical radius, r_c, where

$$r_c = -\frac{2\sigma v}{\Delta G} \qquad \text{eqn. (2.18)}$$

The work necessary to form this nucleus is

$$E_c = \frac{16\pi\sigma^3 v^2}{3(\Delta G)^2} \qquad \text{eqn. (2.19)}$$

and represents the free energy barrier to the formation of the second phase (ΔG_c). The rate of formation of nuclei (nuclei/cm^3 s) is given by

$$I = A.\exp(-\Delta G_c/kT) \qquad \text{eqn. (2.20)}$$

where A is the nucleation factor.

It can be seen from these equations that the interfacial energy at the melt/nucleus boundary is a major component of the total energy required to form a stable nucleus. For the homogeneous nucleation of oxides in molten steel, the interfacial energy at the oxide/molten steel boundary is about 1.0 J/m^2 (1000 erg/cm^2) but in some cases is greater. This means that exceptionally high supersaturation ratios

are necessary for nucleation by this mechanism.

The first experimental evidence came from von Bogdandy, Meyer and Stranksi[39] who studied the formation of oxides in iron-oxygen melts by equilibrating a column of the melt with a quantity of deoxidiser added to the top surface. Convection currents were virtually eliminated and penetration of the deoxidiser into the melt occurred only by diffusion. The column was quenched after pre-determined diffusion periods and the diffusion zone was examined metallographically and analytically. Their results on aluminium deoxidation showed that the oxygen combined to form alumina in the aluminium-rich zone and iron oxide in the aluminium-deficient zone. Only a few traces of hercynite, $FeO.Al_2O_3$, were observed throughout the experiments. The oxygen content was found to remain constant along the column and so it was concluded that the inclusions remained in their position of formation. Using the aluminium and oxygen concentrations measured at the boundary between the unaffected melt and the zone rich in alumina particles, the critical supersaturation ratio was determined as 3.6×10^{14} at 1550°C.

Woehlbier and Rengstorff[40] used a similar technique to that of von Bogdandy et al with a very pure iron-oxygen melt and an Fe-10% Al alloy as deoxidiser. They reported exceptional nucleation difficulties at 1600°C and oxide nuclei were not formed in the diffusion zone, although the aluminium concentration was 2.9% and inclusions formed on quenching showed a high concentration of oxygen. The same experiment was repeated using a less pure iron containing 0.07% oxygen instead of 0.16% and this was found to be partially deoxidised by the Fe-Al alloy. It was concluded that a very high degree of supersaturation is required for homogeneous nucleation of alumina but a much lower degree of supersaturation is sufficient to cause the precipitation of alumina on small heterogeneous nuclei without the appearance of hercynite.

Further work by Woehlbier and Rengstorff in which pure aluminium was stirred into the upper zone of the pure iron-oxygen melt resulted in the formation of alumina inclusions by homogeneous nucleation at the point of addition. These inclusions were then carried down into the undeoxidised portion of the melt where they reacted with residual oxygen to form hercynite.

For aluminium, the experimentally determined critical supersaturation ratios agree very well with the values calculated using Volmer's theory assuming the maximum possible frequency factor. The temperature dependence of the supersaturation ratio is also in agreement with Volmer's theory.

The final proof of the applicability of Volmer's hypotheses came from the fact that oxide nucleation in iron is facilitated by surface-active elements such as manganese, which lowers the surface tension of molten iron. Frohberg and Pötschke[41, 42] were able to show that these hypotheses could be applied to other metals, e.g. oxide formation in molten copper. They found that surface-active elements such as sulphur facilitated the formation of oxides.

Few reliable measurements have been made of interfacial energies between deoxidation products and liquid iron, but Turpin and Elliott[43] calculated the following interfacial energies between oxide and melt at 1536°C:-

	Interfacial Energy, J/m^2 (erg/cm^2)
$Fe_{(l)}$ - $FeO_{(l)}$	0.25 (250)
$Fe_{(l)}$ - $SiO_{2(s)}$	1.25 (1250)
$Fe_{(l)}$ - $Al_2O_{3(s)}$	2.4 (2400)
$Fe_{(l)}$ - $FeO.Al_2O_{3(s)}$	1.7 (1700)

The experiments were carried out by equilibrating iron-oxygen melts with various residual silicon or aluminium contents and then quenching. The critical supersaturation for homogeneous inclusion nucleation was assumed to result from the high

degree of oxygen segregation to the liquid during solidification. Their results are summarised in Figs. 2.13 and 2.14, which show the calculated lines at 1536°C for nucleation of silicon and aluminium deoxidation products for various values of the appropriate interfacial energy. The lines marked (eq) are for the formation of the deoxidation product when the size of the precipitate particle is such that the interfacial energy makes an insignificant contribution to the total energy (i.e. the bulk equilibrium conditions).

At low concentrations of the deoxidising element, the nucleation of FeO may occur more readily than the formation of the equilibrium reaction product. The shaded bands on the diagrams show the experimental composition ranges in which it was found that FeO was nucleated first and subsequently changed to the stable product. At higher concentrations of deoxidiser, the stable product was nucleated directly from the melt. This transition occurs at lower concentrations for aluminium than for silicon and shows that the higher value of σ for the Fe-Al_2O_3 interface is more than compensated by the larger value of ΔG for the precipitation of alumina.

An alternative view of this effect was obtained by calculation of the degree of undercooling required to achieve the necessary degree of supersaturation for homogeneous nucleation. Figure 2.15 shows that if σ(SiO_2-Fe) = 1.3 J/m^2 (1300 erg/cm^2), the melt would have to be equilibrated with SiO_2 at approximately 1950°C if homogeneous nucleation is to occur at 1536°C. For σ(FeO-Fe) = 0.25 J/m^2 (250 erg/cm^2), the same degree of undercooling would be required for nucleation of FeO in a melt containing approximately 0.5% Si. At lower silicon contents, FeO would require less supersaturation and, consequently, would nucleate in preference to SiO_2.

Sigworth and Elliott[44] recently reviewed the nucleation of oxides in Fe-O-Si alloys. According to these workers, investigations of the nucleation process during deoxidation have been limited by the lack of accurate interfacial energy data and also

by the experimental techniques available. In the latter case, it is difficult to provide the necessary supersaturation quickly and in a controlled manner, and it is even more difficult to detect exactly when nucleation occurs. They concluded that in the earlier experiments of Turpin and Elliott, homogeneous nucleation of oxides in the Fe-O-Si system did not occur. These experiments were later duplicated by Torssell, Gatellier and Olette[45] and the absence of any significant degree of supersaturation was confirmed by electrochemical measurements, which showed that the oxygen activity in the melt followed very closely the value calculated for equilibrium with the melt silicon content, Fig. 2.16. It appears, therefore, that heterogeneous nucleation occurred and the deoxidation reaction had ready access to particles of the stable phase throughout the cooling process. However, the test was not a particularly severe one because the cooling rate was relatively slow. In addition, homogeneous nucleation would not have been expected in the experiment because the temperature interval for cooling was only 75°C and the maximum supersaturation ratio possible (in the absence of heterogeneous nucleation) was only about 4, compared to the estimated value required of 100 or more.

Sigworth and Elliott reported that the experimental technique used first by von Bogdandy et al and later by many other workers was also inadequate for obtaining an accurate value of the critical supersaturation ratio, its main limitation being the complexity of the theoretical analysis. All that could be concluded from these studies was that substantial supersaturation is necessary for the homogeneous nucleation of oxides during deoxidation and that homogeneous nucleation can occur when the deoxidising element is first introduced into the melt.

In their own experimental work, Sigworth and Elliott measured the critical supersaturation necessary for homogeneous nucleation of oxides in Fe-O-Si alloys by means of an electrochemical cell. Their results are summarised on the composition

triangle in Fig. 2.17 and the same information is presented in the more familiar form of the deoxidation diagram in Fig. 2.18. Included are the lines for the formation of silica and liquid FeO at equilibrium, i.e. when the interfacial energy is zero. A value of 0.25 J/m^2 (250 erg/cm^2) was used for the nucleation of liquid FeO. The interfacial energy for the boundary between liquid iron and iron silicate was assumed to be near to that of the FeO/liquid iron interface.

They found that the homogeneous nucleation of silica occurred at supersaturation ratios of about 80 and showed that, when ferro-silicon is added to a ladle of low-carbon steel during the tapping of a basic oxygen or open-hearth furnace, homogeneous nucleation can occur quite easily. The conditions necessary can be achieved even in the presence of particles suitable for heterogeneous nucleation if the supersaturation is provided rapidly. This was illustrated in the work of Jaeger et al[46] who found that homogeneous nucleation of water droplets in air could occur even in the presence of numerous dirt particles.

The problem of competition between different phases which may be precipitated has also been studied by Vorobnev and Levin[47] and by Plöckinger et al[48] for the Fe-O-Al system. In the latter case, these workers studied the deoxidation of nominally pure iron melts containing different manganese contents by aluminium at 1630°C. It was observed that the primary deoxidation products underwent a marked change in composition during the course of their formation. Immediately after the aluminium addition, the inclusions were very low in alumina and consisted essentially of iron and manganese oxides. The proportion of the latter depended upon the manganese content of the melt. The alumina content of the inclusions then increased very rapidly during the next few seconds until the composition reached that of the spinel $(Fe,Mn)O.Al_2O_3$. During this period the inclusions were in a fluid or partly fluid state and possessed good coagulation properties. In addition, microanalysis showed that each inclusion

had a uniform composition. This situation persisted for only a short interval and with further increase in time, the large inclusions developed two regions having different compositions. The core of the inclusions contained about 60% Al_2O_3, 40% (FeMn)O, and had, therefore, a spinel-like composition in which the FeO:MnO ratio depended on the manganese content of the melt. In contrast, the outer layers consisted of pure alumina.

According to Plöckinger et al, the solution and distribution of the aluminium in the melt takes a definite although short time. Within a small volume element of the melt, the aluminium content rises rapidly, but not instantaneously, from zero up to a point at which the solubility product for the formation of mixed oxides is exceeded. This occurs with very small aluminium contents and the deoxidation products consist essentially of iron and manganese oxides with very small proportions of alumina, e.g. 85% FeO, 10% MnO and 5% Al_2O_3. With this composition they are liquid at the melt temperature of 1630°C.

As the aluminium content of the melt increases, there is a corresponding increase in the alumina content of the mixed oxides. So long as the inclusions are liquid, conditions are favourable for the homogenisation of their compositions. Only when the alumina content increases further up to a value corresponding to that of the spinel does complete solidification of the inclusions occur. After this stage, the inner core regions of the large deoxidation products are no longer involved in a reaction with the now aluminium-rich melt, and pure alumina deposits on their surfaces leaving the cores with a constant composition.

The mechanism put forward by Plöckinger et al postulates that the liquid mixed oxides are precipitated homogeneously. Fröhberg and Pötschke[49], and Förster[50] consider that this suggestion is contradicted by nucleation theory and that the phase for which the system is able to supply the nucleation energy will be

precipitated first. This implies that solid nuclei of alumina would have to form on to which iron and manganese oxides would then be precipitated heterogeneously. Consequently, Fröhberg et al have postulated that solid alumina particles are formed at the surface of the aluminium immediately after its addition to the melt. (It is significant that aluminium deoxidants already have a coating of oxide as a result of air oxidation.) Convection and stirring effects result in a rapid distribution of these alumina particles throughout the melt. In regions where sufficient supersaturation exists, iron and manganese oxides are precipitated heterogeneously on the alumina, which then dissolves in the mangano-wüstite to form a fully molten oxide. This then reacts with further aluminium according to Plöckinger's mechanism.

Förster[50] has carried out similar experiments using zirconium instead of aluminium. The inclusions observed shortly after the addition of the deoxidant consisted of a core of zirconia surrounded by mangano-wüstite. This result points to the primary formation of zirconia which had not dissolved in the liquid (FeMn)O.

Vorobnev and Levin[47] have suggested that during aluminium deoxidation, the formation of complex nuclei of the $FeO-Al_2O_3$ type in the liquid state is possible owing to a decrease of the melt/nucleus interfacial energy caused by chemical reaction between the two phases, and that the compositionof such nuclei are determined by the soluble oxygen content of the melt prior to deoxidation. Their results are summarised in Fig. 2.19 where lines 1-5 are based on various equations derived by the authors. The areas A-E between the lines represent the areas of formation of nuclei of various compositions. A represents the region of unsaturated metal where the formation of nuclei cannot occur; B is the area of supersaturated metal where the supersaturation is insufficient for the formation of stable nuclei; C is the area of supersaturated metal where only liquid mixed oxides can form; D is the area where liquid mixed oxides and pure alumina can form; E is the area where only alumina nuclei can precipitate.

According to these workers, when aluminium is introduced into a melt, the processes of solution of the deoxidant and deoxidation occur simultaneously throughout the volume of the melt. The concentration of aluminium at any point increases with time from zero. Consequently, the initial state of the system is in area A. With increasing time, the concentration of aluminium at a given point reaches a value which is in equilibrium with the dissolved oxygen (line 1), after which the metal becomes supersaturated (area B). With further increase in the aluminium concentration, the degree of supersaturation of the metal becomes sufficient for the oxide phase to separate. With a sufficiently high concentration of oxygen in the melt, for example 0.05%, the nuclei which form will be liquid mixed oxides (area C). If the oxygen concentration is less than 0.01% before deoxidation, the oxide phase will separate in the form of alumina (area E).

If deoxidation is carried out by the simultaneous use of silicon and aluminium, then according to the nucleation theory, that phase which provides for the greatest rate of nucleation, namely alumina, must occur first. The silica can then be precipitated heterogeneously on the alumina particles. This mechanism has been confirmed in laboratory experiments by Fröhberg and Pötschke[42].

Applying the nucleation theory to normal deoxidation practice, it can be predicted, on the basis of the discussion so far, that when a deoxidiser is added to the bath, the supersaturation of the melt, and consequently the nucleation frequency, will be a maximum in the immediate vicinity of the deoxidiser as it dissolves in the melt. If the degree of supersaturation achieved is high, many small nuclei are formed which cannot grow to a large size before equilibrium is attained and may remain suspended in the bath. At lower degrees of supersaturation only a few nuclei are formed before the level falls below that at which further stable nuclei can be formed. The degree of local supersaturation achieved can be controlled to some extent by the mode of deoxidation, e.g. by the use of finely divided deoxidisers or, more particularly, by lowering the deoxidiser concentration in the ferro-alloy.

Similarly, additions of a relatively weak deoxidiser such as manganese will decrease the supersaturation and encourage the formation of larger inclusions when a strong deoxidiser is subsequently added.

Once the supersaturation has been relieved, homogeneous nucleation will cease, although it may continue adjacent to the slag/metal interface owing to oxygen transfer from slag to metal[29]. Heterogeneous nucleation will continue at lower degrees of supersaturation, but the growing precipitates steadily reduce the metal oxygen content towards the equilibrium level. If the growing particles are carried rapidly away from the regions where the deoxidiser is dissolving into more remote parts of the bath where the concentration of deoxidiser is low, subsequent growth may involve the formation of a layer with a lower deoxidiser:oxygen ratio (e.g. $FeO.Al_2O_3$) relative to the initially formed nucleus (e.g. Al_2O_3). Alternatively, they may act as heterogeneous nuclei for the precipitation of MnO and SiO_2.

Degrees of supersaturation required for heterogeneous nucleation are always less than those for homogeneous nucleation and in industrial practice, the former is very important. In addition to any nuclei formed by homogeneous nucleation in the immediate vicinity of the deoxidiser, all industrial deoxidants, weak or strong, introduce into the steel a certain quantity of oxide particles, either through their surface oxidation film or through inclusions contained in their mass. These oxide particles can also act as nuclei for heterogeneous precipitation. Most weak deoxidants contain variable quantities of metallic elements with a very strong affinity for oxygen, e.g. calcium, aluminium and titanium[51]. The oxides of such elements, formed by homogeneous nucleation, can constitute nuclei during deoxidation by weaker deoxidants[52], which may also account for the complex nature of some primary inclusions during deoxidation.

The practical significance of heterogeneous nucleation has been stressed by Förster and Richter[53,54] who attribute the major role for the success of

deoxidation to the 'nucleation' stage. In the case of deoxidation by aluminium, they explained that the nuclei and primary inclusions separate from steel in a state of supersaturation which is too weak to produce further effective nucleation, i.e. in the area below the nucleation curve and above the equilibrium curve in Fig. 2.20. Part of their work involved the electrochemical determination of oxygen activity during the teeming of an aluminium-killed melt at a point about 60 cm above the bottom of a 120 tonne ladle, Fig. 2.21. The dissolved oxygen varied considerably between 0.003% and 0.011%. They attributed this to areas differently supersaturated with alumina and to varying aluminium contents. It can be seen that in the aluminium-killed melt, the degree of freedom from oxide inclusions varied considerably from ingot to ingot. In contrast, the oxygen content of a silicon-killed steel was uniform during casting. These authors proposed two practical measures to increase the efficiency of the deoxidation process:-

(i) the introduction of foreign nuclei, either simultaneously with or subsequently to the addition of the deoxidant,

(ii) the reduction of the melt/oxide interfacial tension by the use of a deoxidant with a relatively high manganese content.

As discussed previously, there is a second moment when conditions are favourable for homogeneous nucleation of inclusions, this being during solidification as a result of a high local concentration of oxygen and deoxidant produced in the residual liquid phase. It is generally assumed that the oxides which form during solidification are not harmful to the properties of the steel because of their fine distribution. However, finely distributed oxides can affect the transformation behaviour of a steel[54].

Another important aspect of the solidification stage is that several different non-metallic phases are formed, in particular oxides and sulphides. The latter can

cause anisotropy of the mechanical properties of the steel[55]. The important question then arises as to which phase has the greater nucleation rate and therefore is the first to form, thus determining the distribution of the other phases which are precipitated heterogeneously on the primary particles.

A decisive factor in the formation of oxides and sulphides during solidification is that oxygen and sulphur are almost insoluble in solid iron and so accumulate ahead of the solidification front, Fig. 2.22. The concentration of oxygen in advance of the front must increase until an oxide nucleus can form. This may happen in the extreme case as early as the achievement of the equilibrium concentration but more probably it occurs much later because nucleation is inhibited. If this is the case, then as a result of the enrichment of oxygen, the supersaturation ratio increases to the critical value at which nucleation occurs. The reaction then proceeds rapidly and the concentration of oxygen ahead of the solidification front falls to a lower value[56], Fig. 2.23. When the oxide particle is overtaken by the solidification front, the build-up of oxygen and deoxidant begins again. This concept is greatly simplified, however, in that it assumes a planar solidification front.

These hypotheses were examined experimentally by measuring the content of oxygen in solution electrochemically[56]. The particle distribution depended to a large extent on the solidification rate and also on the dissolved oxygen content. The experiments also showed that the oxygen content is more important than the sulphur content in determining sulphide distribution. Similar observations have often been reported, for example the effect of aluminium deoxidation on sulphide distribution[57].

Förster and Richter[53] have considered the question as to whether large clusters of alumina inclusions which result in defects in the rolled product might not also originate from dissolved oxygen during solidification in the mould. The quantity of dissolved oxygen (0.002 - 0.007%) in normal aluminium-killed steels could easily

be enough to form large inclusions. On this basis, they referred to work by Knüppel, Brotzmann and Förster[58] who established from investigation of an aluminium-killed steel that the clusters of alumina inclusions present in the product were, in most cases, not present in the ladle and must, therefore, have formed between ladle and ingot, or in the ingot. Knüppel et al suggested that the most likely cause appeared to be agglomeration of very small inclusions in the flow conditions of the uphill-teeming system. However, Förster et al consider that it is also possible, in principle, that these alumina clusters formed from dissolved oxygen during solidification of the ingot, presumably by the agglomeration of small alumina particles formed in the oxygen-rich liquid ahead of the solidification front. This mechanism would appear to require that the alumina particles are not overtaken by the solidification front but are entrained in the convection currents within the bulk melt where they form clusters with other entrained particles. Although this mechanism is theoretically possible, it seems unlikely that it can account for the formation of the large alumina clusters which lead to defects in the rolled product. The main reason for this is that, as previously mentioned, the solidification front is not planar but dendritic and many of the small alumina particles which form during solidification are likely to be precipitated between dendrites, which then thicken and envelop the inclusions, so that there is very little opportunity for the inclusions to be swept into the bulk liquid by the convection currents.

Förster et al have also discussed a further problem of practical interest, that of the formation of blowholes in fully aluminium-killed steels. The formation of alumina nuclei at the solidification front requires a high degree of supersaturation whereas the nucleation of carbon monoxide bubbles is evidently catalysed at the solidification front compared with nucleation in the melt. It is clear from Fig. 2.24 that owing to oxygen enrichment ahead of the solidification front and the inhibition of nucleation of alumina, the formation of carbon monoxide at preferred locations can be more probable than the nucleation of oxides.

2.3.3 Growth of Nuclei

In practice, the growth of nuclei overlaps to a very large extent with the flotation stage and it is difficult to discuss either of them individually. There are four major growth processes:-

(i) Brownian motion

(ii) Ostwald ripening (diffusion coalescence)

(iii) Diffusion

(iv) Collision

On the basis of both experimental and theoretical results, Lindborg and Torssell[59] proposed the mechanism summarised in Fig. 2.25 for the growth and elimination of silica particles during deoxidation. The transition from a nucleus (of diameter several Å) to an inclusion (of diameter several μm) is explained by the diffusion of solutes in liquid steel. This mechanism reaches completion very rapidly, however, through the reduction of dissolved oxygen in the melt. From this moment, growth can continue by means of collisions owing to movements in the bath. These workers consider that in the initial stage, Brownian motion can also have some effect but it is only secondary and is reduced very quickly by the increase in the size of the particles. The growth of large particles at the expense of small ones by the Ostwald ripening effect is also too slow to be of any importance.

Turkdogan[60] has carried out a theoretical analysis of the kinetics of nucleation, growth, and flotation of oxide inclusions in liquid steel and shown that the number of nuclei has a pronounced effect on the growth of oxide inclusions, on the extent of the deoxidation reaction and on the rate of flotation of oxide inclusions out of the melt. His analysis was based on a model which assumed that, starting with an homogeneous solution of oxygen and the deoxidant in liquid steel, oxide inclusions were precipitated on nuclei present in the melt. The nuclei were considered to be formed initially by homogeneous nucleation of the deoxidation product in solute-rich regions of the melt. Assuming that a phase boundary equilibrium was readily established at

the metal/oxide interface, a rate equation was derived for the growth of inclusions by a diffusion-controlled process. With the additional assumptions that the diffusion sphere around the inclusion was not affected by the upward movement of the inclusion, and that Stokes' law was applicable, the instantaneous inclusion size for any time, t, during its ascent in the liquid, and the distance, l, travelled by a growing inclusion were calculated. The results obtained are summarised in Figs. 2.26 and 2.27, which show that in the presence of a large number of nuclei, the diffusion-controlled reaction, in accordance with the proposed model, is completed in a relatively short time. For example, when $Z > 10^5/cm^3$, growth of inclusions is essentially completed in less than about 30 s. In these cases, the particles attain a constant velocity of rise within a short time, and this velocity may be calculated from the final particle size. However, this simplification does not apply for $Z < 10^5/cm^3$ where particles grow throughout the whole of their ascent in the melt, causing an acceleration of their upward movement.

According to Turkdogan, as the inclusions grow and rise in the melt with increasing reaction time, the liquid steel is progressively depleted of inclusions from bottom to top. Owing to an insufficient degree of supersaturation, new nuclei cannot form and therefore the deoxidation reaction ceases in the inclusion-depleted part of the steel before reaching the final equilibrium state. The dependence of the average total oxygen content of the steel on the number of nuclei and the holding time is shown in Fig. 2.28. The plateaux in the diagram indicate that when all the inclusions have floated out of the melt, no further deoxidation takes place.

The expected net result of these effects is shown in Fig. 2.29 where the average total oxygen content of the steel is plotted against the number of nuclei assumed to be present at the time of addition of deoxidisers. The critical value of Z, Z_m, corresponding to the minimum point on the curve for a given reaction time has a particular significance. If the number of nuclei, Z, is less than the critical value, Z_m, the relatively large inclusions float out of the melt quickly, leaving behind

unreacted high residual oxygen in solution. Therefore, the portion of the curve to the left of the minimum point gives the average oxygen in liquid steel which is essentially free of inclusions. Within this region, an increase in reaction time beyond about 5 min has little effect on the final oxygen content of the steel, because the deoxidation reaction cannot proceed in the absence of nuclei. If the number of nuclei, Z, is greater than Z_m, the inclusions attain their full growth in a relatively short time, i.e. the residual oxygen in solution approaches the equilibrium value in a short time. Under these conditions the inclusions are small in size and hence their separation from the melt takes a long time, as indicated by the curve for infinite time in Fig. 2.29. Therefore, the curve to the right of the minimum point gives the average oxygen present as oxide inclusions in the steel which is deoxidised almost to the equilibrium value. As seen from Fig. 2.29, with increasing number Z, the holding time should be increased in order to obtain the lowest oxygen in the steel.

The practical significance of Turkdogan's theoretical observations as summarised in Fig. 2.29 is as follows. For the case of $Z > Z_m$, the steel is effectively deoxidised (i.e. the oxygen in solution is low), but, even after prolonged holding time, the inclusion content of the steel is high and may lead to poor quality in the finished product. On the other hand, for $Z < Z_m$, the steel may be essentially free of inclusions at the time of casting, but contains a high percentage of oxgen in solution leading to the formation of blowholes, or to the precipitation of further inclusions during cooling and solidification.

A diffusion-controlled growth model such as the one suggested by Turkdogan assumes an homogeneous precipitation of inclusions all having approximately the same diameter, and growing by the combination of elements which have diffused to the inclusion surface. However, the very large deoxidation inclusions sometimes found in practice which float out almost instantaneously on addition of the deoxidant, cannot achieve such a size by a diffusion process alone and therefore must be a result of inclusion collision and coalescence.

Growth by diffusion always occurs to some extent but recent experiments and calculations indicate that collisions are more important than previously realised. In laboratory experiments using about 5 cm deep melts, Grevillius[61] found that the rate of deoxidation by silicon or silicon-manganese was much faster in stirred melts relative to those in unstirred melts, Fig. 2.30. Similar observations have also been made by numerous other investigators.

Several workers[58,59,62-64] have measured the size distribution of inclusions in steel samples taken at intervals during deoxidation and found that in the initial stages of deoxidation, $Z \simeq 10^7/cm^3$ for inclusions of 1-2 μm diameter and $Z \simeq 10^5/cm^3$ for inclusions of 6-8 μm diameter, Figs. 2.31 and 2.32. It should be remembered in such instances that the inclusion distribution found in samples taken after prolonged deoxidation times is that arising from the formation of oxides during solidification. For example, the lower curve in Fig. 2.31 gives the inclusion distribution arising from the residual equilibrium oxygen that was in solution in liquid steel (free of inclusions) after a reaction time of 200 s. Turkdogan considers that it is reasonable to take $Z \simeq 10^7/cm^3$ or higher for the number of nuclei forming at the time of addition of deoxidisers. For a homogeneous distribution of such a large number of nuclei, the diffusion-controlled deoxidation reaction approaches equilibrium rapidly. From Turkdogan's theoretical model, it is predicted that with $Z = 10^6/cm^3$, 0.05% oxygen reacts almost completely in about 5 s, and oxide removal by flotation becomes the primary rate-controlling process. The time for flotation of oxide inclusions (equivalent to 0.05% oxygen in the metal) is shown in Fig. 2.33 as a function of Z and particle size for 5, 50 and 200 cm deep melts. If this mechanism applied, it would take about 40 min for 4 μm diameter inclusions (corresponding to $Z = 10^7/cm^3$ and 0.05% oxygen) to float out of a 5 cm deep melt. This flotation time is much longer than that observed experimentally. Furthermore, the size measurements indicate that the majority of the oxide inclusions are in the 30-40 μm range, and which escape from the melt in a much shorter time. It has, therefore, been inferred by several

investigators that the oxide inclusions grow by collision with each other resulting in a faster rate of flotation.

Lindborg and Torssell[59] have calculated the size distribution function brought about by collisions of different sized particles, and although they showed good agreement between the measured and calculated inclusion size distribution, Fig. 2.31, there are inconsistencies in the proposed growth mechanism by collision when compared with experimental observations. In their experiments with molten steel (~4.5 cm deep) stirred by induction heating, the macroscopic flow velocity was estimated to be about 1 cm/s. They showed that growth caused by collision in these stirred melts (gradient collisions) was less than that caused by the collision of different sized particles whilst rising in the melt with varying velocities (Stokes collisions), Fig. 2.25. If this is the case, then the observed effect of stirring on the rate of deoxidation in Fig. 2.30 cannot be explained in terms of growth by collision. According to Turkdogan[10], the major weakness of this growth mechanism is that the trajectory of the moving particle is assumed to be unaffected by an approaching particle and that every collision results in coalescence. On the basis of theoretical calculations, Turkdogan has concluded that the chances of collision between inclusions as they rise in the melt (Reynolds number Re <1) are negligibly small.

Turkdogan has suggested that the complexity of the rate pheomena in deoxidation is the result of side effects caused by the interplay of several variables which cannot readily be accounted for in mathematical models of the deoxidation process. However, he has summarised the following observations based on theoretical and experimental analyses:-

(i) The number of nuclei formed at the time of addition of deoxidisers is of the order of $Z = 10^8/cm^3$ or higher.

(ii) The diffusion-controlled deoxidation reaction is essentially complete within a few seconds when $Z > 10^6/cm^3$.

(iii) The deoxidation reaction may cease prematurely in parts of the melt depleted of nuclei or oxide inclusions.

(iv) The inclusion size during deoxidation is in the range 1 to 40 μm.

(v) In laboratory experiments with inductively stirred melts ($\sim$ 5 cm deep), most of the oxide inclusions float out of the melt in 5 to 10 min; shorter flotation times are even reported for unstirred melts.

(vi) Because of the distortion of the trajectories of approaching particles, the growth by collision and coalescence of ascending inclusions in unstirred or moderately stirred melts is not significant.

These observations are mutually inconsistent. For example, in the absence of growth by collision in essentially stagnant melts, there cannot be large inclusions of 10-40 μm diameter when the total number of nuclei is of the order of $10^8/cm^3$. One possible explanation which Turkdogan has put forward is that the nuclei formed at the time of dissolution of deoxidisers are unevenly distributed in the molten steel. That is, there is a spacial frequency distribution of nuclei in the melt immediately after the addition of deoxidisers. The initial frequency distribution of dispersed nuclei is likely to change from one experimental situation to another. In parts of the melt where the number of nuclei is small, e.g. $10^4/cm^3$ to $10^5/cm^3$, the inclusions 20-40 μm in diameter rapidly float out of the melt prior to the completion of the deoxidation reaction. In regions of the melt containing about 10^8 nuclei/cm^3, the inclusions grow only to a micron size and ascend in the melt very slowly. Convection currents or other means of stirring eventually bring about a more uniform distribution of these small inclusions. The particles brought to the parts of the melt where the deoxidation reaction was incomplete bring about further deoxidation, growth and flotation. The curve in Fig. 2.28 for non-uniform distribution of Z, though drawn

arbitrarily, illustrates the net effect of an uneven distribution of nuclei.

Another interesting aspect of inclusion growth is the formation of alumina clusters. Castings of aluminium-killed steels and samples taken from laboratory melts deoxidised by aluminium sometimes contain relatively large clusters of alumina crystals. Such clusters have been observed by many investigators and a detailed discussion of their formation and flotation is included in the following section on inclusion elimination.

2.3.4 Elimination of Inclusions

The escape of the deoxidation products from the liquid metal is the factor which determines how successful is the removal of oxygen from the metal by the deoxidation procedure. Thus, whilst it is possible to kill the steel and decrease the dissolved oxygen to a very low level, unless the oxides which are formed are able to escape, the steel will have a high total oxygen content and be inherently dirty.

Before 1957, it was generally accepted that the rate of flotation of inclusions was governed by Stokes' law:-

$$R = \frac{2gr^2 (d_1 - d_2)}{9v} \qquad \text{eqn. (2.21)}$$

where R = rising velocity

g = gravitational acceleration

r = radius of inclusion

d_1 = density of liquid metal

d_2 = density of inclusion

v = viscosity of liquid metal

It can be seen that the most important variable is r, the radius of the inclusion, since the rate of rise increases as r^2 when the other factors remain constant. Effective deoxidation has therefore been based on the formation of liquid inclusions which can grow by coalescence and thus escape from the steel more rapidly.

The importance of particle radius was shown by Herty and Fitterer[65], when

they found that silicon-manganese deoxidation gave the cleanest steel if the Mn:Si ratio was between 4 and 7, corresponding to the ratio range which resulted in the largest size of inclusions. The composition of the inclusions resulting from this deoxidation practice was found to be in the very low liquidus temperature range of compositions at approximately 35-45% SiO_2, 45-55% MnO, 10% FeO, leading to the conclusion that low melting point products were advantageous because their fluidity enabled them to coalesce, thus increasing their size and improving their rate of flotation.

In 1957, however, Plöckinger, Rosegger and Wahlster[66,67] showed that, contrary to the ideas of the time, primary inclusions rich in alumina could be eliminated several times more quickly than silicates, and that the size of inclusions was of limited importance. These first results mark the beginning of what Grethen and Phillippe[36] have called the 'Controversy on Stokes' law'.

Figure 2.34 is taken from a later investigation by Plöckinger and Wahlster[32]. Starting with a uniform initial oxygen content and using a constant addition of various deoxidants, the variation in the total oxygen content at various stages between tapping and solidification of the ingot is clearly shown. The differences in behaviour of these deoxidants cannot be explained solely in terms of the different equilibria with oxygen in the liquid metal, inferring that the physical properties of the inclusions must influence their escape.

Thus, the two main questions to be answered are:-

(i) is the elimination of inclusions governed by a hydrodynamic law such as Stokes' law?

(ii) how otherwise can the differences in the rate of elimination of inclusions having different chemical compositions be explained?

Numerous investigations, both theoretical and experimental, have been carried out in an attempt to answer these questions. The effects of turbulence,

deoxidant composition and furnace lining on inclusion removal have been studied. In view of the importance of this stage relative to the success of the overall deoxidation process, and because of the current differences of opinion regarding the applicability of Stokes' law and the influence of melt/oxide interfacial energy, a detailed review of past work is presented in an attempt to clarify the situation.

A great number of authors have stated that in deoxidation by silicon-manganese, fluid deoxidation products are formed, which by their ability to coalesce, are rapidly removed according to Stokes' law. In general, the experimental work has been concentrated on trying to establish a suitable Mn:Si ratio in the melt. According to Korber and Oelsen[14], the conditions necessary for the formation of fluid inclusions at 1520°C are shown in Fig. 2.35. Kulikov and Samarin[68] have stated that the Mn:Si ratio of the silicon-manganese alloy should be 3-8 for liquid manganese silicates to form at 1600°C. As mentioned previously, Herty and Fitterer[65] found in laboratory experiments that the Mn:Si ratio of the deoxidant ought to be 4-7 in order to obtain large fluid silicates.

Determinations on a laboratory scale of the rate of removal of inclusions resulting from silicon-manganese deoxidation are rather scarce, although in recent years some relevant articles have been published in Japan and Sweden. Kawawa et al[69] studied the separation process after additions of 0.3% Si, 0.3% Si + 0.5% Mn, and 0.3% Si + 1.0% Mn at 1600°C. In each case, separation occurred faster during the first 30 s than later and the separation rate in the steel containing the highest manganese addition was considerably greater than for the other two. This was attributed to the fact that the inclusions resulting from the highest addition had a thicker 'rim' of more fluid manganese silicate than those from the 0.5% Mn addition, thus facilitating coalescence and thereby increasing the rate of rise according to Stokes' law.

Tajiri et al[70] have also studied the inclusions formed during silicon-manganese

deoxidation on a laboratory scale and found that for melt Mn:Si ratios less than 1, the inclusions consisted of pure silica, whereas for Mn:Si ratios greater than 2, manganese silicates containing about 40% MnO were formed. For Mn:Si ratios of 1-2, there was a continuous transition of inclusion composition and the inclusion volume, determined 5 min after the addition, increased with increasing silicon content for a constant manganese content. This was attributed to the lower ability of silica-rich inclusions to coalesce and thereby be rapidly removed. For Mn:Si ratios of less than 2, instances of two or more inclusions in the process of coalescence were observed. The contact zones were found to be very rich in silica, whilst the centres of the inclusions were richer in manganese oxide. Scanning electron micrographs[71] of such partially coalescing silicate inclusions are shown in Fig. 2.36. Manganese silicates surrounded by a silica-rich 'rim' have also been observed by Kiessling et al[72] and by Hultgren[73]. These inclusions showed a finely dispersed precipitation of silica in the matrix.

Recently, Grevillius[61] has examined the rate of removal of deoxidation products resulting from manganese-silicon deoxidation of laboratory melts. The added silicon content was 0.45% accompanied by manganese additions between 0 and 14%, and the addition was made by blowing the deoxidant directly into the bath. Both simultaneous and separate additions in both successions were performed.

With simultaneous additions it was found that the separation rate increased with increasing Mn:Si ratio of the deoxidant. This effect was weak in the interval $0 < \text{Mn : Si ratio} < 1.4$ but became very strong in the interval $1.4 < \text{Mn : Si} < 1.9$. Microanalysis showed that the strong increase in separation rate coincided with the break-up of the silica shells surrounding the inclusions at Mn:Si ratios of less than 1.4, and the high viscosity of the silica shell was assumed to be the factor delaying coalescence. At Mn:Si ratios greater than 1.9, the separation rate continued to increase rapidly with increasing manganese content of the deoxidant. This was

attributed to a decrease in the melt viscosity caused by manganese. It was concluded that the rate of removal of the inclusions was dependent both on Stokes' law and on the stirring effect within the bath. When the inclusions were large the first effect was dominant, while the stirring effect alone determined the separation rate when the inclusions were small. The surface conditions were almost the same for all Mn:Si ratios and were assumed not to have contributed to the different separation rates.

When silicon and manganese were added separately with a time interval between them, the same separation rate was reached, independently of the sequence of addition, as with silicon-manganese alloy additions having the same Mn:Si ratio.

Lindon and Billington[74] have examined the formation and separation of oxide inclusions in a quiescent bath using manganese-silicon-aluminium alloys of different compositions. They melted a prepared iron-oxygen alloy containing 0.045 to 0.055% oxygen in an alumina crucible and deoxidised at 1550°C by plunging a thin steel cartridge containing the alloy below the melt surface. An inert atmosphere was maintained by passing a continuous stream of argon over the melt. The silicon addition was kept constant at about 0.29% and accompanied by manganese between 0.25 and 0.95% and aluminium between 0.002 and 0.036%. They found that the separation rate increased with increasing Mn:Si and Al:Si ratio of the deoxidiser. In the experiments with a low rate of removal, inclusions rich in silica were found and it was evident that the coalescence of such inclusions was delayed because of a higher viscosity. It was also concluded that in a well deoxidised, quiescent bath, the flotation rate of alumina is approximately described by Stokes' law. However, fluid manganese alumino-silicate deoxidation products separate more slowly than predicted by Stokes' law and this retardation appears to be associated with a low interfacial energy between the product and the melt.

Anderson[75,76] has studied the rate of separation of inclusions produced by manganese-silicon-aluminium complex deoxidation on a laboratory scale. The apparatus employed was the same as that used by Grevillius[61]. The silicon addition

was maintained constant at 0.45% whilst the silicon and aluminium contents were varied between the limits 0-15% and 0.02-0.18% respectively. The separation rate was influenced by both the Mn:Si and Al:Si ratio of the deoxidant. For Al:Si ratios of 0.05 and 0.10, there was a rapid increase in the rate of removal as the Mn:Si ratio was increased from 1.0 to 1.8. This was attributed to a decrease in the viscosity of the inclusions which facilitated coalescence. The separation rates for Mn:Si ratios greater than 1.8 were approximately the same as those for normal silicon-manganese deoxidation. The surface energy conditions were almost constant at these Al:Si ratios and it was therefore assumed that they did not affect the separation rate.

For an Al:Si ratio of 0.20, a further increase in the rate of removal was observed for Mn:Si ratios in the range 0-1.8. This increase was caused by the formation of clusters of alumina-rich inclusions in addition to the spherical complex oxides. These clusters escaped very rapidly. For Mn:Si ratios greater than 1.8, the separation rates were the same as those at Al:Si ratios of 0.05 and 0.10.

At an Mn:Si ratio of 1.75 and when varying the Al:Si ratios between 0.05 and 0.41, an increase in separation rate was evident up to an Al:Si ratio of 0.20. At higher ratios, however, it was unaffected.

The separation process was studied for different inclusion volumes to be removed. The separation rate in the initial period increased with increasing initial inclusion volume, presumably caused by more favourable collision conditions. When an oxygen level of 100-200 ppm was reached, however, the rate of removal was determined by the amount of stirring.

Kawai and Kobayashi[77] applied Stokes' law to silica particles of a given size distribution in static and agitated baths. They found that the rising velocity of inclusions in agitated baths was faster than predicted by Stokes' law and attributed this to the coalescence of particles which increased their size, whilst the particles in the static bath obeyed Stokes' law.

Fischer[78] described a kinetic study of deoxidation with silicon in high frequency induction furnaces, which also showed that separation of primary deoxidation products was very much more rapid in turbulent conditions than in quiescent ones. This effect of turbulence has also been observed by many other workers including Plöckinger and Rosegger[66], and Duderstadt and Weller[79], who used aluminium and other deoxidants to confirm the effects found with silicon. Fischer reported from the same work that primary silica products were separated very rapidly in basic lined furnaces (CaO or $CaO-CaF_2$) but only slowly with acid linings. Further observations were that the time for total elimination of products decreased with increasing melt temperature, decreasing silicon addition, and decreasing furnace size which increased the surface area to volume ratio.

Imai[80] reported that stirring a melt of low carbon killed steel together with a synthetic slag in a ladle by means of a rotating propeller resulted in a cleaner steel. The total oxygen content decreased from 75 ppm to 30 ppm in 5 min. Increasing the stirring rate apparently caused a more rapid decrease in total oxygen although no figures were quoted in this case. For melts which were not stirred, the inclusions present in the finished product were calcium aluminates of 50-100 μm diameter resulting from furnace slag entrained in the metal during tapping. For casts which were treated with a synthetic slag and stirred in the ladle, the inclusions in the product were about 10 μm in diameter and consisted of alumina particles with only very small amounts of lime. It was concluded that the turbulence accelerated the removal of the large $CaO-Al_2O_3$ inclusions by the synthetic slag and by the ladle lining.

The importance of stirring for accelerating metallurgical reactions in steel melts was also discussed by Linder[81]. A short account was given of the theoretical background of turbulent flow occurring during stirring and of the effects on homogenisation and inclusion removal.

Ohkubo et al[82,83] proposed a model to explain the effects of turbulence and of furnace lining material on the rate of removal of inclusions. The deoxidation

experiments were carried out in a high frequency induction furnace using various temperatures, deoxidisers and furnace linings[82]. They found that the oxide content of the steel could be expressed as a function of time by the equation:-

$$C = C_o e^{-kt} \qquad \text{eqn. (2.22)}$$

where C is the oxide concentration at a time t following deoxidation at t = 0, C_o is a constant and corresponds to the maximum oxide concentration, i.e. the concentration after the addition of deoxidiser but before any products have separated and k is the rate constant which depends upon temperature, deoxidiser, and crucible material. The surface area:volume ratio of the melt was included as a factor influencing k[88].

The model of Ohkubo et al appears to assume that removal of deoxidation products by flotation, according to Stokes' law, is completely absent and proposes that the mechanism of inclusion removal in an agitated bath is essentially one of reaction between the particle and crucible material. According to Lindon[6], this model is very reasonable provided that the turbulence is sufficient to present a melt surface in contact with the crucible which is continually changing and representative of the oxide concentration in the bulk melt. Under these conditions, it is likely that an equation of the form shown below would apply:-

$$\frac{dc}{dt} = -k.C.\frac{A}{V} \qquad \text{eqn. (2.23)}$$

where $\frac{dc}{dt}$ is the rate of change of oxide concentration, C is the average oxide concentration of the bulk melt, k is the rate constant and A/V is the surface area:volume ratio of the melt. Upon integration between limits of $c = C_o$ at t = 0 and c = C at t = t, this would give equation (2.22).

The increase in separation rate of SiO_2 in a basic-lined furnace was confirmed and attributed to chemical reaction between particle and furnace lining. Removal of silica by an acid lining would not involve chemical reaction and would depend only on surface action between particle and lining. The lowering of the separation rate by increased silicon addition was also confirmed, and can be explained by the fact that

the residual dissolved oxygen after low silicon additions was approximately 0.09%. The deoxidation product, therefore, would have been a liquid iron silicate which could react with, and adhere to, a siliceous lining to a greater extent than could solid silica products resulting from higher silicon additions. Rate constants determined after manganese-silicon deoxidation were greater than those determined for silicon alone, and similarly the rate constant for alumina separation was improved by the addition of manganese.

Lindskog[84] has carried out laboratory and full scale industrial experiments to study the removal of inclusions in a stirred melt. The deoxidisers, aluminium and silicon, were marked with the radioactive isotopes zirconium-97 and silicon-31 respectively. By measuring the radioactivity in the slag and on the lining after complete separation of the deoxidation products, it was shown that the inclusions were removed mainly by adsorption on the lining and not by elimination into the slag. Figures 2.37 and 2.38 show the amount of SiO_2 on different parts of the crucible wall after deoxidation of 500 g pure iron with 0.5% radioactive silicon in a high frequency furnace. It can be seen from Fig. 2.37 that 85% of the SiO_2 inclusions was found on the wall of the silica crucible and 15% in the slag. For an alumina crucible, 90% of the SiO_2 inclusions was found on the wall and 10% in the slag, Fig. 2.38.

Industrial experiments using aluminium mixed with radioactive zirconium were also carried out in a 140 t ASEA-SKF ladle unit fitted with two straight stirrers. Slag and metal samples were taken at short intervals during the 30 min treatment. The radioactivity in these samples was measured and this showed that the slag samples were almost inactive, indicating that very few deoxidation products were present in the slag. After the steel had been teemed from the ladle furnace, the activity on different parts of the lining was measured. This was a maximum at about the 1 m level and rather low at the slag-line (2.5 m level), which was in agreement with the

low activities found in the slag samples. The results showed, therefore, that the majority of deoxidation products were removed by the lining and not by the slag. The flow pattern was also found to influence greatly the removal process.

Kjellberg[85] has studied the removal of inclusions after deoxidation with aluminium and rare earth metals (Ce, La, Nd and Pr) in a small high frequency furnace. It was found that with the intensive induction stirring, La_2O_3 and Nd_2O_3 inclusions were removed more rapidly than Al_2O_3 particles. Microscopic examination indicated that the crucible wall was involved in the deoxidation process, although the mechanism and extent of this were not determined.

It should be noted at this point that inclusion removal by adsorption on the furnace lining is particularly suited to the experimental conditions of the high frequency induction furnace and the ASEA-SKF ladle unit, i.e. high rate of metal circulation as well as high ratio of wall area:bath volume.

Torssell, Gatellier and Olette[45] showed that stirring within a certain intensity range promoted the removal of inclusions, as shown in Fig. 2.39 which refers to deoxidation by silicon, aluminium and titanium in laboratory crucibles. The fact that stirring is a valuable means of eliminating inclusions has now been confirmed in many industrial trials and is also in line with the known improvement in steel cleanness associated with the turbulence created during decarburisation, electro-magnetic stirring, stirring with argon or another inert gas and, of course, vacuum degassing.

As previously mentioned, Plöckinger and Wahlster[67] made a series of experiments in high frequency induction furnaces and found that solid alumina particles separated from the melt more rapidly than fluid silicate inclusions. Holding the melt quiescent in a ladle after deoxidation resulted in further separation of silica particles, but very little further decrease in residual alumina was observed, all the separable particles having been removed in the initial period. They concluded from the difference in inclusion behaviour that Stokes' law is not entirely valid when comparing inclusion types and that the major reason for this is the difference in surface properties.

They suggested that wetting of the silica, and silica-rich particles, by the steel hinders their separation, whereas alumina particles having a high surface energy are not wetted and are therefore unaffected by the melt/oxide interface properties.

Koenitzer and Hammer[86] have also pointed out that liquid products, in spite of their ability to increase their size by coalescence, do not escape as quickly and completely as some solid products, e.g. alumina, the reason given again being the high interfacial energy of solid alumina particles with steel as against silicates with steel.

Lindon and Billington[87] have studied the deoxidation of steel at 1550°C by complex deoxidants (Ca-Si-Al and Mg-Si-Al) and made comparison with deoxidation by silicon, aluminium and silicon-aluminium alloys. It was concluded that in a quiescent bath, product separation rates increase as the interfacial energy between inclusions and the melt increases, thus confirming Plöckinger's results and supporting his theory of the influence of surface properties on inclusion removal.

Knüppel, Brotzmann and Förster[58] have suggested that with the rising of oxide particles in liquid steel, there exist a lifting force and a flow resistance which are opposing each other. The lift depends on the difference in density between the steel and the oxide particles, and the flow resistance on the shape and size of the particles and the viscosity of the steel. The type of boundary surface energy between steel and particles, whether wettable or not, affects the rising rate only indirectly via the formation of agglomerates or clusters of oxide particles. For the individual particles, the movement process through the liquid steel is approximately the same on wetting and on non-wetting.

The small wettability of alumina particles by liquid steel is considered by many workers to be a predominant factor in the rapid removal of these particles. However, according to Plöckinger and Wahlster[88], the favourable boundary surface properties of alumina no longer apply to the elimination process if the particles are below certain 'critical' sizes. This size factor possibly accounts for the observation

that residual alumina particles are reluctant to separate from a quiescent bath. In this case, the only alternative mode of separation is by coagulation, and this can occur if the melting point of the alumina inclusions is appreciably lowered. Previous studies have shown that even with normal aluminium deoxidation, a considerable degree of coalescence or agglomeration of the alumina inclusions is experienced, but that this is confined to a very short time interval immediately after the addition of the aluminium to the steel melt. In order to obtain a liquid phase for a longer period of time after the aluminium addition, an appreciable lowering of the melting point of the deoxidation products can be achieved by the addition of fluxes, enabling the inclusions to coalesce or agglomerate over a longer period of time. In so doing, however, the favourable surface properties of the alumina particles, i.e. small wettability by liquid steel, must not be influenced adversely to any appreciable extent.

Very little is published regarding the use of fluxes for lowering the melting point to accelerate the separation of alumina inclusions by means of coagulation. Speith, Ende and Seelisch[89] found during study of inclusion separation in casting runners, that by adding ground fluorspar to the casting trough during the casting of aluminium-killed heats, the chemical composition of the separated products in the casting runners changed, and their melting points were considerably lowered. In addition, Bailey, Onuscheck and Turfa[90] reported that the number of alumina agglomerates directly under the ingot skin was lowered by the addition of fluoride-containing fluxes during the casting.

Choudhury and Wahlster[91] studied the effect of fluorspar (CaF_2) and cryolite ($3NaF.AlF_3$) on the separation in the ladle of the inclusions formed during aluminium deoxidation. From the Al_2O_3-CaF_2 equilibrium diagram, Fig. 2.40, it is apparent that the melting point of Al_2O_3 can be lowered to a eutectic temperature of 1270°C by the addition of CaF_2. From the $3NaF.AlF_3$-Al_2O_3 equilibrium diagram, Fig. 2.41,

it is apparent that at the eutectic composition of 18% Al_2O_3 and 82% $3NaF.AlF_3$, the melting point of the mixture is lowered to 935°C. In the Al_2O_3-CaF_2-$3NaF.AlF_3$ ternary system, Fig. 2.42, the eutectic temperature is lowered even further to 867°C.

Choudhury et al found that the average oxide content of the sheet product was lowered by deoxidation with aluminium/fluorspar and aluminium/cryolite mixtures, compared with straight aluminium deoxidation. The ductility properties were also improved. It was assumed that this was a result of the fluorspar and cryolite influencing the coalescing of the alumina inclusions. A direct proof of this was not obtained, however, because the basic elements of the fluxes could not be detected by the microanalyser.

The comparatively recent development of solid electrolyte cells for determining dissolved oxygen has shown that these are extremely valuable aids for understanding the deoxidation process. Moreover, by taking samples and analysing the steel for oxygen using vacuum fusion and neutron activation techniques, it is possible to monitor the total oxygen content of the bath. Consequently, the difference in these two values enables the amount of oxygen in the form of inclusions in suspension in the bath to be determined and the variation of this parameter with time to be followed.

Gatellier, Torssell and Olette[45,92] have applied this technique to the deoxidation of steel with various elements, e.g. silicon, aluminium and titanium. Figure 2.43 shows the results of an experiment on deoxidation with silicon at 1600°C. It can be seen that the dissolved oxygen content falls very rapidly, and nucleation and growth of inclusions in these operating conditions appears to occur within 5 s (and probably much sooner). The inclusions themselves disappear completely in the test conditions within about 10 min and after this time, all the residual oxygen, i.e. 0.010% which corresponds to equilibrium, is present in the form of dissolved oxygen. A proportion of this oxygen will precipitate during cooling and the remainder during solidification. The resulting inclusions will have difficulty in floating out as previously mentioned.

Figure 2.44 shows a similar test using aluminium. In this case too, most of the oxygen is reacted with the aluminium within a few seconds. The apparently slower reaction process compared to silicon deoxidation arises from the difficulty in dissolving an added fragment of aluminium owing to the increase in bath viscosity with alumina precipitation. It is again evident that most of the alumina inclusions floated out within the first 10 min. However, very small particles remained in suspension in the bath for a long period.

On the basis of the preceding discussion, the indications are that the answer to the first question, as to whether the elimination of inclusions is governed by a hydrodynamic low such as Stokes' law, is negative as far as practical steelmaking is concerned. It is not true to say, as some investigators have, that Stokes' law never has any relevance to steelmaking, because it is applicable under the conditions for which it was derived. However, it is certainly not correct to expect it to predict inclusion elimination when convection currents exist, particularly for smaller inclusions (less than about 20 μm), the movement of which is probably governed more by the fluid velocity than by buoyancy effects. With increasing inclusion size, the effects of buoyancy will probably become more dominant, however.

In the case of the second question, the hypothesis most generally advanced to explain the differences observed in the rate of removal of inclusions having different chemical compositions is the effect of interfacial phenomena. However, opinions differ widely as to the mechanism by which such phenomena are effective. The possibilities are:-

(a) by their direct effect on flotation

(b) by their effect on growth

(c) by their effect on emergence and adsorption

Although the relative importance of the first effect has not been extensively investigated, the small amount of experimental evidence which is available indicates

that it is unimportant, i.e. variation in the steel/inclusion interfacial energy has little effect on movement of the inclusion within the liquid steel. However, the assimilation of inclusions when they impinge upon a collecting surface, e.g. slag, refractory lining, depends very much on surface energy effects, as apparently does the growth and formation of inclusion clusters.

The role of surface phenomena in the mechanism of removal of solid inclusions and the formation of inclusion clusters in liquid steel has been studied in detail by Kozakevitch, Lucas, Torssell and Olette[34,45,92,93]. According to these investigators, the rate at which solid inclusions are removed from a liquid metal bath is the overall result of several processes, and some of these depend on surface phenomena at the various inclusion/metal/slag interfaces.

Considering the escape of solid inclusions at a metal/gas interface, an inclusion of microscopic dimensions approaching the surface of the liquid metal may either remain just below the surface of the metal without escaping (the inclusion is thoroughly wetted by the metal) or escape and float on the surface (no wetting). In the former case, the inclusion may easily be re-entrained into the metal by a descending current. In the case of complete escape, this entrainment seems much less probable.

Emergence of the inclusion can take place spontaneously only if it leads to a reduction in the surface free energy, G, of the system, i.e. $\Delta G < 0$. The free energy change, ΔG, is given by:-

$$\Delta G = \gamma_s - \gamma_m - \gamma_{sm} \qquad \text{eqn. (2.24)}$$

where γ_s is the surface energy of the solid oxide, γ_m is that of the liquid metal, and γ_{sm} the interfacial energy at the inclusion/metal interface. In other words, a new solid/gas surface is formed and a metal/gas and metal/solid surface disappear. It follows that $\Delta G < 0$ when $\gamma_{sm} > \gamma_s - \gamma_m$. The escape of a solid inclusion is thus promoted by:-

(a) a high interfacial energy, γ_{sm}

(b) a low surface energy of the solid oxide, γ_s

(c) a high surface energy of the liquid metal, γ_m

The surface energies of solid oxides of practical interest appear to be always lower than those of iron or steels with low oxygen and sulphur contents. Thus, ΔG will normally be negative. However, the numerical value of ΔG and, therefore, the practical tendency towards emergence can vary greatly from one case to another.

It should be noted that ΔG is identical with the spreading coefficient, S[94]. It might also be said that emergence can occur when the adhesion energy of the liquid metal relative to the material of the inclusion, $W_A = \gamma_s + \gamma_m - \gamma_{sm}$, is lower than the cohesion energy of the liquid metal, $W_C = 2\gamma_m$. The difference, $W_A - W_C$, is identical with the expression given for ΔG in equation (2.24).

Among the values which enter the base equation (2.24), only γ_m can be measured directly. For γ_s, the surface energy of different substances forming solid inclusions, it is possible only to make some estimations based on the surface energy of the same materials in the liquid state. According to measurements on solid metals using the zero creep method of Hondros and McLean[95], the surface energy of metals in the solid state is 0.1 - 0.3 J/m^2 (100 - 300 erg/cm^2) higher than that of the corresponding liquid. By adopting this rule, somewhat arbitrarily, the values of γ_s applicable to oxides can be obtained providing their surface energy in the liquid state is known. Unfortunately, the only data available refer to Al_2O_3 (0.69 J/m^2), 'FeO' (0.585 J/m^2) in equilibrium with solid iron at 1450°C, SiO_2 (0.307 J/m^2) and some silicates, e.g. $CaO.MgO.2SiO_2$ (0.5 J/m^2).

Knowing γ_s and γ_m, it is possible to calculate γ_{sm} quite easily by measuring the contact angle, θ, relating to a droplet of liquid metal on a solid oxide support, Fig. 2.45. The equilibrium of the surface forces involved can be written as:-

$$\gamma_s - \gamma_m \cos\theta - \gamma_{sm} = 0 \qquad \text{eqn. (2.25)}$$

Combining equations (2.24) and (2.25) gives:-

$$\Delta G = \gamma_m (\cos \theta - 1) \quad .. \quad .. \quad .. \quad .. \quad .. \quad \text{eqn. (2.26)}$$

This latter equation, although of limited validity, makes it possible to predict the tendency of inclusions to emerge when γ_m and θ are known. The condition $\theta = 0°$, which prohibits any formation of a new inclusion/gas interface, corresponds to the condition $\gamma_{sm} = \gamma_s - \gamma_m$. It gives the maximum value of γ_{sm} where there is complete wetting. The condition $\theta = 90°$ corresponds to $\gamma_s = \gamma_{sm}$ and $\theta = 180°$ corresponds to $\gamma_{sm} = \gamma_s + \gamma_m$ and $\Delta G = -2\gamma_m$.

The above calculation makes use of a vectorial model, Fig. 2.45, and is therefore valid only for the range $0° \leq \theta \leq 180°$, i.e. in the range $\gamma_s - \gamma_m \leq \gamma_{sm} \leq \gamma_s + \gamma_m$. Cases where $\gamma_{sm} < \gamma_s - \gamma_m$, which cannot be covered by the contact angle method, are frequent in solid + liquid + gas systems where there is good wetting, but not in metal + inclusion systems. On the other hand, cases where $\gamma_{sm} > \gamma_s + \gamma_m$, which also cannot be covered by the contact angle method, do not occur in solid + liquid + gas systems, and the limiting condition $\gamma_{sm} = \gamma_s + \gamma_m$, i.e. $\theta = 180°$ is never attained in practice as the angles measured are always less than 180°. However, this limit is frequently exceeded in systems composed of a solid and two imiscible liquids as, for instance, inclusion + metal + slag systems.

The contact angle, θ, for several systems of practical interest is shown in Table 2.3. The values of ΔG can be estimated* from this data using equation (2.26).

Using the above equations, Kozakevitch et al[93] examined the emergence of alumina inclusions and concluded that:-

(i) the tendency of pure alumina inclusions to emerge at the surface of pure iron and carbon steels is very pronounced, even in the presence of normal amounts of sulphur, Table 2.4.

---

* When an inclusion emerges at the surface of the bath, the metal leaves the surface of the inclusion. It is, therefore, the contact angle known as the 'receding angle' which must be used. Unfortunately, the available experimental results usually refer to advancing angles so that the calculation is less precise.

(ii) Reoxidation of the metal by the surrounding atmosphere may well hinder the emergence of inclusions, Table 2.4.

The reasoning outlined for the emergence of inclusions at a metal/gas interface is equally valid for the metal surface covered by slag, the solid/slag interfacial energy, γ_{sl}, then replacing γ_s and the metal/slag interfacial energy, γ_{ml}, taking the place of γ_m. The basic equation then becomes:-

$$\Delta G = \gamma_{sl} - \gamma_{ml} - \gamma_{sm} \quad .. \quad .. \quad .. \quad .. \quad \text{eqn. (2.27)}$$

The interfacial energy between the solid inclusion and the liquid slag, γ_{sl}, is not measured directly and must be calculated using the slag/inclusion contact angle by means of estimations based on γ_s. The contact angle formed by a slag in contact with the surface of a solid oxide is always acute, even when there is no reaction between the oxide and the slag. For example, θ is about 20° for the interface between alumina and a silicate slag droplet saturated with Al_2O_3. Assuming an average value for the surface energy of the liquid slag, γ_l, of 0.5 J/m^2 (500 erg/cm^2) this gives $\gamma_{sl} = \gamma_s - \gamma_l \cos\theta$ = 0.43 J/m^2 (430 erg/cm^2). When the surface of the alumina is attacked by the slag, the interfacial energy**, γ_{sl}, tends towards zero. Values of γ_{sl} will therefore almost always be less than those of γ_s quoted previously. The effect of a covering slag is, in this sense, always beneficial and is all the more so when solution takes place.

The metal/slag interfacial energy, γ_{ml}, can be measured directly. In general, for two liquids which cannot be mixed at all or which mix only slightly and which are in equilibrium with each other, it is frequently found that $\gamma_m > \gamma_{ml} > \gamma_m - \gamma_l$, the case of $\gamma_{ml} = \gamma_m - \gamma_l$ being the limiting condition of spread of the light liquid (slag) on the heavy liquid (metal). However, γ_{ml} can be less than $\gamma_m - \gamma_l$, for instance, when a double ionic layer is formed at the interface of the two liquids. The repulsion of the like charges constituting the double layer in each of the two elementary layers greatly

---

** Dynamic interfacial energy, i.e. in a state of non-equilibrium

reduces the interfacial tension as appears to be the case in practice, particularly at a metal/slag interface.

Values of γ_m, γ_l and γ_{ml} are given in Table 2.5[93]. It can be seen that the spreading coefficient, S, of the slag on the liquid metal is positive in some cases. The values of γ_{ml} being lower than those of γ_m, it may be concluded that a covering slag adversely affects this term, particularly when a double ionic layer is formed at the interface as is most frequently the case. In practice, however, the beneficial influence of γ_{sl} is greater than the adverse effect of γ_{ml}. Consider, for example, the escape of a pure alumina inclusion at the interface between pure iron and a covering slag consisting of $CaO + Al_2O_3 + SiO_2 + 20\% CaF_2$, Table 2.5. This slag is a good solvent for alumina at 1600°C and the interfacial energy, γ_{sl}, therefore tends towards zero. The values of γ_{ml} and γ_{sm} are 1.205 J/m^2 (1205 erg/cm^2) and 2.279 J/m^2 (2279 erg/cm^2) respectively. Substituting these values in equation (2.27) gives $\Delta G = -3.484$ J/m^2 (-3484 erg/cm^2). For the escape of an alumina inclusion at a pure iron/gas interface, $\Delta G = -3.179$ J/m^2 (-3179 erg/cm^2), Table 2.4. With the covering slag, therefore, the reduction in surface free energy for the escape of an alumina inclusion is 0.305 J/m^2 (305 erg/cm^2) greater than without the slag. It can be seen that in this case, $\gamma_{sm} > \gamma_{ml} + \gamma_{sl}$ and, as previously discussed, direct calculation of ΔG using the contact angle method is therefore not possible.

The concepts outlined above refer to an ideal situation, revealing only the tendency of inclusions to emerge as a result of surface phenomena. Kozakevitch et al have suggested, however, that in the case of small inclusions up to several microns in diameter, the conclusions based on this simple model might well be sufficiently close to reality.

Cosma[96] has calculated the effects of surface phenomena on the removal of alumina and silica inclusions in austenitic stainless steel alloyed with nitrogen. The steel composition was 0.05% C, 0.61% Si, 9.25% Mn, 4.75% Ni, 18.21% Cr and the nitrogen content was varied between 0.03% and 0.27% giving the steel types A-D in

Table 2.6. Contact angles and surface energies were measured using the sessile drop method. It was concluded, on the basis of the results shown in Table 2.6, that inclusion removal in terms of surface energy phenomena is rendered more difficult by the presence of nitrogen, which varying within relatively small limits, lowers both the steel/inclusion interfacial energy and the surface energy of the steel.

Cosma also considered the emergence of the inclusions when there was a slag layer present at the melt surface. The results obtained are shown in Table 2.7 from which it can be seen that there is a more pronounced tendency for the inclusions to escape, as well as a difference in the capacity of the various slags to adsorb inclusions. It can also be seen that because of a high value of γ_{sm}, alumina inclusions will tend to escape from the steel into all the slags except slag no. 9, whereas SiO_2 inclusions, having a low value of γ_{sm}, will only do so for about half of the experimental slags.

Iyengar and Philbrook[97] developed a mathematical model to predict the growth and elimination of inclusions in liquid steel stirred by natural convection. The model was based on the hypothesis that the motion of inclusions is influenced by the fluid flow resulting from natural convection. Only when the fluid flow is negligible can a modified Stokes' law be applied to predict the rate of removal of inclusions. It was shown that the rate is dependent upon the growth rate of inclusions, the intensity of stirring in the liquid steel and the efficiency with which an inclusion can be assimilated by a bounding surface. Of particular interest was the fact that the model explained that some large inclusions can remain in the liquid steel because of a low efficiency of assimilation caused either by a small residence time at the collecting surface or by insufficient surface energy being released during the assimilation process. This indicates, therefore, that surface phenomena may also be important for the removal of large inclusions as well as for small ones.

Kozakevitch et al also examined the formation of inclusion agglomerates in terms of the variation in surface free energy, ΔG. As discussed previously, they

studied the deoxidation of iron by aluminium at 1600°C, Fig. 2.44. Observation of the size distribution of the particles formed during this experiment and its variation with time proved to be extremely interesting. As Fig. 2.46 shows, the size of these particles (3-4 μm) changed very little with time. The application of Stokes' law to these inclusions showed a rate of rise of only 20 mm/h, which would certainly not produce almost complete removal of these inclusions in 10 min as was observed. However, optical examination showed that instead of being relatively well distributed throughout the sample, the inclusions tended to gather together in clusters. The size of these clusters was usually between 50 and 200 μm, although much larger ones up to 3 mm have also been observed. By successive polishing, it was shown that the alumina particles in the clusters were all in contact, pair by pair, and formed a three-dimensional unit. This contact was not apparent when the clusters were observed on a two-dimensional micrograph. This clustering effect has since been observed by many workers using the scanning electron microscope, as in Fig. 2.47 which shows a cluster of alumina particles[98].

Knüppel, Brotzmann and Förster[58] were the first to publish a clearly formulated theory regarding the maintenance of inclusion agglomerates. According to these workers, two alumina particles which collide by chance in the molten steel can stick to each other without having to coalesce in any way at the point of contact. This process takes place on the impact of two particles, assumed for calculation purposes to be of the same spherical size, in which the steel can draw back from the gap which occurs between the spheres at the point of contact, Fig. 2.48. As a result of this, the total steel/oxide boundary surface is reduced over the two spheres. If this reduction in surface area is ΔA, then the energy released, ΔE_γ, is given by:-

$$\Delta E_\gamma = \gamma_{sm} \Delta A \qquad \text{eqn. (2.28)}$$

where γ_{sm} is the surface energy of the steel/inclusion interface.

The movement of the surface of the steel must occur against the external pressure, which consists of the ferrostatic pressure, p_f, and the pressure at the melt

surface, p_a, with a residual pressure, p_r, inside the gap promoting the movement. The energy necessary to form the gap is then given by:-

$$\Delta E_p = \Delta V\ (p_f + p_a - p_r) \qquad \text{eqn. (2.29)}$$

where ΔV is the volume of the gap. If $\Delta E_\gamma > \Delta E_p$, then the steel may spontaneously draw back from the gap in the manner described and form a tube-like skin between the two alumina spheres, which presses the spheres tightly together. Other values being equal, the melt/oxide interfacial energy is the predominant factor in deciding whether the two inclusions adhere or not. Thus, the high interfacial energy between liquid steel and alumina favours agglomerate formation.

Kozakevitch et al[93] extended the mechanism proposed by Knüppel et al by stating the conditions necessary for such contacts to occur spontaneously. It is not easy to define on a molecular scale what constitutes contact between two solid surfaces of microscopic dimensions which are not strictly flat. Assuming that it is a question of one or more very small projections or points situated on a surface element which is approximately flat, contact between these points and a surface element of an adjacent inclusion is improbable if the material forming these inclusions is wetted by the metal (contact angle $\theta = 0°$) with a very fine film of liquid still 'sticking' to each of the two surfaces which should come into contact. This extreme case never happens, however, in metal + inclusion systems. If the adhesion forces between the metal and the inclusions are only slight, a small input of external energy would be sufficient to allow some points to 'touch' a surface element of the adjacent inclusion. At this moment, the two small surface elements of two adjacent inclusions would be a very short distance apart. The very thin layer of metal separating the elements will only be able to withdraw spontaneously if the variation in the surface free energy of this process is negative. The process consists of the disappearance of two metal/inclusion interface elements and the formation of two inclusion/void interface elements. The change in surface free energy ΔG is given by:-

$$\Delta G = 2(\gamma_s - \gamma_{sm}) \qquad \text{eqn. (2.30)}$$

and ΔG is negative when $\gamma_{sm} > \gamma_s$, i.e. 'contact' between two approximately flat elements may be spontaneously established only when $\gamma_{sm} > \gamma_s$. It is conceivable that even the establishment of contact between one point and the surface element of another inclusion is subject to the same mechanism of metal withdrawal. Certainly, an increased input of kinetic energy (vigorous stirring) should allow contact to be established between points on adjacent elements even when $\gamma_{sm} < \gamma_s$, but in this case the metal could not withdraw spontaneously from the points which have come into contact. The condition of $\Delta G < 0$ is thus of critical importance for the initial stage of agglomerate formation, and thus makes it possible to classify all (inclusion + metal bath) systems into two groups: one group in which agglomerate formation is, in principle, possible, and another group in which this process is thermodynamically improbable. By combining equations (2.25) and (2.30), equation (2.31) is obtained:-

$$\Delta G = 2\gamma_m \cos\theta \qquad \text{eqn. (2.31)}$$

It follows that agglomerate formation is probable when $\theta > 90°C$ but not probable when $\theta < 90°C$, thus highlighting the importance of experimental determination of the contact angle.

Consider, for example, Al_2O_3 and TiO_2 inclusions. In the case of a bath of pure iron, $\gamma_m = 1.8$ J/m^2 (1800 erg/cm^2), $\theta = 140°$ for Al_2O_3 and 72° or 84° for TiO_2 (Table 2.3). Consequently, $\Delta G = -2.758$ J/m^2 (-2758 erg/cm^2) for Al_2O_3 inclusions and $\Delta G = +1.112$ J/m^2 (+1112 erg/cm^2) or +0.378 J/m^2 (+378 erg/cm^2) for TiO_2 inclusions. It follows from this that agglomerate formation is very probable in the case of Al_2O_3 but not very probable for TiO_2, and this is in general agreement with the experimental data.

The coagulation of solid particles has also been studied by Baptizmanskii, Bakhman and Dmishreiv[99]. In particular, these authors calculated the effect of the angle of contact between steel and inclusion, the radius of the particles and the ferrostatic pressure on the strength of agglomeration. As predicted by Kozakevitch et al, the strength of agglomeration increased with increasing contact angle, increasing

particle radius and decreasing ferrostatic pressure, Fig. 2.49.

Another interesting aspect of alumina clusters is the formation of dendritic alumina particles. For example, Fig. 2.50, is an electron micrograph of a carbon replica of alumina dendrites found by Torssell and Olette[100]. Figure 2.51 is a scanning electron micrograph of dendritic alumina clusters in as-cast steel taken from the work of Rege, Szekeres and Forgeng[101]. The dendrites appear to have grown from a single nucleus. Similarly, Fig. 2.52 also shows dendritic alumina crystals[98].

Turkdogan has stated that although the gross dimensions of the clusters are relatively large, they do not seem to float out of the melt very readily. Because of their intricate shape, metal entrapped between the dendrite arms increases the overall density of the cluster such that its rate of rise is markedly decreased. This effect is possibly even more marked when alumina clusters are present in the ingot during teeming. With relatively low teeming temperatures, solid iron may nucleate on the clusters and prevent them from escaping. They become entrained in the convection currents during cooling and solidification and eventually segregate to the bottom of the ingot.

Kozakevitch et al[93] have considered the application of Stokes' law to the displacement of agglomerates. The latter were considered as relatively large spheres (100-3000 μm) composed of iron and alumina and in Stokes' law, the rate of rise varies with the square of the particle radius. The difference in density is naturally small, but this is apparently compensated for by the size. Figure 2.53 shows how the rate of rise of a cluster varies in accordance with Stokes' law as a function of its diameter for clusters containing 10^2-10^5 inclusions. For example, a cluster of 200 μm diameter containing 10^4 inclusions, or 5% inclusions by volume exhibits a displacement velocity of 50 mm/min. In this particular case, however, the displacement is a result of differences in density and is retarded by frictional forces under these conditions of lamellar flow, i.e. for a Reynolds number lower than 10. Figure 2.53 also shows the

area (shaded) corresponding to the characteristics of the clusters observed in the experiments of Kozakevitch et al. On the left, the diagram is limited by the application of Stokes' law to a single inclusion (f = 1).

According to Kozakevitch, with stirring of the bath, a cluster has evidently more chance of being eliminated because of its larger size compared with a single inclusion, as, in principle, it is sufficient for any single inclusion in the cluster to adhere to the refractory lining or to emerge at the surface of the bath for the entire cluster to remain there.

In concluding this section, the question still to be answered is which of the four elementary stages which have been discussed in the present section (solution, nucleation, growth and flotation) is the most important for the production of clean steel. Certain authors attribute a predominant role to nucleation and growth and have proposed measures to break up persistently high degrees of supersaturation. For many others, chemical equilibrium is quickly attained and it is the elimination stage which remains the most important. From the point of view of the overall deoxidation reaction and freedom from non-metallic inclusions, however, the latter stage must be regarded as the most important.

The considerations discussed so far show that recent advances have been made in our knowledge of the parameters controlling the formation and elimination of non-metallic inclusions during deoxidation. Some of these advances have enabled cleaner steels to be produced on a more consistent basis.

2.4 FORMATION OF INCLUSIONS DURING STEELMAKING

2.4.1 Effect of Process Variables

The type, size and composition of the inclusions in the molten steel changes at various stages during the steelmaking process. Small changes in several different operations during steelmaking may have a marked effect on the inclusions present in the steel. Typical of the important steelmaking variables are the duration of the boil,

the deoxidation practice, the tapping and teeming operations and the composition of refractories. Unfortunately there are only a few investigations reported in the literature dealing with these important factors which govern the occurrence of non-metallic inclusions in the solid steel.

Pickering, Blank, Morgan and Salter[102-104] have made a detailed study of the inclusions present at different stages during the manufacture of steel by basic electric arc and open-hearth processes. Because their work gives important information on the relation between different inclusion types and various steelmaking parameters, and because it forms the background to the investigations reported in this thesis, a detailed review is presented here.

The majority of the investigations were concerned with double slag basic electric arc steelmaking and involved the production of 0.65-0.70% C[103], 1% C-Cr[104] and low carbon 2% Ni-Mo steels. Liquid metal bomb or tube samples were taken at various stages during the steelmaking, tapping and teeming processes in order to determine the nature of the non-metallic inclusions.

(i) Oxidation Period

The inclusions present at melt out, a cold charge being used in all cases, were mainly manganese-aluminium silicates resulting from oxidation of the charge. As the boil progressed during the oxidation period, the Al_2O_3 and MnO contents of the silicates decreased, Figs. 2.54 and 2.55 as the aluminium and manganese were oxidised out of the charge. The most interesting feature of the composition of the silicates was the progressive increase in their CaO content during the boil, Fig. 2.56. Silicon was also oxidised out of the bath, but the SiO_2 content of the silicates did not change appreciably throughout the oxidation period. The reason for this was that the inclusions formed by oxidation probably nucleated on existing inclusions in the bath and were eliminated to the slag by the turbulence during the boil, but this same turbulence also caused slag particles to be mixed into the bath. Thus, the turbulence created by the

boil can account for the increased CaO content of the silicates being produced by the entrainment of slag in the bath. Further confirmation of the role of the slag in forming the inclusions present during the oxidation period was given by the observation that when considerable turbulence was created by charging material, a sample taken immediately afterwards showed large numbers of the highly calcareous slag inclusions. Also, as occasionally happened, when slag had to be removed during the boil, the bath was partially deprived of its slag cover and the metal surface oxidised to produce iron-manganese silicates and these were entrapped in the bath by the turbulence. Consequently, a sample taken immediately after such an intermediate slagging off contained simple iron-manganese silicates, which were free from CaO. A typical average analysis of such inclusions from three separate trials was 38% MnO, 25% FeO, 37% SiO_2 .

Although slag entrapment accounted for an ever-increasing proportion of the inclusions present throughout the boil, there was not a 1:1 correspondence between the composition of the slag and that of the calcareous silicates at the end of the boil. In fact the inclusions were richer in MnO and SiO_2 and less rich in CaO than the slag, and this was explained on the basis that oxidation products tended to nucleate on entrapped slag particles.

The size of the silicate inclusions varied systematically throughout the boil, being largest at the start of the boil when the reaction was most vigorous, and decreasing in size towards the end of the boil when the turbulence was subsiding[103]. Superimposed on this general trend, there was also a marked effect produced by the vigour of the boil, as indicated by the average rate of carbon removal, Fig. 2.57. It can be seen that as the rate of carbon removal increased, so the size of the slag-based silicates increased. This effect cannot increase indefinitely because eventually, with very great turbulence, the particles of slag will be so large that they will separate almost immediately without being detected. Also, with a very turbulent boil, the energy will be sufficient to create the surface area associated with small particles,

and hence the slag will be more effectively emulsified. Consequently, at very rapid rates of carbon removal, smaller particle sizes may again be detected. There was evidence for this in some work carried out on the oxygen injected basic open-hearth (AJAX) process, as shown in Fig. 2.57. At the most rapid rate of carbon removal, smaller silicates were in fact observed, but as the rate of carbon removal decreased towards the end of the boil, the particle size increased and was in agreement with the trend observed for the boil during electric arc steelmaking.

When the initial charge to the furnace contained some chromium, e.g. in a low alloy steel, it was observed that small, individual particles of spinels were formed during the oxidation period. At melt out, the spinels were mainly galaxite, $MnO.Al_2O_3$, formed by oxidation of any aluminium in the charge, but also containing some Cr_2O_3 replacing Al_2O_3. As the oxidation period proceeded, the aluminium and also the manganese in the charge were removed and the composition of the spinels moved rapidly towards that of chromite, $FeO.Cr_2O_3$. At the same time, chromite inclusions were also seen to be associated with silicate inclusions. Two forms were observed, one being a fairly large angular chromite within a silicate containing only a trace of chromium. It was suggested that the silicates coalesced or nucleated around these fairly large spinel particles. The other form consisted of chromite dendrites which had been precipitated within a complex silicate containing about 12-15% Cr_2O_3. In this case, considerable Cr_2O_3 had been dissolved in the silica, yet the solubility of Cr_2O_3 in SiO_2 is very limited[105]. This solubility can, however, be increased by the presence of other oxides in the silicate, the average composition of which was 34% SiO_2, 16% MnO, 11% FeO, 20% CaO, 3% Al_2O_3, 1% MgO, 15% Cr_2O_3, but only at a temperature of about 1800°C[106]. It was suggested by Pickering et al, therefore, that oxygen lancing had caused a locally very high temperature, and in these conditions the silicates had been able to dissolve sufficient Cr_2O_3 to result in the precipitation of chromite dendrites on subsequent cooling.

The evidence that slag-based inclusions were picked up during the oxidation period, whilst being obtained mainly during experiments on electric arc furnaces, was also confirmed during more limited investigations on the oxygen-lanced basic open-hearth process. As shown in Fig. 2.58, there was a progressive increase in the CaO content during the oxidation period. Therefore, whilst it was not suggested that the inclusions present in the bath during the boil would persist and appear in the final product, this obviously not being the case, there was ample evidence to show that the type of inclusions could be closely related to the actual processes occurring during this period of steelmaking.

(ii) Refining Period

At the start of refining, after slag removal and prior to deoxidation, the inclusions present were calcium-manganese silicates persisting from the oxidation period. Silicon deoxidation was effected either by the use of calcium silicide or ferro-silicon The addition of calcium silicide led to a pronounced change in the silicate inclusions, those being produced by deoxidation containing up to 40% Al_2O_3 due to the presence of about 1.5% Al in the calcium silicide, Fig. 2.59. The ferro-manganese added also increased the MnO content of the silicates and dilution effects greatly lowered the CaO and SiO_2 contents of the silicates, even though calcium silicide had been used. The inclusions still contained about 15% CaO, however, due either to the calcium deoxidation or to the nucleation of deoxidation products on small pre-existing slag particles. Providing no further deoxidation alloys were added, the silicate composition gradually reverted to a lower Al_2O_3 and MnO content and a higher CaO and SiO_2 content as the first formed silicates were removed to the slag and were replaced by further silicates formed from oxygen picked up from the hearth, banks and possibly the slag. Any pick-up of slag inclusions would also give rise to calcium-rich silicate inclusions. The effect of small amounts of aluminium in the silicon deoxidation alloy in causing the formation of highly aluminous silicates was clearly established by a number of investigations. That slag also contributed to the silicates was shown by the fact that when

ferro-silicon alone was used for deoxidation, the silicates still contained CaO, Fig. 2.60. They also contained appreciable Al_2O_3 due to the ferro-silicon containing more than 1% Al. However, the CaO content at the end of refining when ferro-silicon had been used was 20-25%, compared with almost 50% when calcium silicide was used, and it seems therefore that some CaO was being introduced into the silicates from the calcium-bearing deoxidant.

Another feature observed was the gradual increase in the Al_2O_3 content of the silicates if additions of the aluminium-bearing silicon deoxidation alloy were made progressively throughout the refining period, in order to bring the steel to specification, Fig. 2.61. If such an addition was made immediately prior to tapping, the alumina content of the silicates increased sharply even though immediately prior to the addition, the Al_2O_3 content of the silicates was less than 2%. It was shown that some of the CaO in these silicates, which were primarily deoxidation products, originated from the slag even though the bath was relatively quiescent. This will be discussed later, but Pickering et al did suggest that general turbulence near the arcs could be responsible for some admixture of slag and metal.

According to Pickering et al, the aluminous silicates which also contained CaO, particularly if formed in quantity by a late addition of ferro-silicon or calcium silicide, can be retained in the bath long enough to be tapped into the ladle. Also, they have been found in the final product where they can give rise to problems with respect to quality. These inclusions were often quite large, and they appeared to increase in size with increasing Al_2O_3 content. It was observed that if selected ferro-silicon containing very little aluminium was used for deoxidation, the Al_2O_3 content of the silicates was greatly decreased, as also was their size, and fewer quality problems were encountered. Consequently, it was found beneficial to use silicon deoxidants containing a minimum of aluminium, and to ensure that no such deoxidant was added late in the refining period[103].

Several investigations were made in which ferro-silicon and aluminium were added simultaneously at the start of refining. This gave rise to manganese-aluminium silicates, the compositions of which depended upon the local concentrations of aluminium and silicon. The aluminium and silicon each accomplished its own deoxidation to produce alumina or silicates respectively in regions rich in aluminium or silicon. These two types of inclusion were observed simultaneously in the bath immediately after the joint deoxidation, but such a coexistence was very temporary because circulation within the bath took these primary inclusions into regions of differing deoxidation states. If the alumina particles entered a region rich in silicon, manganese-aluminium silicates were precipitated around them. Alternatively, if the silicates moved into an aluminium environment, reaction occurred to give a silicate rich in Al_2O_3 so that mullite or alumina was precipitated from the alumino-silicate. If such a reaction went to completion, almost all the silicate was converted to an alumina aggregate. In rare circumstances, coalescence occurred between a shower of alumina and silicates, giving rise to very irregular silicates enveloping one or more alumina particles.

The complexity of these reactions resulted in inclusions having a wide range of composition and morphology, but the most important observation was that large amounts of alumina were not formed. Consequently, the rate of deoxidation was decreased because the aluminous silicates were less rapidly eliminated to the slag compared with alumina.

As the aluminium was consumed, the Al_2O_3 content of the silicates decreased throughout refining, Fig. 2.62. The CaO content increased, indicating the role of slag in providing nuclei for deoxidation products, because no calcium-bearing deoxidant was used in this case. The band of results shown in Fig. 2.62 was probably caused by variability in the initial state of oxidation of the bath, and also to variable rates of oxygen pick-up and reaction with aluminium. Because of the dynamic effect of continual removal of inclusions to the slag and the formation of new inclusions from

oxygen pick-up, the Al_2O_3 content of the slag increased throughout refining, Fig. 2.63, and was at a higher level with increasing aluminium used in the deoxidation process.

Other investigations were made in which aluminium deoxidation was carried out prior to the addition of ferro-silicon or calcium silicide. Alumina showers were produced and the average Al_2O_3 content of the inclusions increased sharply to ~80%, Fig. 2.64. The inclusions formed, apart from alumina produced by direct deoxidation, comprised spinels and calcium aluminates, the latter originating from the pre-existing inclusions which reacted with the aluminium addition. Providing an adequate aluminium addition was made, the subsequent addition of silicon-bearing ferro-alloys did not produce any silicate inclusions. A similar series of changes was also observed when ferro-aluminium was used instead of aluminium. Because the alumina thus produced was rapidly eliminated to the slag, and no silicates were formed, a very clean bath was produced. If, however, the initial deoxidation reactions used up most of the aluminium, any oxygen pick-up resulted in silicates being formed. At the same time, calcium-bearing silicates from the slag were also observed. On the other hand, if the aluminium addition was sufficient to leave an adequate cover in the bath, further oxygen pick-up resulted in the formation of more alumina particles, and the slag inclusions reacted to form calcium aluminates and spinels ($MgO.Al_2O_3$). Pickering et al found that, depending upon the amount of aluminium added, the original oxygen content prior to deoxidation, the amount of oxygen pick-up during refining, and the extent of reaction between the aluminium in the bath and the refining slag, then the aluminium cover can persist for various lengths of time. A high oxygen content at the end of the boil, e.g. with a very low carbon content, can cause a very much decreased aluminium cover and necessitate the formation and elimination of a larger volume fraction of alumina, which takes time, and thus the primary deoxidation may be neither uniform nor complete when the ferro-silicon is added.

The presence of an adequate aluminium cover, however, preserved a clean bath, but the effective aluminium content decreased with time during refining, and eventually silicates were formed unless steps were taken to add further aluminium. Some observations on a particular practice indicated that an addition of 0.05% Al preserved an adequate cover for 40-45 min, whilst 0.15% Al increased this time to 85-90 min, the precise effects varying with the particular practice used. As the aluminium cover decreased in effectiveness, so the Al_2O_3 content of the inclusions decreased, as already shown for the silicates in Fig. 2.62. A similar effect was observed for the calcium aluminates formed from the entrapped slag particles. The greater the aluminium cover, the higher was the Al_2O_3:CaO ratio in the calcium aluminates, as shown by the following data. Immediately after an addition of 305 kg ferro-aluminium to a 120 t melt, the Al_2O_3:CaO ratio of the calcium aluminates was 9.6, which decreased over the next 35 min to 1.67 as the aluminium cover diminished. A further addition of 102 kg ferro-aluminium immediately restored the aluminium cover, and the Al_2O_3:CaO ratio of the calcium aluminates immediately increased to 11.1. This clearly showed that an addition of aluminium later during refining readily restored a fading aluminium cover. The presence of an aluminium cover to the end of refining therefore preserves a clean bath containing a minimum of inclusions, which also ensures that a minimum of inclusions are tapped into the ladle. Consequently, it was suggested by Pickering et al that aluminium should be added as early as possible during refining, and always before the silicon. The amount of aluminium added should be sufficient to preserve an adequate aluminium cover until tapping, and corrective silicon additions should not be added just prior to tapping when the aluminium cover is weakest, unless preceded by enough aluminium to restore an effective cover, or unless the remnant cover is strong. Also, more aluminium should often be added if the refining period is inadvertently extended.

The role of slag inclusions, even in the relatively quiescent refining period, has already been mentioned. The fact that any disturbance or turbulence created in

the bath can cause admixture of slag into the bath was observed on many occasions in these investigations. Immediately after such a disturbance of the bath, an increase in the CaO content of the silicates, in a process not primarily deoxidised by aluminium, was frequently observed. Two particular causes of such entrapment were identified with additions of slag-forming materials and ferro-alloys, and with mechanical stirring of the bath, as shown in Fig. 2.65. The fact that these silicates always contained considerably less CaO than did the slag can be attributed to them acting as nuclei upon which deoxidation products were precipitated. It was emphasised, however, that the effects produced by such disturbances were only transient.

In general, the inclusion size decreased progressively throughout the reducing period, Fig. 2.66. The silicates in a silicon deoxidation practice were always much larger (45 μm) than the alumina, spinel and calcium aluminates (5-15 μm) in an aluminium-deoxidation practice. The reason given for the trend shown in Fig. 2.66 was that at the start of refining, the supersaturation was relatively great so that each inclusion had ample opportunity to grow more than later in refining, when the supersaturation was small and only caused by oxygen pick-up.

(iii) Tapping

Several effects were observed during tapping. The first was the pick-up of launder erosion products during tapping down a siliceous (gannister) launder. The result was large, highly siliceous globules, which invariably contained particles of silica (cristobalite), and these occurred in the metal stream issuing from the end of the launder in a silicon-killed steel. These inclusions often contained a little CaO from slag glaze on the launder. Replacing the siliceous launder by a magnesite launder completely removed this type of inclusion. Also, in an aluminium-treated steel, such launder erosion products were much less prevalent as a result of their reaction with the dissolved aluminium.

During tapping, the major effect was produced by tapping through the refining slag in order to promote more effective desulphurisation. This always resulted in

the occurrence of large inclusions which undoubtedly originated from the admixture of the slag with the steel during tapping. Two distinct types of inclusions were observed in the ladle immediately after tapping, depending upon whether the steel was silicon-killed or aluminium-killed.

In a silicon-killed steel, not treated with aluminium, the inclusions in the ladle invariably comprised large calcium-rich silicates originating from the slag, as shown by the close correspondence of the analysis of the inclusions and the slag in Fig. 2.67. The inclusions in the ladle were always considerably larger than those in the furnace immediately prior to tapping, Fig. 2.68, and always occurred in much greater amounts.

In an aluminium-treated steel, whilst slag inclusions were picked up during tapping through the slag, these reacted with the aluminium dissolved in the steel to form quite large calcium aluminates containing $MgO.Al_2O_3$ spinel particles[104]. Again the size of these calcium aluminates was very much greater than that of the inclusions occurring at the end of the refining period, Fig. 2.69. The composition of the calcium aluminates was very dependent on the amount of aluminium in the steel. The greater the aluminium addition, the higher was the Al_2O_3:CaO ratio of the calcium aluminates, and the smaller was the particle size.

It seems, therefore, that despite the improvements which can be made by varying the deoxidation procedures during the refining period to improve the cleanness of the steel before it is tapped, much of this improvement can be rendered useless if the metal is tapped through the slag in an attempt to produce lower sulphur contents. Using this technique, it seems that the lower sulphur contents can only be obtained at the risk of an increased oxide content. These oxides, i.e. the calcium-rich silicates or calcium aluminates originating from the slag, are therefore largely exogenous but their nature can be altered by reaction with a strong deoxidant added to the ladle. According to Pickering et al, therefore, the necessity for tapping through the slag

must be seriously considered and even questioned.

On the basis of a very simple calculation of the energy available to disperse the slag into globules within the steel, it was shown that the size of the slag-based inclusions should decrease as the amount of slag tapped with the steel decreases. Evidence for this was obtained from a number of investigations into the effect of slag-metal mixing. The results showed that in seven trials using normal slag-metal mixing, the mean maximum inclusion size was $\sim 90\ \mu m$, whereas in two trials with very restricted slag-metal mixing, it was $\sim 60\ \mu m$. It was also concluded that the number of larger slag-based inclusions should decrease whilst there should also be a larger number of very small slag-based particles. This conclusion was also verified by considering the ratio of slag-based to other inclusions, with sizes greater than $25\ \mu m$:-

	Ratio slag: other inclusions
Normal slag-metal mixing	2.28
Very restricted slag-metal mixing	0.87

Finally, on the evidence that a restriction of slag-metal mixing produces fewer of the larger inclusions, it would be expected that for a constant amount of oxygen pick-up and precipitation of deoxidation products on the slag inclusions, more dilution of the CaO content of the inclusions should be observed when slag-metal mixing is restricted. This was also observed, as shown by the following results:-

	% CaO in Inclusions
Normal slag-metal mixing	35
Very restricted slag-metal mixing	21

It can be seen therefore that a cleaner steel, containing fewer of the larger inclusions, can be produced in the ladle if the slag and metal are not mixed during tapping.

(iv) Deoxidation in the Ladle

In a silicon deoxidation practice, experiments were made to investigate the effect of additions of ferro-silicon or calcium silicide to the ladle. These additions also contained 1 - 1½% Al. It was observed that the aluminium in the silicon alloys entered the deoxidation products which were formed, and greatly increased the Al_2O_3 content of the silicates. This is shown in Fig. 2.70 and these more highly aluminous silicates were quite large and led to quality control problems[103], particularly as they were formed in the ladle and therefore had a greater opportunity to enter the ingot. It was concluded, therefore, that wherever possible, ferro-silicon additions to the ladle should be avoided in a silicon-killed steel, and the implementation of this suggestion led to a marked improvement in cleanness[103].

In an aluminium-killed steel, in which an addition of aluminium was also made to the ladle, the mixing of slag and metal during tapping resulted in the formation of calcium aluminates from the reaction between the slag and the aluminium in the steel. The Al_2O_3:CaO ratio of the calcium aluminates increased with increasing amounts of aluminium added to the ladle, changing from $CaO.Al_2O_3$ through $CaO.2Al_2O_3$ to $CaO.6Al_2O_3$. With increasing Al_2O_3:CaO ratio in the calcium aluminates, their size decreased as shown in Fig. 2.71. The reason given for this was that $CaO.Al_2O_3$ and calcium aluminates less rich in Al_2O_3 melt at temperatures below the ladle temperature, and thus are molten and can coalesce and grow to form larger particles. On the other hand, $CaO.2Al_2O_3$ and $CaO.6Al_2O_3$ are solid and thus form much smaller particles.

Some observations were also made on the effect of calcium silicide additions to the ladle in a steel which was aluminium-killed and therefore contained calcium aluminates. The effect of the calcium silicide was to cause considerably smaller calcium aluminates for a given Al_2O_3:CaO ratio, the size for an Al_2O_3:CaO ratio of 2.0 being about 20 μm compared with 40 μm for a steel not treated with calcium silicide. The reason for this effect was not given.

(v) Effect of Ladle Holding

During a holding period in the ladle, the larger inclusions can float out into the ladle slag. However, there is always the danger that the longer the steel is in contact with the ladle lining, the more tendency there will be for ladle erosion. In a silicon-killed steel, a short holding period of about 5 min caused a decrease in the maximum size of the silicates from 57 μm to 43 μm, which was explained on the basis of the larger inclusions floating into the ladle slag. As a result of cooling in the ladle, further deoxidation products were precipitated, and as the steel cooled, MnO was precipitated in larger amounts than SiO_2. Consequently the $MnO:SiO_2$ ratio of the deoxidation products in a silicon-killed steel increased with increasing time in the ladle, Fig. 2.72.

In an aluminium-killed steel, it was observed that the Al_2O_3 content of the calcium aluminates increased as the time in the ladle increased. At first, this was believed to be an adjustment towards equilibrium, but such a change would involve Al_2O_3 replacing CaO in the calcium aluminate, which is thermodynamically improbable. Alternatively, some further precipitation of alumina on existing calcium aluminates might be possible, but in a heavily aluminium-killed steel this tendency will be very slight. Instead, the authors attributed the effect to the larger size of the less aluminous calcium aluminates, Fig. 2.71, which allowed them to float out more quickly, leaving the smaller, more aluminous calcium aluminates in the steel. Such a flotation effect was confirmed by the marked increase in the Al_2O_3 content of the ladle slag with increasing time. There was also clear confirmation of flotation of the larger calcium aluminates by the generally decreasing size of the calcium aluminates remaining in the ladle with increasing time.

(vi) Effect of Vacuum Degassing

Investigations were made into the effect of vacuum degassing on the inclusions present in the steel during two degassing processes. In the first, the whole ladle was put under vacuum (the Stokes process) and this was applied to heavily aluminium-killed

basic electric arc steels. There was no evidence that there was any dissociation of the very stable calcium aluminates under vacuum, but the size of the inclusions definitely decreased. This was simply due to the holding period of 9-14 min brought about by vacuum degassing, which allowed flotation of the larger inclusions, aided by the evolution of gas and the associated turbulence. At the same time, the Al_2O_3:CaO ratio of the calcium aluminates increased during degassing, caused by the flotation of the larger, more calcareous inclusions during the vacuum degassing period, as shown by the following data:-

	Al_2O_3:CaO ratio of calcium aluminate	
	Before degassing	After degassing
Trial No. 1	1.18	1.94
Trial No. 2	1.07	2.00
Trial No. 3	1.36	2.14

In a second investigation, a vacuum lift process was examined (the R-H process) using a silicon-killed basic open-hearth steel. Prior to degassing, the inclusions comprised calcareous silicates originating from furnace slag, and manganese silicate deoxidation products which contained some Al_2O_3 from the aluminium present in the ferro-alloy additions. During degassing, a complex series of changes was observed. At the start of and during the early stages of degassing, the calcareous silicates tended to decrease in CaO and increase in Al_2O_3 content. After about 6 min these inclusions were no longer observed, the circulatory action having apparently eliminated them to the slag, and this was confirmed by the slag analysis. The deoxidation products decreased in Al_2O_3 content during the early stages of degassing as some were eliminated to the ladle slag and the remainder were diluted by manganese silicate secondary deoxidation products, free from Al_2O_3, which were precipitated on them during cooling in the ladle. Later, during degassing, the Al_2O_3 content tended to increase, caused probably by contamination from ladle and degasser refractory material, the degasser body, legs and snorkel comprising high alumina refractories.

On the other hand, it was suggested that there may have been some dissociation of the MnO and SiO_2 of the silicates during degassing, giving rise to a relative increase in Al_2O_3. Evidence for the elimination of some of these inclusions to the slag was shown by the increase in the Al_2O_3 and MnO content of the slag. Still later in the degassing process, the cooling caused more secondary deoxidation products to precipitate on existing inclusions, which increased the MnO and SiO_2 contents. After about 6 min degassing, a new type of silicate was observed which persisted to the end of the degassing period. This was a highly aluminous silicate containing about 35% Al_2O_3, 25% SiO_2, and it was suggested that it resulted from degasser refractory erosion. Further confirmation that some inclusions originated from the highly aluminous degasser refractories was provided by the fact that they frequently contained spinel (galaxite) or alumina particles. At the end of the degassing process, a number of secondary deoxidation manganese silicates, virtually free from Al_2O_3, were observed. In general, the inclusions observed in the ladle prior to degassing were completely eliminated, but the erosion products persisted through to the end of degassing. There was apparently little systematic variation in size of each of the various types of inclusion throughout degassing, but a very significant difference in size between the different types was observed. The Al_2O_3-rich erosion products were nearly twice as large as the deoxidation products, 110 μm against 60 μm respectively. From the results of extensive oxygen analyses, it also seemed that little oxygen was removed during the later stages of degassing but extensive mixing of the steel occurred. According to Pickering et al, this and other evidence indicates that little dissociation of the silicates takes place under vacuum. Consequently, the effectiveness of increased mixing and homogenisation must be offset against the possibility of greater refractory erosion, although the circulatory action does apparently help to eliminate inclusions to the ladle slag.

(vii) Teeming Period

In silicon-killed basic electric arc furnace steels, the inclusions observed

were both deoxidation products of the manganese aluminium silicate type and calcareous slag-based inclusions. During teeming, there was a pronounced tendency for these inclusions to increase in Al_2O_3 content, Fig. 2.73(a). This was attributed to progressive contamination by ladle refractory erosion products. It was shown that a very low contamination rate was required to account for the observed increase in the Al_2O_3 content[103]. It was concluded that the upper and lower limits of the band shown in Fig. 2.73(a) probably represented the extremes of ladle lining condition. Further evidence for the contamination with ladle erosion products is shown in Fig. 2.73(b) in which the TiO_2 content increased with time, TiO_2 being a tracer in the refractories.

Ladle linings which were maintained by a sprayed gannister coating were observed to give rise to many more erosion products than either bricked or rammed linings. These ladle erosion products also frequently contained a little CaO resulting from the slag-contaminated ladle glaze.

Using a simple flotation model for inclusions in the ladle, the maximum size of inclusions of the silicate type was predicted for any time during the teeming process, as shown by the full line in Fig. 2.74. The maximum observed particle size should increase with time during teeming, and this was in fact observed in practice. The largest calcium-rich, slag-based silicates were in general never bigger than the predicted maximum, but the largest ladle erosion products were considerably greater than the predicted maximum size. The reason given for this was that ladle erosion products were produced continually throughout teeming in a wide spectrum of sizes and at a time dependent upon the local softening and scouring action of the reaction layers. Consequently, flotation models cannot readily be used to predict their sizes, which are much greater than would be predicted. It was observed that whilst ladle holding allowed flotation to occur, the extra time involved for the steel in contact with ladle refractories could give rise to more erosion products. The conditions for forming the minimum of erosion products are therefore complex, involving a critical

interaction between holding time, teeming speed, temperature and above all the initial condition and type of the ladle lining.

In the case of silicon-killed basic open-hearth steels, the inclusions present during teeming were mainly deoxidation products and ladle erosion products. The calcareous slag-based inclusions had largely been eliminated to the ladle slag during vacuum degassing. The $MnO:SiO_2$ ratio of the primary deoxidation products was observed to increase during teeming, as more MnO than SiO_2 was precipitated upon them during cooling in the ladle. Typical results have already been shown in Fig. 2.72. The primary deoxidation products also increased in Al_2O_3 content in a similar manner to the silicates already described in the basic electric arc steels, the suggested reason again being contamination by ladle erosion products, but this contamination did not usually commence until some minutes after the start of teeming. No clearly defined trend in the size of these inclusions was, however, observed during teeming.

A predominant type of inclusion throughout much of the teeming process was the manganese aluminium silicate ladle erosion product. Some of these also originated from nozzle and stopper erosion. These were usually very large, as shown by the following maximum sizes observed:

Primary deoxidation products	49 μm
Secondary deoxidation products	32 μm
Ladle erosion products	107 μm

In general, these inclusions tended to increase in size towards the end of teeming as larger masses of glaze were scoured from the ladle lining due to softening becoming more pronounced as the time of contact between the steel and refractory increased.

In steels which had been heavily killed by aluminium, the occurrence of ladle erosion products was by no means so readily observed, because reaction occurred between the silicates and the aluminium dissolved in the steel, tending to form alumina and spinels and even calcium aluminates from the CaO often present in the erosion

products. Nevertheless, clearly defined erosion products were observed in samples taken from the ladle stream, when they had had less time to react with aluminium, but not in the ingot itself when the reactions had probably gone more or less to completion. The silicates contained rather high Al_2O_3 contents of 20-50%, and it was suggested that they were erosion products, the high and variable Al_2O_3 content probably being the result of partial reaction with aluminium. Inclusions of this type have been observed in laboratory investigations into the reaction between silicates and aluminium dissolved in the steel(22,98,107). It was suggested that they were probably nozzle and stopper erosion products which had not had sufficient time for complete reaction before the sample was taken, and this was to a large extent confirmed because they contained no CaO, which would have been present had they originated from ladle glazes. It was not implied that ladle refractory erosion did not occur, but rather that such erosion products had time to react with aluminium during their residence in the ladle. In some of the erosion products, second phase particles of alumina were also observed. This alumina was not thought to result from reaction with aluminium because the mullite typically observed in laboratory experiments(107) was not seen. Rather the alumina was thought to arise from the erosion reactions, it having been shown that large amounts of corundum can be formed in the surface layers of aluminosilicates which have been immersed in liquid steel.

There was no systematic variation in the Al_2O_3 content of the erosion products during teeming, probably because they varied in Al_2O_3 at the time of their formation, and the analysis would be randomised further by variable reaction with aluminium dissolved in the steel. There was, however, a tendency for the largest erosion products to increase in size as teeming progressed, Fig. 2.75 and this was particularly observed towards the end of teeming, and when teeming was inadvertently prolonged. This showed the detrimental effect of an increasing time of contact between steel and refractory on the formation of erosion products.

In addition to erosion products, there were also calcium aluminates and alumina present during teeming. There was a tendency for the Al_2O_3:CaO ratio of the calcium aluminates, which often contained second phase $MgO.Al_2O_3$ particles, to increase with time during teeming, and for the size of the calcium aluminates to decrease. These effects are mutually compatible; the larger, low-melting-point calcium aluminates having a lower Al_2O_3:CaO ratio, Fig. 2.71, float out of the ladle more readily during teeming. The alumina particles, and the calcium aluminates of the $CaO.6Al_2O_3$ type were very small in size (less than 5 μm) throughout teeming, and together with $MgO.Al_2O_3$ spinels, were formed by reaction between entrapped slag and the aluminium added in the ladle. It was concluded, however, that the main sources of alumina were direct deoxidation, or from the pick-up of oxygen during teeming.

The average sizes of these various inclusions were very different, as shown by the following data:-

	Average diameter, μm
Alumina and $CaO.6Al_2O_3$	~5
Other calcium aluminates	27
Erosion silicates	64

The reason given for the smaller size of these erosion silicates compared with those in the silicon-killed steels was that they never had time to grow or coalesce because they were altered by reaction with the aluminium in the steel. Also, it has been shown that aluminium in steel decreases the amount of liquid in the erosion layer and that this tends to decrease the size of the erosion products scoured from the ladle lining.

According to Pickering et al, the most deleterious place in which inclusions can be formed is probably the ingot because they will then have the least chance of escaping from the steel, although there is evidence that inclusions can float out to

some extent in the mould itself[103,104].

The oxygen required in the solidification of rimming steel ingots is more than that available in the liquid steel teemed into the ingot mould[108], and must be supplied from the atmosphere at the turbulent surface of the ingot. One source of such oxygen is the scum which forms by atmospheric oxidation on the surface of the liquid metal in the ingot mould, and ciné films of this surface have shown that large masses of scum can be entrained in the solidifying ingot. In a study of the inclusions in rimming steels, Pickering[108] observed that some large inclusions consisted of (FeMn)O dendrites in a silicate matrix. An examination of the scum from the ingot revealed that it had virtually an identical structure and there can be little doubt that in rimming steels, some large inclusions are a direct consequence of the entrapment of large masses of the scum. Similar observations of scum entrapment have been reported by Bruch, Grisar and Müller[110], Houseman[111] and Ichinoe et al[112].

In the manufacture of balanced or semi-killed steels, a technique which can be used is to add sufficient deoxidant to the mould to regulate the gas evolution so that a balanced condition results. Pickering considers that such a practice is not perhaps the best because it forms fairly large amounts of deoxidation products within the mould, and ladle balancing is a more effective method to produce clean balanced steel. Two methods of mould balancing were investigated. In the first, an aluminium-silicon alloy was fed into the mould to regulate the rimming action and it was found that a large proportion of plates were rejected because of deoxidation inclusions formed directly by mould balancing. An investigation into this practice revealed that when samples were taken from the ingot mould before and after the addition of the aluminium-silicon alloy, those taken after the addition contained considerably greater Al_2O_3 contents in the silicates, Fig. 2.76. Prior to the addition of the deoxidants to the mould, the inclusions were primary deoxidation products of manganese silicate or MnO, but after the aluminium-silicon deoxidant had been added, they were very fluid manganese aluminium silicates, and frequently of large size. They formed either by a direct deoxidation

reaction with dissolved oxygen or by a reaction between the added aluminium and silicon and the pre-existing inclusions. When the rimming reaction ceased, these manganese aluminium silicates then segregated into the bottom third of what behaved as a killed ingot[109] and gave rise to lamination defects.

In the second method, a rimming steel was uphill-teemed and the last metal was treated with aluminium to produce a killed or stabilised steel core within a rimmed periphery. In the rimmed peripheral layers of the ingot, the inclusions were mainly silicates but in the core of the ingot they abruptly changed to aluminous silicates or alumina clusters depending on the amount of aluminium used. These aluminous inclusions were formed by direct deoxidation, and by reaction with existing inclusions[107]. The compositions of the inclusions formed from the aluminium deoxidation were dependent upon the amount of aluminium used, increasing in Al_2O_3 content with increasing aluminium additions. An interesting feature of this investigation was that the more aluminous the inclusions, i.e. the more aluminium added to the mould, the cleaner was the steel.

The use of exothermic feeder head compounds, which contain free aluminium in a thermite mixture, can lead to unusual inclusions in the ingot. For example, in a silicon-killed $1\frac{1}{2}\%$ Mn steel, Pickering et al observed groups of large alumina inclusions in the upper part of the ingot, although no aluminium had been used at any stage during their manufacture. The alumina inclusions occurred at positions down to 30% from the top of the ingot, and were attributed to aluminium deoxidation of the top of the ingot by the free aluminium in the exothermic feeder head compound. Apparently convection currents within the solidifying ingot were capable of drawing the inclusions down into the body of the ingot.

A second example concerned the formation of duplex $MgO.Al_2O_3$ spinels with calcium aluminium silicates, which were confined to billets from the top part of ingots of a basic electric high carbon steel. This steel also had at no stage in its manufacture been treated with aluminium, and the ferro-silicon used for deoxidation had been

specially selected to contain a low residual aluminium content. The steel had, however, been tapped through slag in order to achieve a low sulphur content, and a very effective exothermic feeder head compound had been used on the ingots. The presence of the calcium aluminium silicate associated with the spinel indicated that entrained slag was partially responsible for the inclusions, and it was also suspected that the exothermic feeder head compound played a part in their formation. Experiments in which non-reactive feeder head compounds such as vermiculite were used, showed a marked decrease in the frequency of occurrence of the detrimental inclusions, Fig. 2.77 but did not entirely eliminate them. However, the very effective restriction of slag-metal mixing during tapping, coupled with a non-reactive feeder head compound, virtually eliminated the inclusions. It was suggested that slag inclusions were entrained in the steel during tapping and some also passed into the ingot during teeming. As they floated up to the top of the ingot, they reacted with the exothermic feeder head compound to form spinel particles within the calcium-rich silicates from the slag, which also became enriched in aluminium as a result of the free aluminium in the exothermic compound. Particles of the spinel-slag complex then became detached from the reacted layer and were carried by convection currents into the body of the ingot, although they were mainly confined to near the top. The reason given to explain why the use of a vermiculite insulating layer did not entirely eliminate the inclusions was that vermiculite can, at high temperature, break down to form $MgO.Al_2O_3$ spinel, which was entrapped by slag. The lower frequency of occurrence of the inclusions using a non-reactive compound pointed to the additional effect caused by the exothermic reaction in promoting the reactions or in helping the detachment of inclusions into the main body of the ingot. In fact, confirmation of these suggested mechanisms was obtained from experimental work in which slag and exothermic compounds were stirred into a laboratory melt. Samples taken from the melt showed the presence of the spinel-calcium silicate inclusions.

The use of oxidic materials to help in promoting good surfaces and adequate

feeding in ingots may be expected to lead to some complex inclusions from time to time. For example, it is known that a mould flux can react with an exothermic feeder head compound and impair its performance and the reaction products could then be entrained in the ingot. Further reactions could also be envisaged with the feeder head tiles, giving very complex oxide inclusions. Pickering has concluded, therefore, that in future, it will be necessary for such materials as mould fluxes, feeder head compounds and tiles to be mutually compatible so as not to impair each others performance and moreover so as not to form exogenous inclusions which might be detrimental to the quality of the steel.

On the basis of the steelmaking trials carried out, Pickering et al attempted to assess the detrimental nature of different types of inclusions. In general, it is the very large inclusions which provide the greatest quality control problems, particularly if they occur in segregates. The relative average volumes of the various types of inclusions can be taken as an index of their likely deleterious nature, and the data obtained by Pickering et al is shown in Table 2.8. These figures show that it is the primary silicate deoxidation products and the erosion products which are likely to cause the most problems. Steps can be taken to eliminate deoxidation silicates by varying the deoxidation practice, but, as Pickering pointed out, more effort is required to eliminate refractory erosion products.

Several other investigators have studied the origin of inclusions during steelmaking, although not quite in such a comprehensive manner as Pickering et al. Thus, before going on to consider in greater detail the formation of inclusions as a result of atmospheric reoxidation and refractory erosion, the main conclusions of these other studies are discussed, with particular reference to the use of radioactive isotopes to label inclusion sources.

Leach[113] discussed the general approach to the production of high quality alloy and stainless steels made in large electric arc furnaces. The importance of

correct deoxidation practice was emphasised, and methods of employing aluminium treatment and vacuum degassing to best effect were discussed. The various difficulties which inclusions can give rise to in stainless steel plate and sheet were described, together with remedial actions taken as a result of investigations of inclusions present at various stages of steelmaking by a bomb sampling technique similar to that used by Pickering et al.

König and Ernst[4] carried out a detailed investigation of the composition and origin of oxide inclusions in liquid steel. The formation of inclusions and the subsequent changes in their chemical composition were discussed in terms of:-

(i) The physical state of the inclusions (solid/liquid)

(ii) contact and coalescence with other inclusions

(iii) reaction with the liquid steel (to approach chemical equilibrium)

(iv) holding time at reaction temperatures; the melt temperature; the inclusions size

(v) reactions with refractory material and with slag

(vi) atmospheric oxidation.

In general, their main conclusions were very similar to those of Pickering et al and other workers.

Franklin, Rule and Widdowson[51] studied the effect of various deoxidation techniques on the oxygen contents and types of oxide inclusions in single slag melts of 0.2% C steel made in a basic electric arc furnace. Furnace and ladle deoxidation was investigated using ferro-silicon, ferro-manganese, ferro-aluminium, silicon-manganese and aluminium deoxidants. One tonne heats were made and experimental work was based on vacuum fusion oxygen analyses and electron probe microanalyses of inclusions. Their results showed that shortly after melt-out, residual deoxidation products introduced by the charge materials were present. The persistence of such oxide inclusions coincided with abnormally high bath oxygen contents. The carbon-oxygen product decreased during refining as the residual deoxidation products were removed until a

value of approximately 250 ppm oxygen was reached at 0.2% C, corresponding to a product of 0.005. Before deoxidation, the steel was virtually free from inclusions.

Silicon-manganese deoxidation in the ladle was the least efficient method of oxygen removal, there being a drop of 40 ppm in oxygen in the ladle and a further drop of 50 ppm in the ingot, so that final ingot average oxygen levels were about 150 ppm. The same deoxidation in the furnace produced a much cleaner steel, mainly because during the 10-15 min taken for deoxidation, sampling, and tapping, there was a gradual fall of 150 ppm in oxygen to a ladle level of 100 ppm. A subsequent further drop on teeming and ingot solidification meant that mean ingot oxygen levels of 80 ppm were obtained.

Aluminium deoxidation was the most efficient for oxygen removal, a rapid drop of 100 ppm in oxygen content being obtained within 1 or 2 min of the aluminium addition, whether in furnace or ladle. Further gradual decrease in oxygen content occurred when silicon and manganese were added. Addition of aluminium in the furnace or ladle produced average ingot oxygen contents of about 30 ppm.

The composition of inclusions in the deoxidised steel depended entirely on the alloys added. Ferro-silicon containing 1.8% Al resulted in oxide inclusions containing up to 40% Al_2O_3. Small amounts of CaO (3%) and TiO_2 (1%) were traced to calcium in the ferro-silicon, and titanium in the ferro-manganese and silico-manganese. The authors found it unnecessary to assume that any of the constituents of the inclusions in the steel originated in refractories or furnace slags.

Aluminium added either as aluminium stick, ferro-alloy, or as a trace element in the ferro-silicon, was always a major constituent of the inclusions. The balance of SiO_2 and MnO depended on the original oxygen content of the bath combined with the recovery of the ferro-alloys. The range of compositions tended to lie on a tie-line connecting pure alumina with the low melting-point region of the Al_2O_3-SiO_2-MnO ternary diagram, between spessartite and rhodonite.

Lunner[114,115] examined the occurrence of macro-inclusions (larger than

about 30 μm) in non-stabilised austenitic stainless steel made in electric arc furnaces by sampling the liquid steel at different stages of the steelmaking, tapping and teeming processes. The compositions of the inclusions observed during these processes are given in Table 2.9. It was found that the frequency of large inclusions was relatively low in the furnace, increased somewhat in the ladle, and was highest in the ingot mould.

When the melt was tapped into the ladle, it was found that the number of macro-inclusions had markedly increased. This was a result of the entrainment of furnace slag and oxidation by air during tapping of the melt. The time during which the melt was held in the ladle was found to have a favourable effect on the separation of the larger inclusions. Slag particles greater than 50 μm were effectively separated.

Ingots which were teemed late in the casting period contained more macro-inclusions than those teemed at an earlier stage. This was attributed to the growth of slag inclusions present in the ladle as a result of coalescence and also, possibly, reoxidation.

Lunner also observed the following trends when comparing direct and uphill-teemed ingots:-

(i) uphill-teemed ingots contained fewer macro-inclusions

(ii) micro-inclusions were mainly present in the top part of uphill-teemed ingots

(iii) uphill-teemed steel had an insignificantly lower total inclusion content throughout

(iv) coarse inclusions which were present were more uniformly distributed throughout the uphill-teemed ingots whereas in the direct-teemed ones, they were mainly located in the bottom cone region.

The effect of argon bubbling on the separation of slag particles was also studied, although only on two casts. Argon bubbling in the furnace before tapping resulted in a marked reduction in the number and size of the spherical silicate inclusions.

However, with argon bubbling in the ladle, carried out on aluminium-killed steels, no significant removal of inclusions was observed. Lunner suggested that in this case, the aluminate particles were already too small to be effectively separated by the bubbles, and also that argon bubbles adhere to silicates more effectively than to aluminates.

Wahlster, Choudhury and Rohde[116,117] investigated the origin of inclusions in steel containing 1.0-1.2% Mn. Liquid metal samples were taken by a bomb sampling technique from 5 t and 100 t melts. Figure 2.78 shows the influence of the amount of the deoxidiser addition on the composition of the primary deoxidation products in the ladle. In each case, aluminium was added together with calcium alloys. With increasing aluminium addition, the Al_2O_3 content of the primary inclusions increased and after an aluminium addition of 0.7-1.1 kg/t, they comprised calcium aluminates with little or no SiO_2 present. Figure 2.79 shows that the composition of primary oxide inclusions was shifted towards higher SiO_2 contents during teeming. The reasons given by the authors for this growing SiO_2 content were the temperature-dependence of the silicon-oxygen reaction in steel, the rapid separation of alumina inclusions containing CaO, and reaction between the steel and the firebrick lining of the ladle.

Figure 2.80, also taken from the work of Wahlster et al, illustrates the influence of different processes on the solubility product of aluminium and oxygen. The value of 10^{-9} at 1600°C obtained in normal technical melts (electric arc furnace, black slag) is taken as standard. This value, which the authors consider is better defined as a characteristic number for inclusion separation, can be lowered by the application of certain metallurgical measures such as vacuum treatment, argon stirring, fluorspar 'bombs' and calcium treatment, with best results obtained by using unsaturated refining slags. In the electro-slag remelting process or by using $CaO-Al_2O_3$ slags in laboratory melts at 1600°C, the thermodynamic equilibrium value for $[\%\,Al]^2\,[\%\,O]^3$ has been achieved.

According to Wahlster et al, application of calcium during deoxidation with aluminium and silicon has proved to be a most effective measure in achieving favourable inclusion content and composition. From the fact that exogenous inclusions are formed as a result of chemical reaction between liquid steel and firebrick, they also concluded that in this case, improvements in steel cleanness can only be achieved by using better quality refractories such as higher alumina firebrick, dolomite or magnesite.

Kohn et al[118,119] studied the origin of aluminous inclusions in electric arc steels using radioactive cerium as a tracer with the aluminium. The steel was made in a 40 t furnace by a double slag practice and the average composition was 0.15% C, 0.35% Si, 0.75% Mn, 0.007% S, 0.012% P, 1.30% Ni, 1.04% Cr, 0.10% Mo and 0.025% Al. Four heats were made and details of the deoxidants used are given in Table 2.10. In heats A and C, the aluminium addition to the furnace was labelled with cerium. In heat B, the aluminium added to the ladle was labelled and in heat D, the ladle slag was labelled by means of a small amount of sintered oxide mixture having the composition 31% SiO_2, 35% CaO, 16.7% Al_2O_3, 4.2% CaF_2 and 12.5% CeO_2 (radio-active). In each cast, half of the metal in the ladle was teemed into a continuous casting machine, whilst the other half was teemed into ingots (direct and uphill). The results of activity measurements on slag and scum samples are shown in Table 2.11. The main conclusion of this investigation was that the inclusions present in the aluminium-deoxidised steels were not pure alumina crystals but were in fact aluminates containing magnesia or lime.

Kohn et al proposed that on adding the aluminium, alumina inclusions were formed initially but these were rapidly eliminated. The deoxidation products subsequently formed, as a result of reoxidation of the metal, were complex aluminates. These aluminate inclusions were precipitated directly by the simultaneous oxidation of aluminium, magnesium, calcium and radioactive cerium present in solution in the liquid metal. It was calculated that 0.05% oxygen requires 0.055% Al, 0.007% Mg and 0.012% Ca to fix the whole of this oxygen, half as $MgO.Al_2O_3$ and half as $CaO.Al_2O_3$

Although the vapour pressures of calcium and magnesium are very high at 1600°C, these workers consider that it is reasonable to assume that about 0.01% Mg and 0.01% Ca can exist in solution in the liquid steel.

According to Kohn et al, the calcium probably originated from the calcium-silicon addition, Table 2.10, and the magnesium possibly from the ferro-alloys and from the calcium-silicon alloys in which it was found as impurity (about 2% Mg). It might also have formed by the reduction of MgO present in the furnace lining or by introduction into the slag as a result of refractory erosion. The thermodynamic data show that the aluminates have a high stability and that they can be formed in liquid steel containing aluminium, calcium and magnesium when the steel is reoxidised.

A white powder was deposited on the interior of the tundish nozzles during continuous casting and radiographic analysis showed that it was composed of $MgO.Al_2O_3$, $CaO.2Al_2O_3$ and $CaO.6Al_2O_3$ together with traces of alumina. Chemical analysis gave 62-67% Al_2O_3, 9-11% MgO, 12.5% CaO and less than 3% SiO_2. As this deposit was composed of crystals of the same nature as the inclusions present in the metal, it was concluded that the deposit was produced as a result of the poor wetting of the aluminous inclusions by liquid steel according to the mechanism of Kozakevitch et al discussed previously. If such a mechanism is assumed, the inclusions which come into contact with the nozzle wall remain attached to it and accumulate, one on the other to form a powdery deposit. This phenomenon is related to the high surface area: volume ratio of the liquid stream flowing through the nozzle. It may even be intensified by the break in the metal stream caused by opening and closing the stopper. The current theories on nozzle blockage are discussed in more detail in section 2.4.3.

Two types of aluminate cluster were observed in the finished product, those containing less than ten particles and those with several hundreds. It was considered that the small clusters formed in the mould as a result of collisions whilst the larger groups, consisting of too many inclusions to have formed by random encounter of inclusions during flotation, were already agglomerated when they entered the mould

and originated from the nozzle deposit which periodically became detached from the wall by the flow of metal.

The trials also showed that a significant proportion of the aluminate inclusions escaped from the liquid metal into the ladle slag and ingot scum. However, a certain number were not eliminated, either because they were impeded by the various currents, especially convection currents present in the ladle or ingot, or because they acted as nuclei for the precipitation of iron crystals during cooling in the ingot.

Kohn et al concluded that the presence of these aluminous inclusion clusters in basic electric arc steels killed with aluminium is inherent to the traditional method of casting, even when the production of the steel in the furnace is conducted with great care. In order to minimise their occurrence, it would be necessary to prevent reoxidation during casting (by casting under vacuum or in a protective atmosphere) and to promote the elimination of inclusions in the ladle.

Ericsson[120] studied the effect of tapping and teeming practices on the macro-inclusion content of electric arc, open-hearth and Kaldo steels using a radioactive tracer technique. Four main types of steel were studied, these being low carbon ($\sim$0.1%), low carbon ($\sim$0.15%) with 1.0-1.5% Mn, low alloy (0.25% C, 1.0% Cr, 0.25% Mo or 0.20% C, 0.7% Cr, 1.5% Ni) and 18-8 stainless. It was concluded that with open-hearth steel, furnace slag is unlikely to contribute to the inclusions in the ingot. However, this is apparently not the case with Kaldo and electric arc steels where slag-based inclusions can be a problem. It seems likely that the difference lies in the fact that during tapping from the furnace into the ladle, there is a much more powerful mixing of slag with steel in the case of Kaldo and electric arc furnaces compared with open hearth furnaces. An instance was quoted in which non-metallic isolates from 6 t ingots of arc furnace steel were found to contain 4-5% of ladle slag. This observation is in agreement with that of Pickering et al discussed previously.

It was also observed that after labelling the furnace slag in one cast, significant activities were obtained in the following, unactivated cast in the same ladle. The

activity was also apparent in the next cast as well. This effect was attributed to the ladle slag adhering to the refractory lining as the slag cover moves slowly down the wall of the ladle during teeming. In the next heat, this slag/refractory glaze can react with oxide and/or alloying elements in the steel. This mechanism has been described by König et al[4] and by Sims[3]. Cox and Charles[121,122] detected K_2O in addition to CaO in a number of inclusions and since the K_2O must have come from alumino-silicate refractories, it was concluded that they resulted from a reaction between the ladle slag and lining.

By means of studies on step-down testpieces and plate testpieces, Ericsson found that high teeming temperatures resulted in steel which was less contaminated by macro-inclusions compared with low teeming temperatures and suggested that the highest possible teeming temperatures should be aimed for. According to Ericsson, this results in the cleanest steel in terms of macro-inclusions, even if the attack on refractories is intensified, because separation of the large inclusions from the steel is considerably improved. Bruch et al[110] consider that hot teeming is especially important for fully aluminium-killed steels. These conclusions should not be taken too literally as there is sufficient evidence available to indicate that in some circumstances the opposite effect is true, i.e. that increased teeming temperatures result in a dirtier steel because of increased refractory erosion. In addition, there are other problems associated with reoxidation and dissolved gases to be considered.

In tests that were carried out at the Azovstal' Works in the U.S.S.R., strontium-89 was introduced into the slag on a 350 t open-hearth furnace cast at the start of the refining period[111]. The steel produced was rolled to rail section which was sampled both by measurement of the intensity of radioactivity and by autoradiography. The presence of finely-divided inclusions on the autoradiographs confirmed that open-hearth furnace slag was a source of inclusions in this cast. In a similar study of ball-bearing steel made in 55 t electric furnaces, the results indicated that

about 10% of the total inclusion content had originated from the furnace slag.

A series of investigations described by Richardson[123] included one trial in which lanthanum-140 in the form of oxide was added to the slag on a 140 t open-hearth rimming steel heat some 30 min before tapping. Sampling showed that approximately uniform activity in the slag was obtained in 10 to 15 min. Metal samples were taken from the bath, ladle and ingots. None of these showed significant readioactivity, the amount of labelled material in the metal not exceeding 0.01%.

Houseman[111] considers that the possibility of inclusions originating from furnace slag is rather greater with electric arc steelmaking than with open-hearth steelmaking of similar grades of steel, although not to the extent of the 10% reported previously for ball-bearing steel. Under the action of the forces in the electric arc, the slag may be broken down to form droplets so small that they do not float out from the bath very readily, but remain throughout the steelmaking and teeming processes and even to some extent during solidification of the ingot. Such droplets would have to be very small, possibly below 1 μm according to Houseman, though once in the ingot there exists the possibility of their combination with other small droplets to form larger inclusions.

2.4.2 Atmospheric Reoxidation

Until relatively recent times, reoxidation and its relation to product quality have not received nearly the same amount of attention as other aspects of steelmaking. This is not meant to imply lack of awareness. Twenty-three years ago, Bower, Bain and Larsen[124] presented rather convincing circumstantial evidence to indicate that reoxidation of tapping streams was the main source of alloy losses in open-hearth heats. The estimated additional amount of oxides formed in this way was in the range of 1-4 kg/t. In the course of their report, they cited the classic work done by Hultgren[125] in 1945 showing that large silicates, often rich in MnO, were present in ladle samples of high carbon basic electric arc steel which had been deoxidised in the furnace and which contained no large inclusions prior to tapping. Furthermore, these inclusions

were more numerous when the metal stream was made to spray in a turbulent manner.

In 1959, Vingas and Caine[126] ascribed the origin of macro-inclusions in steel castings to reoxidation. More recently, Van Vlack and Flinn[127-130], in an extensive investigation of the origin of ceroxides in steel castings deoxidised with aluminium, specifically discussed the role of reoxidation. Whilst their work was in progress, Hoffmann, Bailey and Holmes[131] published the results of experiments on the use of argon shrouding during casting for improving steel quality. They used the teeming stream protector shown in Fig. 2.81 for distributing argon around the metal stream and providing a mechanical barrier between the argon and air. An inert argon atmosphere was also established in the mould cavity prior to teeming. In their tests, complete argon shrouding resulted in a 30-65% decrease in oxide inclusions, a 3-24% decrease in surface grinding losses and a retention of the effects of vacuum treatment.

In an attempt to decrease the reoxidation during tapping from the furnace, Ericsson[120] used a "submerged nozzle" technique which reduced the height of fall of the tapping stream of 18-8 stainless steel melted in a 6 t basic H.F. furnace from 1-2 m to 0.1-0.2 m. The effect was followed by analysing for nitrogen and total oxygen and the results are given in Table 2.12. During normal tapping, a more extensive reaction took place with the air as shown by the nitrogen contents. Assuming that the reaction with oxygen was equally as strong, the results indicate that oxygen in the form of inclusions was eliminated during tapping. This elimination also proceeded during holding in the ladle.

Adilstam and Döbeln[132] studied the reoxidation of carbon, low alloy and 13% Cr steels during teeming and showed that a considerable quantity of macro-inclusions were formed by air oxidation, Table 2.13.

In a further series of experiments by Ericsson, protection against atmospheric reoxidation during teeming was achieved by pouring the steel through a tube of about 275 mm diameter which was connected to the ladle by a gas-tight seal and which had

its outlet about 100 mm above the bottom of the ingot mould. Immediately before and also during teeming, argon was blown into the tube at a rate of about 250 litre/t of steel. In this way, an inert atmosphere was obtained around the metal stream as shown by continuous gas analysis. At the same time, the ingot scum which formed on the surface of the rising metal in the mould was prevented from being entrained into the liquid steel by the teeming stream. In experiments on carbon steel (0.2% C, 0.75% Mn and 0.25% Si), the quantity of coarse inclusions over 25 μm decreased slightly in the bottom part of the ingot, but not to the same extent as in the related experiments of Adilstam et al, Table 2.13. In the case of smaller inclusions, no effect was observed and the total oxygen content of the steel had not changed significantly as a result of shielded teeming. A very small decrease in the nitrogen content (0.001%) was confirmed.

The principal difference in the methods of teeming in an inert atmosphere used by Adilstam et al and by Ericsson was that in the former case, even the surface of the steel in the mould was completely shielded from oxidation. Since this technique gave a considerably greater reduction in the content of macro-inclusions in the ingot, it seems that atmospheric reoxidation of the surface of the metal in the mould could make an essential contribution to the macro-inclusion content. One way to avoid this problem without having recourse to complicated teeming in a protective gas atmosphere, ought to be uphill-teeming with a suitable mould additive.

Radioisotopes have been used to study the phenomena of reoxidation of ball-bearing steel[111]. The steel was made in electric furnaces, but the results are clearly applicable to open-hearth practice. The isotopes used were zirconium-95 and tantalum-192. Zirconium is fairly similar in behaviour to aluminium since both have a high affinity for oxygen and form an oxide that is solid at steelmaking temperatures. Tantalum somewhat resembles manganese in its oxidation behaviour so that between them these two isotopes can be used to obtain information applicable to both types of deoxidation practice. In each case the isotope was introduced into the deoxidised bath

and distributed by careful mixing. Slag and metal samples were taken from the bath and the ladle and further metal samples from the first three ingots after rolling. The inclusions were extracted electrolytically and the radioactivity of both the extracted inclusions and the electrolyte was determined. Both were radioactive showing that, while some of the zirconium had been oxidised and formed inclusions, some had remained unoxidised in the steel. The results showed that there was a decrease in the specific activity of the metal as zirconium was removed by oxidation. The most rapid removal took place during tapping. There was a corresponding rise in the specific activity of the extracted inclusions. In this case, however, the results were less consistent, possibly because the inclusions were complex aggregates so that the balance of non-active material in each sample was highly variable[111]. Nevertheless, the general tendency was towards a rise in specific activity as teeming progressed.

König et al[4] consider that the relative importance of atmospheric reoxidation during teeming in contributing to the total inclusion content should not be underestimated. Of the inclusions present in an ingot, 30-60%, depending on the type of steel, come from reoxidation of the metal stream. Changing from covered to open teeming can double the oxygen content. Conversely, the oxygen content can be markedly decreased (30-60%) by pouring under a protective gas. According to these investigations, the mean composition of the inclusions formed by atmospheric reoxidation of the teeming stream differs from that of the ladle deoxidation products because the composition of the teeming stream is not usually the same as that of the ladle metal during deoxidation. If the amount of primary deoxidant at the surface of the metal stream is insufficient to bind completely the oxygen, increased amounts of other oxides such as FeO and MnO will be present in the oxides[133,134]. However, the mixing of the steel in the ingot or tundish assists the approach to equilibrium and the (FeMn)O is subsequently reduced by the stronger deoxidising elements.

A process of special interest from the standpoint of reoxidation is continuous casting[134,138]. Up to the point where molten steel is introduced into the tundish,

the process is similar to conventional ingot practice with regard to reoxidation. However, the surface:volume ratio existing in the tundish-to-mould stream(s) results in an unusually high degree of additional exposure of steel to the atmosphere. Furthermore, the reoxidation products, which can normally float to the surface in ingots, may be driven back down into the liquid core by the tundish-to-mould stream.

Little, Van Oosten and McLean[137] studied the factors influencing reoxidation of molten steel during continuous casting and showed that the reoxidation products could be a major source of inclusions in the finished product. They concluded that when steel is teemed in the conventional manner, reoxidation can occur by direct contact of air with the stream and the molten pool surface. In addition, immediately the steel leaves the nozzle, boundary layer attachment occurs and a continuous supply of air, entrained by the stream, is carried down into the metal pool. This entrained air is a major cause of metal reoxidation. The extent of this reoxidation depends on a number of factors, e.g. temperature and chemistry of the steel, the physical nature of the stream and the oxygen potential of its surroundings, the character of the gas boundary layer, and the duration and total area of exposure of molten steel to the atmosphere. A good indication of stream quality is the amount of splashing or sparking which occurs when the stream enters the tundish or mould. The effect observed by Little et al when rough and smooth ladle streams enter a tundish are shown in Fig. 2.82. In general, a rough or irregular stream is accompanied by more splashing, more fume and greater disturbance in the liquid pool than would be the case with a smooth stream. While stream roughness is difficult to define quantitatively, it does have a strong bearing on the question of reoxidation. Not only does it increase the surface area of the stream exposed to the air, it also increases the amount of air entrained by the stream and carried down into the metal pool. This in turn has a strong influence on the flow patterns and the behaviour of inclusions in the pool, and consequently on the cleanness of the final product.

Three sets of consecutive frames taken by Little et al from a high speed film

of a ladle stream are shown in Fig. 2.83. Within each sequence the time interval between frames is 1/2000 s. The stream appearance approximately 5, 20 and 35 min after the start of teeming is shown on the left, centre and right frame respectively. Particularly evident from these photographs is the increase in stream diameter with time caused by nozzle erosion, accompanied by a progressive decrease in both stream roughness and stream flaring. All of these factors tend to produce a decrease in the extent of reoxidation. Reoxidation will increase with duration of stream exposure and this will vary with stream length and velocity. Figure 2.84 shows the change in character of a ladle stream as the stopper rod is lowered at the end of a teeming period. The stream first becomes highly irregular, air entrainment is greatly increased, and this is accompanied by splashing and fume formation. The stream becomes thinner and finally degenerates into a series of droplets. The surface:volume ratio of the metal exposed to the atmosphere is now a maximum, conditions for direct oxidation of the metal are optimised and excessive fuming is observed. Similar effects are apparent when the stopper rod is raised at the commencement of the teeming period, and here again conditions are favourable for reoxidation. Thus, during the teeming of a heat, the amount of reoxidation which occurs would be diminished if a smooth ladle stream could be maintained without interruption until the casting operation was complete.

The extent of oxygen pick-up is difficult to estimate as it depends very much on the flow conditions and the type of teeming practice. Turkdogan[10] demonstrated the effect of increasing the free-fall height of a water stream on the amount of entrained air bubbles in a column of water. The latter increased with increasing free-fall height and "ropiness" of the stream. For zero fall (glass tube immersed in water) no bubbles were observed. This is one of the situations pertinent to teeming liquid steel as in many continuous casting operations, the liquid pool is covered with a low melting silicate and the steel is poured into the mould below the slag cover using a submerged nozzle. This is one of the methods used in the continuous casting of aluminium-killed steels to suppress oxidation which may lead to poor surface quality.

Kenney[138] examined the effects of reoxidation during continuous casting. The similarities and differences between ingot casting and continuous casting were discussed. It was concluded that, because of the rapid rate of solidification associated with the latter process, entrapment of reoxidation products can be a major problem. When an argon shroud was used to exclude oxygen from the tundish stream, this resulted in very substantial reductions in both the size and number of inclusions in the continuously cast billets. The products rolled from the cast billets consistently showed inclusion ratings which were equivalent to the best ratings observed in high quality products from conventional ingot casting.

In 1970, Farrell, Bilek and Hilty[139] carried out a series of laboratory experiments on fully-killed carbon steels to study the types of inclusions originating from reoxidation of liquid steel. Their results showed that inclusions resulting from reoxidation of pouring streams during the casting of steel can be identified and differentiated from normal deoxidation products on the basis of size and composition. In general, reoxidation products are usually very much larger than deoxidation products and tend to be richer in the weaker oxide-forming elements, e.g. silicon and manganese, than the indigenous inclusions. The growth of these two inclusion types is shown schematically in Fig. 2.85 for a steel deoxidised with silicon and manganese and containing only a residual amount of aluminium ($<0.01\%$). Their composition is a direct function of the composition of the molten steel and the amount of exposure to an oxidising atmosphere during teeming. In steels containing an excess of strong oxide-forming elements such as zirconium and aluminium, several types of reoxidation products may occur depending on the amount of exposure to the atmosphere. This is illustrated schematically in Fig. 2.86 for a fully-killed steel containing silicon and manganese together with sufficient aluminium ($>0.01\%$) to control deoxidation.

Application of the same experimental technique to commercial steels showed that a major source of inclusions causing defects in both wrought and cast steels was

reoxidation of the molten metal during teeming. Farrell et al concluded, therefore, that reoxidation of steel may be more serious than has been considered previously. Reoxidation can completely mask the beneficial effects of otherwise excellent furnace practice and deoxidation treatments. Steels containing sufficient aluminium for this element to be in control of deoxidation, e.g. most fine-grained steels, should contain no silicate inclusions. The presence of silicates in such steels, excluding siliceous erosion products, is direct evidence for pouring stream reoxidation. Solution of the problem is most likely mechanical rather than chemical in nature. That is, reoxidation products cannot be eliminated by changes in deoxidation practice. Whilst changes in deoxidation may modify the composition of these inclusions because of a change in the steel composition, they do not prevent them. The only remedy is isolation of the metal from contact with air or other oxidising atmosphere during casting.

Farrell et al consider that the elimination of reoxidation as a source of inclusions would be a major step in improving steel cleanness. Furthermore, unless reoxidation of teeming streams is prevented, the full benefit conferred by advanced techniques, such as vacuum treatment and sophisticated deoxidants, cannot be realised.

2.4.3 Steel - Refractory Interaction

Ericsson[120] has stated that erosion of refractories is not a major source of inclusions, providing there is careful selection of refractory materials and tapping temperatures. On the other hand, bearing in mind the possibility of variations in melting and casting conditions, it is a factor which should be closely observed at all times. In support of this, Ericsson quoted the work of Cottingham and Vincent[140] on the continuous casting of silicon-killed steel billets for tube production. These authors concluded that it was necessary to study the use of higher quality refractories and also the flow of metal during teeming in order to minimise refractory erosion and eliminate large, exogenous inclusions. They suggested, for example, the replacement of fireclay ladle nozzles by nozzles made of zirconium silicate, magnesite or high alumina material, additionally ensuring that the area around the ladle nozzle was

lined with high quality refractory to resist erosion in this particular part of the ladle.

In his own investigations on refractory erosion, Ericsson found considerable differences between steel types. For example, higher manganese steels e.g. 0.15% C, 0.3% Si and 1.2% Mn are known for their strong chemical attack on refractory material and with such steels, 25% of the macro-inclusion content was contaminated with material from the nozzle (20%) and the stopper (3-6%), both of these being fireclay. Graphite nozzles were found to give less erosion products than fireclay ones. It was also found that wear on fireclay nozzles was reduced by impregnation with tar.

The bottom of the ladle is subject to considerable erosion when the steel flows out through the nozzle. This has been clearly shown by model experiments[141,142]. The quality of the cement in the ladle bottom can therefore be of considerable importance from the point of view of bottom wear. According to Ericsson, erosion in this region can be diminished by inserting the nozzle so that it stands up from the bottom of the ladle. It is even better, apparently, if the nozzle is surrounded by a wall or dam in the ladle bottom, probably because of the more favourable flow conditions.

Ericsson reported that during uphill-teeming of killed 0.4% C steel involving two different alumino-silicate runner brick qualities containing 32% Al_2O_3 and 17% Al_2O_3, the latter resulted in fewer inclusions in the steel even though it spalled more than the higher Al_2O_3 quality. This indicates that high abrasion of any refractory material does not necessarily imply an increase in the inclusions present in the ingot, although possible reasons for the effect were not discussed.

Investigations in the USSR showed that, under particularly unfavourable conditions, up to 8% of the inclusions in the steel may originate from magnesite used for the taphole[111]. Pieces of magnesite are swept into the ladle by the metal stream during tapping. This is certainly a surprising result and indicative of careless "housekeeping', since for a 350 t cast having a total inclusion content of 0.1%

(average value), 8% of inclusions as referred to above is equivalent to the erosion of about 28 kg magnesite.

In an investigation into the possible contribution of ladle lining material to the non-metallic content of the ingot, several kilograms of refractory impregnated with calcium-45 solution were placed on the bottom of a ladle prior to tapping steel into it. Autoradiographs of rolled metal samples showed that as much as 5% of the total inclusions could arise from this source. This work also emphasised the importance of carefully cleaning loose refractory materials and dirt from launders, ladles, and ingot moulds.

(i) Ladle Erosion

It is relevant at this stage to discuss the types of refractory materials used for ladle linings as it will be shown later than these can have a marked effect on the nature of the erosion products present in the liquid steel. The local conditions at a particular Works govern the size and shape of a ladle, but the ladle lining is normally a compromise between cost and the chemical and mechanical requirements[143]. Only in very few instances does cost not play an important part and this only happens when the application is so arduous that there is no alternative choice of material. In the majority of cases, the cost effectiveness is the criterion by which the final choice of lining material and technique are chosen. As steel quality requirements become more exacting, however, the importance of this parameter may well become less.

In certain cases such as vacuum degassing, continuous casting and after-furnace steelmaking, ladle linings have more stringent requirements placed on them because of the higher tapping temperatures, the increased slag covering for insulation purposes and the longer holding (residence) times. Before discussing lining details, it is necessary to summarise how a lining wears. Wear occurs by three basic mechanisms:-

(a) Chemical attack by slag and steel.

(b) Physical damage by temperature and ingress of the slag or steel into the refractory surface.

(c) Mechanical damage by thermal and physical stresses being set up in the refractory.

The slag layer is generally more destructive towards the ladle lining than is the steel itself and the attack will be more pronounced the thicker the slag layer. The degree of corrosion and rate of chemical reactions depend on the chemical composition of the slag and the steel, the teeming temperature, and the physico-chemical composition of the refractories. Operating conditions such as standing time and casting time will also affect the rate of corrosion. In addition, the refractory working surface does not operate under the same conditions throughout. The upper part of the refractory material will be generally more severely attacked since it will be in contact with fresh unsaturated high temperature slag, and will be in contact with slag for a longer period of time than the other parts of the refractory lining. The corrosion is mainly caused by manganous oxide, iron oxide and lime, which react strongly with the silica and other materials in the refractory lining material. The volume of slag is one of the most important factors in determining the life of a ladle lining. Basicity of the slag is also an important factor in controlling the rate of solution.

Fireclay brick is the most commonly used ladle lining material. Increasing the alumina content at low levels has been shown to increase slag-lining reactivity. However, it has also been shown that increasing alumina content over 30% causes a reduction in reactivity and at levels over 60% the reactivity is considerably reduced. The chemical nature of the lining is also influenced by ladle working temperature in that if the ladle is preheated or the metal is superheated prior to the metal being continuously cast, then a higher grade alumina refractory may be required e.g. 85% Al_2O_3.

Over the firebrick range of composition, little basic slag absorption is needed to convert the working face of the ladle brick to the wholly molten state at steel teeming temperatures. The controlling factor regarding the rate of attack of the

lining has been shown to be the viscosity of the reaction layer. The viscosity of the reaction products increases with increase in silica content, thereby diminishing the ladle attack. Therefore the benefits of higher Al_2O_3 content in fireclays are only to be obtained by producing bricks of low porosity. Owing to the low thermal conductivity of firebrick, only a very thin layer of the brick is subject to a working temperature near its melting point.

The surface area of brick in contact with slag or metal is clearly one of the factors governing the rate of ladle attack. Therefore an important feature of an effective brick lining is that it should not shrink, thereby developing gaps and cracks. For this reason an expansile cement is generally preferred. It is also essential that the jointing material is at least as chemically efficient as the bricks it is supporting, otherwise the joints will become preferentially eroded. Surface area is also governed by brick porosity. The denser the material, the less is the area exposed to attack. However, a very dense material may well have bad thermal shock resistance, and therefore there must be a compromise between the two properties. Fluid slag or metal may be drawn up into the brick pores by a capillarity effect and if the ladle undergoes heating and cooling cycles, solidified slag may block the pores and inhibit further attack.

Mechanical wear of the ladle lining occurs when steel is tapped into the ladle and strikes the lining. Metal turbulence occurs as the steel is continued to be tapped into the ladle and also if the ladle is bottom-teemed, leading to pronounced wear on the bottom few courses of brickwork. Deskulling also causes mechanical wear. The solidified metal tends to get in between the brickwork and when the skull is removed, serious damage can be caused to the brickwork. Monolithics have been used in an attempt to get over this problem, but there is danger of considerable erosion from the metal stream on large ladles. Due to rapid heating, considerable thermal stresses

are set up in the ladle and this can lead to spalling. Monolithics, however, have a less rigid texture and are therefore able to better absorb these stresses.

Although firebrick linings are still extensively used[144], longer holding times, higher teeming temperatures and the demand for higher quality steel have led to considerable interest in high alumina refractories[145-147], which, however, have certain disadvantages. A conventional ladle lining surface tends to 'clean itself' whereas high alumina does not. The latter also tends to produce a solid skull and on removal of the skull, lining damage occurs: also, as a result of the large heat capacity of high alumina refractories, the metal tends to be chilled. However, temperature drop and skull formation can be lowered to acceptable limits by the use of a firebrick safety layer together with adequate preheating of the ladle. Schroth and Bays[146] found that with 50% Al_2O_3 bricks, there was no skulling problem whereas 70% Al_2O_3 gave moderate skulling.

It is well known that high alumina refractories do not expand enough to close joints and prevent metal penetration. In order to overcome this problem, phosphate-bonded high alumina mortar is used. This develops strength at low preheat temperatures (approx. 250°C) and becomes stronger with heating. It also shows low permeability and appears to resist wetting by slag and molten metal.

(ii) Runner Erosion

The runner brick assembly in uphill teeming systems has long been recognised as a source of non-metallic inclusions, which originate from erosion of the alumino-silicates, particularly by higher-manganese steels. Such erosion products are very readily observed in silicon-killed steels, but they are not so readily observed in heavily aluminium-treated steels because of reaction between the erosion products and the aluminium dissolved in the steel to form alumina and spinels[102]. Nevertheless, such reaction products can contribute to the total inclusion content of the steel.

It has already been stated that the surface layers of alumino-silicate refractories

which have been in contact with liquid steel can contain appreciable amounts of corundum, and Pickering reported a particularly severe example of the entrapment of a large mass of alumina from this source. This type of refractory erosion has also been observed to give rise to quality control problems in higher manganese stainless steels[148], and it is clear that where such erosion problems are likely to occur, particular attention should be paid to the quality of the runner bricks.

In 1943, Rait[149] published the results of a detailed investigation into the formation of inclusions from casting pit refractories. It was shown that manganese in the liquid steel reduced the free silica of firebrick and the resulting MnO fluxed the refractory, Fig. 2.87, to form a liquid manganese alumino-silicate phase. This was washed off the runner bricks and carried into the ingots. The compositions of the manganese alumino-silicate reaction layers were discussed in terms of the $MnO-Al_2O_3-SiO_2$ phase diagram. It was found that a line drawn from the MnO corner of the diagram through the composition of the reaction layer intersected the Al_2O_3-SiO_2 side of the diagram at the approximate composition of the firebrick from which it was derived.

Following the investigations of Rait, several workers studied inclusion pick-up from uphill-teeming refractories, notably Post and Luerssen[150], Snow and Shea[151], Fedock[152], Carney and Rudolphy[153], and Van Vlack and his co-workers[127,128].

Smith and Banks[154] studied the reactions that take place when liquid steel comes into contact with refractory runner bricks. In the first part of their investigation, they examined the effects of steelmaking and casting pit variables on the degree of attack of the bricks. It was observed that the runner bricks suffered considerable erosion as a result of attack of the free silica in the fireclay refractory by aluminium and manganese in the steel. At the working surface, very little free silica remained in the fireclay and a (mullite + liquid) phase was formed. The steel/refractory reaction in rimmed steel was promoted by manganese, in the absence of aluminium,

producing glassy reaction products and a general glazing of the refractory. In killed steel with a low aluminium content in addition to manganese, the steel/refractory reaction was modified and the reaction layer contained some precipitated alumina. In the case of killed steel with a high aluminium content, the reaction layer was rich in alumina and appeared as a whitish, powdery deposit. Refractory attack was most severe in runners on the first plate to be teemed, the attack progressively decreasing in severity during teeming of the cast. The reason for this was not obvious although the investigators tentatively suggested that the decrease in the temperature of the steel and its aluminium and manganese contents during teeming may have been the cause. This suggestion seems reasonable in the case of the ladle temperature and aluminium content, but the decrease in manganese content between the first and last plates to be teemed was generally less than 0.1% and therefore not likely to affect significantly the rate of refractory attack. The degree of attack did not appear to be dependent upon the teeming speed. Although a proportion (unspecified) of the steel/refractory reaction products, which passed along the runners into the ingot being teemed, floated into the surface scum, some were found to contaminate the steel in the form of exogenous inclusions.

In the second part of their investigation, Smith et al carried out a programme of laboratory work to study the effect of steel composition, temperature and time of contact with the refractory on the degree of attack suffered by the runner bricks. It was found that the bricks having the greater alumina content and the smaller free silica content were superior in all respects. Higher manganese contents in the liquid steel increased the glassy nature of the steel/refractory reaction layer. In contrast, the addition of aluminium had very little effect and the formation of an alumina-rich layer similar to that observed in the first part of their investigation was not reproduced. They attributed this to the fact that the aluminium contents of the laboratory melts were considerably less than those of the production casts in Part 1 and therefore a glassy reaction layer was to be expected. However, other investigators[155,156] have

observed a similar difference in the effect of aluminium in the steel on the alumina content of steel/refractory reaction layers produced in laboratory dip-tests and those produced on actual runner bricks during teeming, i.e. the white, powdery alumina deposit formed on runner bricks during teeming could not be duplicated in laboratory immersion experiments. The reason for this anomolous behaviour is not fully understood although it is possibly a result of the very different steel flow conditions existing in the two situations. It is also observed that the surface appearance of steel solidified in a runner brick having an alumina-rich reaction layer is comparatively smooth whereas in a runner brick having a glassy manganese alumino-silicate layer, the solidified metal is rough and pitted. It has been suggested[155] that the formation of a compact, infusible layer of alumina on the surface of runner bricks is superior, in terms of overall steel cleanness, to a glassy liquid layer and should therefore be sought. Not only is erosion less, but the dendritic alumina layer acts as a 'filter' for the liquid steel and removes, for example, alumina deoxidation products present in the metal. (The steel flow conditions in the runner bricks are probably comparable to those immediately adjacent to the lining in an HF induction furnace or ASEA - SKF ladle unit, i.e. high rate of metal circulation, and as previously discussed in section 2.3.4, these conditions can result in the removal of large numbers of inclusions by the refractory lining.) This is an interesting theory and experimental work is being initiated to examine it on a quantitative basis. The only reservation is that if large clusters of alumina are torn from the refractory surface by the metal flow, particularly in the final stages of teeming, then they may not escape very readily in the mould. However, this is a matter which needs further investigation.

Smith et al observed that reaction between erosion products and aluminium dissolved in the liquid steel resulted in the formation of highly aluminous inclusions associated with showers of alumina particles. A similar reaction mechanism was also suggested by Pickering. Although a proportion of the erosion products were found in the ingot scum, some large inclusions were found in sections of the solidified

ingots. Forging and examination of the sections showed that these inclusions were identical to those found in ultrasonically rejected tube material.

(iii) Mechanism of Refractory Attack

Stephenson, Gladman and Pickering[156] studied the effect of manganese and aluminium in molten steel on the erosion of an alumino-silicate brick containing 42% Al_2O_3. According to these investigators, manganese in liquid iron reacts with solid silica according to the equation:-

$$2\,\underline{Mn} + (SiO_2) \longrightarrow (MnO) + \underline{Si} \qquad \text{eqn. (2.32)}$$

The free energy change, ΔG, for this reaction is negative mainly because of the very low activity coefficient of silicon in liquid iron. Aluminium should also react with silica in a similar manner:-

$$4\,\underline{Al} + 3\,(SiO_2) \longrightarrow 2\,(Al_2O_3) + 3\,\underline{Si} \qquad \text{eqn. (2.33)}$$

Under the experimental conditions of their investigation, the behaviour of manganese and aluminium were expected to be very similar.

If the SiO_2 reacts exclusively with manganese, the composition of the surface layers moves from a position on the Al_2O_3-SiO_2 binary into the MnO-Al_2O_3-SiO_2 system following the line AB in Fig. 2.88, where A represents the initial brick composition and B represents complete conversion of SiO_2 to MnO. The constitution changes from mullite and cristobalite to mullite, cristobalite and a liquid of composition a. As the MnO content increases, cristobalite disappears and the liquid composition moves along the 1550°C isotherm until, at point b, mullite disappears completely. The viscosity of the liquid decreases as the SiO_2 content decreases, so that the probability of erosion increases as the liquid composition changes along ab. With a further increase in the MnO content, the composition enters the corundum primary phase field and alumina is precipitated from the melt.

Once the liquid phase forms on the surface of the brick, complex silicate polyanions, e.g. SiO_4^{4-} and $Si_2O_7^{6-}$, react with manganese in the metal to give

silicon of low activity in liquid iron:-

$$SiO_4^{4-} + 2\,\underline{Mn} \longrightarrow \underline{Si} + 2\,Mn^{2+} + 4O^{2-} \quad .. \quad .. \quad \text{eqn. (2.34)}$$

$$Si_2O_7^{6-} + 4\,\underline{Mn} \longrightarrow 2\,\underline{Si} + 4\,Mn^{2+} + 7O^{2-} \quad .. \quad .. \quad \text{eqn. (2.35)}$$

Some of the O^{2-} ions dissolve in the molten steel, but others, together with Mn^{2+} ions, diffuse through the liquid surface layers and effectively reduce the degree of polymerisation of the silicate polyanions.

If some of the SiO_2 reacts with aluminium, the compositional changes occur to the right of AB and the constitution shows an enrichment in mullite or even in corundum if sufficient reaction with aluminium takes place. In conditions where the aluminium-silica reaction predominates, an alumina-rich layer would be expected to form on the surface of the brick, perhaps acting as a barrier to further attack.

In their laboratory dip tests with an alumino-silicate brick containing 42% Al_2O_3, Stephenson et al found that increasing the manganese content of the liquid steel caused an increase in the rate of refractory erosion. Manganese penetration occurred in the silica-rich regions of the brick and the compositional changes resulted in the formation of a single-phased liquid at the hot face. The composition of this liquid was approximately 30% MnO, 30% Al_2O_3 and 40% SiO_2. Aluminium additions to the liquid steel caused no significant change in either the rate of refractory erosion or the composition of the hot face. In these experiments, therefore, erosion apparently proceeded according to equation (2.32).

Wahlster et al[116,117,157] showed that the reduction of silica in firebrick by manganese in liquid steel proceeds stoichiometrically according to equation (2.32) and the MnO produced by this reaction decreases the melting point of firebrick to quite an extent so that a liquid alumino-silicate phase containing high amounts of MnO forms at the surface of the refractory in contact with the molten steel. This liquid oxide layer is eroded from the surface of the firebrick and distributed as inclusions in the melt. A summary of the results obtained by Wahlster et al is presented in

Fig. 2.89. The upper part shows the identical nature of the reaction layers at the firebrick surfaces and manganese alumino-silicate inclusions in heavy plate. In the lower part of Fig. 2.89, the direction of reaction between silica and manganese is clearly shown. These workers concluded that decisive improvements can be obtained by using ladle linings with higher Al_2O_3 contents, mullite or bauxite linings, or magnesite- or dolomite- based linings.

The mechanism of refractory attack has been similarly discussed by Narita[158], and by König et al[4]. In the latter case, these workers postulated that reaction (2.32) proceeds preferentially in steels with low or medium carbon contents having high Mn : Si ratios. With increasing residual aluminium content, reaction (2.33) is then possible.

Schwerdtfeger and Schrewe[159] discussed the chemical equilibria between aluminium - deoxidised steel and refractory oxides at 1550°C. Their results for the systems Fe-Al-Cr-O, Fe-Al-Si-O and Fe-Al-Zr-O are given in Fig. 2.90. The upper part of the diagram shows that the respective oxide systems Cr_2O_3 and Al_2O_3 form a continuous series of solid solutions. Hence, the relationship between the chromium and aluminium contents of the metal phase (lower part of Fig. 2.90a) depends very much on the composition of the solid solution. SiO_2 and Al_2O_3 form a compound, mullite, $3Al_2O_3 . 2SiO_2$, as shown in Fig. 2.90b. Hence, two equilibrium curves exist for the composition of the liquid steel, one for the equilibrium $Fe-SiO_2-3Al_2O_3-2SiO_2$, and the other for the equilibrium $Fe-3Al_2O_3.2SiO_2-Al_2O_3$. At compositions between the two curves, only mullite is stable. At silicon contents higher than those given by the upper curve, silica is the coexisting phase; and at silicon concentrations smaller than those represented by the lower curve, alumina is the equilibrium oxide. The $ZrO_2-Al_2O_3$ system is a simple eutectic system, Fig. 2.90c. Both oxides coexist with each other. Hence, there is

only one curve in the lower diagram which limits the stability regions for ZrO_2 and Al_2O_3. Figure 2.90 shows that aluminium is a strong reducing agent with respect to chromium oxide and silica. In contrast, zirconia is very stable and may be considered an ideal refractory oxide from the standpoint of possible chemical attack. However, the rate of actual reduction is governed by kinetic factors and refractories may behave well although equilibrium conditions are unfavourable. For instance, if aluminium-deoxidised iron is brought into contact with Cr_2O_3, the resulting Al_2O_3 may form a dense layer on the Cr_2O_3 and further reaction may be very slow because the inter-diffusion in the oxide solid solution will be rate controlling. The same is true of attack on silica in the case where a protective layer of alumina or mullite is formed.

(iv) Flow of Steel Through Nozzles

Another very important aspect of steel-refractory interaction is that associated with the flow of steel through nozzles. Depending upon the chemical composition of the steel being cast and the type of nozzle being used, two contradictory behaviours can be observed, i.e. an increase in nozzle bore caused by erosion of the refractory, Fig. 2.83, or a reduction of the nozzle bore as a result of the deposition of non-metallic inclusions on the surface of the nozzle.

The state of oxidation of the metal is of paramount importance in determining nozzle wear and/or blockage. Chemical attack and erosion are enhanced by the large contact surface and the continuous renewal of material caused by the flow of metal. Low carbon steels which are often high in oxygen are also teemed at higher temperatures than carbon and alloy steels and this also enhances erosion.

It is a well known fact that aluminium-deoxidised steels are more difficult to teem through nozzles than silicon-deoxidised steels, because the former tend to 'block' the nozzle[160,161]. In the past, however, the problem was not considered as a major one and in practice, whenever the nozzle showed signs of becoming constricted, teeming rates could be maintained by clearing the nozzle with an oxygen lance.

Consequently, very little attention was given to the mechanism of nozzle blockage. Occasional studies were undertaken, e.g. Snow and Shea[151] reported the occurrence of "corundum-glass tufts" covering the bore surface of nozzles used to teem aluminium fine-grained steels, but no systematic attempt to follow up such observations was made.

With the increasing application of continuous casting during the 1960's, however, teeming difficulties resulting from the use of aluminium became acute. In some instances, the addition of aluminium was discontinued and vanadium or niobium were used for the production of fine-grained steels[138]. In addition, the use of oxygen lancing to clear nozzles was recognised as an operation which was likely to result in a dirtier steel. Consequently, investigators began to study in detail the mechanism of nozzle blockage characteristic of aluminium-treated steels in the hope of eliminating or at least minimising the problem.

In 1967, Duderstadt, Iyenger and Matesa[162] showed that nozzle blockage, which occurred while casting steels deoxidised with various amounts of aluminium, was associated with the precipitation and agglomeration of alumina in the nozzle bore.

Farrell and Hilty[163] carried out a detailed laboratory study of the effects of various deoxidising elements on the flow of liquid steel through nozzles. Equipment was constructed for comparing flow rates and the causes of nozzle blockage were evaluated by metallographic techniques. Their observations indicated that any deoxidation treatment producing an oxide phase that is solid at steel teeming temperatures, e.g. aluminium, zirconium, titanium, the rare earth metals and even silicon in the absence of manganese, can be expected to impede the flow of steel through a nozzle and ultimately cause the nozzle to become completely blocked by precipitation and accumulation of the oxide in the nozzle bore. They postulated that, as the steel enters the nozzle bore during teeming, it is chilled significantly by contact with the relatively colder nozzle refractory. The net result of this temperature drop is the precipitation of oxide inclusions to satisfy a new oxide solubility product. Once under way, this

process accelerates and since the oxide phase is a solid, its formation at the nozzle throat restricts the opening. When this occurs, the flow rate is reduced and the residence time of the steel at the nozzle inlet increases, resulting in a greater degree of cooling followed by more precipitation until complete blockage occurs.

According to Farrell et al, the nature of the bonding force between the precipitates and the nozzle material is not clearly understood. For example, metallographic examination of the interface between the refractory and the oxide precipitate shows no apparent reaction. Nevertheless, the precipitate adheres very strongly. In addition, while the up-stream growth of dendrites correlates with the mechanism of precipitation, it is difficult to explain why the relatively fragile branches remain in place and continue to accumulate in spite of the washing action of the steel flow.

At the 1970 Electric Furnace Conference, Schwerdtfeger and Schrewe[159] presented a paper discussing the results of their work on the contribution of reoxidation products formed by reaction between aluminium in steel and tundish refractories to nozzle blockage. In their experiments, the precipitation of indigenous alumina-type deoxidation products was minimised by vacuum carbon deoxidation of the heat prior to final deoxidation with aluminium. They concluded that interaction between aluminium in the steel and oxides in the refractories (particularly moisture and iron oxides in magnesite tundish linings) contributed to the nozzle blockage problem, although the role played by such reaction in production heats was not as serious as in laboratory scale experiments. (This source of reoxidation is not to be confused with atmospheric reoxidation discussed earlier.) In the experiments of Farrell and Hilty, it is probable that, because of the short flow times, the formation of indigenous deoxidation products outweighed any reaction between refractories and the deoxidisers present in the steel.

Fortunately, not all continuous casting operations are as vulnerable to nozzle blockage as those using small diameter metering nozzles. Aluminium is used daily in the ladle deoxidation of steel in the production of large billets and slabs by continuous casting. In these cases, the problem is dealt with adequately through use of large

diameter nozzles and/or stopper rod control which helps to break loose accumulations of precipitated alumina.

Several real or potential process techniques have been cited for dealing with the nozzle problem. One of the most interesting approaches to preventing blockage while continuously casting aluminium-killed steel is that described by Meadowcroft and Milbourne[164]. Their process involves the use of an inert gas to purge a porous refractory nozzle during a cast, thereby preventing the build-up of alumina in the bore.

Two other suggestions which have been made are somewhat related to one another. Since it is a drop in temperature which causes alumina to precipitate, these call for maintaining the temperature of the nozzle at or above the temperature of the steel in the ladle during a cast, or preventing any temperature loss between the furnace and mould. The mechanics of either approach could prove formidable.

Self-eroding nozzles may work adequately, although the metering feature of the nozzle would have to be sacrificed. In addition, excessive erosion of refractory material into the steel could adversely affect steel cleanness, particularly in continuous casting.

Problems of nozzle blockage have been avoided in some Works by feeding aluminium wire or granules to the metal stream during teeming. Whilst this technique does provide sufficient aluminium for grain size control, the primary deoxidation products formed in the mould may not escape very readily. In addition, unless carried out under controlled conditions, reoxidation can lead to a very dirty steel.

The simplest solution would be a chemical one in which the melting temperature of the oxides produced by the strong deoxidisers would be lowered below that of the steel, as occurs with silicon-manganese deoxidation. In this respect, the use of calcium-containing deoxidants to produce certain types of calcium aluminate and calcium alumino-silicate inclusions which are liquid at steel casting temperatures might prove extremely beneficial.

2.5 PURPOSE OF PRESENT WORK

The main purpose of the present work was to improve the cleanness of several different types of steel by first determining the nature and origin of the inclusions formed at various stages during the steelmaking, tapping and teeming processes. At the same time, it was also possible to study in greater detail the effects of many of the process variables discussed in Section 2.4 on the inclusions present in the liquid metal. This was particularly so in the case of exogenous inclusions picked up during tapping and teeming as it may be seen from the preceeding review that information concerning the effect of slag entrainment, reoxidation and refractory erosion on product quality is to a certain extent inconclusive.

SECTION 3

DETAILS OF INVESTIGATIONS AND EXPERIMENTAL PROCEDURE

SECTION 3 - DETAILS OF INVESTIGATIONS AND EXPERIMENTAL PROCEDURE

3.1 BASIS OF WORK

The basis of the work comprised a number of planned investigations into the types of oxide inclusions present at various stages during the steelmaking, tapping and teeming of several qualities of steel made by basic electric arc and open-hearth processes. A series of trials were carried out at various Works within the Special Steels Division, and it was possible to study the effects of numerous process variables during steelmaking on the nature of the non-metallic inclusions present in the liquid metal. Full details of the trial casts are given in Section 3.7.

3.2 METHODS OF SAMPLING

Liquid metal samples were taken from the furnace, ladle and ingots at various stages during the steelmaking, tapping and teeming processes. The sampling device employed is shown schematically in Fig. 3.1. It consisted of a 0.61 m long cardboard tube of the type used in the construction of 'Temtip' thermocouples. Into the bottom end of this tube was fitted a small metal mould so that the bottom of the mould was level with the end of the tube. Approximately 25 mm above the top of the mould, a small hole was cut in the cardboard tube. This hole was then covered with several layers of tape. A second hole (not shown in Fig. 3.1) was cut in the tube approximately 100 mm from the top end. This hole was left uncovered for gases to escape.

The tube was then fitted on to the tapered end-piece of a long sampling rod and metal samples were taken by immersing the bottom end of the tube containing the mould in the liquid steel, the tape preventing slag from entering the mould as the tube was immersed. The steel eventually burned through the tape and flowed into the mould. In the case of furnace or ladle samples, car masking tape was used to cover the metal entry hole. For the ingot samples, however, Selotape was found to be adequate for preventing the ingress of mould additive.

The liquid metal samples were not further killed in any way in the sampling mould: consequently, the inclusions present in the solidified samples consisted of:-

(i) relatively large inclusions which were present in the liquid metal

(ii) very small inclusions which were precipitated from the melt during the rapid cooling and solidification of the samples.

In general they were reasonably sound and it was possible to obtain many examples of the inclusions present simply by preparing metallographic sections.

Metal samples were taken from the top of the ladle immediately after the completion of tapping, and at various stages of vacuum degassing for those casts which were degassed. Again, these samples were not further killed in any way.

During teeming, metal samples were also taken from the tops of certain ingots as the level of liquid metal approached the tiles, and from the ladle stream. In the latter instance, the sample was normally taken by reducing the flow of metal through the nozzle and collecting the sample in a spoon. The liquid metal was then poured from the spoon into a small mould. In other cases, the sample was taken directly from the stream into the mould. Again, these samples were not further killed in the sampling mould.

In addition to the liquid metal samples, furnace slag samples were also taken whenever possible during steelmaking, and in some cases, ladle slag samples were taken before and after teeming. The analyses of all the steelmaking and slagmaking additions were obtained, the types of refractories used throughout steelmaking, tapping and teeming were recorded, and the amount of furnace and/or ladle wear was estimated for each cast. Where appropriate, sections of billets, bars, etc., from the cast were also taken for examination in order to compare the inclusions present in the liquid metal with those in the rolled product.

During the whole of the steelmaking, tapping and teeming processes, a detailed chronological record was kept of all the operations carried out including the sampling. In this way, it was possible to relate the analyses of the metal, slag and inclusions

directly with the actual details of the steelmaking practice.

3.3 METALLOGRAPHIC EXAMINATION

All the metal samples were sectioned and prepared for metallographic examination on $\frac{1}{4}$ μm diamond. Even though the samples sometimes contained blowholes, it was always possible to obtain solid material containing the types of non-metallic inclusions present. By normal optical metallographic examination, a representative number of the different types of inclusions in each sample were selected and marked for subsequent examination by electron-probe microanalysis. Where appropriate, the inclusions in sections from the finished and semi-finished products (billets, bars, plates, forgings, etc.) were also examined in this way. It should be emphasised that the examination was particularly aimed at establishing the types, sizes and analyses of the inclusions which occurred at different stages of the steelmaking process and not in the quantitative assessment of the number or volume fraction of the inclusions. However, when occasional quantitative work was carried out to provide details of the approximate variation in the inclusion content during the steelmaking, tapping and teeming processes, the results were remarkably consistent.

3.4 ELECTRON-PROBE MICROANALYSIS

Inclusion compositions were determined 'in situ' by the use of electron-probe microanalysis. The instrument used was a Cambridge Microscan Mark V.

3.4.1 The Principles of the Instrument

When a beam of electrons is emitted from a hot cathode source and accelerated via a high potential (25 kV in the present case) and made to hit a target, the absorbed electrons cause X-rays to be emitted from the target characteristic of the elements present in the irradiated volume. The important feature of the microanalyser is the fact that the incident beam of electrons is very finely focused when it hits the target or sample, being of the order of one micron or even less in diameter. This fine beam is focused via the condenser and objective lenses of the optics system, in addition to

which there are two sets of scanning coils present allowing the focused 'spot' to be systematically scanned over selected areas or lines as required. The X-rays which are emitted are incident upon the analysing crystal of the fully-focussing spectrometer, which can be set in accordance with Bragg's Law:-

$$n\lambda = 2d \sin \theta \quad .. \quad .. \quad .. \quad \text{eqn. (3.1)}$$

to select the particular X-radiation characteristic of the element in question. The X-rays are subsequently detected by a proportional counter and the resultant signal is amplified and fed into the display and recording sections of the instrument.

The 'back-scattered' electrons are also detected via a phosphor, photomultiplier and scintillation counter, the resultant signal also being amplified and fed into the display equipment. These back-scattered electrons are dependent upon two main properties of the sample. Firstly, the higher the atomic number of a region, the greater is the degree of back-scatter from that region as opposed to a region of lower atomic number. Thus, if a known element, e.g. iron in a steel sample, is used for reference, an area appearing lighter or darker (signal intensity) will have a correspondingly higher or lower mean atomic number than the reference area. Secondly, the surface finish of the sample is of great importance. With rough surfaces, different incident angles of the electrons will result giving rise to light and dark adjacent regions caused by varying degrees of back-scatter.

3.4.2 Problems of Analysis

As stated in the previous section, the surface finish of the sample is of great importance and for accurate quantitative analysis, it is essential that the specimen and the comparison standards be as flat as possible. Because of variations in the effective X-ray take-off angle, rough surfaces will also cause different X-ray intensities to be registered depending upon topography rather than upon composition. For example, it has been shown[165] that for a 20° take-off angle, if an error of 2° occurs in the inclination of the specimen surface to the incident beam, or if the analysis takes place

in a $\frac{1}{2}$ μm deep groove, then when analysing for magnesium in iron, an error of about 10% will occur. Similar effects have been obtained by Salter[166], who has shown that, even with semi-focusing spectrometers, an error of 1% will occur for a specimen height variation of about $\frac{1}{2}$ μm. Hence, for all accurate quantitative analysis, a good metallographically polished surface is essential.

The method of analysis is to compare the intensity of X-rays for a specific element from the sample with those obtained from a pure standard of the element. Then, to a first approximation:-

$$C_A = I_A/I_{(A)} \quad .. \quad .. \quad .. \quad .. \quad \text{eqn. (3.2)}$$

where C_A is the true concentration of A in the alloy

I_A is the intensity of X-rays from A in the alloy (usually K_α or L_α lines are used)

$I_{(A)}$ is the intensity of X-rays from the pure standard of A

Unfortunately, the relationship is not quite as simple as this. There are several factors which have, in certain circumstances, a marked effect upon the ratio. Hence, it is more usual to write equation (3.2) in the form:-

$$K_A = I_A/I_{(A)} \quad .. \quad .. \quad .. \quad .. \quad \text{eqn. (3.3)}$$

where

$$K_A = (F).C_A \quad .. \quad .. \quad .. \quad .. \quad \text{eqn. (3.4)}$$

where K_A is the measured or apparent concentration of A in the alloy and (F) is some function which can be greater or less than unity depending upon the prevailing conditions These factors are generally very complex, and only a brief outline will be given here. The factors involved can be considered under three main headings as follows:-

(i) Absorption

This condition prevails between all elements, including self-absorption, and occurs where the emitted X-rays are absorbed by the material before they are able to escape and be detected. The absorbing power, given in terms of the mass absorption coefficient, is a maximum at the lower wavelength side of the absorption edge and is

considerably less at the higher wavelength side. This is because as the wavelength decreases, so the energy increases and penetration increases, hence decreasing absorption. At the absorption edge there is an abrupt change which signifies a further release of electrons and the utilisation of the X-rays of this wavelength and energy, and those of immediately shorter wavelength; thereafter the mass absorption coefficient decreases once more. The magnitude of this absorption depends upon the elements present and, therefore, differs between sample and standard. As a result, the apparent concentration, K_A, is less than the true concentration, C_A.

(ii) Fluorescence

If the energy of the characteristic X-rays of one element is slightly greater than the absorption edge energy of a second element in the same sample, then strong absorption of the characteristic X-rays by the second element occurs. The absorbing element is excited and in returning to the ground state it may emit characteristic radiation. These secondary X-rays add to the intensity of the primary X-rays of the same wavelength emitted by that element as a result of absorption of electrons from the incident beam. This increase in intensity of the characteristic X-rays of one element caused by the absorption of the characteristic X-rays of another is termed the characteristic fluorescence effect. The fluorescence of iron by nickel and copper are good examples of this effect in steels.

(iii) Atomic Number Effect

The number of characteristic X-rays produced in the sample per incident electron is a function of the average atomic number of the sample. Thus, the number of Fe K_α X-rays produced in a sample of Al-1% Fe is quite different from the number produced in a sample of U-1% Fe for the same excitation conditions. Differences in back-scattering and stopping power for electrons have been shown to be the cause of this effect.

3.4.3 Methods of Analysis and Correction Procedures

It is not intended that a critical examination be given of the various absorption and fluorescence correction formulae which have been evolved, as these are well covered in the literature[166-173]. Hence, passing reference only is made to the formulae used. However, a detailed description of the correction procedure is presented, including a worked example.

The surfaces of all the specimens examined were prepared on $\frac{1}{4}$ μm diamond and then coated with 100-200Å thick layers of copper to eliminate charging-up effects. Count rates for various elements were determined and compared with the count rates from standard oxides, sulphides and fluorides. Quantitative analysis for the different oxides, e.g. FeO, MnO, P_2O_5, Al_2O_3, SiO_2, CaO, MgO, K_2O, TiO_2, were then obtained from correction curves based on Philibert's absorption formula[168] and Duncumb and Reed's atomic number formula[170] as discussed by Salter[166]. In general, the correction required for fluorescence in these oxide systems was negligible[167]. Normal operating conditions involved an accelerating voltage of 25 kV and a specimen current of approximately 0.1 μA. The X-ray take-off angle was 75° for a normally-incident electron beam.

A typical binary correction curve is shown in Fig. 3.2, whilst Fig. 3.3 shows typical ternary correction curves[167]. The ternary curves are constructed such that the uncorrected concentration K_i for a component i (in the case of Fig. 3.3 this is an oxide) is represented by a linear ordinate indicated on the left-hand side of each family of curves. The other two components are presented as a ratio function on the horizontal scale. The co-ordinates, therefore, define a point in the diagram. The true concentration C_i corresponding to K_i is then found by relating the point to the positions of the immediate iso-concentration curves, the values of which are given by the non-linear ordinate on the right-hand side of the diagram.

Unfortunately, this procedure is unsuitable for quaternary or larger component systems as the number of graphs required would be inconveniently large. In these

cases, it is necessary to adopt a 'matrix correction' procedure[166] based on the assumption that the determination of one element is subject to corrections proportional to the amounts of the other elements present. It can be seen from Fig. 3.3a that this is not always so, although in many cases (Figs. 3.3b and c) the variation is almost linear. The more complex the system, the less the concentration of any particular element is in general and, as in Fig. 3.3a, these lower concentrations tend more closely towards a linear relationship. Thus, the correction factors are linear to a first approximation over small ranges of composition.

The relationships used in the 'matrix correction' procedure are given below:-

The uncorrected concentration of element i is K_i ($i = 1,2,3 \ldots$)

The corrected concentration of element i, in a binary system with element j, from the binary diagrams is K_i^j ($j = 1,2,3 \ldots$ but $i \neq j$).

The approximate estimated concentrations of i and j are $K_{(i)}$ and $K_{(j)}$.

The final corrected concentration of i is C_i. The process involved is an iterative one and initially it is necessary to obtain an approximate estimate $K_{(i)}$ of the various components. This is simply done by calculating the approximate contribution of each separate binary correction and summing for all the corrections which should be added to K_i to give $K_{(i)}$. Thus, for each component separately,

$$K_{(i)} = K_i + \sum \frac{(K_i^j - K_i) K_j}{100 - K_i^j} \qquad \text{eqn. (3.5)}$$

The next stage of the calculation is to weight the individual values of K_i^j from the pure binary systems by each of the intermediate corrected values $K_{(j)}$ as fractions of the total minus $K_{(i)}$ itself. In this way the proportional effects of each element are summed to give

$$C_i = \frac{\Sigma (K_i^j . K_{(j)})}{\Sigma K_{(i)} - K_{(j)}} \qquad \text{eqn. (3.6)}$$

A typical correction is given in Appendix 1 (take-off angle 20° at 25 kV).

3.5 OXYGEN ANALYSES

The total oxygen contents of the metal samples were determined by vacuum fusion analysis[174].

3.5.1 Apparatus

The furnace section of the apparatus consisted of a pyrex outer shell cooled by means of an air blower. A quartz test tube was suspended inside the outer shell by means of platinum wires. This tube was partially filled with sub -300 mesh graphite powder. Supported and surrounded by the powder was a graphite crucible with a capacity of about 150 g of liquid steel. The graphite crucible was fitted with a graphite funnel to ensure that the samples fell into the crucible. The furnace was heated by an induction unit and the temperature measured by means of an optical pyrometer.

The evolved gases (CO, H_2 and N_2) were removed from the furnace chamber by a mercury diffusion pump and passed over a copper oxide catalyst. This was contained in a quartz 'U' tube connected into the gas line immediately after the furnace diffusion pump. Its function was to oxidise the CO and H_2 in the evolved gases to CO_2 and H_2O respectively. The catalyst was operated at a temperature of 600°C and this was achieved by a resistance winding on the outside of the quartz tube.

Immediately following the catalyst was a water vapour trap consisting of phosphorus pentoxide in a silica boat, which was contained in a pyrex tube fitted with a ground joint and cap to facilitate renewal of the dessicant.

The remaining gases (CO_2 and N_2) were then collected in a constant volume reservoir. The total pressure of the gases collected was automatically measured by a transducer and recorded on a pen-recorder chart. The gas temperature could also be measured at any time.

The collected gases were then circulated through a liquid oxygen trap where the CO_2 was frozen out and retained. The remaining N_2 was then passed into the constant

volume reservoir and its pressure recorded in the same way as before. The difference between the two readings gave the pressure of CO_2.

3.5.2 Test Procedure

The apparatus was out-gassed at a temperature of 2300°C. The blank rate (prior to adding sample) of gas evolution was then determined at the test temperature (1860°C).

The surface oxide was removed from the specimen, which was then introduced into the furnace via a vacuum lock. The test was commenced and the gases collected until the gas evolution rate dropped to that of the blank rate. The collected gases were then analysed for CO_2 and N_2 as before. The time taken to return to the blank rate at the end of a determination occasionally seemed excessive, due usually to the sluggish evolution of N_2. This could be confirmed in any particular case by analysing the gases evolved, collecting a second fraction and establishing that this further fraction contained no CO_2. Under these circumstances, there was no necessity to remove completely all N_2 before proceeding with the next sample.

The transducer and recorder were calibrated against a McLeod gauge, using CO_2 from the liquid oxygen trap. The factor, F, for the weight of oxygen (g) equivalent to 1 chart division at 0°C was then given by:-

$$F = \frac{V \times 0.000714}{d} \qquad \text{eqn. (3.7)}$$

where V = volume of CO_2 at STP measured by the McLeod gauge

d = recorder divisions corrected to standard temperature (0°C)

The factor 0.000714 converts ml CO at STP to g oxygen

Then

$$\text{wt \% oxygen} = \frac{(A - B) - (a - b) \times F \times 273 \times 100}{W \times (273 + t)} \qquad \text{eqn. (3.8)}$$

where A = total gas pressure from specimen (recorder divisions)

B = nitrogen gas pressure from specimen (recorder divisions)

a = total gas pressure from blank for equivalent time (recorder divisions)

b = nitrogen gas pressure from blank for equivalent time (recorder divisions)

F = weight of oxygen (g) equivalent to 1 chart division at 0°C

W = specimen weight in g

t = ambient temperature in °C

3.6 CHEMICAL ANALYSES

In a number of the trials, the metal samples were analysed for aluminium and/or silicon. In the latter case, the analyses were carried out according to the British Standard Photometric Method No. 1121, Part 19 for acid soluble silicon. Within the limits of experimental error, the values obtained by this method were the same as the corresponding spectrographic analyses for total silicon content, i.e. using the photometric method, the silicate inclusions present in the sample must also have dissolved in the acid so that the acid-soluble silicon content was in fact equivalent to the total silicon content.

Acid-soluble and acid-insoluble aluminium determinations were based on the direct eriochrome cyanine R photometric method[175].

3.7 DETAILS OF INVESTIGATIONS

3.7.1 Occurrence of Inclusions in Vacuum Degassed Low Alloy Steel

This investigation was concerned with the cleanness of $2\frac{1}{4}$% Cr, 1% Mo steel produced by an open-hearth steelmaking/R.H. degassing route. Problems were being experienced owing to the occurrence of an excessive number of non-metallic inclusions in the billets and a sampling trial was therefore carried out to determine the nature and origin of the inclusions present in the liquid metal.

The trial (A.1) was on a 120 t open-hearth cast which had the following pit analysis:-

	Analysis, wt. %									
C	Si	Mn	S	P	Cu	Ni	Cr	Mo	Sn	Al
0.12	0.44	0.52	0.029	0.027	0.13	0.13	2.26	1.01	0.008	<0.005

The chronological record of the trial is given in Table 3.1 and a brief description of the procedure is as follows:-

A metal sample was taken from the furnace prior to tapping. The steel was tapped at a temperature of 1670°C and additions of 0.03% aluminium, 0.71% ferro-manganese, 0.36% ferro-silicon and 4.72% ferro-chromium were made to the ladle. Part of the ferro-chromium addition was placed in the bottom of the ladle before tapping. The ladle of steel was then transferred to the vacuum degassing unit and the steel was degassed for 32 min. The temperature of the steel at the end of degassing was 1570°C. The steel was uphill-teemed using a sliding-gate stopper and the mould additive was vermiculite.

3.7.2 Occurrence of Inclusions in Low Silicon Leaded Free-Cutting Steel

The composition of this steel is based on the specification A.I.S.I. 12L14 with an 0.01% max. silicon content for improved machinability. The analysis range is:-

	C	Si	Mn	P	S	N	Pb
Range, %	0.08 max.	0.010 max.	0.85/ 1.05	0.07/ 0.11	0.27/ 0.34	0.006/ 0.010	0.22 min.

This necessitates the careful control of silicon during steelmaking, tapping and teeming, including the use of special, low-silicon ferro-alloys. Despite these controls, the silicon content of ladle stream samples taken during teeming was found to be greater than 0.01% in some instances, indicating that pick-up of silicon over and above that present in the ferro-alloy additions had occurred. It was necessary therefore, that the source of this additional silicon be located so that steps could be taken to eliminate it.

Steelmaking trials were carried out on four casts of free-cutting steel to follow the variation in silicon content and to determine the nature of the oxide inclusions present in the metal. The chronological records of the four trial casts are shown in Tables 3.2 - 3.5. Trial cast B.1 was sampled from melt out whereas

casts B.2, B.3 and B.4 were only sampled from tap onwards as this was found to be the important period from the point of view of silicon pick-up.

The steel was made in a 120 t basic electric arc furnace using a single-slag practice. The charge to the furnace consisted of scrap, lime and coke, and melting down was accompanied by the use of oxygen which also helped to form an active oxidising slag. At melt out, the bath carbon content was normally about 0.15%. During the oxidising period, the bath carbon was lowered to 0.05/0.06% and the bath silicon to less than 0.005%. The melt was then blocked with low carbon, low silicon ferro-manganese. The furnace was tapped at a temperature of 1630/1640°C, and during tapping, ferro-manganese, ferro-phosphorus and rock sulphur were added to the ladle. The bulk of the steel was uphill-teemed, lead being added down the trumpet during the teeming of each plate. Occasional non-leaded ingots were direct-teemed for comparison with the uphill-teemed ingots. An oxygen lance was used on the ladle nozzle during casts B.2, B.3 and B.4. A summary of the steelmaking details for the trials casts is presented in Table 3.6.

3.7.3 Occurrence of Inclusions in Carbon-Manganese-Niobium Steel

This investigation was concerned with the production of C-Mn-Nb plate steel, which was required to have adequate resistance to lamellar tearing. The steel chosen for the application was modified B.S.4360, Grade 50D steel, which is basically a C-Mn-Nb quality supplied as plates in the normalised condition. The testing procedure specified for determining the susceptibility to lamellar tearing was the through-thickness tensile test. The steel was required to meet a minimum average reduction of area value from six tests on each plate. The basic electric arc steelmaking practice included a tight control of residual elements, a restricted carbon equivalent value and aluminium treatment.

The average through-thickness test results for the first series of production casts were approximately as follows:-

Average Reduction of Area Value, %		
Centre	Edge	Overall
26	42	34

In some instances, these tensile properties were below those required by the customer. In addition, the through yield (ingot to plate) for this material was low. The failure to meet the through-thickness properties, when this occurred, was caused by the presence of Al_2O_3 and/or MnS inclusions. Consequently, a steelmaking development programme was initiated, aimed at improving the quality of C-Mn-Nb plate steel so that a minimum reduction of area value of 40% average could be achieved on a regular basis. Steelmaking trials were carried out on three casts of C-Mn-Nb steel. The first (trial C.1) was made according to the original standard practice involving primary ferro-silicon deoxidation. The two subsequent trials (C.2 and C.3) were on development casts made to a modified steelmaking practice. Details of the original and modified practice are now given.

(i) Trial C.1

This cast was made according to the original standard practice involving a ferro-silicon bath block. The chronological record of the trial cast is summarised in Table 3.7 and a brief description of the procedure is as follows:-

The charge to the furnace was made in three baskets and consisted of 120 tonne scrap, 2.1 tonne breeze and 5.08 tonne lime. Melting down was accompanied by the use of oxygen which also helped to form an active oxidising slag. At melt out, the bath carbon content was 0.585%.

The bath was then blown and the slag was flushed over the sill during this period. The total time for oxidation was approximately 1 h and the bath carbon was lowered to 0.061%.

The slag was removed and then the bath was blocked with 0.67% ferro-silicon. This was followed almost immediately by the addition of 1016 kg Desulfex 75* to form

* Proprietary desulphurising agent - see Table 3.11 for full composition

a refining slag. Approximately 15 min later, 0.11% aluminium was added to the furnace. Near the end of the refining period, final additions of ferro-manganese and ferro-niobium were made to achieve the required specification.

The furnace was then tapped at a steel temperature of 1635°C. A large taphole was used to promote slag-metal mixing and a further 0.11% aluminium was added to the ladle in the normal manner. The metal temperature after tapping was 1600°C.

The steel was uphill-teemed into 5 x 20 t ingots using wide end up moulds. Stelotol 15** mould additive was placed in the bottom of each mould prior to teeming. Extra Stelotol was sprinkled into moulds 1 and 2 during teeming. Oxygen was used on the ladle nozzle after the 3rd and 4th ingots.

(ii) Trial C.2

This cast was made to a modified steelmaking practice involving, among other things, blocking the bath with aluminium and the maintenance of an effective aluminium cover (>0.025% Al) during refining, tapping and teeming. The chronological record of the trial cast is summarised in Table 3.8 and a brief description of the procedure is as follows:-

The charge to the furnace was made in 5 baskets and consisted of 123 tonne scrap, 2.3 tonne breeze and 5.08 tonne lime. At melt out, the bath carbon content was 0.305%.

The bath was then blown and slag flushed over the sill during this period. The total time for oxidation was approximately 30 min and the bath carbon was reduced to 0.115%.

The bath was slagged off and then blocked with 0.37% aluminium. This was followed by the addition of a normal lime refining slag. 11 min after the aluminium block, ferro-silicon was added to the bath. 39 min later, a further addition of 0.09% aluminium was made. The slag was then flushed off and more ferro-silicon

** Proprietary mould additive - approximate composition 40% SiO_2, 20% Al_2O_3, 10% Na_2O

was added followed by Desulfex 75 to form a second refining slag. Final additions of ferro-manganese and ferro-niobium were made prior to tapping.

The steel was then tapped at a temperature of 1640°C and 0.05% aluminium was added to the ladle. This was carried out by interrupting the tapping of the furnace when the ladle was approximately one third full. The aluminium, suspended from the crane, was lowered into the metal and the remainder of the metal and slag was then tapped into the ladle. A large taphole was again used to promote slag-metal mixing and desulphurisation. The metal temperature after tapping was 1600°C.

The steel was uphill-teemed into 4 x 20 t wide end up ingots and 1 x 25 t wide end up ingot with a superimposed head. The metal stream was protected by argon during teeming. The mould additive was suspended about 30 cm from the base of each mould. Additional mould additive was added to moulds 1, 2 and 5 during teeming. Oxygen was used on the ladle nozzle after teeming the third and fourth ingots.

(iii) Trial C.3

The steelmaking practice for this cast was similar to trial C.2 except that part of the Desulfex 75 was injected into the bath. The chronological record of the trial cast is summarised in Table 3.9 and a brief description of the procedure is as follows:-

The charge to the furnace was made in 5 baskets and consisted of 105 tonne scrap, 2.1 tonne breeze and 5.08 tonne lime. At melt out, the bath carbon content was 0.38%. The bath was then blown and slag flushed over the sill during this period. The total time for oxidation was approximately 30 min and the bath carbon was reduced to 0.055/0.045%.

The bath was slagged off and then blocked with 0.37% aluminium followed by the addition of a normal lime refining slag. The electrodes were dipped for 3 min and an addition of 0.40% ferro-silicon was then made 16 min after the primary

aluminium block. The bath was paddled and sampled, and 437 kg Desulfex 75 was then injected into the melt using nitrogen as the carrier gas. After sampling and flushing the slag, a further addition of 0.09% aluminium was made followed by 1500 kg Desulfex added in the normal manner. About 20 min later, final additions of ferro-manganese, ferro-silicon and ferro-niobium were made prior to tapping.

The steel was then tapped at a temperature of 1640°C and 0.05% aluminium was added to the ladle in the same manner as in trial C.2. A large taphole was again used and the ladle metal temperature after tapping was 1600°C. The steel was uphill-teemed into 2 x 18 t wide end up, 2 x 18 t narrow end up, and 1 x 20 t wide end up ingots. Argon shrouding of the teeming stream was again carried out. The mould additive was suspended, additional amounts being added to ingots 1, 2, 4 and 5. Oxygen was used on the ladle nozzle after teeming the 3rd and 4th ingots.

The final pit analyses for the 3 trial casts are given in Table 3.10.

(iv) Modifications in Practice

The following main changes from the original standard practice (trial C.1) were adopted for the two development casts (trials C.2 and C.3).

(a) Although a sulphur content of 0.006% was being achieved previously, there appeared to be real advantage in reducing this to 0.004%. In trials C.2 and C.3 desulphurisation was carried out bymeans of a double refining slag, the first one being the normal lime slag and the second consisting of Desulfex 75 which is of higher purity and quicker fluxing. The analysis of Desulfex 75 is given in Table 3.11. When this second refining slag was fluxed and hot, the metal was teemed through the slag. The main difference between the three casts in terms of the desulphurisation practice was in the amount of Desulfex used. In an attempt to achieve a sulphur content of 0.004%, the amount of Desulfex used was increased from about 1 t (trial C.1) to 1.5 - 2.0 t (trials C.2 and C.3). In trial cast C.3, part of the Desulfex 75 was also injected into the bath.

(b) Initial deoxidation was with 0.37% aluminium before the normal refining slag was made up. Ferro-silicon was added only after the first refining slag was fluxed. When the sulphur content was down to about 0.012%, 0.09% aluminium was added and the first refining slag was removed. The Desulfex 75 slag was then added and when this slag was fluxed and hot and the temperature and composition correct, the furnace was tapped at a temperature of 1640°C.

(c) 0.05% aluminium was added to the ladle during tapping. This was done by interrupting the tapping of the furnace when the ladle was approximately one third full. The aluminium was immersed and then the remainder of the metal and slag was tapped into the ladle.

(d) Following the initial aluminium addition, the total aluminium content of the metal was maintained above 0.025% throughout refining, tapping and teeming.

(e) The teeming temperature was 1590°C and the teeming stream was protected by an argon shroud of similar design to the one shown in Fig. 2.81.

(f) The ladle bricks were alumino-silicate containing 70% Al_2O_3 and no highly siliceous refractory material was in contact with the steel at any time. Details of the refractories for the three trial casts are given in Table 3.12.

(g) The mould additive was suspended in the moulds prior to teeming, instead of being placed in the bottom.

SECTION 4 - EXPERIMENTAL RESULTS

The nature and composition of the oxide inclusions present in the metal samples from the eight trial casts are described in the following pages. The microprobe analyses of all the inclusions are presented together in Table 4.1. On the basis of this information, the possible origins and mechanisms of formation of the inclusions are discussed. This is followed by a more detailed discussion in Section 5 of the thesis.

4.1 TRIAL CAST A.1 (LOW ALLOY STEEL)

4.1.1 Inclusions Present in Furnace

Metal 1

This sample, which was taken immediately before tapping, was relatively free from inclusions, only occasional small silicates of the type shown in Fig. 4.1a being observed. The presence of 40-50% CaO in these inclusions indicates that they originated from furnace slag entrained in the metal during the boil.

4.1.2 Inclusions Present in Ladle After Tapping

Metal 2 and 3

Typical inclusions observed in these samples are shown in Figs. 4.1b and 1c. They were glassy manganese alumino-silicates containing small amounts of Cr_2O_3 and CaO. These inclusions were deoxidation products originating from the additions made to the ladle during tapping and the CaO probably arose as a result of slight contamination by slag mixed into the metal.

4.1.3 Inclusions Present in Ladle During Vacuum Degassing

Metal 5

The inclusions observed in this sample were single-phased, manganese alumino-silicate deoxidation products, Fig. 4.2a.

Metal 6

(i) Large, glassy alumino-silicate deoxidation products, Fig. 4.2b.

(ii) Complex inclusions consisting of an $MnO-SiO_2-Cr_2O_3$ phase surrounded by a silica shell, Fig. 4.2c. These were probably erosion products resulting from attack by manganese (and to a lesser extent by chromium) in the steel on siliceous refractory material. The most obvious source of the latter was the siliceous cement used to repair the bottom of the ladle between heats.

Metal 7, 8 and 10

(i) Manganese alumino-silicates containing varying amounts of Al_2O_3, Figs. 4.2d and 2e. It is unlikely that they were pure ladle deoxidation products because their Al_2O_3 contents were too high, indicating that they originated in part from another more highly aluminous source. It would appear that these inclusions had originated from two possible sources, either the ladle refractories or the high alumina cement of the degassing vessel and that agglomeration with ladle deoxidation products had probably occurred to some extent. In a few instances, these alumino-silicates also contained alumina particles, Fig. 4.3a.

(ii) Duplex inclusions consisting of mullite, $3Al_2O_3.2SiO_2$, within a manganese alumino-silicate matrix containing a trace amount of K_2O, Fig. 4.3b. Only a few inclusions of this type were observed. They were erosion products resulting from manganese attack on the fireclay refractories of the ladle.

(iii) Single-phased manganese alumino-silicates containing about 1% K_2O, Fig. 4.3c, which were also fireclay erosion products.

Metal 11 and 12

(i) Manganese alumino-silicates containing trace amounts of K_2O, Fig. 4.3d. These were undoubtedly ladle erosion products, the presence of CaO indicating contamination by slag, possibly from slag glaze on the refractories although 12% CaO seems a rather large amount to originate solely from such a source. An alternative explanation is that it was picked up as a result of agglomeration with calcareous slag inclusions entrained in the liquid metal during degassing.

(ii) Duplex inclusions consisting of cristobalite particles within a manganese silicate matrix, Fig. 4.3e. Only small amounts of Al_2O_3 and Cr_2O_3 were present in these inclusions, which probably originated from the siliceous material used to repair the ladle.

(iii) Large, complex inclusions comprising MgO-Cr_2O_3 particles within a calcium silicate matrix, Fig. 4.3f. The composition of the MgO-Cr_2O_3 phase, A, was close to that of picrochromite, MgO.Al_2O_3 (stoichiometric composition 79% Cr_2O_3, 21% MgO). Slight substitution of MgO by MnO and of Cr_2O_3 by Al_2O_3 in the spinel lattice had occurred in this case. The matrix itself was duplex, containing lath-like crystals, but only an average matrix analysis was obtained because of the electron beam 'shining through'. These inclusions consisted of slag globules containing spalled particles from the magnesite-chromium refractories of the degassing vessel.

4.1.4 Inclusions Present in Ladle Stream During Teeming

Metal 15, 18, 20 and 22

(i) Complex inclusions consisting of cristobalite, chromium galaxite and cristobalite-chromium galaxite eutectic within a manganese silicate matrix, Fig. 4.4. At first sight the morphology of the inclusion in Fig. 4.4c suggests that it could have dropped into the sampling pot from the end of the nozzle as the sample was taken. However, it was certainly not a nozzle erosion product as it only contained a small amount of Al_2O_3 whereas the refractories of the sliding gate nozzle were highly alumi-nous. It seems likely that these inclusions were ladle erosion products originating from the siliceous cement used to repair the ladle and which had picked up chromium from the melt.

(ii) Duplex inclusions consisting of manganese chromium silicate surrounded by a silica shell, Fig. 4.5a. These were also siliceous ladle erosion products.

(iii) Manganese alumino-silicates containing trace amounts of K_2O, Fig. 4.5b. They were erosion products resulting from manganese attack on fireclay ladle refractories.

4.1.5 Inclusions Present in Ingots During Teeming

Metal 14, 16, 17 and 19

(i) Duplex particles consisting of alumina within a manganese alumino-silicate matrix containing approximately 2% K_2O, Fig. 4.6a. The exact origin of these inclusions was difficult to determine. Despite their relatively high K_2O contents, it seems unlikely that they formed as a result of entrapment of vermiculite mould additive because their Al_2O_3 contents were too high and their MgO contents too low. (The full analysis of vermiculite is given in Table 4.2.) These particular inclusions must therefore have resulted from erosion of highly aluminous refractory material and the only two possible sources of this were the high alumina cement used on the vacuum degassing vessel and the refractories of the sliding gate stopper. It is tentatively suggested that erosion of the cement was the more likely one as subsequent examination of the sliding gate stopper revealed very little wear.

(ii) Glassy alumino-silicates containing varying amounts of CaO and MgO, Fig. 4.6b. Only a few of these inclusions were observed and they originated in part from entrained slag as evidenced by the presence of CaO and MgO. They probably agglomerated with reoxidation products formed during teeming although their relatively high Al_2O_3 contents also indicate contamination by refractory erosion products.

(iii) Manganese alumino-silicate erosion products containing 1-2% K_2O, Figs. 4.6c and 6d.

(iv) Large, duplex inclusions consisting of cristobalite particles within a manganese alumino-silicate matrix, Fig. 4.7a. These were holloware erosion products, probably originating from siliceous jointing cement.

(v) Complex inclusions consisting of cristobalite and chromium galaxite - cristobalite eutectic within a manganese silicate matrix, Fig. 4.7b. They were probably ladle erosion products which had picked up chromium.

4.1.6 Inclusions Present in Billets

Despite the generally high level of inclusions present in the liquid metal during tapping, degassing and teeming, the billet samples from this trial cast contained very few non-metallic inclusions, only occasional alumino-silicate stringers of the types shown in Fig. 4.8 being observed. They also appeared to be duplex but it was not possible to differentiate between the different phases when using the electron probe microanalyser and so only average analyses are given. The presence of up to 80% Al_2O_3 indicates that they comprised alumina within an alumino-silicate matrix. Their origin was difficult to determine but because of their high Al_2O_3 contents, it is very unlikely that they were deoxidation products. Rather they were erosion products originating from highly aluminous refractory material and this was supported by the fact that occasionally, trace amounts of K_2O were detected, Fig. 4.8b. The only two possible sources of this erosion were the highly aluminous cement of the degassing vessel and the sliding gate refractories. It was not possible to determine, on the basis of composition, from which of these two sources the inclusions originated. However, other highly aluminous inclusions were observed during degassing and teeming and in addition, subsequent visual examination of the sliding gate stopper revealed very little wear of the high alumina refractories. Consequently, the indications are that the alumino-silicates in Fig. 4.8 resulted from erosion of cement used on the degassing vessel.

The relative freedom from inclusions was confirmed by total oxygen determinations, Table 4.3.

4.2 TRIAL CAST B.1 (FREE-CUTTING STEEL)

4.2.1 Inclusions Present in Furnace During Steelmaking Period

Metal 1

The use of oxygen during melting down meant that oxidation had occurred prior to melt out. The resulting inclusions present in this sample were manganese alumino-silicates containing about 10% CaO, Figs. 4.9a and 9b. The presence of P_2O_5, TiO_2

and sulphur in addition to lime in these inclusions indicates that they had originated from slag entrapped in the metal by the turbulence caused by oxygen blowing. However, they were considerably richer in MnO, SiO_2 and Al_2O_3 than the bulk slag at the expense of a decreased CaO content, Table 4.4. This indicates a dilution effect produced by the precipitation of oxidation products on the entrapped slag particles. A similar effect has been observed previously during basic electric arc steelmaking[102], the SiO_2, MnO and at this early stage, the Al_2O_3 being readily available from the oxidation of silicon, manganese and aluminium in the charge.

Metal 2

This sample was taken approximately one minute after an oxygen blow and the resulting inclusions were very large, Figs. 4.9c and 9d. The inclusion in Fig. 4.9c consisted of (FeMn)O.$(CrAl)_2O_3$ dendrites within a manganese alumino-silicate matrix containing a small amount of lime. The presence of lime indicates that it originated in part from entrained slag, the MnO, SiO_2 and Al_2O_3 contents increasing as a result of oxidation of manganese, silicon and aluminium from the bath. The Cr_2O_3 in this inclusion must also have resulted from oxidation of chromium in the metal, the dendritic spinel being precipitated within the liquid silicate matrix on cooling.

The inclusion in Fig. 4.9d was a single-phased calcium manganese silicate containing approximately 5% Al_2O_3 and 20% CaO. It originated from slag entrapped in the metal during the turbulence caused by oxygen blowing, the MnO and SiO_2 contents increasing owing to oxidation of manganese and silicon from the melt.

Metal 3

Typical inclusions present in this sample are shown in Figs. 4.10a and 10b. Although much smaller, they were very similar in composition to those observed in the previous sample and had originated from slag entrained in the metal during oxygen blowing.

Metal 4

There were very few oxides in this sample. The duplex inclusion in Fig. 4.10c was the only one of its type observed and consisted of (FeMnMg)O particles within a calcium silicate matrix. It is suggested that this particular inclusion originated from erosion of the hearth refractories, the resulting MgO - rich erosion particles then agglomerating with entrained slag.

Metal 5

This sample was taken only $2\frac{1}{2}$ min after the addition of ferro-manganese and with the electrode power on. Consequently, the inclusions present were entrapped slag particles of the type shown in Fig. 4.10d. They were entrained in the metal as a result of the turbulent conditions under which this sample was taken.

4.2.2 Inclusions Present in Ladle After Tapping

Metal 6

Typical inclusions observed in this sample are shown in Fig. 4.11. They were large manganese silicates containing varying amounts of Al_2O_3, CaO and sulphur. The complex inclusion in Fig. 4.11a apparently consisted of laths of tephroite, 2MnO. SiO_2, together with finely crystallised MnS. Because of the fine nature of these phases, however, only an average inclusion analysis was possible. Small amounts of CaO and Al_2O_3 were also present and it is suggested therefore that this inclusion originated in part from slag mixed into the metal during tapping. The entrained slag particle then reacted with manganese, sulphur and oxygen in the steel so that its MnO and MnS contents increased and its CaO content decreased by dilution. The overall mechanism of this reaction probably involved the following individual reactions:-

(i) reduction of the small amount of FeO in the slag particle

(ii) solution of sulphur in the liquid inclusion

(iii) precipitation of MnO-rich deoxidation/reoxidation products on the entrained slag particle.

The single-phased silicate in Fig. 4.11b contained much more Al_2O_3 than the latter inclusion. In addition, it contained a trace of K_2O and this suggests that it was a refractory erosion product, probably originating from the ladle. Chemical analysis showed that none of the ladle additions contained any K_2O. The 5% CaO in this inclusion probably came from slag glaze on the ladle refractories. Alternatively, it was picked up as a result of agglomeration with slag mixed into the metal during tapping.

The inclusion in Fig. 4.11c consisted of MnO and MnS dendrites within a calcium manganese silicate matrix and had also originated from slag entrained in the metal during tapping. In this case, however, extensive precipitation of MnO-rich deoxidation/reoxidation products on the entrained slag particle had occurred.

4.2.3 Inclusions Present in Ladle Stream During Teeming

Metal 8, 10 and 12

Typical inclusions present in these samples are shown in Fig. 4.12. The large, glassy manganese alumino-silicate in Fig. 4.12a contained a trace amount of K_2O and was a ladle, stopper or nozzle erosion product.

The inclusions in Figs. 4.12b and 12c consisted of galaxite spinel, $MnO.Al_2O_3$ within a manganese alumino-silicate matrix containing about 1% K_2O. They were ladle, stopper or nozzle erosion products. The faceted morphology of the $MnO.Al_2O_3$ phase in Fig. 4.12b indicates that it was present prior to cooling, whereas the dendritic morphology of the spinel in Fig. 4.12c indicates that it formed during cooling.

The complex inclusion in Fig. 4.12d consisted of (FeMn)O and MnS dendrites in a manganese silicate matrix containing small amounts of Al_2O_3 and Cr_2O_3. It is suggested that this was a deoxidation/reoxidation product formed during tapping and/or teeming.

The inclusion in Fig. 4.12e consisted of (FeMn)O and MnS dendrites within a manganese silicate matrix containing small amounts of Al_2O_3, CaO and TiO_2. Because of the fine nature of the individual phases, however, only an average analysis is given. The origin of this particular inclusion type was difficult to determine.

Despite the fact that K_2O could not be detected, it is still possible that it formed as a result of refractory erosion. Alternatively, it originated from slag entrained in the metal during tapping and subsequently acted as a hetergeneous nucleus for the precipitation of deoxidation/reoxidation products and the solution of sulphur. This resulted in a dilution of the CaO content and the precipitation of (FeMn)O and MnS dendrites.

4.2.4 Inclusions Present in Ingots During Teeming

Metal 7, 9 and 11

Typical inclusions observed in these samples are shown in Fig. 4.13. The manganese alumino-silicate inclusion in Fig. 4.13a contained a trace amount of K_2O and was therefore a ladle, stopper, nozzle or holloware erosion product.

The inclusions in Figs. 4.13b and 13c consisted of MnO and MnS dendrites within a manganese silicate matrix. As no CaO, K_2O, TiO_2 or P_2O_5 was detected in these silicates, it is suggested that they were deoxidation/reoxidation products formed during tapping and/or teeming.

The inclusion in Fig. 4.13d consisted of MnO and MnS within a manganese silicate matrix containing small amounts of Al_2O_3, CaO and TiO_2. Although K_2O could not be detected, it could still have formed as a result of refractory erosion, although it is also possible that it originated from slag entrained in the metal during tapping and subsequently reacted with manganese, sulphur and oxygen in the steel.

4.2.5 Inclusions Present in Billets

Typical stringer inclusions observed in selected billet samples from the present trial cast are shown in Fig. 4.14. They consisted of galaxite spinel, $MnO.Al_2O_3$ and MnS particles within a manganese silicate matrix containing a trace amount of K_2O. The presence of $MnO.Al_2O_3$ particles together with K_2O indicates that these stringer inclusions were erosion products originating from glaze on refractories. The majority of these inclusions were present in the bottom billet samples: by comparison, the middle and top billet samples were relatively clean. The latter observation was

confirmed by determining the total oxygen and silicon contents of the billet samples. Figure 4.15 shows the variation in total oxygen content from billet edge to centre, Fig. 4.16 illustrates the variation in total oxygen content from ingot top to bottom and Fig. 4.17 shows the corresponding variation in total silicon content (determined on centre samples only).

4.2.6 Variation in Total Silicon Content During Steelmaking, Tapping and Teeming

The variation in the silicon content of the bath, ladle and stream samples is shown by the solid line in Fig. 4.18. The corresponding variation in the silicon content of the ingot samples is shown by the broken line.

4.3 TRIAL CAST B. 2 (FREE-CUTTING STEEL)

The results of this trial cast are summarised in Figs. 4.19 - 4.22, from which it can be seen that they were very similar to those of the previous one. This is not surprising in view of the similarities in practice. The only difference in the types of inclusions present in the metal samples was that during the teeming of trial cast B.2, occasional complex calcium silicates containing MgO particles were observed, Fig. 4.23. It is suggested that these silicates originated during tapping as a result of the pick-up of MgO particles by the slag from the magnesite-coated launder of the furnace. They were entrained in the metal by the force of the tapping stream and subsequently passed into the ingots during teeming. Although it is surprising that an inclusion of the size shown in Fig. 4.23 was not eliminated in the ladle, it is emphasised that only a few such inclusions were observed in the liquid metal samples and they were not observed in the billet samples.

4.4 TRIAL CAST B.3 (FREE-CUTTING STEEL)

The results of this trial cast, which are summarised in Figs. 4.24 - 4.27, were again very similar to those of trial cast B.1. As there was no difference in the types of inclusions observed, micrographs of inclusions from the present cast are not shown.

4.5 TRIAL CAST B.4 (FREE-CUTTING STEEL)

The results of this final free-cutting steel trial are summarised in Figs. 4.28 - 4.31. Once again they were very similar to the results of the previous trial casts in this series. In particular, there was no difference in the types of inclusions observed in the metal samples and therefore inclusion micrographs are again omitted. However, a major difference was observed in the variation in silicon content shown in Fig. 4.31. In this final trial, two samples were taken from the ladle after tapping and the second of these had a much higher silicon content than the first, i.e. in this trial, silicon pick-up by the liquid metal was directly observed in the ladle whereas in the three previous trials, it was observed only in the stream samples. The reasons for this are discussed in Section 5.

4.6 TRIAL CAST C.1 (CARBON-MANGANESE-NIOBIUM STEEL)

4.6.1 Inclusions Present in Furnace During Steelmaking Period

Metal 1, 2 and 3

During the oxidation period, the inclusions present were calcium silicates containing varying amounts of Al_2O_3, MgO and MnO together with trace amounts of P_2O_5, TiO_2 and S, Fig. 4.32a. They originated from slag entrained in the metal during the turbulence caused by oxygen blowing. In some cases, however, they were considerably richer in MnO and SiO_2 than the bulk slag at the expense of a decreased CaO content. This was the result of a dilution effect produced by the precipitation of oxidation products on the entrained slag particles.

Metal 4

The inclusions present in this sample which was taken after the addition of the ferro-silicon, were glassy silicates containing approximately 70% SiO_2 together with varying amounts of MnO and Al_2O_3, Fig. 4.32b. They were conventional deoxidation products.

Metal 5

The inclusions in this sample taken after the initial addition of aluminium were duplex manganese alumino-silicates containing alumina particles, Fig. 4.32c. They resulted from reaction between the aluminium and the pre-existing silicate deoxidation products.

Metal 6

(i) Calcium silicate inclusions resulting from the entrainment of slag in the liquid metal, Fig. 4.32d.

(ii) Manganese alumino-silicates containing particles of alumina, Fig. 4.32e. These duplex particles were products of reaction between pre-existing silicates resulting from ferro-silicon deoxidation and the aluminium added to the steel.

Metal 7 and 8

(i) Calcium silicate inclusions resulting from the entrainment of slag, possibly when the ferro-manganese and ferro-niobium additions were made, Fig. 4.32f.

(ii) Single-phased manganese alumino-silicate deoxidation/reoxidation products, Fig. 4.32g.

4.6.2 Inclusions Present in Ladle After Tapping

Metal 9

(i) Glassy calcium alumino-silicates resulting from the entrainment of slag in the liquid metal during tapping, Fig. 4.33a.

(ii) Duplex inclusions consisting of MgO dendrites within a calcium alumino-silicate matrix, Fig. 4.33b. These inclusions also resulted from the entrainment of slag during tapping. However, their MgO contents were increased as a result of contamination by magnesite refractory erosion products from the furnace, taphole or launder.

4.6.3 Inclusions Present in Ladle Stream During Teeming

Metal 11, 13, 15 and 17

(i) Glassy manganese silicates containing varying amounts of Al_2O_3, Fig. 4.34a. These inclusions were either deoxidation products, or more likely reoxidation products formed during tapping and teeming.

(ii) Single-phased manganese alumino-silicates containing trace amounts of K_2O, Fig. 4.34b, which were ladle glaze erosion products.

4.6.4 Inclusions Present in Ingots During Teeming

Metal 10, 12, 14 and 16

(i) Single-phased manganese alumino-silicates, Fig. 4.35a. Their size and shape as well as their composition and the fact that there were very many similar inclusions in these samples indicate that they originated from the mould additive placed in the bottom of the moulds prior to teeming. During teeming, the turbulent flow of the metal into the moulds resulted in the entrainment of mould additive in the liquid metal. This mould additive then reacted with manganese and aluminium in the steel.

(ii) Manganese alumino-silicates containing small amounts of CaO together with trace amounts of K_2O, Fig. 4.35b. In some cases, these alumino-silicates also contained alumina particles. They were erosion products resulting from attack by manganese in the steel on alumino-silicate refractories. As these were ingot samples, the inclusions were ladle or holloware erosion products.

(iii) Duplex inclusions consisting of $(MnMg)O.Al_2O_3$ particles within a manganese alumino-silicate matrix containing a trace amount of K_2O, Fig. 4.35c. They were complex erosion products originating in part from magnesite refractory material, and only a few such inclusions of this type were observed compared with those from the mould additive.

(iv) Duplex inclusions consisting of $MgO.Al_2O_3$ particles within a calcium aluminate matrix, Fig. 4.35d. They resulted from reaction between aluminium in the

steel and the slag/magnesite erosion products entrained in the metal during tapping. Again, only a few inclusions of this type were observed compared with those from the mould additive.

4.6.5 Variation in Aluminium Content

The variation in the aluminium content of the furnace, ladle and ingot samples is shown in Fig. 4.36. The corresponding variation in the aluminium content of the ladle stream samples is shown in Fig. 4.37. In each case, the total aluminium content is given in terms of the acid soluble and insoluble components. The former is approximately equivalent to the aluminium present in solution in the metal, and the latter to the aluminium present as Al_2O_3. It can be seen from Fig. 4.36 that the total aluminium content increased to 0.009% after the initial ferro-silicon and aluminium additions, this aluminium being present mainly as Al_2O_3. Subsequently, the total aluminium content decreased during the refining period to 0.003%.

The total aluminium content of the sample taken from the ladle after tapping was 0.010%, 0.006% of this being soluble aluminium. During teeming, the soluble aluminium content of the ingot samples remained constant at 0.006% but the insoluble aluminium content fluctuated quite considerably as a result of variations in the amounts of Al_2O_3 inclusions present in the samples. This was particularly high in the cases of the samples taken after teeming the 3rd and 4th ingots.

The total aluminium content of the ladle stream samples, Fig. 4.37, also varied slightly as a result of corresponding variations in the insoluble aluminium content.

4.6.6 Through-Thickness Tensile Results

The average through-thickness reduction of area values for the whole cast were as follows:-

Edge	Centre	Total
36%	31%	34%

4.7 TRIAL CAST C.2 (CARBON-MANGANESE-NIOBIUM STEEL)

4.7.1 Inclusions Present in Furnace During Steelmaking Period

Metal 1

The inclusions in this sample taken after the initial addition of aluminium were large showers of alumina deoxidation products, Fig. 4.38a.

Metal 2

This sample was taken $5\frac{1}{2}$ minutes after the ferro-silicon addition. However, the inclusions present were still showers of alumina deoxidation particles, Fig. 4.38b, indicating that the level of aluminium in the melt at this stage was sufficient to prevent the formation of globular silicate deoxidation products.

Metal 3

(i) Small, isolated alumina deoxidation products, Fig. 4.38c.

(ii) Small, spherical manganese alumino-silicates probably resulting from slight reoxidation of the metal, Fig. 4.38d. This sample was relatively free from non-metallic inclusions.

Metal 4

(i) Small, isolated alumina deoxidation products, Fig. 4.38c.

(ii) Duplex inclusions consisting of alumina within a calcium alumino-silicate matrix, Fig. 4.38f. They resulted from the entrainment of slag in the liquid metal when the bath was paddled.

Metal 5

This sample contained very few inclusions, only small, secondary alumino-silicates which were formed on cooling being observed, Fig. 4.38g. (Because of the electron beam 'shining through' the small inclusion in Fig. 4.38g into the surrounding iron matrix, its analysis is not given.)

Metal 6

(i) Small, isolated alumina deoxidation products resulting from the further addition of aluminium, Fig. 4.38h.

(ii) Rings of alumina crystals resulting from the complete reduction of alumino-silicate inclusions by aluminium, Fig. 4.38i. The mechanism of formation of these alumina rings has been studied in detail previously[22, 107].

(iii) Duplex inclusions consisting of MgO dendrites within a calcium aluminate matrix, Fig. 4.38j. They resulted from the entrainment of slag in the liquid metal when the bath was paddled. The relatively high MgO content of the slag was caused by erosion of magnesite furnace refractories.

(iv) Glassy manganese alumino-silicates which in some cases contained particles of galaxite, $MnO.Al_2O_3$, Fig. 4.38k. These inclusions probably resulted from slight reoxidation of the metal when the bath was paddled.

Metal 7

This sample contained duplex inclusions consisting of MgO dendrites within a calcium alumino-silicate matrix, Fig. 4.39a. They again resulted from the entrainment of slag, possibly caused by the turbulence created when the ferro-manganese and ferro-niobium additions were made.

Metal 8

This sample also contained duplex MgO/calcium aluminates resulting from slag entrainment, Fig. 4.39b, possibly caused by the turbulence created by the arc during heating to 1640°C prior to tapping.

4.7.2 Inclusions Present in Ladle After Tapping

Metal 9

As expected, this sample contained calcium aluminates resulting from the entrainment of slag in the liquid metal during tapping, Fig. 4.40a. Many of these inclusions, however, contained considerable quantities of MgO in the form of second phase particles, Fig. 4.40b. This indicates contamination of the slag by magnesite refractories as Desulfex 75 contains only about 1% MgO. The MgO in these inclusions originated from the furnace and/or taphole and/or launder refractories.

4.7.3 Inclusions Present in Ladle Stream During Teeming

Metal 12, 14, 16 and 18

(i) Large, single-phased manganese silicates containing varying amounts of Al_2O_3, Fig. 4.41a. As these inclusions contained no CaO, K_2O, or MgO, they were almost certainly exogenous reoxidation products formed during sampling. As stated previously, the ladle stream samples were taken with the argon shroud turned off and therefore the sampling conditions were the same as those for a normal air-teemed cast. The inclusion in Fig. 4.41b also appeared to be a reoxidation product although in this case it contained small angular particles. Unfortunately, these particles were too small for accurate analysis and therefore only an average inclusion analysis is given.

(ii) Duplex inclusions consisting of alumina particles within a manganese alumino-silicate matrix containing a trace amount of K_2O, Fig. 4.41c. They were erosion products resulting from attack by manganese in the steel on alumino-silicate refractories. As these were stream samples, they were ladle, stopper or nozzle erosion products. Their exact origin is considered in greater detail later when the types of refractories used in the trial casts are discussed.

(iii) Duplex inclusions consisting of galaxite, $MnO.Al_2O_3$, particles within a manganese alumino-silicate matrix containing a trace amount of K_2O, Fig. 4.41d. These were also ladle, stopper or nozzle erosion products resulting from manganese attack.

4.7.4 Inclusions Present in Ingots During Teeming

Metal 10, 11, 13, 15 and 17

(i) Duplex inclusions consisting of $MgO.Al_2O_3$ within a manganese alumino-silicate matrix containing a trace amount of K_2O, Fig. 4.42a. The presence of MgO indicates that they originated as a result of magnesite refractory erosion. However, unlike MgO-rich inclusions observed previously, they contained very little CaO and

were not therefore derived from the ladle slag. It is suggested that these inclusions originated from MgO-rich furnace refractory (i.e. furnace, taphole, launder) dispersed in the steel during tapping. Subsequently, they acted as exogenous nuclei for the precipitation of MnO, SiO_2 and Al_2O_3 to give inclusions of the type shown in Fig. 4.42a.

(ii) Duplex inclusions consisting of alumina particles within a manganese alumino-silicate matrix containing a trace amount of K_2O, Fig. 4.42b. These inclusions were very similar to those observed in the stream samples, cf Fig. 4.41c. They were erosion products resulting from manganese attack on alumino-silicate refractories.

(iii) Duplex inclusions consisting of $MgO.Al_2O_3$ particles within a calcium aluminate matrix, Fig. 4.42c. These resulted from reaction between aluminium in the steel and slag/magnesite erosion products entrained in the metal during tapping.

(iv) Single-phased manganese alumino-silicates containing small amounts of K_2O and CaO, Fig. 4.42d. These were also alumino-silicate erosion products typical of manganese attack on fireclay refractories.

(v) Small, isolated alumina deoxidation products, Fig. 4.42e.

(vi) Single-phased manganese silicates containing varying amounts of Al_2O_3, Fig. 4.42f. The exact origin of these inclusions was difficult to determine on the basis of composition. Although they contained no K_2O, they could still have originated as a result of refractory erosion. Alternatively, they were reoxidation products formed during tapping and/or teeming.

4.7.5 Variation of Aluminium Content

The variation in the aluminium content of the furnace, ladle and ingot samples with time is shown in Fig. 4.43 and the corresponding variation of the ladle stream samples is shown in Fig. 4.44. It can be seen from Fig. 4.43 that the soluble aluminium content was maintained above 0.025% during the refining period and was about 0.030% prior to tap. After tapping, it dropped to approximately 0.026% in the

ladle. During teeming, the soluble aluminium content of the ingot samples was 0.01 - 0.02%, Fig. 4.43 and that of the stream samples was 0.015 - 0.023%, Fig. 4.44.

The total aluminium content of the samples again fluctuated quite considerably during refining, tapping and teeming as a result of a corresponding variation in the insoluble aluminium content caused by differences in the number of aluminous inclusions present in the samples.

4.7.6 Variation in Sulphur Content

The variation in the sulphur content of the furnace, ladle and ingot samples with time is shown in Fig. 4.45 and the corresponding variation in the sulphur content of the stream samples is shown in Fig. 4.46. During tapping, the sulphur content was lowered from 0.012% to 0.005%. The sulphur content of the ingot samples was 0.006/0.007%, Fig. 4.45 and the sulphur content of the stream samples was 0.005/0.007%, Fig. 4.46.

4.7.7 Through-Thickness Tensile Results

The average through-thickness reduction of area values for the whole cast were as follows:-

Edge	Centre	Total
51%	52%	51%

These results were very good and they showed a marked improvement over the average through-thickness results obtained with the previous standard practice.

4.8 TRIAL CAST C.3 (CARBON-MANGANESE-NIOBIUM STEEL)

4.8.1 Inclusions Present in Furnace During Steelmaking Period

Metal 2

(i) Clusters of alumina deoxidation products, Fig. 4.47a.

(ii) Calcium alumino-silicates resulting from entrainment of slag in the liquid metal, Fig. 4.47b.

Metal 3

This sample contained very few inclusions, those observed being mainly duplex particles consisting of alumina within a manganese alumino-silicate matrix, Fig. 4.47c. They were probably reoxidation products formed when the bath was paddled following the FeSi addition. Some of the alumina particles may have acted as nuclei for the precipitation of the MnO, SiO_2 and Al_2O_3. Alternatively, they were precipitated within the inclusion matrix as a result of reaction with aluminium in the steel.

Metal 4

This sample also contained very few inclusions, only small isolated alumina deoxidation products being observed, Fig. 4.47d.

Metal 5

The inclusions present in this sample were spherical calcium alumino-silicates resulting from the injection of Desulfex, Fig. 4.47e.

Metal 6 and 7

(i) Small, isolated alumina deoxidation products, Fig. 4.47f.

(ii) Calcium alumino-silicates resulting from slag entrainment, Fig. 4.47g.

(iii) Manganese alumino-silicate inclusions, Fig. 4.47h. These possibly resulted from slight reoxidation of the metal.

Metal 8

This sample, which was taken about $3\frac{1}{2}$ min after the final ferro-alloy additions, contained duplex inclusions consisting of alumina particles within a calcium manganese alumino-silicate matrix, Fig. 4.47i. They were probably slag/reoxidation products. However, the morphology of the inclusion in Fig. 4.47i was very unusual. It appears that the alumino-silicate phase was precipitated on the alumina which acted as an exogenous nucleus. The following mechanism is therefore proposed for the formation of this particular inclusion. Initially, the large alumina particle, which originated

either from aluminium deoxidation/reoxidation of the melt or from alumina present in the Desulfex, was present in the furnace slag layer. It was subsequently entrained in the metal by the turbulence created when the ferro-alloys were added. At this stage, the alumina particle was contained within a globule of liquid slag. Precipitation of MnO and SiO_2 reoxidation products on the entrained slag particle then caused its MnO and SiO_2 contents to increase and its CaO content to decrease by dilution, giving the inclusion in Fig. 4.47i.

4.8.2 Inclusions Present in Ladle after Tapping

Metal 9

This sample contained calcium aluminates resulting from the entrainment of slag in the liquid metal during tapping, Fig. 4.48. They again contained considerable quantities of MgO in the form of second phase magnesite particles, but because of their small size, only an average analysis is given. This indicates contamination by magnesite refractory, but unlike the previous trial, very few MgO-rich inclusions were observed in the furnace during steelmaking. It is suggested, therefore, that in this case they were slag/magnesite taphole or launder erosion products rather than pure furnace slag.

Again compared with the corresponding inclusions in the previous trial cast, they were considerably smaller and this indicates perhaps that there was less slag-metal mixing during tapping in this cast. This is supported by the fact that sulphur removal during tapping was less (0.010% to 0.007%) than in the previous trial cast (0.012% to 0.005%).

4.8.3 Inclusions Present in Ladle Stream During Teeming

Metal 11, 14, 16 and 18

(i) Single-phased manganese silicates containing varying amounts of Al_2O_3, Fig. 4.49a. As these inclusions contained no K_2O, CaO or MgO, they were almost certainly exogenous reoxidation products formed during sampling. The ladle stream samples were taken with the argon shroud turned off and therefore the sampling

conditions were the same as those for a normal air-teemed cast.

(ii) Duplex inclusions consisting of alumina particles within a manganese alumino-silicate matrix containing a trace amount of K_2O, Fig. 4.49b. They were erosion products resulting from attack by manganese in the steel on alumino-silicate refractories. As these were stream samples, they were ladle, stopper or nozzle erosion products.

(iii) Duplex inclusions consisting of $MnO.Al_2O_3$ particles within a manganese alumino-silicate matrix containing a trace amount of K_2O, Fig. 4.49c. These were also ladle, nozzle or stopper erosion products resulting from manganese attack. In the inclusion shown, metal globules have acted as nuclei for galaxite precipitation from the solid matrix during cooling of the sample. A similar reaction mechanism has been observed previously by Kiessling[1].

4.8.4 Inclusions Present in Ingots During Teeming

Metal 10, 12, 13, 15 and 17

(i) Duplex inclusions consisting of alumina particles within a manganese alumino-silicate matrix containing a trace amount of K_2O, Fig. 4.50a. These inclusions were erosion products resulting from manganese attack on alumino-silicate refractories.

(ii) Single-phased manganese alumino-silicates containing small amounts of K_2O and CaO, Fig. 4.50b. These were erosion products typical of manganese attack on fireclay refractories.

(iii) Single-phased manganese silicates containing varying amounts of Al_2O_3, Fig. 4.50c. Although they contained no K_2O, they could still have originated as a result of refractory erosion. Alternatively, they were reoxidation products formed during tapping and/or teeming.

4.8.5 Variation in Aluminium Content

The variation in the aluminium content of the furnace, ladle and ingot samples with time is shown in Fig. 4.51. The corresponding variation of the ladle stream

samples is shown in Fig. 4.52. It can be seen from Fig. 4.51 that the soluble aluminium content was maintained above 0.035% during the refining period and was about 0.05% prior to tap. After tapping, it dropped to approximately 0.04% in the ladle. During teeming, the soluble aluminium content of both the ingot and ladle stream samples was 0.035/0.04%, Figs. 4.51 and 4.52.

In this cast, the total aluminium content followed the soluble aluminium content quite closely as a result of the generally consistent and low insoluble aluminium content, the latter remaining at about 0.01% throughout.

4.8.6 Variation in Sulphur Content

The variation in the sulphur content of the furnace, ladle and ingot samples with time is shown in Fig. 4.53 and the corresponding variation of the ladle stream samples is shown in Fig. 4.54. It can be seen from Fig. 4.53 that injection of part of the Desulfex before the second addition of aluminium was not effective in removing sulphur. However, during the final stages of refining with the full Desulfex slag, the sulphur content dropped from 0.016% to about 0.010% prior to tapping. After tapping, it dropped to approximately 0.007% in the ladle. During teeming, the sulphur content of the ingot samples was 0.006/0.007%, Fig. 4.53 and the sulphur content of the stream samples was 0.005/0.006%, Fig. 4.54.

4.8.7 Through-Thickness Tensile Results

The average through-thickness reduction of area values for the whole cast were as follows:-

Edge	Centre	Total
56%	49%	53%

These results were again very good in comparison with the average through-thickness results obtained with the original standard practice.

SECTION 5 - DISCUSSION OF RESULTS

5.1 OCCURRENCE OF INCLUSIONS IN VACUUM DEGASSED LOW ALLOY STEEL

Prior to tapping the open-hearth furnace, the steel was relatively free from oxide inclusions, only occasional small silicates resulting from slag entrainment being present.

During tapping, ferro-silicon, ferro-manganese, ferro-chromium and aluminium were added to the ladle. The practice for making these additions consisted of placing about 30% of the ferro-chromium on the bottom of the ladle prior to tapping. The ferro-manganese, ferro-silicon and remaining ferro-chromium were added together when the ladle was approximately one quarter full, and finally the aluminium addition was made. The resulting inclusions were liquid manganese alumino-silicate deoxidation products containing small amounts of Cr_2O_3. Very few calcareous slag inclusions were observed in the ladle after tapping, thus supporting Houseman's[111] view that slag entrainment is not a major problem in open-hearth steelmaking.

The liquid manganese alumino-silicates were also present in the metal during the early stages of vacuum degassing, but as degassing progressed, their number appeared to decrease gradually, presumably as a result of coalescence and flotation, until only occasional inclusions of this type were observed. The approximate variation in the average size of these ladle deoxidation products with time is shown in Fig. 5.1. It can be seen that in the time interval during which the ladle was transferred from the furnace to the vacuum degassing unit, the average diameter of the deoxidation products changed very little because of the relatively quiescent conditions existing in the ladle. Coalescence and elimination of inclusions was therefore minimal. However, once vacuum degassing was underway, the turbulence resulted in extensive coalescence and agglomeration of the deoxidation products which then

escaped much more rapidly and after approximately 10 min degassing they were no longer observed in the metal samples.

During the later stages of degassing, various types of erosion products were present in the liquid steel as follows:-

(a) Manganese alumino-silicates containing about 30% Al_2O_3 together with trace amounts of K_2O. These were typical of erosion products originating from fireclay refractories as a result of attack by manganese(156).

(b) Manganese silicates containing particles of cristobalite. They originated as a result of attack by manganese on the highly siliceous cement (>90% SiO_2) used to repair the ladle between heats.

(c) Calcium silicates containing particles of picrochromite, $MgO.Cr_2O_3$. These inclusions were only observed during the final stages of degassing and were products of reaction between ladle slag and the magnesite-chromium refractories of the degassing vessel.

(d) Alumino-silicate inclusions containing about 60% Al_2O_3. These inclusions were also erosion products but their Al_2O_3 contents were far too high for them to have originated from the normal fireclay ladle refractories which only contained 30-40% Al_2O_3. The most likely source of these inclusions was the high alumina cement (>80% Al_2O_3) used on the degassing vessel. Secondary deoxidation products formed during cooling probably precipitated on these inclusions and caused their MnO and SiO_2 contents to increase.

The effect of ladle and degasser refractory erosion during the later stages of degassing is shown in Fig. 5.2, where the variation in total oxygen content of some of the metal samples taken from the ladle during vacuum degassing has been plotted against time. Unfortunately, not all the samples were suitable for oxygen analysis but nevertheless, the available results show that during the early stages, the total oxygen content gradually decreased as many of the ladle deoxidation products escaped

into the slag. During the later stages, however, the total oxygen content increased again owing to excessive erosion of ladle and degassing vessel refractories. A similar variation has been observed previously during R.H. vacuum degassing by Pickering[102] and Blank[174]. The oxygen content decreased initially and then increased again as the rate of refractory erosion exceeded the rate of inclusion elimination.

The majority of inclusions present in the ladle stream samples were complex manganese silicates containing cristobalite, chromium galaxite and cristobalite-chromium galaxite eutectic. Although inclusions were frequently observed containing these four distinct phases, other inclusions were also observed which only contained cristobalite or cristobalite + eutectic. All these silicates were ladle erosion products which had picked up varying amounts of Cr_2O_3 and they probably originated from the siliceous cement used to repair the bottom of the ladle. It is interesting to note that very few of these inclusions were observed in the samples taken from the ladle during vacuum degassing, being present mainly in the stream samples. It is suggested therefore that they formed as a result of reaction between the siliceous cement on the bottom of the ladle and the ferro-chromium and ferro-manganese additions made to the ladle before and during tapping. This reaction commenced immediately the molten metal began to fill the ladle. Manganese and chromium dissolved in the siliceous cement according to the mechanisms discussed in Section 2.4.3, i.e.

$$2\underline{Mn} + (SiO_2) \longrightarrow 2(MnO) + \underline{Si} \quad .. \quad .. \quad .. \quad .. \quad \text{eqn. (5.1)}$$

$$4\underline{Cr} + 3(SiO_2) \longrightarrow 2(Cr_2O_3) + 3\underline{Si} \quad .. \quad .. \quad .. \quad \text{eqn. (5.2)}$$

Solution of chromium in the silicate occurred quite rapidly in this instance because of the heavy segregation of chromium at the bottom of the ladle (~30% of the ferro-chromium was placed in the ladle prior to tapping). This resulted in the formation of a manganese chromium silicate reaction layer containing less than 5% Al_2O_3. With increasing time, softening of this layer occurred and particles were eroded away.

This erosion was apparently much greater during teeming than during vacuum degassing, thus confirming previous observations[141,142] that the bottom of the ladle (including the cement used for repairs) is subject to considerable erosion when the steel flows out through the nozzle. The quality of the cement and the manner in which it is applied are therefore of considerable importance from the point of view of bottom wear and the passage of erosion products into the ingots.

In order to understand the mechanism of formation of the inclusion types shown in Fig. 4.4, it is first necessary to have some knowledge of the ternary relationships in the system $MnO-SiO_2-Cr_2O_3$. However, this system has not been examined thoroughly and there is no convenient experimental equilibrium diagram. Nevertheless, assuming there are no ternary compounds in the system, it is possible to sketch a qualitative liquidus surface, Fig. 5.3. This surface is similar to the liquidus surfaces of the $MgO-SiO_2-Cr_2O_3$ and $MnO-SiO_2-Mn_2O_3$ systems[105,106] in that:-

(a) The three phases Cr_2O_3, MnO and $MnO.Cr_2O_3$ occupy a large part of the composition triangle, whereas the primary phase fields of the silicon-containing phases $MnO.SiO_2$, $2MnO.SiO_2$ and SiO_2 are restricted to a relatively narrow area adjacent to the $MnO-SiO_2$ boundary.

(b) There is a large liquid immiscibility gap which extends across the diagram from the $Cr_2O_3-SiO_2$ binary to the $MnO-SiO_2$ binary.

(c) There is a steep temperature gradient across the diagram falling from about 2250°C (the melting point of Cr_2O_3) to about 1200°C (the ternary eutectic point).

It can be seen from Fig. 5.3 that on cooling manganese silicate inclusions containing only small amounts of Cr_2O_3, e.g. 50% MnO, 45% SiO_2 and 5% Cr_2O_3, they should solidify in the cristobalite phase field and subsequently down the trough between the cristobalite and chromium galaxite phase fields. Complete solidification should occur at the ternary eutectic point. However, one or more of these

precipitation reactions may be suppressed depending upon the rate of cooling and solidification. The eutectic regions in Fig. 4.4 appeared to consist of two phases and although accurate analysis of the constituents of the eutectic was not possible, it appears that the ternary eutectic reaction was suppressed.

As the Cr_2O_3 content of the inclusions increased, their compositions passed into the (spinel + liquid) phase field and angular particles of chromium galaxite were precipitated, Fig. 4.4c. During cooling and solidification, cristobalite-chromium galaxite eutectic was precipitated from liquid adjacent to the spinel particles. The remaining liquid apparently solidified as a single-phased glass. The presence of two primary phases, i.e. cristobalite and chromium galaxite within some of the inclusions is indicative of non-equilibrium solidification associated with the relatively rapid cooling of the samples.

The majority of inclusions present in the samples taken from the ingots during teeming were duplex cristobalite/manganese silicate erosion products. In this case, they were almost certainly holloware erosion products originating from the siliceous refractory cement used on the runner bricks of the uphill-teeming system. Manganese chromium silicates resulting from erosion of ladle cement, manganese alumino-silicates resulting from erosion of fireclay ladle and/or runner bricks, and highly aluminous silicates resulting from erosion of degassing vessel cement were also observed in the ingot samples.

Despite the relatively high level of inclusions present in the liquid metal during tapping, degassing and teeming, the billet samples from this trial cast contained very few inclusions, only occasional, highly aluminous silicate stringers being observed. These alumino-silicates were almost certainly exogenous erosion products as evidenced by the fact that they occasionally contained trace amounts of K_2O. It has been suggested that they resulted from erosion of the highly aluminous cement used on the degassing vessel refractories, although it was not possible to confirm this directly.

The overall cleanness of the billet samples was confirmed by the total oxygen determinations, Table 4.3, and shows therefore, that in this particular cast, the majority of inclusions present in the liquid metal in the ingot escaped and were not entrapped during solidification.

5.2 OCCURRENCE OF INCLUSIONS IN LOW SILICON LEADED FREE-CUTTING STEEL

5.2.1 Oxidation Period

During the oxidation period, the inclusions observed were mainly calcium manganese silicates containing varying amounts of Al_2O_3 and Cr_2O_3 together with trace amounts of MgO, P_2O_5 and TiO_2. They originated from slag entrapped in the metal by the turbulence caused by oxygen blowing. However, the SiO_2 content of these inclusions was considerably higher than that of the bulk slag (35% against 13%). The MnO content was also much higher (25% against 7%) whereas the CaO content was lower (15% against 40%). In other words, these inclusions were considerably richer in SiO_2 and MnO than the bulk slag at the expense of a decreased CaO content. This indicates a dilution effect produced by the precipitation of oxidation products on the entrained slag particles. The same effect has been observed previously by Pickering[102] during basic electric arc steelmaking.

Aluminium was also available for oxidation in the initial charge and it is clear that more than sufficient was available from this source to give inclusions having a higher Al_2O_3 content that that of the bulk slag. However, the oxidation of the aluminium would be expected to occur very early in the oxidation period and this appeared to be the case in the present investigation as shown in Fig. 5.4.

The initial charge to the furnace must also have contained some chromium as it was observed that dendritic particles of the spinel, $(FeMn)O.(CrAl)_2O_3$, associated with silicate inclusions were formed during the oxidation period, Fig. 4.9c. These dendrites had been precipitated within the silicate matrix which contained $\sim$10% Cr_2O_3

in solution. As Pickering[102] has pointed out, the solubility of Cr_2O_3 in SiO_2 is very limited but can be increased by the presence of other oxides in the silicate, the average composition of which was approximately 12% FeO, 27% MnO, 32% SiO_2, 18% Al_2O_3, 10% Cr_2O_3, 5% CaO, 1% MgO, but only at a temperature of about 1800°C. It appears, therefore, that oxygen lancing had caused a locally very high temperature and under these conditions the silicates had been able to dissolve sufficient Cr_2O_3, in addition to Al_2O_3, to result in the precipitation of dendrites of spinel on subsequent cooling.

During the oxidation period, the inclusion sampling technique used in the present work (unkilled samples) gave very similar results for acid soluble silicon content as the normal furnace spoon samples (aluminium-killed). Thus, despite the fact that the inclusion samples were unkilled in order not to modify the inclusions, and consequently they contained a certain amount of porosity owing to the relatively high oxygen content of the metal during the oxidation period, they were nevertheless suitable for chemical analysis as well as for metallographic inclusion examination.

At the end of the oxidation period, the bath was blocked with ferro-manganese. A sample taken shortly after this operation whilst the power was still on (trial B.1) indicated that the turbulent conditions under which the sample was taken had resulted in the entrainment of slag particles in the bath. The MnO-rich deoxidation products resulting from the ferro-manganese addition had nucleated on or agglomerated with entrained slag particles to form calcareous inclusions containing globules of (FeMn)O.

5.2.2 Tapping Period

The samples taken from the top of the ladle immediately after the completion of tapping contained large manganese silicates. Within this group, there were two distinct types having the following approximate compositions:-

	MnO	SiO_2	Al_2O_3	MnS	CaO	P_2O_5	TiO_2	K_2O
(a)	45	25	15	5	5	-	tr	1
(b)	50	25	5	10	5	tr	tr	-

No potassium was detected in the ferro-phosphorus so that the presence of 1% K_2O together with 15% Al_2O_3 in the first type suggests that they originated as a result of ladle refractory erosion. The 5% CaO in these inclusions probably came from slag glaze on the ladle refractories, or was possibly picked up as a result of their reaction with slag mixed into the metal during tapping.

The second type of inclusion also contained approximately 5% CaO but no K_2O and much less Al_2O_3 than the first type. It is suggested therefore that these inclusions originated in part from slag entrained in the metal during tapping. The presence of relatively large amounts of MnO in these inclusions indicates that MnO-rich deoxidation products resulting from the ladle addition of ferro-manganese had nucleated on or agglomerated with the entrapped slag particles, the CaO content of which had correspondingly decreased by dilution. As the ladle samples were taken only about 2 min after the completion of tapping, this CaO dilution effect was apparently very rapid, much more rapid in fact than has been observed with previous slag-metal mixing. This may have been a result of the very high Mn:Si ratio of the steel and/or the more rapid flotation of the higher CaO content inclusions. The ladle addition of rock sulphur also resulted in the solution of appreciable amounts of sulphur in the entrapped slag particles. This would again accelerate the CaO dilution effect and produce the observed changes in inclusion composition.

5.2.3 Teeming Period

The following types of inclusions were present in the ladle stream samples:-

(a) Large, glassy manganese alumino-silicates containing about 1% K_2O. These were erosion products from the ladle, stopper or nozzle refractories.

(b) Complex manganese silicates containing essentially (FeMn)O and (FeMn)S. These inclusions were probably deoxidation/reoxidation products formed during tapping and teeming.

The following types of inclusions were present in the samples taken from the ingots:-

(a) Complex manganese silicates containing small amounts of CaO and Al_2O_3 together with K_2O. These were refractory erosion products.

(b) Complex manganese silicates containing small amounts of CaO and Al_2O_3 but no K_2O. Despite the fact that K_2O could not be detected in these inclusions, it is still possible that they originated from the erosion of refractories. However, at this stage, apart from the K_2O content, the composition and constitution of all the inclusions were very similar as a result of coalescence and reaction with manganese in the steel, and it was therefore very difficult to determine their exact origin. The indications are, however, that they were mainly erosion products together with some deoxidation/reoxidation particles.

During the teeming of trial cast B.2, occasional complex calcium silicates containing MgO particles were also observed, Fig. 4.23. These silicates possibly originated during tapping as a result of the pick-up of MgO particles by the slag from the magnesite-coated launder of the furnace. They were entrained in the metal by the force of the tapping stream and subsequently passed into the ingots during teeming. However, it is surprising that such large inclusions were not eliminated in the ladle and also that their compositions were changed very little during their residence in the steel. These facts tend to suggest an alternative mechanism of formation at a much later stage but it is difficult to account for a CaO-MgO composition other than during tapping. As they were observed during the earlier stages of teeming, they were unlikely to result directly from the teeming of ladle slag. It may be that these inclusions became attached to the ladle lining and were washed off again by the flow of the metal during teeming. However, this still does not explain their

very high CaO content.

The bottom billet samples from each of the four free-cutting steel casts were extremely dirty. Long silicate stringers containing MnS and $MnO.Al_2O_3$ particles together with trace amounts of K_2O and CaO were present. By comparison, the middle and top billet samples were relatively clean. This difference in inclusion content between the bottom 30% of the ingot and the remainder was a result of the bottom cone segregation of silicate inclusions. The presence of galaxite spinel particles together with K_2O indicates that these stringer inclusions were chemical erosion products originating from fireclay refractories, i.e. because of the high Mn:Si ratio (~100:1) this steel was proving to be extremely susceptible to attack by manganese on alumino-silicate refractories. The small amounts of CaO in these inclusions probably came from slag glaze on ladle refractories.

The metallographic observations were confirmed by the total oxygen contents of the billets, e.g. Figs. 4.19-4.21 for trial cast B.2. Apart from the high inclusion content of the bottom billet samples relative to the middle and top samples, Fig. 4.19 also showed that there was very little difference in cleanness between the uphill-teemed ingots (1, 7 and 12) and the direct-teemed ingot (6). In fact the bottom billet samples from ingot 6 were slightly dirtier than those from the other ingots in the cast yet the inclusion types were identical in all the billet samples, i.e. manganese alumino-silicate erosion products. This indicates, therefore, that holloware erosion during uphill-teeming was not a problem in this cast. Rather it was erosion of the ladle refractories which resulted in the pick-up of silicon after tapping and the presence of alumino-silicate stringer inclusions in the billets. It appears, therefore, that one of the main factors determining the extent of erosion was the length of time the steel was in contact with the refractories. It is significant that the residence time of the steel in the ladle was considerably longer than that of the steel in the runner bricks, allowing reaction with manganese and softening of the surface layer of ladle refractory

in contact with the steel to be proportionately greater.

5.2.4 Variation in Silicon Content throughout Steelmaking, Tapping and Teeming

The variation in silicon content for the four trial casts are shown in Figs. 4.18, 4.22, 4.27 and 4.31. It can be seen that the silicon content of the bath dropped during the oxidising period as silicon was oxidised to silica which was then assimilated into the slag.

In each of the four trial casts, B.1-B.4, the silicon content of the sample taken from the top of the ladle shortly (1-3 min) after the completion of tapping was approximately the same, within the limits of analytical error (±0.002% Si), as the bath silicon content prior to tapping. At this stage, therefore, it is apparent that neither the small amount of silicon present in the ladle additions (Table 3.6) nor the silicon present in the form of silicate inclusions (deoxidation products, entrained slag particles, refractory erosion products) caused the total silicon content of the liquid steel to increase significantly. In trial cast B.4, however, a second sample was taken from the top of the ladle 5 min after the completion of tapping and the silicon content of this sample (0.011%) was considerably higher than that of the first ladle sample (0.002%) taken 2 min earlier, Fig. 4.31. This pick-up of silicon after tapping was also reflected in the ladle stream samples from all four trial casts and in most cases, this increase in silicon content was significantly greater than that present in the ferro-alloy additions made to the ladle, even allowing for maximum recovery from the additions. The metallographic evidence indicates that the number of entrained particles of furnace slag was small and they were rapidly eliminated into the ladle slag layer, whereas manganese alumino-silicate refractory erosion products persisted throughout the teeming period and were present in the ladle stream, ingot and bottom billet samples. Thus, the increase in silicon content after tapping to a value of 0.010% or more was apparently caused by the presence of manganese/ladle refractory reaction products in the metal.

The fact that this ladle erosion was not detected in the samples taken from the top of the ladle 1-3 min after the completion of tapping was probably that a longer period of time than this was necessary for the manganese in the steel to react with the silica in the ladle refractories to form a fluid manganese alumino-silicate reaction layer, for significant amounts of this reaction layer to be washed into the steel and for these entrained erosion products to rise to the top of the ladle where the sample was taken. In the case of trial cast B.4, this occurred after ~5 min. With increasing residence time of the steel in the ladle, erosion probably increased, particularly during teeming as a result of the washing action of the steel on the bottom of the ladle.

It has already been mentioned that the condition of the ladle lining is an important factor from the steel cleanness point of view. In any clean steel practice, the steelmaker normally chooses a ladle which is not new, having been used for a few heats, and which has not been repaired with siliceous refractory cement. This was confirmed in the present series of trials as the following results show:-

Trial Cast	Ladle Life	$(Si)_{Pit} - (Si)_{Tap}$
B.1	18 heats (repaired)	0.009%
B.2	1 heat	0.006%
B.3	4 heats	0.004%
B.4	12 heats (repaired)	0.008%

One final point of interest in connection with the present investigation is the mechanism of bottom cone inclusion formation in steel ingots. It is not intended that a critical examination be given of this phenomenon as it could quite easily form the basis of a separate thesis. However, a review of the bottom cone of inclusions in steel ingots has been published by Standish[178] and it is evident from this that there is still a great deal of controversy concerning the mechanism of bottom cone formation. In this respect, it is pertinent to mention the work of Hunt[179] on the formation of A - segregates. Although bottom cone formation was not specifically referred to

in Hunt's model work, it seems reasonable to assume that the mechanism which was proposed to account for the formation of A - segregates during solidification might also go a long way towards explaining the formation of the bottom cone of inclusions, particularly as these two phenomena invariably occur together (see Section 5.3.4).

5.3 OCCURRENCE OF INCLUSIONS IN CARBON-MANGANESE-NIOBIUM STEEL

5.3.1 Trial Cast C.1

During the oxidation period, the inclusions observed were mainly calcium silicates containing varying amounts of Al_2O_3, MgO and MnO together with trace amounts of P_2O_5, TiO_2 and S. They originated from slag entrained in the metal by the turbulence caused by oxygen blowing. However, the SiO_2 content of these inclusions was considerably higher than that of the bulk slag. In some cases, the MnO content was also much higher whereas the CaO content was lower. As in previous work therefore, this indicates a dilution effect produced by the precipitation of oxidation products on the entrapped slag particles. There seemed to be little systematic variation in the sizes of the inclusions during the oxidation period, most of the inclusions having diameters of 15-40 μm.

During the refining period, the majority of inclusions present in the liquid metal were globular manganese alumino-silicate deoxidation products resulting from the ferro-silicon, ferro-manganese and aluminium additions. Calcium silicates resulting from slag entrainment were also present.

Immediately after tapping, the inclusions present in the liquid metal were mainly calcium alumino-silicates resulting from reaction between aluminium and entrained slag particles. In some cases, these inclusions contained considerable amounts of MgO as a result of contamination by magnesite refractory material from the furnace, taphole or launder.

During teeming, the majority of inclusions present in the ingots were manganese alumino-silicates resulting from entrainment of the mould additive.

However, other types of inclusions were also observed including:-

(a) alumino-silicate refractory erosion products

(b) magnesite refractory erosion products

(c) slag/magnesite refractory reaction products.

5.3.2 Trial Cast C.2

The samples taken during the refining period of this first development cast showed that the high aluminium cover, i.e. very low dissolved oxygen content, was sufficient to prevent the formation of globular silicate deoxidation products following the ferro-silicon addition. Unlike the previous trial cast, very few direct deoxidation products were observed and the majority of inclusions present were entrained slag particles. In many cases, these slag particles were rich in MgO as a result of contamination of the slag by magnesite furnace refractory.

Immediately after tapping, the inclusions present in the liquid metal were calcium aluminates resulting from slag entrainment. Many of these inclusions contained considerable quantities of periclase (MgO), picked up from the furnace, taphole or launder refractories.

During teeming, the main types of inclusions observed were alumino-silicate refractory erosion products, magnesite refractory erosion products, and slag/magnesite refractory reaction products.

5.3.3 Trial Cast C.3

The steelmaking practice for this cast was similar to the previous one except that part of the Desulfex was injected into the bath. As expected therefore, the inclusions observed during the steelmaking, tapping and teeming processes were very similar to those observed in the previous cast. The main difference was that in this cast, fewer MgO-rich inclusions resulting from magnesite refractory erosion were observed. This difference is discussed in Section 5.3.4.

5.3.4 Comparison of Trial Casts C.1, C.2 and C.3

(i) Through-Thickness Results

The through-thickness tensile results for the two development casts C.2 and C.3 were significantly better than those for cast C.1 made according to the original ferro-silicon deoxidation practice, the overall average reduction of area values for casts C.1, C.2 and C.3 being 34%, 51% and 53% respectively. Thus, for the two development casts, the modifications in steelmaking practice were very successful in improving the through-thickness ductility and have since been adopted as standard practice for C-Mn-Nb steel production.

(ii) Non-Metallic Inclusion Content

The improvement in through-thickness ductility is attributed to a decrease in the volume fraction of inclusions in the liquid and hence in the solid steel. However, the sampling technique employed during the steelmaking, tapping and teeming processes was primarily aimed at establishing the types of non-metallic inclusions present in the liquid metal and not at a quantitative assessment of the number or volume fraction. Consequently, it was not possible to quantify accurately the differences in inclusion content at corresponding stages during the three trial casts. An attempt was made to follow the variation in inclusion content by determining the total oxygen contents of the metal samples. However, the results were very variable, fluctuating quite considerably not only from sample to sample but also along the length of a single sample. Similar effects have been observed previously with aluminium-killed steels both in laboratory induction furnaces and in large arc furnaces. In contrast, total oxygen determinations on equivalent samples from silicon-killed steels have been found to be very consistent and to reflect changes in the bath inclusion content very precisely. These effects are presumably similar to those observed by Förster and Richter[53,54] and discussed earlier, the variable oxygen content of the

aluminium-treated steel resulting from the variable distribution of alumina inclusions.

Nevertheless, optical metallographic examination did reveal a marked cast to cast difference in both the size and number of inclusions present in samples taken from the furnace during the refining period, from the ladle after tapping and from the ingots during teeming. Such differences were not obvious in the case of the ladle stream samples, and this may have been a direct result of this particular method of sampling giving rise to numerous reoxidation products.

During the refining period, the size and number of deoxidation products observed in cast C.1 were greater than those observed in the two development casts. This difference was a result of the use of a full aluminium deoxidation practice for the development casts in place of the previous ferro-silicon practice, and is discussed in greater detail below.

There was also a difference in inclusion content observed between the samples taken from the ladle after tapping. In this case, however, the main difference was between the two development casts. The size and number of inclusions present in the sample taken from the ladle after tapping were much greater for cast C.2 than for cast C.3. The possible reasons for this difference are also discussed below.

Finally, there was a marked reduction in the number of inclusions observed in the ingot samples from the two development casts compared with those from cast C.1. There were probably several reasons for this reduction including the use of higher alumina ladle refractories to minimise erosion and the use of an argon shroud to minimise reoxidation. However, the main reason was undoubtedly the improved method of adding the mould additive. Previous work has shown that placing the mould additive in the bottom of the mould prior to teeming results in considerable entrainment of the additive in the liquid metal. This entrainment was again observed during the teeming of cast C.1 but not for casts C.2 and C.3, in which the mould additive was suspended in the moulds so that its addition was made after the start of teeming

when there was a pool of metal in the mould. This particular difference in inclusion content also provided evidence that the sampling technique was capable of obtaining representative samples.

A point of considerable interest is the fact that although the majority of inclusions observed in the liquid metal in the ingots during teeming were globular alumino-silicates resulting from refractory erosion and slag entrainment, these inclusions were rarely observed on the fracture faces of the through-thickness tensile specimens. Poor ductility and premature failure of the test-pieces from the earlier production casts were invariably caused by alumina-rich agglomerates, Figs. 5.5a and 5b, and/or sheets of manganese sulphide, Fig. 5.5c. The aluminate particles, which were primarily observed at the centres of plates rolled from the bottom of the ingots, i.e. associated with bottom cone segregation, were frequently found to contain small amounts of MgO and CaO, and very occasionally a trace amount of K_2O was also detected. The sheets of manganese sulphide were mainly observed at about the 25% depth level of plates rolled from the top of the ingots, i.e. associated with A - segregation. Particles of niobium carbide were also present with the manganese sulphide. The metallographic evidence indicated that in 'bad' ingots, heavy bottom cone segregation of aluminate particles was invariably associated with marked A - segregates whereas in 'good' ingots, there was a more general distribution of the aluminate inclusions and only very weak A - segregates.

It is very unlikely that all the globular alumino-silicates present in the ingots during teeming escaped at this late stage. It is suggested, therefore, that although many of these larger particles did in fact escape from the liquid metal in the ingot, some of the smaller alumino-silicates were entrapped and continued to react with dissolved aluminium and were eventually converted to alumina. Evidence for this type of reduction reaction has been obtained by laboratory studies of the reaction between silicate inclusions and aluminium in both liquid and solid iron[22,107].

During rolling, these reduced alumino-silicates are broken down and spread out to form stringers of alumina particles which are very similar in appearance to some of the stringers observed in plate samples from the present work, e.g. Fig. 5.5a. Further evidence that this type of reaction occurred was provided by the fact that, as mentioned previously, the aluminate particles present on the fracture surfaces of through-thickness tensile specimens frequently contained small amounts of MgO and CaO indicating that they originated in part from slag and/or refractory material. These oxides are very stable and are not reduced by aluminium to the same extent as SiO_2 and MnO. They are therefore useful tracers for determining the origins of non-metallic inclusions. Modifications in practice aimed at lowering the volume fraction of silicate inclusions in the liquid metal, e.g. full aluminium deoxidation, suspension of mould additive and high Al_2O_3 content refractories, should therefore result in a lower volume fraction of aluminate inclusions in the finished product.

It is not suggested, however, that reduction of alumino-silicates by aluminium was the only mechanism by which the aluminate clusters were formed. Deoxidation and reoxidation reactions also need to be considered, particularly for explaining the formation of the very small alumina particles (<5 μm) in Fig. 5.5b which are not easily accounted for in terms of the above reduction reaction. Clusters of alumina deoxidation products were not observed in the samples taken from the ladle after tapping or from the ladle stream during teeming in any of the three trial casts. This is apparently typical of sampling trials on double slag basic electric arc casts, similar observations having been reported by Knüppel et al[58]. It suggests that relatively few, if any, alumina clusters were present in the ladle of metal during teeming compared with the globular alumino-silicate inclusions, and that if alumina deoxidation/reoxidation products were contributing to the clusters observed on the fracture faces, e.g. Fig. 5.5b, then they must have formed by the agglomeration of very small inclusions such as that shown in Fig. 4.38h. This agglomeration possibly

occurred on the sides of the nozzle during teeming and these large clusters were periodically flushed into the ingot. However, it is emphasised that alumina agglomeration on the sides of the nozzle is normally associated with the formation of dendritic clusters and this type was not observed on the fracture faces of the tensile specimens. Further agglomeration of small alumina particles in the uphill-teeming channel may also have contributed to the overall clustering effect but a major factor leading to the formation of very large clusters of the type shown in Fig. 5.5b was undoubtedly segregation during solidification of the ingot. This not only resulted in the formation of a bottom cone of alumina particles but also in the formation of sheets of manganese sulphide in the A - segregates, even with an average pit sulphur content of only 0.006 wt. %.

Reoxidation of fully aluminium-deoxidised steel can result in the formation of alumina clusters. Evidence for this has been obtained during laboratory experiments with iron-silicon-oxygen-aluminium melts in a 50 kg induction furnace[22,107]. Reoxidation, as shown by the variation in the total oxygen content of the melt after the preliminary deoxidation stage, resulted initially in the formation of alumina clusters and then, as the soluble aluminium content of the melt decreased with time, in the formation of duplex alumino-silicate inclusions containing alumina. With further increase in time, single-phased alumino-silicates were formed. This sequence of reaction products has been discussed by Farrell et al[139] and is illustrated schematically in Fig. 2.86. It shows quite clearly that the type of reoxidation product which is formed depends on the relative concentrations of the reacting elements. As discussed previously, Kohn et al[118,119] consider that the reaction products which precipitate as a result of reoxidation of aluminium-killed steel in the furnace and ladle are complex aluminates containing small amounts of CaO and MgO, the latter originating from trace concentrations of calcium and magnesium (from refractories, slag and deoxidants) in solution in the steel. These aluminates accumu-

a r· dicall flushed into the in ot. Althou h not ostulated

by Kohn et al, similar aluminates formed as a result of reoxidation of the ladle stream during teeming could also enhance this effect, agglomeration in this case occurring in the uphill-teeming channel and/or in the ingot. Segregation of alumina in the ingot would occur as discussed in the previous paragraph. Whilst this mechanism can account for the formation of aluminates containing MgO and CaO, it must be pointed out that these oxides were not detected in globular manganese alumino-silicate reoxidation products present in ladle stream samples, e.g. Figs. 4.41a and 41b. However, this could have been a result of the large dilution effect caused by the excessive reoxidation. Nevertheless, the present work did confirm the results of Kohn et al in that many of the inclusions present in the final product were aluminates rather than pure alumina, indicating that the problem was associated with secondary deoxidation/reoxidation products and not primary deoxidation products.

(iii) Deoxidation Practice

Following the first trial cast C.1, it was recommended that a clean steel practice for the production of C-Mn-Nb steel should involve a primary aluminium bath block followed by the maintenance of an effective aluminium cover during refining, tapping and teeming. The use of such a deoxidation practice results in the formation of alumina or spinel-type inclusions which are known to escape from the liquid metal more readily than silicates, and the rapid elimination of such deoxidation products into the slag results in a cleaner steel. Also, the addition of ferro-silicon after the aluminium bath block does not give rise to silicate deoxidation products because of the lack of available oxygen in the steel. Thus, the presence of siliceous inclusions is confined to entrained slag, reoxidation and erosion products. Also, if there is a sufficient aluminium cover, i.e. a sufficiently high level of soluble aluminium in the steel, any entrained silicates react with this aluminium and are eventually converted to alumina/spinel particles which again escape readily. In the absence of

an aluminium cover, these silicates tend to remain in the steel for a longer period of time.

The present investigation has confirmed the above theory in that for cast C.1 involving a ferro-silicon bath block, large globular silicates and alumino-silicates were present in the liquid metal throughout the refining period. These were deoxidation products resulting from the ferro-silicon, ferro-manganese and aluminium additions. However, for casts C.2 and C.3, a high aluminium cover was maintained during refining and only small, isolated alumina deoxidation/reoxidation products were observed during this period.

In general, the entrained slag particles present during the refining periods of casts C.2 and C.3 were smaller than the corresponding inclusions of cast C.1 indicating that the high aluminium cover was possibly also assisting in the elimination of these exogenous slag particles.

During the teeming of the two development casts, the soluble aluminium content of the stream and ingot samples from C.3 ($\sim$0.04%), Figs. 4.51 and 4.52, was approximately twice that of the corresponding samples from C.2 ($\sim$0.02%), Figs. 4.43 and 4.44. In addition, the soluble aluminium content of cast C.2 tended to drop below 0.02% during the later stages of teeming. Thus, the effective aluminium cover was significantly higher for cast C.3 than for cast C.2 throughout all stages of steelmaking, tapping and teeming. However, no obvious difference in terms of type and number of inclusions was observed as a result, indicating that the level of aluminium in both casts was sufficient to prevent the formation of globular alumino-silicate inclusions.

Apart from these differences in aluminium content, the most striking aspect was the close correlation between the soluble and total aluminium contents for cast C.3, as a result of the relatively consistent level of insoluble aluminium, Fig. 4.51.

(iv) Tapping Practice

In each of the three trial casts, a large taphole was used to promote slag-metal mixing and desulphurisation. The inclusions present in the ladle samples taken after the completion of tapping were mainly calcium aluminates containing particles of periclase (MgO), resulting from the entrainment of slag particles in the metal. However, their general content of MgO was also high as a result of contamination of the slag by magnesite refractory erosion products from the furnace, taphole or launder.

As mentioned previously, there were considerably fewer slag inclusions in the ladle sample taken after tapping cast C.3 compared with cast C.2. This could have been a sampling problem but more likely it was the result of a difference in the degree of slag-metal mixing as supported by the fact that sulphur removal for cast C.3 was only 0.003% compared with 0.007% for cast C.2.

Although the majority of the $CaO-MgO-Al_2O_3$ particles entrained in the metal during tapping appeared to escape into the ladle slag layer, some of these inclusions remained entrapped in the steel and were carried through into the ingots during teeming. The presence of varying amounts of MgO and CaO associated with aluminates on some fracture surfaces further indicates that these slag-based inclusions were possibly contributing to the overall inclusion content of the final product, either directly or indirectly. In order to reduce the amount of slag mixed into the metal during tapping and thus improve steel cleanness, it would be necessary to slag off partially prior to tapping and then hold back the remaining slag for as long as possible during tapping. However, the necessity to obtain as low a sulphur content as possible dictates that the metal be tapped through the slag. Nevertheless, an alternative desulphurisation technique, such as reladling, should enable the slag-metal mixing during tapping to be minimised and lead to a cleaner steel in the ingot. These conclusions are in agreement with those of Pickering[102] who has also pointed

out that slag-metal mixing during tapping can lead to an increase in the number of inclusions present in the final product. It may be that in steels where a low sulphur content necessitates tapping through the slag, and other desulphurisation techniques are not available, then inert gas bubbling through a porous plug in the bottom of the ladle might accelerate the removal of entrained slag particles and result in a cleaner product.

(v) Argon Shrouding

There were no obvious indications from the liquid metal samples that argon protection of the teeming stream in the two development casts was reducing the volume fraction of inclusions in the ingots by minimising atmospheric reoxidation. The ladle stream samples, which were taken with the argon flow turned off in the two development casts, contained large manganese alumino-silicate reoxidation products, e.g. Fig. 4.41a. These were formed as a result of the sampling technique allowing excessive oxidation of the metal stream to occur. If such inclusions were actually formed during teeming into the ingots, they would probably agglomerate with other pre-existing inclusions (entrained slag, refractory erosion products). Such a mechanism would lead to an increase in the volume fraction of liquid silicates in the ingots during teeming. On the other hand, with only slight reaction of the liquid steel with atmospheric oxygen, the resulting inclusions would be more highly aluminous and possibly even consist of solid particles of alumina. The latter could then agglomerate in the narrow confines of the uphill-teeming system, such a mechanism leading to an increase in the numbers of alumina clusters in the ingots during teeming, as discussed previously. Although it was not possible to investigate these effects in detail in the present work, the practice of argon shrouding is to be continued and further work is to be carried out.

(vi) Refractories

Results from the first trial cast C.1 indicated that in a clean steel practice for the production of C-Mn-Nb steel, careful attention should be paid to the magnesite refractory material of the furnace, taphole and launder, and the alumino-silicate fireclay refractories of the ladle, stopper, nozzle and holloware. Immediately after tapping this cast, entrained slag particles were present in the metal and many of these inclusions contained MgO particles as a result of contamination by magnesite refractory from the furnace, taphole or launder. Slag/magnesite inclusions of this type were also present in the ingots during teeming. MgO-rich inclusions consisting of spinel within a manganese alumino-silicate matrix were also present in the ingot samples. They were not associated with slag and therefore probably formed by the precipitation of MnO, SiO_2 and Al_2O_3 reoxidation/secondary deoxidation products on eroded magnesite refractory. Reaction with aluminium in the steel then resulted in the formation of spinel particles.

For cast C.2, magnesite erosion appeared to be even more marked. Slag/magnesite reaction products were present in the furnace, ladle and ingots. Manganese alumino-silicates containing $(MnMg)O.Al_2O_3$ particles were also observed in the ingots.

For cast C.3 however, apart from the inclusions present in the ladle after tapping, none of the inclusions analysed in the furnace or ingot samples were rich in MgO. Magnesite erosion therefore, did not appear to be as great in this cast as in the previous two. It is interesting to note that this cast to cast variation corresponds fairly closely with the variation in furnace lining life:-

Cast No.	Lining Life
C.1	74%
C.2	94%
C.3	58%

It was not possible to determine the individual contribution from the furnace

lining, taphole and launder. All that can be stated is that for cast C.3, magnesite erosion products were not observed in the furnace or ingots; for cast number C.1 magnesite erosion products were observed in the ingots; and for cast number C.2 they were present in the furnace and ingots. In all three casts, MgO-rich calcium aluminates were present to varying extents in the ladle after tapping. Experimental data on the effect of increasing MgO content on the elimination of calcium aluminates and calcium alumino-silicates from liquid steel have not been published. However, the results of the present trials indicate that MgO-rich calcium aluminates having diameters up to 35 μm can remain in the steel for periods as long as 38 min after the completion of tapping and can eventually pass into the ingots during teeming.

For cast C.1 another major source of inclusions in the liquid metal was alumino-silicate refractory erosion. Manganese attack on the fireclay refractories of the ladle and/or holloware resulted in the formation of a liquid layer at the refractory/melt interface. The viscosity of this layer decreased with decreasing SiO_2 content so that the ease of removal or erosion of the layer increased. The resulting inclusions were manganese alumino-silicates containing trace amounts of K_2O. Because of the relatively high manganese content therefore, this steel was proving to be susceptible to refractory erosion. The major source of this erosion was probably the ladle rather than the holloware because of the higher temperature and longer contact period.

Consequently, in the two development casts, the ladle refractories were made of high alumina brick (70% Al_2O_3) instead of the normal firebrick ($\sim$30% Al_2O_3) in an attempt to reduce the number of erosion products in the liquid metal during teeming. Details of the refractories for all three trial casts are given in Table 3.12. For the same reasons as stated previously, it was impossible to quantify the difference in inclusion content resulting from this change in ladle refractory. However, optical examination of the ladle stream and ingot samples from the three casts did indicate

some differences in the mean compositions of the manganese alumino-silicate erosion products. For cast C.1 they were mainly single-phased particles typical of manganese attack on an alumino-silicate brick containing ~30% Al_2O_3. A few duplex inclusions containing alumina were also observed and these possibly resulted from further reaction with aluminium in the steel. For casts C.2 and C.3, however, they were mainly duplex inclusions containing spinel and alumina phases. This higher Al_2O_3 content may have been a result of the higher soluble aluminium content of the two development casts. However, as some single-phased erosion products were observed in both these casts, it is considered that it was also a result of the use of 70% Al_2O_3 ladle bricks, duplex alumino-silicates containing alumina being the typical equilibrium reaction products with manganese in this case. The single-phased erosion products having lower Al_2O_3 contents probably originated from the holloware or some other fireclay-type refractories. Thus, although the higher Al_2O_3 ladle bricks still appeared to be giving rise to some alumino-silicate erosion products, it is suggested, on the basis of the optical metallographic results, that the volume fraction of these products in the liquid steel during tapping and teeming was less than with the normal firebrick ladle.

SECTION 6

SUMMARY AND CONCLUSIONS

SECTION 6 - SUMMARY AND CONCLUSIONS

6.1 VACUUM DEGASSED LOW ALLOY STEEL

Prior to tapping the open-hearth furnace, the steel was relatively free from oxide inclusions.

During tapping, the addition of ferro-manganese, ferro-silicon, ferro-chromium and aluminium to the ladle resulted in the formation of liquid manganese alumino-silicate deoxidation products containing small amounts of Cr_2O_3.

These liquid manganese alumino-silicates were also present in the steel during the early stages of vacuum degassing. With increasing degassing time, however, their number gradually decreased as a result of coalescence and flotation until only occasional inclusions of this type were observed.

During the later stages of degassing, ladle erosion products were present in the liquid metal. In addition, Cr_2O_3-rich and MgO-rich erosion products which had originated from the magnesite-chromium refractories of the degassing vessel were also present. Alumino-silicate inclusions containing varying amounts of Al_2O_3 were occasionally observed as well. The most likely source of these was the high alumina cement used on the degassing vessel refractories. During vacuum degassing, the total oxygen content of the steel decreased initially and then began to increase again as the rate of refractory erosion exceeded the rate of inclusion flotation. This increase occurred approximately 18 min after the commencement of degassing, although the rapid rate of inclusion removal finished after only 14 min of the degassing cycle.

Complex manganese chromium silicate erosion products containing cristobalite and in some cases chromium galaxite were present in the ladle stream samples. They originated from the siliceous material used to patch the ladle and had picked up chromium from the liquid steel.

The majority of inclusions present in the ingots during teeming were large,

duplex cristobalite/manganese silicate erosion products. In these cases, they were holloware erosion products originating from the siliceous cement used to joint the runner bricks together.

Despite the generally high level of inclusions in the liquid metal during tapping, degassing and teeming, the billet samples from the present trial cast were relatively free from non-metallic inclusions, only occasional, highly aluminous silicates being observed. It has been suggested that they resulted from erosion of the high alumina cement of the degassing vessel, although this could not be confirmed directly. The indications are therefore, that in this particular cast, the majority of inclusions present in the molten metal escaped and were not trapped in the ingot during solidification. Nevertheless, the occurrence of certain of the inclusion types, particularly the erosion products, could be minimised, thus resulting in a cleaner steel prior to solidification.

One suggestion for improving the cleanness of the steel in the ladle would be to add more aluminium during tapping, preferably in the form of ferro-aluminium. This should result in the formation of more highly aluminous inclusions and therefore an increase in their rate of escape.

A further possible improvement in the rate of inclusion removal and therefore in steel cleanness in the ladle might be achieved by adding the aluminium before the ferro-manganese, ferro-silicon and remaining ferro-chromium providing the mixing conditions for the latter three additions could still be met. This suggestion is contrary to some of the ideas discussed in Section 2.3.2 where it was proposed that additions of a relatively weak deoxidiser such as manganese will decrease the degree of supersaturation and encourage the formation of larger inclusions when a strong deoxidiser is subsequently added. However, by adding the aluminium before the ferro-alloys, it might be possible to form alumina inclusions which should escape very rapidly, particularly as there is a great deal of turbulence during tapping. There would then be less oxygen available for reaction with the ferro-alloys and,

therefore, fewer liquid manganese silicate deoxidation products which escape less rapidly than alumina would be formed. The implication of this proposal is that inclusion composition is more important than inclusion size for the removal of the deoxidation products and therefore for the success of the overall deoxidation process. The only limitation on this practice is that a certain time interval should occur between the aluminium and ferro-alloy additions to allow the alumina inclusions to escape. This may not be possible in actual practice because of the relatively short time available to make the additions.

A further suggestion for improving steel cleanness is that careful consideration should be given to the condition of the ladle and degassing vessel refractories. Erosion of the siliceous material used to repair the bottom of the ladle was a problem in this cast and was aggravated by the locally high concentration of ferro-chromium during tapping. Erosion of the magnesite-chromium refractories and high alumina cement of the degassing vessel was also a problem. A reduction in the number of inclusions arising from this source might be obtained by lowering the turbulence of the steel flowing through the vessel. As this steel was degassed for cleanness and analytical purposes rather than for hydrogen removal, this could possibly be achieved by not using the final steam ejector of the RH unit, i.e. by operating the unit at a slightly higher pressure.

The fact that this steel was not degassed for the purpose of hydrogen removal but for cleanness and analysis reasons raises the question as to whether equivalent results might not be obtained by simple inert gas purging through a porous plug in the bottom of the ladle. This would allow the degassing unit to concentrate more on those qualities for which hydrogen removal was essential. The only problem is that the ladle slag is an oxidising one and argon bubbling could promote phosphorus reversion as a result of slag-metal mixing. This is not too much of a problem during R.H. degassing because the slag tends to remain relatively quiescent.

It is also clear from the present trial cast that approximately 15 min after the start of degassing, the total oxygen content reached a minimum and then began to increase again as a result of refractory erosion. Therefore, some consideration should be given to reducing the degassing time.

A final suggestion is that careful attention should be paid to the condition of the holloware refractories, particularly the siliceous material used to joint the trumpet and runner bricks, as a major source of inclusions in the present trial cast was holloware erosion during uphill-teeming.

6.2 LOW SILICON LEADED FREE-CUTTING STEEL

On the basis of the silicon contents of the samples taken before and after tapping, neither the silicon present in the ladle additions nor silicon present in the form of siliceous slag inclusions mixed into the metal during tapping appeared to contribute significantly to the overall silicon content of the steel.

Pick-up of silicon in the form of silicate inclusions occurred in the ladle after tapping. The majority of these silicates originated from erosion of the ladle refractories. They persisted throughout the teeming period and were present in the ladle stream, ingot and billet samples. There was no direct evidence that slag entrainment during tapping was a problem.

The bottom billet samples were extremely dirty, containing long alumino-silicate stringers whereas by comparison, the middle and top billet samples from these ingots were relatively clean. This difference in inclusion content between the bottom 30% of the ingot and the remainder was a result of the bottom cone segregation of alumino-silicate inclusions.

There was no significant difference in cleanness between the uphill-teemed ingots and the direct-teemed ones. Manganese alumino-silicates resulting from refractory erosion were present in all of them. This indicates therefore that holloware erosion during uphill-teeming was not a problem. Rather the pick-up silicon after tapping and the presence of alumino-silicates in the billets were a result of ladle

erosion. This probably included erosion of the stopper and nozzle as well as the actual ladle lining. Thus, because of the very high Mn:Si ratio, this steel is very susceptible to attack by manganese on alumino-silicate ladle refractories. The condition of the ladle lining had a marked effect on the degree of ladle erosion and therefore on the extent of the pick-up of silicon. Ladles which had been used about four times previously and which had not been repaired or patched were found to give the best results.

The main recommendation therefore, for improving the cleanness of the steel is that careful attention should be paid to the condition of the ladle refractories, as the major source of inclusions was ladle erosion. In this respect, it might prove beneficial from the steel cleanness point of view to reinforce the refractories in the region of the ladle bottom, e.g. the use of more highly aluminous refractories for the bottom part of the ladle and stopper rod, and a magnesite nozzle or insert together with a magnesite or high alumina ramming compound.

6.3 CARBON-MANGANESE-NIOBIUM STEEL

For the two development casts, the modifications in steelmaking practice were very successful in improving the through-thickness ductility of the plates.

Although it was not possible to quantify the differences in inclusion content at corresponding stages during the three trial casts, optical metallographic examination indicated that, in general, there were fewer inclusions present in the liquid metal for the two development casts than for the original standard practice cast.

The use of a full aluminium deoxidation practice instead of one involving a ferro-silicon block, resulted in a marked reduction in the number of deoxidation products present during refining.

Slag-metal mixing during tapping resulted in the entrainment of calcium aluminates in the metal. These inclusions contained considerable amounts of MgO

as a result of contamination by magnesite refractory from the furnace, taphole or launder. These MgO-rich inclusions were also present in the ingots during teeming.

Final sulphur contents were very similar in all three casts. The indications are therefore that the improvement in through-thickness ductility of the two development casts was a result of a lower oxide inclusion content rather than a reduction in total sulphur content. In particular, the incidence of gross aluminate clusters at the bottom of the ingot and A - segregates of manganese sulphide at the top was considerably reduced. The composition and morphology of the aluminate particles in the clusters indicated that they were not primary aluminium deoxidation products but secondary deoxidation/reoxidation inclusions together with aluminium/alumino-silicate reaction products. Segregation and agglomeration of these inclusions in the bottom of the ingot occurred during cooling and solidification. However, the severity of this segregation was less, and therefore, the through-thickness ductility of the plate greater, for the two development casts than for the original standard cast. As the teeming conditions, in particular the temperature, were approximately the same in each case, this difference in quality was presumably a result of an improvement in steel cleanness, i.e. a lower volume fraction of inclusions in the liquid metal during teeming. The fact that, for the same metal sulphur content, there was also a corresponding improvement in ductility at the top of the ingot as a result of weaker A - segregate formation, implies that the ingot solidification pattern was influenced by the oxide inclusions in the liquid metal. Oxide particles possibly acted as nuclei for the precipitation of iron dendrites, thus promoting a more equiaxed ingot structure and therefore, according to McDonald and Hunt[179], more favourable conditions, i.e. increased solid/liquid regions, for the formation of A - segregates.

Although there were no obvious indications that argon shrouding of the teeming stream was beneficial from the point of view of steel cleanness, the practice should be continued until more detailed results are available.

Placing the mould additive in the bottom of the mould prior to teeming

resulted in considerable entrainment of the additive in the liquid metal. This was not the case in the two development casts where the mould additive was suspended about 30 cm from the bottom of the mould so that it was added after the start of teeming when there was a pool of metal in the mould.

Magnesite refractory erosion was evident in all three casts, but particularly in cast C.2. It was not possible to determine the individual contribution from the magnesite lining, taphole or launder, but the cast to cast variation corresponded with the variation in furnace lining life.

Although the higher Al_2O_3 ladle bricks still gave rise to some alumino-silicate erosion products, the indications were that this was less than with the normal firebrick ladle.

Although a practice for the production of C-Mn-Nb steel with through-thickness properties necessary to meet the required specifications has been developed, it is considered that further improvements in both through-thickness ductility and ingot to plate yield could be achieved by additional after-furnace treatment of the molten steel. Accepting that slag-metal mixing during tapping is unavoidable in terms of obtaining a sulphur content of about 0.005%, then argon purging should help to accelerate the elimination of the entrained slag particles. In addition, effective treatment of the steel with a calcium-containing deoxidant should further inhibit the formation of alumina agglomerates as well as detrimental type II manganese sulphide inclusions. The latter can still cause problems, even with a total sulphur content of only 0.005%, because of the segregation characteristics of the steel solidifying in the 20 t slab moulds. Trials are to be carried out to investigate the effects of these further modifications on steel quality.

6.4 GENERAL CONCLUSIONS AND RECOMMENDATIONS FOR FURTHER WORK

From the results of the investigations reported in this thesis, it is apparent that the entrainment of exogenous inclusions, particularly refractory erosion products,

in the liquid steel during tapping and teeming is a major source of oxide inclusions and can lead to quality problems (rejections and/or reduced yield). These problems are likely to become worse in the future as specifications and qualities become more exacting. Consequently, there is a need for further work to be carried out on the formation of inclusions as a result of:-

(i) Refractory Erosion - with higher manganese steels, attack by the manganese on fireclay refractories is a serious problem. The indications are that this problem can be alleviated to some extent by the use of alumino-silicate refractories having higher Al_2O_3 contents and this requires further investigation, both on a laboratory scale and in production heats.

(ii) Slag Entrainment - the practice of mixing slag and metal during tapping to effect desulphurisation needs careful examination, as there is evidence to indicate that a dirtier steel is produced with this technique. Where possible, argon purging through a porous plug in the bottom of the ladle should be carried out to promote the elimination of entrained slag particles.

(iii) Reoxidation - it was not obvious from the present work what effect argon shrouding of the teeming stream had on the non-metallic inclusion content of the product. However, the available evidence from the literature, although inconclusive, is sufficient to warrant further investigation of this effect.

Obviously, one of the most important factors from the steel cleanness point of view is the elimination of entrained non-metallic material. In this respect, the technique of inert gas bubbling and the effect of temperature on inclusion removal require further study.

A very important area of development is probably the use of reactive elements such as calcium, in the form of alloys with other elements, to modify detrimental Al_2O_3 and MnS inclusions. The physical properties of many calcium-containing alloys are such that they cannot be added to liquid steel in the same way as normal

ferro-alloys. They require to be added in a more carefully controlled manner such as by plunging or even injection. The available evidence indicates that the effective use of calcium alloys can lead to marked improvements in steel quality. It is necessary therefore that suitable techniques for adding reactive elements be investigated. This would apply not only to calcium but to other elements such as cerium, zirconium and magnesium which also appear to have potential as deoxidisers and inclusion modifiers.

The presence of isolated alumina agglomerates in steel products can give rise to major quality problems, as shown in the present work, and the origin, formation and elimination of these agglomerates require further study. Modification with calcium has already been mentioned as one possible method and the application of fluorspar/cryolite bombs is worthy of further consideration. Very recent work is indicating that less detrimental alumina clusters and improved steel quality are obtained by deoxidising with a mixture of aluminium and alumina rather than pure aluminium.

Finally, with the trend towards larger and larger ingots, problems associated with inclusion segregation (oxide and sulphide) during solidification are likely to increase. Consequently, methods of modifying the ingot solidification pattern so as to produce a more favourable inclusion distribution need to be studied.

APPENDIX 1

Example of matrix correction procedure. Operating voltage 25 kV. Take-off angle 20° (After Salter, Refs. 166 and 167)

(a) Corrections in binary systems

	Uncorrected concs K_i	Correction from binary systems K_i^j			
		MnO	CaO	Al_2O_3	SiO_2
MnO	7.9	-	10.8	8.4	8.3
CaO	18.4	23.2	-	23.3	24.3
Al_2O_3	11.5	36.5	24.5	-	14.2
SiO_2	26.6	53.9	42.0	54.7	-

$\Sigma K_i = 64.4$

(b) Calculation of approximate estimate

		Contribution from:				Approximate estimate $K_{(i)}$
Oxide	K_i	MnO	CaO	Al_2O_3	SiO_2	
MnO	7.9	-	0.6	0.06	0.12	8.68
CaO	18.4	1.15	-	1.18	2.08	22.81
Al_2O_3	11.5	3.11	3.16	-	0.84	18.61
SiO_2	26.6	4.68	4.88	7.15	-	43.31

$\Sigma K_{(i)} = 93.41$

(c) Calculation of corrected concentrations-stage 1, first iteration

	Proportional corrections in:				Corrected concs C_i
Oxide	MnO	CaO	Al_2O_3	SiO_2	
MnO	-	2.91	1.80	4.25	8.96
CaO	2.86	-	6.16	14.90	23.92
Al_2O_3	4.26	7.48	-	8.22	19.96
SiO_2	9.35	19.05	20.20	-	48.60

$\Sigma C_i = 101.44$

(d) Calculation of corrected concentrations-stage 2, second iteration

	Proportional corrections in:				Corrected concs C_i
Oxide	MnO	CaO	Al_2O_3	SiO_2	
MnO	-	2.80	1.79	4.39	8.98
CaO	2.71	-	5.90	15.30	23.91
Al_2O_3	4.04	7.15	-	8.45	19.64
SiO_2	9.18	19.00	20.30	-	48.48

$\Sigma C_i = 101.01$

Hence the final corrected values are

MnO	CaO	Al_2O_3	SiO_2	
9.0	23.9	19.6	48.5	$\Sigma C_i = 101.0$

When some experience has been gained in using this technique it is often possible to omit stage (b) and effectively estimate the probable values of $K_{(i)}$. This reduces the amount of calculation required.

REFERENCES

1. R. Kiessling: "Non-Metallic Inclusions in Steel", Part III, I.S.I. Publication No. 115.

2. R. Kiessling: Jernkont. Ann., 153, 1969, 79-89.

3. C. E. Sims: "Howe Memorial Lecture", Trans. A.I.M.E., 1959, 215, 367-393.

4. G. König and Th. Ernst: Radex Rundschau, 1970, 2, 67-98 (B.I.S.I. Translation No. 8584).

5. K. Narita et al: Kobe Steel R. and D. Eng. Report, 1969, 19, (2) 25-42 (B.I.S.I. Translation No. 7658).

6. P. H. Lindon: Ph.D. Thesis, University of Aston in Birmingham, 1967.

7. J. F. Elliott, M. Gleiser and V. Ramakrishna: "Thermochemistry for Steelmaking", Volumes I and II, Addison-Wesley, 1963.

8. O. Kubaschewski and E. LL. Evans: "Metallurgical Thermochemistry", Pergamon Press Ltd.

9. C. Bodsworth and H. B. Bell: "Physical Chemistry of Iron and Steel Manufacture", Second Edition, Longman, 1972.

10. E. T. Turkdogan: "Deoxidation of Steel", Review Paper presented at International Symposium on Metallurgical Chemistry", University of Sheffield, July 1971.

11. E. T. Turkdogan and R. J. Fruehan: Canadian Met. Quarterly, Vol. 11, No. 2, 1972, 371-382.

12. R. J. Fruehan: Trans. Met. Soc. A.I.M.E., 1969, Vol. 245, 1215-1218; Met. Trans., 1970, Vol. I. 2083-2088; Met. Trans., 1970, Vol. 1, 3403-3409.

13. H. Chino, Y. Nakamura, E. Tsunetomi and K. Segawa: Trans. I.S.I. Japan, 1966, Vol. 6, 959-966.

14. F. Korber and W. Oelsen: Mitt. Kaiser - Wilhelm - Inst. Eisenforsch, 1933, 15, 271-309.

15. D. C. Hilty and W. Crafts: Trans. A.I.M.E., 188, 1950, 425-436.

16. H. B. Bell: Iron and Steel, 1954, 27, 493, 531 and 559.

17. H. B. Bell: J.I.S.I. 1963, 201, 116.

18. R. A. Walsh and Ramachandran: Trans. A.I.M.E., 1963, 227, 560-562.

19. Y. Kojima and K. Sano: Tetsu-to-Hagane Overseas, 1965, 5, 282-289.

20. E. T. Turkdogan: Trans. A.I.M.E., 1965, 233, 2100-2112.

21. P. E. Waudby and W. J. M. Salter: J.I.S.I., 1971, July, 518-522.

22. P. E. Waudby: M. Sc. Thesis, University of Sheffield, 1971.

23. H. U. Hopp: Archiv. für das Eisenhüttenwesen, 1969, 40, 4, 265-269 (H.B. Translation No. 7820).

24. H. Schenk et al: Archiv. für das Eisenhüttenwesen, 1970, 41, 131-138 (B.I.S.I. Translation No. 8493).

25. A. McLean and R. G. Ward: J. Metals, 1965, May, 526-528.

26. F. W. Euler and W. Löscher: Hoesch. Ber., 1966, 1, (3), 15-21.

27. L. E. Rohde et al: Archiv. für das Eisenhüttenwesen, 1971, 42, (3), 165-174 (B.I.S.I. Translation No. 9552).

28. G. Gommellini, A. Piaggo and G. Violi: La Metallurgia Italiana, 1969, Vol. 61, No. 7, 295-304 and 309 (H. B. Translation No. 7978).

29. O. Repetylo, M. Olette and P. Kozakevitch: J. Metals, 1967, May, 45-49.

30. N. Gokcen and J. Chipman: Trans. A.I.M.E., 1953, 197, 173.

31. G. Pomey and B. Trentini: "Production and Application of Clean Steels", Proc. Int. Conf., Balatonfüred, Hungary, 23-26 June, 1970, I.S.I. Publication, 1-14.

32. E. Plöckinger and M. Wahlster: Stahl und Eisen, 1960, 80, 659-669.

33. E. Plöckinger: "Clean Steel", I.S.I. Spec. Report No. 77, 1963, 51-56.

34. M. Olette, C. Gatellier and K. Torssell: Berg - Hütten Monatsh, 1968, 113, 484-492.

35. Y. Miyashita: Trans. I.S.I. Japan, 1967, 7, 1-8.

36. E. Grethen and L. Philippe: "Production and Application of Clean Steels", Proc. Int. Conf., Balatonfüred, Hungary, 23-26 June, 1970, I.S.I. Publication, 29-34.

37. A. M. Levin: Izvest. VUZ Cher. Met., 1965, (12), 13-21.

38. J. Chipman: Trans. Met. Soc. A.I.M.E., 1962, 224, 1288-1289.

39. L. von Bogdandy, W. Meyer and I. N. Stranksi: Archiv. für das Eisenhüttenwesen, 1961, 32, 451-460; ibid, 1963, 34, 235-241.

40. F. H. Woehlbier and G. W. P. Rengstorff: J. Metals, May, 1967, Vol. 19, 50-53.

41. M. G. Frohberg and J. Pötschke: Schweizer Archiv., 1968, 10th October, Vol. 10, 318-323 (B.I.S.I. Translation No. 7414).

42. M. G. Frohberg and J. Pötschke: Archiv. für das Eisenhüttenwesen, 1970, 41, 723-729.

43. M. L. Turpin and J. F. Elliott: J.I.S.I., 1966, 204, 217-225.

44. G. K. Sigworth and J. F. Elliott: Canadian Met. Quarterly, Vol. 11, No. 2, 1972, 337-346.

45. K. Torssell, C. Gatellier and M. Olette: Comp. Rend. Acad. Sci., Paris, Vol. 267, Series C, 1968, 869-872.

46. H. L. Jaeger, E. J. Wilson, P. G. Hill and K. C. Russell: "Nucleation of Supersaturated Vapours in Nozzles", Part 1, J. Chem. Phys., 1969, 51, 5380; Part II, ibid, 1969, 51, 5389.

47. A. A. Vorobnev and A. M. Levin: Izv. VUZ. Chern. Met., 1967, 12, 12-18 (B.I.S.I. Translation No. 6580).

48. H. Straube, G. Kühnelt and E. Plöckinger: Archiv. für das Eisenhüttenwesen, 1967, July, 509-518.

49. M. G. Frohberg and J. Pötschke: Freiberger Forschung, 1969, B.144, 31-51 (B.I.S.I. Translation No. 8740).

50. E. Förster: Archiv. für das Eisenhüttenwesen, 1967, July, 607-615.

51. A. G. Franklin, G. Rule and R. Widdowson: J.I.S.I., 1969, September, 1208-1218.

52. H. U. Hopp and E. Piske: Hoesch. Ber., 1966, 1, (3), 21-24.

53. E. Förster and H. Richter: Radex-Rundschau, 1969, 2, 518-523 (HB Translation No. 7666).

54. E. Förster and H. Richter: "Production and Application of Clean Steels", Proc. Int. Conf., Balatonfüred, Hungary, 23-26 June, 1970, I.S.I. Publication, 24-28.

55. M. Espenhahn, H. Bühler and H. Litterscheidt: Thyssenforschung, 1969, 1, (4), 136-143 (B.I.S.I. Translation No. 8211).

56. C. A. Duckwitz, E. Förster and H. Richter: Archiv. für das Eisenhüttenwesen, 1968, 39, 333.

57. R. B. G. Yeo: J. Metals, 1967, June, 29-32 and July, 23-27.

58. H. Knüppel, K. Brotzmann and N. W. Förster: Stahl Eisen, 1965, 85, 675-688.

59. U. Lindborg and K. Torssell: Trans. Met. Soc. A.I.M.E., 1968, 242, 94-102.

60. E. T. Turkdogan: J.I.S.I., 1966, 204, September, 914-919.

61. N. F. Grevillius, Jernkont. Ann., 1969, 153, 547-572.

62. N. Sano, S. Shiomi and Y. Matsushita: Tetsu-to-Hagane, 1965, 51, 19-38.

63. Y. Miyashita: Nippon Kokan Tech. Report, 1965, 4, 41-46.

64. K. Torssell: Jernkont. Ann., 1967, 151, 890-947.

65. C. H. Herty and G. R. Fitterer: U.S. Bureau of Mines, No. 3081 (1931) and No. 3054 (1930).

66. E. Plöckinger and R. Rosegger: Stahl Eisen, 1957, 77, 798-804.

67. E. Plöckinger and M. Wahlster: Radex Rundschau, 1957, 516, 754-770.

68. I. S. Kulikov and A. M. Samarin: Izvestiya Akedemii Nauk U.S.S.R., 1954, 10, 23-30.

69. T. Kawawa, M. Okubo, Y. Sasajima and H. Tokunaga: Tetsu-to-Hagane, 1965, 51, 780-783 (HB Translation No. 6766).

70. I. Tajiri, T. Takei, S. Watanabe, Y. Nagano and H. Haraguchi: Tetsu-to-Hagane, 1966, 52, 554-557 (HB Translation No. 7045).

71. P. E. Waudby: Sorby Memorial Prize Micrograph Competition, 1971, Sheffield Met. and Eng. Association.

72. R. Kiessling, S. Bergh and N. Lange: J.I.S.I., 201, 1963, 509-515.

73. A. Hultgren: Jernkont. Ann., 1945, 129, 633-671.

74. P. H. Lindon and J. C. Billington: Trans. A.I.M.E., 1969, August, 245, 1775-1784.

75. J. Andersson: Jernkont. Ann., 1970, 154, 429-455.

76. J. Andersson: "Clean Steel", Symposium in Sandviken, Sweden, 24-26 March, 1971, Vol. 1, 100-110.

77. M. Kawai and S. Kobayashi: Tetsu-to-Hagane, 1966, 52, 4, 546-551 (B.I.S.I. Translation No. 5118).

78. W. A. Fischer: "The Physical Chemistry of Steelmaking", Wiley, New York, 117.

79. G. C. Duderstadt and R. D. Weller: Journal of Metals, 1966, 18, 71.

80. M. Imai: Rev. Met., 1968, 65, June, 409-416 (B.I.S.I. Translation No. 6814).

81. S. Linder: ASEA Journal, 1971, 44, 4, 83-86.

82. M. Ohkubo, T. Kawawa, Y. Sasajima and H. Tokunaga: Nippon Kokan Tech. Rep., 1966, 37, 161.

83. M. Ohkubo, M. Masui and H. Tokunaga: Nippon Kokan Tech. Rep. Overseas, 1965, 5, 7.

84. N. Lindskog: Proc. Seminar in Process Metallurgy at Imperial College, London, April 9, 1973, 11-17.

85. B. Kjellberg: ibid, 18-24.

86. J. Koenitzer and R. Hammer: Stahl Eisen, 1963, 10, 569-577.

87. P. H. Lindon and J. C. Billington: J.I.S.I., 1969, March, 340-347.

88. E. Plöckinger and M. Wahlster: Stahl Eisen, 60, 1960.

89. K. G. Speith, H. vom Ende and H. J. Seelisch: Stahl Eisen, 1956, 76, 1426-1441.

90. D. R. Bailey, J. W. Onuscheck and A. Turfa jr.: Proc. Open Hearth and Basic Oxygen Steelmaking Conf., A.I.M.M.E., 1963, 390-395.

91. A. Choudhury and M. Wahlster: Rheinstahl - Technik, 1966, 4, 111-121.

92. K. Torssell: "Clean Steel", Symposium in Sandviken, Sweden, 24-26 March, 1971, Vol. 1, 88-99.

93. P. Kozakevitch and M. Olette: "Production and Application of Clean Steels", Proc. Int. Conf., Balatonfüred, Hungary, 23-26 June, 1970, I.S.I. Publication, 42-49.

94. J. T. Davies and E. K. Rideal: "Interfacial Phenomena", 1961 London, Academic Press.

95. E. D. Hondros and D. McLean: Proc. Int. Symposium on the "Surface Phenomena of Metals", Brunel University, London, 1967, Soc. of Chem. Ind. Monograph, No. 28, 39-56.

96. D. Cosma: Metallurgia, 1971, 23, 12, 804-807 (B.I.S.I. Translation No. 10454).

97. R. K. Iyengar and W. O. Philbrook: Met. Trans., 1972, July, 3, 1823-2830.

98. P. E. Waudby: "Formation of Inclusions during Deoxidation", Seminar Paper, Sheffield Polytechnic, 6th June, 1973, to be published.

99. V. I. Baptizmanskii, N. Bakhman and Y. V. Dmishreiv: Izvest. VUZ. Chern. Met., 1969, (3), 42-45.

100. K. Torssell and M. Olette: Rev. Met., 1969, 12, 813-822 (B.I.S.I. Translation No. 8347).

101. R. A. Rege, E. S. Szekeres and W. D. Forgeng: Met. Trans. 1970, 1, 2652-2653.

102. F. B. Pickering: "Production and Application of Clean Steels", Proc. Int. Conf., Balatonfüred, Hungary, 23-26 June, 1970, I.S.I. Publication, 75-91.

103. E. L. Morgan, J. R. Blank, W. J. M. Salter and F. B. Pickering: J.I.S.I., 1968, 206, 987-1001.

104. W. J. M. Salter and F. B. Pickering: J.I.S.I., 1969, 207, 992.

105. M. L. Kieth: J. Am. Ceramic Soc., 1954, 37, 490.

106. A. Muan and E. F. Osborn: "Phase Equilibria among Oxides in Steelmaking", 1965, Addison - Wesley Pub. Co. Inc.

107. P. E. Waudby, W. J. M. Salter and F. B. Pickering: J.I.S.I., July, 1973, 486-492.

108. F. B. Pickering: Jernkont. Ann., 1964, 148, 845.

109. J. R. Blank and F. B. Pickering: "The Solidification of Metals", Proc. Int. Conf., Brighton, 4-7 December, 1967, ISI Publication 110, 370-376.

110. J. Bruch, U. Grisar and E. Müller: Archiv. für das Eisenhüttenwesen, 1965, 36, 799-807.

111. D. H. Houseman: Steel Times, 1966, May, 689-695.

112. M. Ichinoe, H. Mori, H. Kajioka and I. Kokubo: "Production and Application of Clean Steels", Proc. Int. Conf., Balatonfüred, Hungary, 23-26 June, 1970, I.S.I. Publication, 137-166.

113. J. C. C. Leach: ibid., 105-114.

114. S. E. Lunner: ibid., 124-136.

115. S. E. Lunner: J.I.S.I., 1972, March, 168-178.

116. M. Wahlster, A. Choudhury and L. Rohde: Proc. Int. Conf. Science and Technology of Iron and Steel, Part 1, Trans. I.S.I., Japan, 1971, Vol. 11, 601-606.

117. M. Wahlster: "Production and Application of Clean Steels", Proc. Int. Conf., Balatonfüred, Hungary, 23-26 June, 1970, I.S.I. Publication, 205-214.

118. A. Kohn, M. Wanin, J. Arnoult, R. Thomas and L. Backer: ibid., 92-98.

119. A. Kohn et al: Electric Furnace Proceedings, A.I.M.E., 1969, 39-47.

120. C. Ericsson: Jernkont. Ann., 1968, Vol. 152, No. 5, Part 1, 205-212; Part 2, 212-223.

121. P. H. S. Cox and J. A. Charles: J.I.S.I., 1963, 202, 863-872.

122. P. H. S. Cox and J. A. Charles: J.I.S.I., 1965, 203, 493-499.

123. H. M. Richardson: "Clean Steel", I.S.I. Spec. Report No. 77, 1963, 57-63.

124. T. E. Brower, J. W. Bain and B. M. Larsen: Trans. A.I.M.E., 1950, Vol. 88, 851.

125. A. Hultgren: Jernkont, Ann., 1945, Vol. 129, 633-671.

126. G. J. Vingas and J. B. Caine: Foundry, 1959, June, Vol. 87, No. 6, 94.

127. L. H. Van Vlack, R. A. Flinn and G. A. Colligan: Trans. A.F.S., 1960, 68, 132.

128. J. Brokloff, H. C. Chao, L. H. Van Vlack and R. A. Flinn: ibid., 1963, 71, 783.

129. F. E. Rote, V. Sarin and R. A. Flinn: ibid., 1966, 74, 409.

130. R. A. Flinn, L. H. Van Vlack and G. A. Colligan: ibid, 1966, 74, 485.

131. M. F. Hoffman, P. G. Bailey and R. L. W. Holmes: J. Metals, 1961, May 13, 5, 345-349.

132. B. Adilstam and J. v. Döbeln: Jernkont. Ann., 1966, 150, 581-584.

133. C. A. Müller and E. Plöckinger: Radex - Rundschau, 1957, 738.

134. H. Mori, N. Tanaka and M. Hirai: Trans. I.S.I.J., 1971, Vol. 11, 424-438.

135. E. I. Astrov et al: "Continuous Casting of Steel", Metallurgiya Press, Moscow, 1970, 219-222 (HB Translation No. 8679).

136. M. Kurita, T. Ikeda and K. Marukawa: Trans. I.S.I.J., 1971, Vol. 11, 270-274.

137. J. Little, M. Van Oosten and A. McLean: Canadian Met. Quarterly, 1968, Vol. 7, No. 4, 235-246.

138. M. P. Kenney: J. Metals, 1968, March, 88-95.

139. J. W. Farrell, P. J. Bilek and D. C. Hilty: Elec. Furnace Conf. Proc., A.I.M.E., 1970, 64-88.

140. D. M. Cottingham and D. Vincent: Steel Times, 1967, 194, 133-140.

141. C. Jörgensen and A. Wilkström: Jernkont. Ann., 1964, 148, 518-520.

142. A. Robertson: Swinden Laboratories, Private Communication.

143. J. D. Sharp: Iron and Steel, 1970, February, 16-19.

144. D. E. Humphreys: J. Ref. 1969, May, 128.

145. H. Buhr: Elec. Furnace Conf. Proc., A.I.M.E., 1968, 48.

146. P. Schroth and R. J. Bays: J. Metals, 1967, September, 77.

147. G. R. Cope: Metals Progress, 1968, September, 109.

148. W. J. M. Salter: BSC Special Steels Division, Stocksbridge Works, Private Communication.

149. J. R. Rait: Trans. Brit. Ceramic Soc., 1943, 42, 57-94.

150. C. A. Post and G. V. Luerssen: Trans. A.I.M.E., 1949, 185, 15-26.

151. R. B. Snow and J. S. Shea: J. American Ceramic Soc., 1949, 32, 87-94.

152. M. P. Fedock: Elec. Furnace Conf. Proc., A.I.M.E., 1953, 11, 269-274.

153. D. J. Carney and E. C. Rudolphy: J. Metals, 1954, December, 1391-1395.

154. L. Smith and S. W. Banks: BSC Tubes Division, Private Communication.

155. G. Funnell: Tube Investments, Private Communication.

156. I. M. Stephenson, T. Gladman and F. B. Pickering: Swinden Laboratories, Private Communication.

157. M. Wahlster, H. Maas, H. Abratis and A. Choudhury: Archiv. für das Eisenhüttenwesen, 1970, 41, 37-42.

158. K. Narita: Tetsu-to-Hagané Overseas, 1963, June, Vol. 3, No. 2, 106-116.

159. K. Schwerdtfeger and H. Schrewe: Electric Furnace Conf. Proc. A.I.M.E., 1970, 95-102.

160. N. M. Frolovskii et al: Ogneupory, 1970, August, 8, 22-27.

161. A. K. Karklit et al: ibid, July, 7, 27-35.

162. G. C. Duderstadt, R. K. Iyenger and J. M. Matesa: Elec. Furnace Conf. Proc., A.I.M.E., 1967, 25, 61-66.

163. J. W. Farrell and D. C. Hilty: Elec. Furnace Conf. Proc., A.I.M.E., 1971, 31-45.

164. T. R. Meadowcroft and R. J. Milbourne: J. Metals, 1971, June, 11.

165. D. A. Melford: Inst. of Phys. Meeting on Specimen Preparation, November, 1965.

166. W. J. M. Salter: "A Manual of Quantitative Electron Probe Microanalysis", Structural Publications Ltd., London, 1970.

167. W. J. M. Salter: Brit. J. App. Phys., 1968, 2, 1, 541-547.

168. J. Philibert: Proc. 3rd Int. Symp. on X-Ray Analysis, 1962, Stamford, 379-392, Academic Press.

169. P. Duncumb and P. K. Shields: "The Electron Microprobe", Proc. Symp., Washington, 1966, 284-295 (New York - John Wiley).

170. P. Duncumb and S. J. B. Reed: "Quantitative Electron Probe Microanalysis", N.B.S. Spec. Report 298, October, 1968, 133-154.

171. L. S. Birks: "Electron Probe Microanalysis", 1963 (New York - Interscience).

172. S. J. B. Reed: Brit. J. App. Phys., 1965, Vol. 16, 913-926.

173. R. Castaing: Ph.D. Thesis, Paris University, 1951.

174. D. Booth: Swinden Laboratories, Private Communication.

175. D. Shireby: Swinden Laboratories, Private Communication.

176. J. R. Blank: BSC Special Steels Division, Rotherham Works, Private Communication.

177. M. L. Keith: J. Am. Ceram. Soc., 1954, 37, 490.

178. N. Standish: Iron and Steel, 1969, 42, 6, 354-360.

179. R. J. McDonald and J. D. Hunt: Trans. T.M.S.-A.I.M.E., 1969, Vol. 245, 1993.

Equilibrium Constant K	Composition Range	K at 1600°C	log K
$[h_{Al}]^2\,[h_O]^4$	<0.0001% Al	1.1×10^{-15}	$\frac{-71\,600}{T} + 23.28$
$[h_{Al}]^2\,[h_O]^3$	>0.0001% Al	4.3×10^{-14}	$\frac{-62\,780}{T} + 20.17$
$[h_B]^2\,[h_O]^3$	-	1.3×10^{-8}	-
$[h_c]\,[h_O]$ latm. CO	>0.02% C	2.0×10^{-3}	$\frac{-1168}{T} - 2.07$
$[h_{Cr}]^2\,[h_O]^4$	<3% Cr	4.0×10^{-6}	$\frac{-50\,700}{T} + 21.70$
$[h_{Cr}]^2\,[h_O]^3$	>3% Cr	1.1×10^{-4}	$\frac{-40\,740}{T} + 17.78$
$[h_{Mn}]\,[h_O]$	>1% Mn	5.1×10^{-2}	$\frac{-14\,450}{T} + 6.43$
$[h_{Si}]\,[h_O]^2$	>0.002% Si	2.2×10^{-5}	$\frac{-30\,410}{T} + 11.59$
$[h_{Ti}]\,[h_O]^2$	<0.3% Ti	2.8×10^{-6}	-
$[h_{Ti}]\,[h_O]$	>5% Ti	1.9×10^{-3}	-
$[h_v]^2\,[h_O]^4$	<0.1% V	8.3×10^{-8}	-
$[h_v]^2[h_O]^3$	>0.3% V	3.5×10^{-6}	-

Table 2.1

Equilibrium constants for several deoxidants in liquid iron saturated with the respective oxide.
(After Turkdogan and Fruehan, Refs. 10-12).

Solute j	Interaction Coefficient e_o^j	Composition Limit $<\%j$
Al	-3.9	0.2
B	-2.6	0.05
C	-0.13	1.0
Co	0.007	5.0
Cr	-0.037	20.0
Cu	-0.016	15.0
Mn	0	-
N	0.057	-
Nb	-0.14	3.0
Ni	0.006	20.0
O	-0.20	-
P	0.07	0.5
S	-0.091	-
Si	-0.14	-
Ti	-1.15	0.3
V	-0.4	5.0
W	0.008	5.0

Table 2.2

Interaction coefficients, e_o^j, for several elements, together with the composition limits for which equation (2.6) is a reasonable approximation. (After Turkdogan and Fruehan, Ref. 11)

Solid oxide	Liquid metal	Gas	Contact angle, $\theta°$
Al_2O_3	Fe	Ar	141
Al_2O_3	Fe-4.5% C	Ar	133
Al_2O_3	Fe-5.1% Si	Ar	126
Al_2O_3	Fe-12.2% Mn	Ar	103
Al_2O_3	Fe	He	128
Al_2O_3	Fe-3.4% C	He	112
Al_2O_3	Fe-3.9% C	He	104
SiO_2	Fe	N_2	115
CaO	Fe	N_2	132
TiO_2	Fe	Vacuum	72
TiO_2	Fe	H_2	84
Cr_2O_3	Fe	Ar	88

Table 2.3

Contact angles (After Kozakevitch and Olette, Ref. 93)

Melt Composition	$\theta°$	γ_m J/m^2 (erg/cm^2)	ΔG J/m^2 (erg/cm^2)	Estimates	
				γ_s J/m^2 (erg/cm^2)	γ_{sm} J/m^2 (erg/cm^2)
Pure iron	140	1.8 (1800)	-3.179 (-3179)	0.9 (900)	2.279 (2279)
Iron containing 4% C	133	1.73 (1730)	-2.91 (-2910)	0.9 (900)	2.08 (2080)
Iron containing 0.02% S	140	1.39 (1390)	-2.455 (-2455)	0.9 (900)	1.965 (1965)
Iron containing 0.07% O	80	1.1 (1100)	-0.909 (-909)	0.9 (900)	0.709 (709)

Table 2.4

Values of $\Delta G = \gamma_s - \gamma_m - \gamma_{sm} = \gamma_m (\cos \theta - 1)$ obtained at 1600°C for alumina (After Kozakevitch and Olette, Ref. 93)

Slag Composition	Metal Composition	γ_m J/m^2 (erg/cm^2)	γ_l J/m^2 (erg/cm^2)	γ_{ml} J/m^2 (erg/cm^2)	$S = \gamma_m - \gamma_l - \gamma_{ml}$ J/m^2 (erg/cm^2)
33.3% CaO 33.3% Al_2O_3 33.3% SiO_2	Commercially pure iron	1.636 (1636)	0.456 (456)	1.147 (1147)	+0.030 (+30)
As above + 20% CaF_2	Commercially pure iron	1.636 (1636)	0.390 (390)	1.205 (1205)	+0.038 (+38)
30.7% CaO 15.2% Al_2O_3 38.8% SiO_2 15.3% CaF_2	Commercially pure iron	1.636 (1636)	0.386 (386)	1.169 (1169)	+0.087 (+87)
33.3% CaO 33.3% Al_2O_3 33.3% SiO_2	Iron containing 0.01% O	1.511 (1511)	0.456 (456)	1.153 (1153)	-0.098 (-98)
As above + 20% CaF_2	Iron containing 0.01% O	1.511 (1511)	0.390 (390)	1.216 (1216)	-0.095 (-95)

Table 2.5

Relationship between surface energy of slag, γ_l, of metal, γ_m, of the slag/metal interfacial energy, γ_{ml}, and the spreading coefficient, S. A positive value of S corresponds to spreading of the slag at the surface of the molten metal. (After Kozakevitch and Olette, Ref. 93)

		Steel Type			
		A	B	C	D
% N		0.03	0.08	0.10	0.27
$\theta°_{Al_2O_3}$		138	128	130	119
$\theta°_{SiO_2}$		112.5	104	106	97
γ_m	J/m^2 (erg/cm^2)	1.357 (1357)	1.311 (1311)	1.302 (1302)	1.241 (1241)
$\gamma_{sm_{Al_2O_3}}$	J/m^2 (erg/cm^2)	1.698 (1698)	1.497 (1497)	1.527 (1527)	1.291 (1291)
$\gamma_{sm_{SiO_2}}$	J/m^2 (erg/cm^2)	0.826 (826)	0.624 (624)	0.665 (665)	0.458 (458)
$-\Delta G_{Al_2O_3}$	J/m^2 (erg/cm^2)	2.365 (2365)	2.118 (2118)	2.139 (2139)	1.843 (1843)
$-\Delta G_{SiO_2}$	J/m^2 (erg/cm^2)	1.876 (1876)	1.628 (1628)	1.661 (1661)	1.392 (1392)

Table 2.6

Variation in contact angle, θ, steel surface energy, γ_m, steel/inclusion interfacial energy, γ_{sm}, and surface free energy change, $\Delta G = \gamma_m (\cos \theta - 1)$, for alumina and silica inclusions in austenitic stainless steel alloyed with nitrogen at 1500°C. (After Cosma, Ref. 96)

Slag Type	Slag Composition, wt. %			Inclusion Type	
	CaO	Al_2O_3	Other Compounds	Al_2O_3	SiO_2
				$-\Delta G$ J/m^2	$-\Delta G$ J/m^2
1	48.9	51.2	-	0.676	0.186
2	51.0	39.2	9.8 TiO_2	0.477	-0.014
3	38.2	39.5	21.2 TiO_2	0.325	-0.165
4	52.1	44.7	5.0 ZrO_2	0.559	0.073
5	47.2	42.5	10.9 ZrO_2	0.606	0.116
6	44.9	31.5	21.3 ZrO_2	0.770	0.280
7	40.0	50.2	0.55 NaF	0.518	0.028
8	50.4	44.3	6.4 NaF	0.010	-0.480
9	52.5	50.6	10.9 NaF	-0.083	-0.573
10	31.5	33.2	1.9 SiO_2	0.179	-0.311
			19.2 CaF_2		
			11.3 MgO		
11	36.3	54.2	1.2 SiO_2	0.552	0.062
			3.8 CaF_2		
			3.7 MgO		
12	10.3	25.3	2.7 SiO_2	0.014	-0.476
			60.4 CaF_2		

Table 2.7

Variation in surface free energy change, $\Delta G = \gamma_{sl} + \gamma_{ml} - \gamma_{sm}$, for the escape of alumina and silica inclusions from austenitic stainless steel containing 0.08% N into different slags at 1500°C.
(After Cosma, Ref. 96)

Type of inclusion	Average diameter, μm	Approximate relative volume
Alumina, spinel and $CaO.6Al_2O_3$ (other than clusters)	5	1
Other calcium aluminates	27	160
Secondary deoxidation products (Si-killed steel)	32	260
Primary deoxidation products (Si-killed steel)	49	940
Silicate erosion products (Al-killed steel)	64	2100
Silicate erosion products (Si-killed steel)	107	9800

Table 2.8

Relative volumes of various types of inclusions (After Pickering, Ref. 102)

Sampling Stage	Phase	Inclusion Analysis, wt. %							Inclusion Type
		MgO	Al_2O_3	SiO_2	CaO	TiO_2	Cr_2O_3	MnO	
Furnace prior to silicon deoxidation		-	1-2	40-48	10-22	1-2	4-7	18-30	Mn-Ca(Cr) silicate
	1	-	0-1	40-45	2-3	-	7-10	42-48	Mn-Cr silicate
	2	-	1-2	45-50	-	2-3	32-35	15-18	Cr-Mn silicate
Furnace after silicon deoxidation		-	15-30	33-35	1-5	1-2	3-6	30-32	Mn-Al(Cr) silicate
		-	-	45-48	15-22	1-2	4-7	15-28	Mn-Ca(Cr) silicate
Furnace prior to tapping		7-10	5-15	38-40	40-45	-	-	3-5	Ca-Al-Mg silicate
		-	15-30	33-35	-	1-2	8-12	30-35	Mn-Al(Cr) silicate
	1	-	10-15	40-43	-	1-3	7-13	33-40	Mn-Al silicate
	2	-	10-15	-	-	20-22	20-25	40-45	Mn-Cr-Ti-Al spinel
Ladle after tapping		-	1-5	38-40	30-50	-	-	10-20	Ca-Mn silicate
		2-3	10-15	40-45	2-5	1-2	2-4	35-45	Mn-Al silicate
Ingot mould during teeming		2-3	15-20	40-45	15-20	1-2	2-6	10-20	Ca-Mn-Al silicate
		-	10-15	33-35	5-10	1-2	3-6	30-35	Mn-Ca-Al silicate
	1	-	5-10	45-48	-	1-2	1-3	40-45	Mn-Al silicate
	2	-	1-5	-	-	15-20	30-40	35-40	Mn-Cr-Ti spinel

Table 2.9

Compositions of inclusions observed during steelmaking, tapping and teeming. (After Lunner, Refs. 114 and 115

Heat	Furnace additions, wt. %				Ladle additions wt. %		Wt. of slag tapped into ladle t
	Si-Mn	Fe-Si	Si-Al-Ca Si-Ca	Al	Si-Al-Ca Si-Ca	Al	
A	0.375	0.065	1.0	0.7 + 0.15	0.5	0.2	1.4
B	0.320	0.090	1.0	0.9 + 0.25	0.5	0.1	1.9
C	0.280	0.160		0.9 + 0.25		0.2	0.6
D	0.305	0.100	1.0	0.8 + 0.15	0.5	0.1	0.8
Mg content of additions: Si-Mn (1.5%), Fe-Si (2.7%) and Si-Ca (2.5%)							

Table 2.10

Details of deoxidising additions (After Kohn et al, Refs. 118 and 119)

Non-Metallic material	Specific Activities of Non-Metallic Materials, counts/min/mg			
	Heat A	Heat B	Heat C	Heat D
Furnace slag		24		
Ladle slag	59	35	201	321
Tundish flux	470 745	400 490	310 570	14 4
Mould flux (continuous casting)	940 260 690	980 415 385	570 350	4 1 2
Scum on uphill-teemed ingot	780	300	1050	12
Scum on direct-teemed ingot	5080 3165 1000	4480 5100	1670	120 18 23
Deposit in nozzle		6900 10800 6280 11400	22800 18700 21900	

Table 2.11

Specific activities of non-metallic materials
(After Kohn et al, Refs. 118 and 119)

	Content, ppm		Change, ppm	
	O	N	O	N
Normal tapping (4 heats)				
In furnace before tapping	195	944		
In ladle immediately after tapping	210	986	+15	+42
In ladle before pouring	182	994	-28	+8
Shielded pouring (6 heats)				
In furnace before tapping	145	558		
In ladle immediately after tapping	158	568	+13	+10
In ladle before pouring	148	570	-10	+2

Table 2.12

Changes in oxygen and nitrogen contents during tapping and during ladle holding (After Ericsson, ref. 120)

Nominal Steel Analysis, %					Ingot Weight, tonnes	Casting Atmosphere	Macroslag from Stepdown Testpiece, mm/10 dm^2	Microslag Volumetric Proportion, ppm		
C	Si	Mn	Cr	Ni				5-27.5 μm	>27.5 μm	Oxygen Content ppm
0.35	0.30	0.75	-	-	1.25	Argon	3.5	134	149	27
						Normal	17.5	187	224	38
						Oxygen gas	27.5	270	500	34
0.35	0.30	0.60	2.7	-	1.25	Argon	23.5	42	117	27
						Normal	31.0	100	157	32
						Oxygen gas	128.0	170	258	34
0.2	0.30	0.60	13.0	-	1.25	Argon	29.5	100	224	72
						Normal	69.0	137	220	76
						Oxygen gas	100.0	154	270	85
0.20	0.25	0.75	0.80	1.50	1.4	Argon	24(25)*	-	-	46
						Normal	26(26)	-	-	53
0.20	0.25	0.75	0.80	1.50	1.4	Argon	14(11)	-	-	32
						Normal	22(13)	-	-	38
0.17	0.25	0.75	0.80	1.50	1.4	Argon	21(14)	-	-	36
						Normal	44(16)	-	-	40

* The figures in parentheses relate to blue brittleness tests.

Table 2.13

Experiments on teeming in a protective atmosphere (After Adilstam and Döbeln, ref. 132)

Time	Steelmaking Additions	Samples	Comments
13.07		Metal 1	From furnace
13.10			Start of tap, 1672°C
13.11	FeMn, FeSi and Cr Temp		Ladle additions
13.11½	Al		
13.16			End of tap
13.17		Metal 2	From ladle
13.21½		Metal 3	From ladle at degasser
13.23			Start of degassing
13.24			Vermiculite added
13.26		Metal 4	From ladle (failed)
13.30		Metal 5	From ladle
13.30½			1606°C
13.32		Metal 6	From ladle
13.34½		Metal 7	From ladle
13.36½		Metal 8	From ladle
13.38½		Metal 9	From ladle (failed)
13.39			1592°C
13.40½		Metal 10	From ladle
13.45½		Metal 11	From ladle
13.47½		Metal 12	From ladle
13.48½			1580°C
13.52		Metal 13	From ladle (failed)
13.55			End of degassing
14.07			Start teem 1st plate
14.12½		Metal 14	From ingot 1
14.13½			End teem 1st plate
14.14		Metal 15	From ladle stream
14.14			Start teem 2nd plate
14.20		Metal 16	From ingot 7
14.21			End teem 2nd plate
14.22½			Start teem 3rd plate
14.28½		Metal 17	From ingot 13
14.30½			End teem 3rd plate
14.31		Metal 18	From ladle stream
14.32			Start teem 4th plate
14.36½		Metal 19	From ingot 19
14.37			End teem 4th plate
14.38		Metal 20	From ladle stream
14.38			Start teem 5th plate
14.43		Metal 21	From ingot (failed)
14.43½			End teem 5th plate
14.44		Metal 22	From ladle stream

Table 3.1

Chronology of steelmaking trial A.1

Time	Steelmaking Additions	Samples	Comments
9.59			Power on
10.00-11.55	1444 m^3 O_2		
11.57	Spar		Push in
12.06½		Slag 1	Melt out
12.07½			1550°C
12.08		Metal 1	
12.10-12.18	227 m^3 O_2		Slag flush
12.18½		Slag 2	
12.19		Metal 2	
12.19½			1580°C
12.20-12.29	O_2 blow		Slag flush
12.29			1615°C
12.29½		Metal 3	
12.30		Slag 3	
12.34		Slag 4	
12.34½		Metal 4	
12.38			1635°C
12.39		Slag 5	
12.39½	FeMn		Block
12.42		Metal 5	
12.44			Start to tap
12.45	FeMn, N_2FeMn, FeP, S		Additions to ladle
12.50			End of tap
12.50½	Spar, Ferrux		
12.52			1575°C
12.52½		Metal 6	Sample from full ladle
12.57	Lead down trumpet		Start teem 1st plate
13.03		Metal 7	From ingot
13.03½			End teem 1st plate
13.05		Metal 8	From ladle stream
13.05½	Lead down trumpet		Start teem 2nd plate
13.13		Metal 9	From ingot
13.13½		Metal 10	From ladle stream
13.15			End teem 2nd plate
13.15½	Lead down trumpet		Start teem 3rd plate
13.24		Metal 11	From ingot
13.25		Metal 12	From ladle stream
13.26			End teem 3rd plate
13.30		Slag 6	Final ladle slag

Table 3.2

Chronology of steelmaking trial B.1

Time	Steelmaking Additions	Samples	Comments
12. 30			Power on
12. 30 - 14. 30	1500 m^3 O_2		
14. 39			Melt out; 1565°C
14. 42 - 14. 50	240 m^3 O_2		Slag flush
14. 51			1610°C
14. 58			Electrodes dipped
14. 59	FeMn		Block; 1625°C
15. 03			1630°C
15. 08			Start to tap
15. 09	FeMn, N_2FeMn, FeP, S		Additions to ladle
15. 14			End of tap
15. 15		Metal 1	From ladle
15. 24	Lead down trumpet		Start teem 1st plate
15. 30			End teem 1st plate
15. 31			Start teem direct ingot
15. 35		Metal 2	From direct ingot; end teem
15. 36	Lead down trumpet		Start teem 2nd plate
15. 42		Metal 3	From ladle stream
15. 42½			End teem 2nd plate
15. 43		Metal 4	From ingot
15. 44	Lead down trumpet		Start teem 3rd plate
15. 46			Oxygen lance on nozzle
15. 54			Oxygen lance on nozzle
15. 56½			Oxygen lance on nozzle
15. 57			End teem 3rd plate
15. 57½		Metal 5	From ingot

Table 3.3

Chronology of steelmaking trial B.2

Time	Steelmaking Additions	Samples	Comments
7.44			Power on
7.44 - 9.30	1840 m^3 oxygen		
9.30			Melt out; 1570°C.
9.33 - 9.41	230 m^3 oxygen		Slag flush
9.42			1610°C.
9.55			Electrodes dipped
9.56	FeMn		Block; 1630°C.
9.57		Metal 1	
9.58			Start to tap
10.00	FeMn, N_2FeMn, FeP, S		Additions to ladle
10.04			End of tap
10.07		Metal 2	From ladle
10.12	lead down trumpet		Start teem 1st plate
10.21½		Metal 3	From ladle stream
10.22		Metal 4	From ingot
10.22			Slight running stopper
10.22½			Start teem direct ingot
10.24½			End teem direct ingot
10.25		Metal 5	From direct ingot
10.25½	lead down trumpet		Start teem 2nd plate
10.33		Metal 6	From ladle stream
10.35½			End teem 2nd plate
10.36		Metal 7	From ingot
10.36½	lead down trumpet		Start teem 3rd plate
10.38			Oxygen on nozzle
10.44		Metal 8	From ladle stream
10.44½			End teem 3rd plate
10.45		Metal 9	From ingot

Table 3.4

Chronology of steelmaking trial B.3

Time	Steelmaking Additions	Samples	Comments
8.39			Power on
8.39-10.10	1130 m^3 oxygen		
10.10			Melt out; 1555°C
10.15			Electrodes dipped
10.17-10.28	255 m^3 oxygen		Slag flush
10.29			1575°C
10.40			1600°C
10.42-10.46	40 m^3 oxygen		
10.48			1625°C
10.52			Electrodes dipped
10.54	FeMn		Block
10.55			1635°C
10.56		Metal 1	From furnace
10.59			Start to tap
11.00	FeMn, FeP, S		Additions to ladle
11.03			End of tap
11.06		Metal 2	From ladle
11.08		Metal 3	From ladle
11.11	Lead down trumpet		Start teem 1st plate
11.20½		Metal 4	From ladle stream
11.21			End teem 1st plate
11.21½		Metal 5	From ingot on 1st plate
11.22			Start teem direct ingot
11.24			End teem direct ingot
11.24½	Lead down trumpet		Start teem 2nd plate
11.34½		Metal 6	From ladle stream
11.35			End teem 2nd plate
11.35½		Metal 7	From ingot on 2nd plate
11.36	Lead down trumpet		Start teem 3rd plate
11.39			Oxygen on nozzle
11.45		Metal 8	From ladle stream
11.45½			End teem 3rd plate
11.46		Metal 9	From ingot on 3rd plate

Table 3.5

Chronology of steelmaking trial B.4

Trial cast		B.1	B.2	B.3	B.4
Melt carbon, %		0.18	0.14	0.17	0.06
Tap carbon, %		0.06	0.06	0.05	0.06
FeMn bath block, kg		76	76	76	76
Final bath silicon, %		0.004	0.006	0.003	0.002
Launder coating		Siliceous	Magnesite	Magnesite	Siliceous
Ladle life, no. of previous heats		18	1	4	12
Ladle additions	FeMn, kg	1321	1270	1270	1372
	Si content of FeMn, %	0.30	0.28	0.25	0.30
	Si contribution at 100% yield, %	0.004	0.003	0.003	0.004
	FeP, kg	229	76	178	330
	Si content of FeP, %	0.60	1.22	1.70	0.12
	Si contribution at 100% yield, %	0.001	0.001	0.003	<0.001
	N_2FeMn, kg	51	51	51	None
	Si content of N_2FeMn, %	0.41	-	-	-
	Maximum Si contribution from ferro-alloys, %	0.005	0.004	0.006	0.004
Ladle silicon, %		0.006	0.005	0.004	0.003
Mean pit silicon, %		0.013	0.012	0.007	0.010
Mean product silicon, %		0.010	0.007	0.007	0.007

Table 3.6

Summary of steelmaking details for free-cutting casts

Time	Steelmaking Additions	Samples	Comments
17.10			Melt out
17.10 - 17.50	Oxygen blow		
17.50½		Metal 1	
17.51 - 18.12	Oxygen blow		
18.12½		Metal 2	
18.20			Slag off
18.24		Metal 3	
18.30	FeSi		
18.31	Desulfex 75		
18.45		Metal 4	
18.45½	Al		
18.46½			1660°C
18.50			Bath paddled
18.54		Metal 5	
18.54½			1640°C
19.15		Metal 6	
19.28½	FeMn		
19.36		Metal 7	
19.38	FeMn + FeNb		
19.42½		Metal 8	
19.51 - 20.00	Al		Tap
20.00½		Metal 9	From Ladle
20.06			Start teem 1st plate
20.12		Metal 10	From Ingot
20.12½			End teem 1st plate
20.13			Start teem 2nd plate
20.19		Metal 11	From ladle stream
20.19½			End teem 2nd plate
20.20			Start teem 3rd plate
20.27 - 20.29			Breakout; direct teem
20.29½		Metal 12	From Ingot
20.30½		Metal 13	From ladle stream
20.31			End teem 3rd plate
20.32			Start teem 4th plate
20.38½		Metal 14	From Ingot
20.39½		Metal 15	From ladle stream
20.40			End teem 4th plate
20.41			Start teem 5th plate
20.50		Metal 16	From Ingot
20.51		Metal 17	From ladle stream
20.52			End teem 5th plate

Table 3.7

Chronology of steelmaking trial C.1

Time	Steelmaking Additions	Samples	Comments
9.40			Power on
13.40			Melt out
13.40-14.10	Lime + spar + oxygen		Slag flush
14.10			1630°C
14.11-14.16			Slag off
14.17	Al		Block
14.19	Lime		
14.27			1660°C
14.27½		Metal 1	
14.28	FeSi		
14.33½		Metal 2	
14.34			1650°C
14.42½		Metal 3	
14.43			1670°C
14.48-14.50			Bath paddled
14.50½		Metal 4	
15.04			Bath paddled
15.05½		Metal 5	
15.06			1680°C
15.07	Al		
15.08-15.15			Slag flush
15.19	FeSi		
15.20	Desulfex		
15.27-15.29			Bath paddled
15.29½		Metal 6	
15.31	FeNb + FeMn		
15.32	FeMn		
15.36½			1620°C
15.37		Metal 7	
15.43			1640°C
15.43½		Metal 8	
15.48½			Start of tapping
15.51			Stop tapping
15.52	Al		
15.53			Restart tapping
16.01			End of tapping
16.01½			1600°C
16.02		Metal 9	From ladle
16.11½			Start teem 1st ingot
16.16½		Metal 10	From ingot
16.17			End teem 1st ingot
16.18			Start teem 2nd ingot
16.25½		Metal 11	From ingot
16.26		Metal 12	From ladle stream
16.27			End teem 2nd ingot
16.30			Start teem 3rd ingot
16.39½		Metal 13	From ingot
16.40½		Metal 14	From ladle stream
16.42			End teem 3rd ingot
16.43			Oxygen on nozzle
16.44½			Start teem 4th ingot
16.53½		Metal 15	From ingot
16.54		Metal 16	From ladle stream
16.55½			End teem 4th ingot
16.56			Oxygen on nozzle
16.58			Start teem 5th ingot
17.10		Metal 17	From ingot
17.12			Argon shroud off
17.12½		Metal 18	From ladle stream
17.13			End teem 5th ingot

Table 3.8

Chronology of steelmaking trial C.2

Time	Steelmaking Additions	Samples	Comments
6.55			Power on
10.05			Melt out
10.05-11.29½	Lime + spar + scale + oxygen		Slag flush
11.31-11.37½			Slag off
11.38		Metal 1	(failed)
11.40	Al		
11.42	Lime + spar		
11.45			Electrodes dipped
11.54½			1649°C
11.55		Metal 2	
11.56	FeSi		
12.02½-12.06			Bath paddled
12.09½		Metal 3	
12.15		Metal 4	
12.16-12.21	Desulfex		Injected into bath
12.22½		Metal 5	
12.23½-12.31			Slag flush
12.31½			1620°C
12.32	Al		
12.33½	Desulfex		
12.41½			1610°C
12.42		Metal 6	
12.44		Metal 7	
12.48			1620°C
12.53½	FeMn + FeNb + FeSi		Final additions
12.56½			1630°C
12.57		Metal 8	
13.00			1640°C
13.02½			Start tap
13.05			Stop tap
13.05½	Al		
13.07½			Restart tap
13.10			End tap
13.11			1600°C
13.11½		Metal 9	From ladle
13.18½			Start teem 1st ingot
13.24½		Metal 10	From ingot
13.26			End teem 1st ingot
13.26½		Metal 11	From ladle stream
13.27½			Start teem 2nd ingot
13.36½		Metal 12	From ingot
13.39			End teem 2nd ingot
13.40			Start teem 3rd ingot
13.52		Metal 13	From ingot
13.54½			End teem 3rd ingot
13.55		Metal 14	From ladle stream
13.56			Oxygen on nozzle
13.58			Start teem 4th ingot
14.04		Metal 15	From ingot
14.08			End teem 4th ingot
14.08½		Metal 16	From ladle stream
14.09			Oxygen on nozzle
14.10½			Start teem 5th ingot
14.17½		Metal 17	From ingot
14.19			End teem 5th ingot
14.20		Metal 18	From ladle stream

Table 3.9

Chronology of steelmaking trial C.3

Trial Cast	Analysis, wt. %												
	C	Si	S	P	Mn	Cr	Mo	Ni	Cu	Sn	Al	Nb	V
C.1	0.155	0.364	0.006	0.014	1.43	0.09	0.03	0.115	0.12	0.011	0.03	0.019	0.04
C.2	0.165	0.325	0.004	0.015	1.46	0.055	0.01	0.06	0.11	0.010	0.027	0.037	0.01
C.3	0.165	0.355	0.004	0.012	1.26	0.09	0.02	0.14	0.125	0.011	0.059	0.03/ 0.04	0.01

Table 3.10

Pit analyses of CMnNb trial casts

Analysis	Wt. %
SiO_2	1.1
CaO	63.4
MgO	1.3
MnO	< 1
Al_2O_3	17.5
Total Fe	1.8
Cr_2O_3	< 1
TiO_2	< 0.5
V_2O_5	< 1
BaO	< 0.2
C	0.64
S	0.059
CaF_2	9.0
Metallic Al	3.8
Na_2CO_3	3.13
K_2O	0.07

Table 3.11

Analysis of Desulfex 75

Source	Refractory Type		
	Trial C.1	Trial C.2	Trial C.3
Furnace	Magnesite Lining Magnesite Taphole Rammed Magnesite Launder	As for C.1	As for C.1
Ladle	Fireclay (~27% Al_2O_3 probably patched (9 heats)	Stein Ladle Bricks (70% Al_2O_3) KSR Jointing (47% Al_2O_3) not patched (2nd heat)	As for C.2
Stopper	Fireclay (34% Al_2O_3)	As for C.1	As for C.1
Nozzle	Inner - Fireclay (34% Al_2O_3) Outer - Magnesite (91% MgO)	As for C.1	As for C.1
Holloware	Fireclay (34% Al_2O_3)	As for C.1 but with extra precautions	As for C.1 but with extra precautions

Table 3.12

Details of refractories for CMnNb trial casts

Inclusion Figure	Phase*	Analysis (wt. %)										
		FeO	MnO	SiO_2	Al_2O_3	Cr_2O_3	CaO	MgO	S	P_2O_5	TiO_2	K_2O
4.1a	-	15	7	20	1	2	45	8	tr**	tr	tr	-
4.1b	-	2	25	50	25	2	tr	-	-	-	tr	-
4.1c	-	2	25	48	27	3	tr	-	-	-	tr	-
4.2a	-	2	25	42	30	3	tr	-	-	-	1	-
4.2b	-	1	24	34	37	3	tr	-	-	-	tr	-
4.2c	A	-	-	100	-	-	-	-	-	-	-	-
4.2c	B	5	42	48	tr	9	-	-	-	-	-	-
4.2d	-	1	24	28	45	2	tr	-	tr	-	tr	-
4.2e	-	1	20	31	47	1	1	-	tr	-	tr	-
4.3a	A	-	-	-	100	-	-	-	-	-	-	-
4.3a	B	1	18	42	35	1	1	-	tr	-	tr	-
4.3b	A	2	4	33	65	tr	tr	-	-	-	tr	-
4.3b	B	2	30	30	35	2	1	-	tr	-	tr	-
4.3c	-	2	25	40	30	3	tr	-	-	-	tr	1
4.3d	-	2	20	52	12	2	12	2	tr	tr	tr	tr
4.3e	A	-	-	100	-	-	-	-	-	-	-	-
4.3e	B	1	45	49	3	2	-	-	tr	-	-	-
4.3f	A	4	7	tr	5	70	2	12	tr	tr	-	-
4.3f	B	tr	8	32	4	1	45	10	tr	2	tr	-
4.4a	A	-	-	100	-	-	-	-	-	-	-	-
4.4a	B	5	15	50	2	25	-	-	-	-	-	-
4.4a	C	2	50	45	2	5	tr	-	tr	-	-	-
4.4b	A	-	-	100	-	-	-	-	-	-	-	-
4.4b	B	2	30	-	tr	70	-	-	-	-	-	-
4.4b	C	4	16	48	3	23	-	-	-	-	-	-
4.4b	D	3	47	46	1	3	tr	-	tr	-	tr	-
4.4c	A	-	-	100	-	-	-	-	-	-	-	-
4.4c	B	2	28	tr	tr	69	-	-	-	-	-	-
4.4c	C	7	17	52	2	26	-	-	-	-	-	-
4.4c	D	1	52	45	2	5	tr	-	tr	-	-	-
4.5a	A	-	-	100	-	-	-	-	-	-	-	-
4.5a	B	3	40	50	tr	10	-	-	-	-	-	-
4.5b	-	1	20	35	40	3	tr	-	tr	-	1	tr
4.6a	A	-	-	-	100	-	-	-	-	-	-	-
4.6a	B	1	14	42	38	1	1	tr	tr	-	tr	2
4.6b	-	2	2	30	40	tr	15	8	tr	tr	tr	-
4.6c	-	2	20	35	42	2	tr	-	tr	-	1	2
4.6d	-	3	19	45	26	2	5	-	-	-	tr	1

Table 4.1

Analyses of inclusions

* Unless a particular phase is specified, the analysis given is an average one for the inclusion as a whole

** tr = trace amount, i.e. less than 1 wt. %

Inclusion Figure	Phase	Analysis (wt. %)										
		FeO	MnO	SiO_2	Al_2O_3	Cr_2O_3	CaO	MgO	MnS/S	P_2O_5	TiO_2	K_2O
4.7a	A	-	-	100	-	-	-	-	-	-	-	-
4.7a	B	2	40	50	2	8	3	-	tr	-	-	-
4.7b	A	-	-	100	-	-	-	-	-	-	-	-
4.7b	B	3	19	50	-	30	-	-	-	-	-	-
4.7b	C	3	51	45	tr	4	-	-	tr	-	-	-
4.8a	-	tr	3	15	80	1	-	-	-	-	tr	-
4.8b	-	1	4	20	75	1	-	-	-	-	tr	tr
4.9a	-	6	24	36	16	tr	9	-	1	tr	2	-
4.9b	-	9	27	35	15	tr	10	-	2	-	2	-
4.9c	A	13	24	6	35	16	2	2	tr	-	2	-
4.9c	B	12	28	34	16	tr	8	tr	tr	-	tr	-
4.9d	-	9	24	35	5	tr	20	2	2	tr	1	-
4.10a	-	10	25	35	5	tr	20	1	1	tr	2	-
4.10b	-	14	25	30	10	3	15	tr	tr	-	1	-
4.10c	A	42	21	tr	tr	4	3	32	-	tr	-	-
4.10c	B	10	5	20	8	tr	54	1	2	3	tr	-
4.10d	A	40	45	tr	tr	4	5	2	-	-	-	-
4.10d	B	12	15	22	8	tr	38	tr	2	2	tr	-
4.11a	-	6	48	25	4	tr	7	tr	10	tr	tr	-
4.11b	-	3	48	22	16	tr	5	tr	3	-	tr	tr
4.11c	A	10	85	-	-	tr	5	-	tr	-	-	-
4.11c	B	5	25	18	7	-	38	-	5	1	tr	-
4.12a	-	3	34	30	34	tr	tr	tr	3	-	1	tr
4.12b	A	5	40	-	55	1	-	-	-	-	-	-
4.12b	B	3	48	27	16	-	-	-	tr	-	1	1
4.12c	A	4	42	-	54	2	-	-	-	-	-	-
4.12c	B	2	46	25	24	-	-	-	tr	-	1	1
4.12d	A	17	80	-	-	3	-	-	tr	-	-	-
4.12d	B	-	-	-	-	-	-	-	100	-	-	-
4.12d	C	5	50	25	4	tr	2	tr	18	-	tr	-
4.12e	-	9	50	15	3	tr	3	-	18	-	tr	-
4.13a	-	5	38	27	29	-	tr	tr	4	-	1	tr
4.13b	-	9	53	13	4	tr	2	-	18	-	tr	-
4.13c	-	10	47	13	6	tr	tr	-	26	tr	tr	-
4.13d	A	13	85	-	tr	2	-	-	tr	-	-	-
4.13d	B	-	-	-	-	-	-	-	100	-	-	-
4.13d	C	9	45	25	7	tr	3	tr	11	-	tr	-
4.14c	A	-	-	-	-	-	-	-	100	-	-	-
4.14c	B	3	40	-	53	5	-	-	-	-	-	-
4.14c	C	4	59	19	3	-	tr	-	15	-	tr	tr
4.14d	-	4	62	19	2	tr	tr	tr	15	-	tr	tr
4.14e	A	-	-	-	-	-	-	-	100	-	-	-
4.14e	B	3	40	-	55	5	-	-	-	-	-	-
4.14e	C	6	91	2	tr	-	-	-	3	-	-	-
4.14e	D	4	65	23	2	-	tr	-	9	-	-	tr

Table 4.1 (continued)

Inclusion Figure	Phase	Analysis (wt. %)										
		FeO	MnO	SiO_2	Al_2O_3	Cr_2O_3	CaO	MgO	S	P_2O_5	TiO_2	K_2O
4.23	A	1	2	28	2	-	57	8	-	2	-	-
4.23	B	12	tr	-	-	3	tr	80	-	-	-	-
4.23	C	1	2	26	4	-	61	4	-	2	-	-
4.32a	-	4	11	38	6	tr	40	4	tr	1	tr	-
4.32b	-	3	18	67	5	-	tr	-	-	-	2	-
4.32c	A	-	-	-	100	-	-	-	-	-	-	-
4.32c	B	2	22	33	32	-	1	tr	-	-	5	-
4.32d	-	1	2	33	10	-	45	3	tr	2	tr	-
4.32e	A	-	-	-	100	-	-	-	-	-	-	-
4.32e	B	2	26	36	28	-	tr	tr	-	-	4	-
4.32f	-	tr	tr	30	12	-	50	6	tr	2	tr	-
4.32g	-	1	62	35	2	tr	tr	-	tr	-	-	-
4.33a	-	2	tr	20	17	-	53	5	1	2	tr	-
4.33b	A	-	-	-	-	-	-	100	-	-	-	-
4.33b	B	tr	tr	20	18	-	55	5	1	2	tr	-
4.34a	-	1	42	32	22	tr	-	-	tr	-	2	-
4.34b	-	1	42	35	20	-	tr	-	tr	-	1	tr
4.35a	-	2	40	38	22	-	tr	tr	tr	-	tr	tr
4.35b	-	2	35	37	26	-	3	2	-	-	tr	tr
4.35c	A	3	21	3	67	-	tr	10	-	-	-	-
4.35c	B	2	27	35	28	-	3	tr	-	-	tr	tr
4.35d	A	2	3	-	74	-	-	25	-	-	-	-
4.35d	B	tr	tr	2	64	-	35	3	-	1	-	-
4.38a	-	-	-	-	100	-	-	-	-	-	-	-
4.38b	-	-	-	-	100	-	-	-	-	-	-	-
4.38c	-	-	-	-	100	-	-	-	-	-	-	-
4.38d	-	2	20	50	25	tr	tr	-	-	-	1	-
4.38e	-	-	-	-	100	-	-	-	-	-	-	-
4.38f	A	-	-	-	100	-	-	-	-	-	-	-
4.38f	B	3	3	24	45	-	24	tr	-	tr	tr	-
4.38h	-	-	-	-	100	-	-	-	-	-	-	-
4.38i	-	-	-	-	100	-	-	-	-	-	-	-
4.38j	A	-	-	-	-	-	-	100	-	-	-	-
4.38j	B	tr	tr	5	25	-	65	2	1	2	tr	-
4.38k	A	4	38	tr	57	-	-	tr	-	-	1	tr
4.38k	B	2	40	30	22	-	2	-	tr	tr	2	-
4.39a	A	-	-	-	-	-	-	100	-	-	-	-
4.39a	B	tr	tr	15	15	-	65	3	1	2	tr	-
4.39b	A	-	-	-	-	-	-	100	-	-	-	-
4.39b	B	1	2	18	14	-	59	2	tr	1	tr	-
4.40a	-	tr	tr	1	36	-	52	4	1	2	-	-
4.40b	A	-	-	-	-	-	-	100	-	-	-	-
4.40b	B	tr	-	12	20	-	64	1	1	2	tr	-

Table 4.1 (continued)

Inclusion Figure	Phase	Analysis (wt. %)										
		FeO	MnO	SiO_2	Al_2O_3	Cr_2O_3	CaO	MgO	S	P_2O_5	TiO_2	K_2O
4.41a	-	5	56	31	7	tr	-	-	-	-	tr	-
4.41b	-	2	37	30	28	-	-	-	-	-	2	-
4.41c	A	-	-	-	100	-	-	-	-	-	-	-
4.41c	B	1	40	32	27	-	tr	-	-	-	1	tr
4.41d	A	1	34	2	53	-	-	3	-	-	2	-
4.41d	B	1	38	28	27	-	tr	-	-	-	2	tr
4.42a	A	1	3	-	68	-	-	25	-	-	-	-
4.42a	B	1	32	27	31	-	3	1	-	-	2	tr
4.42b	A	-	-	-	100	-	-	-	-	-	-	-
4.42b	B	1	40	35	25	-	tr	-	-	-	2	tr
4.42c	A	tr	tr	-	68	-	2	27	-	-	-	-
4.42c	B	2	tr	1	43	-	49	3	1	1	tr	-
4.42d	-	3	29	33	30	-	3	tr	-	-	1	tr
4.42e	-	-	-	-	100	-	-	-	-	-	-	-
4.42f	-	2	51	35	9	-	tr	-	tr	-	tr	-
4.47a	-	-	-	-	100	-	-	-	-	-	-	-
4.47b	-	tr	tr	15	15	-	65	4	1	1	tr	-
4.47c	A	-	-	-	100	-	-	-	-	-	-	-
4.47c	B	tr	30	30	35	-	4	tr	tr	-	tr	-
4.47d	-	-	-	-	100	-	-	-	-	-	-	-
4.47e	-	1	tr	10	22	-	65	5	tr	2	tr	-
4.47f	-	-	-	-	100	-	-	-	-	-	-	-
4.47g	-	tr	tr	5	24	-	63	4	1	2	1	-
4.47h	-	2	20	50	25	tr	tr	-	-	-	1	-
4.47i	A	-	-	-	100	-	-	-	-	-	-	-
4.47i	B	1	15	30	35	-	15	2	tr	1	tr	-
4.48	-	tr	tr	1	35	-	35	30	1	2	tr	-
4.49a	-	4	55	30	5	-	-	-	-	-	tr	-
4.49b	A	-	-	-	100	-	-	-	-	-	-	-
4.49b	B	1	38	30	27	-	tr	-	-	-	2	tr
4.49c	A	1	35	1	57	-	-	2	-	-	1	-
4.49c	B	1	38	28	29	-	1	-	-	-	2	tr
4.50a	A	-	-	-	100	-	-	-	-	-	-	-
4.50a	B	tr	38	36	27	-	tr	-	-	-	1	tr
4.50b	-	2	30	34	32	-	2	-	-	-	2	tr
4.50c	-	3	49	37	8	-	tr	-	-	-	1	-

Table 4.1 (continued)

SiO_2	39.37%
TiO_2	1.25
Al_2O_3	12.08
Fe_2O_3	5.45
FeO	1.17
MnO	0.30
MgO	23.37
CaO	1.46
Na_2O	0.80
K_2O	2.46
$H_2O + 105°C$	5.18
$H_2O - 105°C$	6.02
CO_2	0.60
P_2O_5	0.15
Li_2O	0.03
ZrO_2	nil
Cr_2O_3	nil
V_2O_3	nil
NiO	nil
CoO	nil
BaO	0.03
Cl	0.02
F	nil
SO_3	0.02
S	0.18

Table 4.2

Chemical analysis of commercial vermiculite

Billet Sample	Position on Billet	Total Oxygen Content wt. %
Middle	Edge	-
	Mid-thickness	0.0023
	Centre	-
Bottom	Edge	-
	Mid-thickness	0.0022
	Centre	0.0029
Top	Edge	0.0019
	Mid-thickness	0.0025
	Centre	0.0016
Middle	Edge	0.0025
	Mid-thickness	0.0026
	Centre	0.0022
Bottom	Edge	0.0025
	Mid-thickness	0.0023
	Centre	0.0028
Top	Edge	0.0038
	Mid-thickness	0.0035
	Centre	0.0033
Bottom	Edge	0.0047
	Mid-thickness	0.0026
	Centre	0.0028
Middle	Edge	0.0034
	Mid-thickness	0.0028
	Centre	0.0038

Table 4.3

Trial cast A.1 - Total oxygen content of billet samples from top, middle and bottom of ingots

Slag Sample	Time after Melt out (minutes)	Details	Analysis (wt. %)											
			SiO_2	CaO	MgO	MnO	Al_2O_3	Total Iron	Cr_2O_3	TiO_2	V_2O_5	BaO	P_2O_5	S
1	0	Bath at melt out	14.9	38.9	3.0	7.9	3.4	19.0	< 1.0	< 0.5	< 1.0	< 0.2	2.89	0.37
2	12	Bath after oxygen blow and slag flush	15.0	43.3	4.6	8.0	4.3	16.3	< 1.0	< 0.5	< 1.0	< 0.2	3.10	0.45
3	23.5	Bath after further oxygen blow and slag flush	12.1	40.5	7.0	6.7	4.7	19.6	< 1.0	< 0.5	< 1.0	< 0.2	2.78	0.45
4	27.5	Bath	10.2	38.6	9.3	5.8	4.3	20.1	< 1.0	< 0.5	< 1.0	< 0.2	2.42	0.38
5	32.5	Bath prior to FeMn block	10.8	36.5	8.0	6.4	5.2	21.7	< 1.0	< 0.5	< 1.0	< 0.2	2.69	0.39
6	83.5	Final ladle slag after teeming ingots	21.7	22.7	6.7	18.5	8.7	13.1	< 1.0	< 0.5	< 1.0	< 0.2	1.43	1.60

Table 4.4

Trial cast B.1 - Analyses of slags

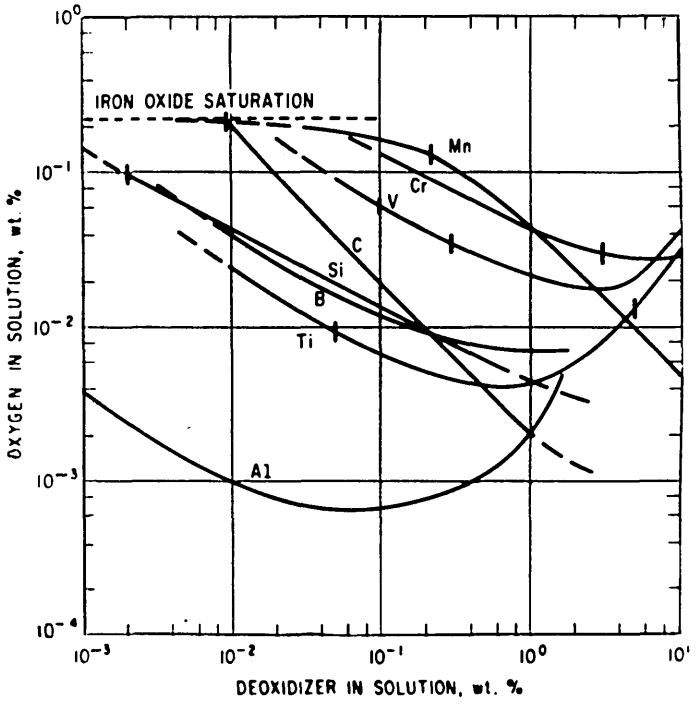

Fig. 2.1

Deoxidation equilibria in liquid iron alloys at 1600°C
(After Turkdogan and Fruehan, Ref. 11)

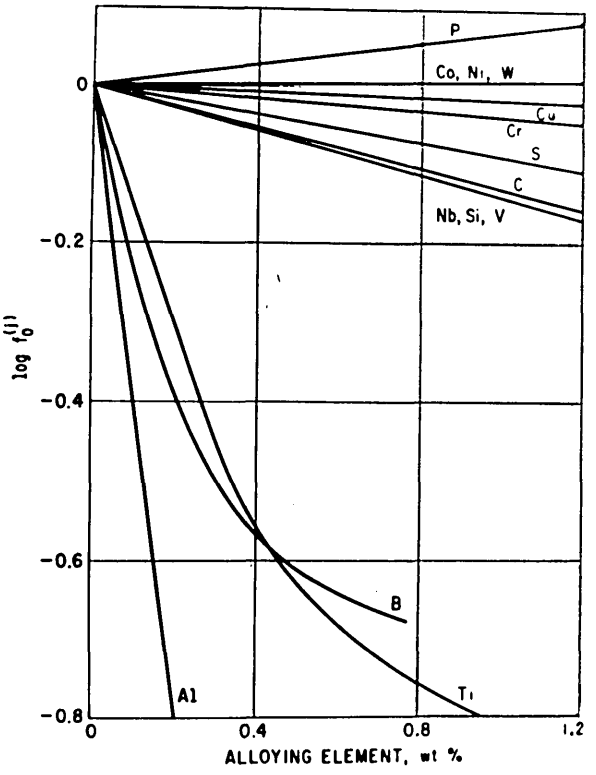

Fig. 2.2

Effect of various elements on the activity coefficient of oxygen in iron at 1600°C
(After Turkdogan and Fruehan, Ref. 11)

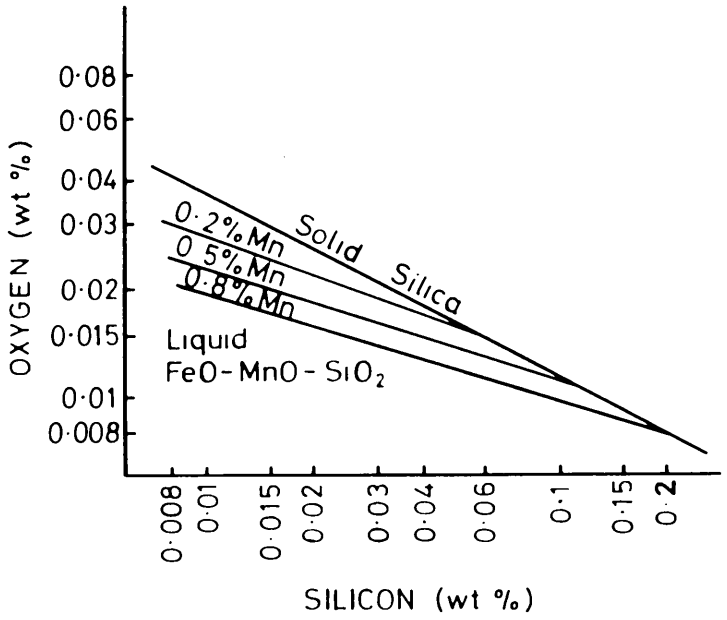

Fig. 2.3

Effect of manganese on the silicon-oxygen equilibrium in liquid iron at 1550°C
(After Bell, Ref. 17)

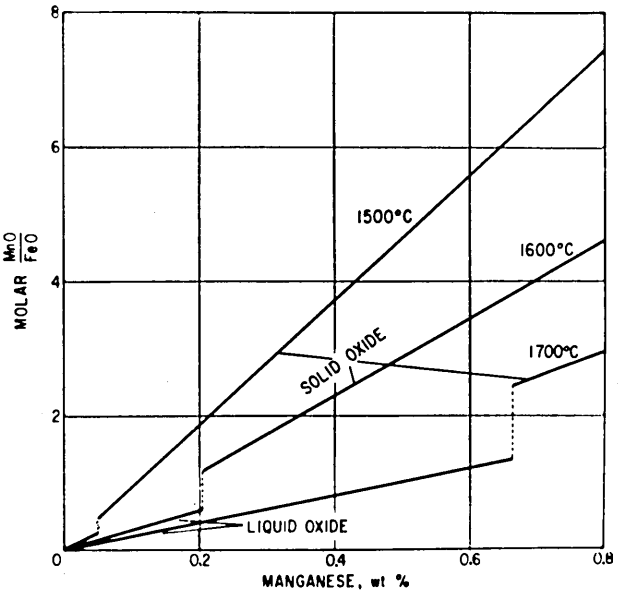

Fig. 2.4

Composition of liquid or solid FeO-MnO deoxidation product in equilibrium with Fe-O-Mn melts
(After Turkdogan, Refs. 10 and 20)

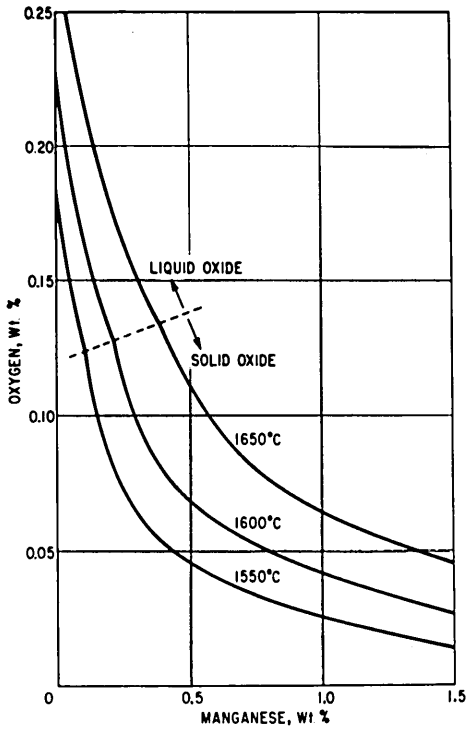

Fig. 2.5

Manganese and oxygen contents of iron in equilibrium with FeO-MnO liquid or solid deoxidation product (After Turkdogan, Ref. 10)

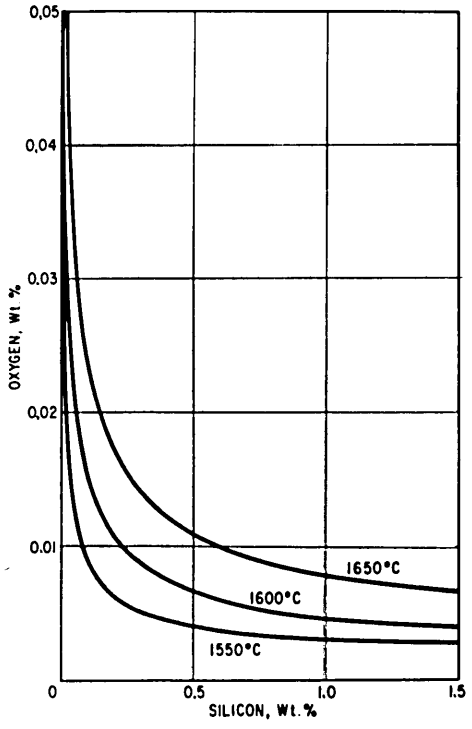

Fig. 2.6

Silicon and oxygen contents of iron in equilibrium with solid silica (After Turkdogan, Ref. 10)

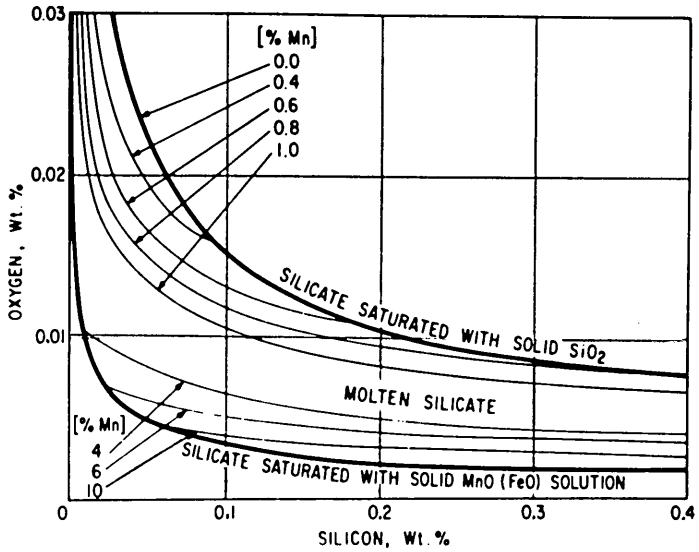

Fig. 2.7

Equilibrium data on simultaneous deoxidation of steel by silicon and manganese at 1600°C
(After Turkdogan, Ref. 10)

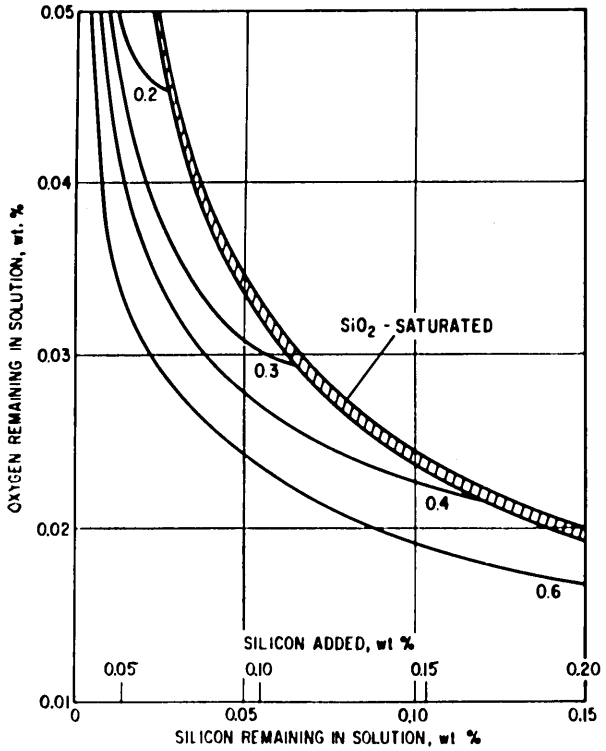

Fig. 2.8

Residual oxygen and silicon contents of iron after deoxidation of 0.1% O steel at 1650°C for various residual manganese contents from 0.2 to 0.6%
(After Turkdogan, Ref. 20)

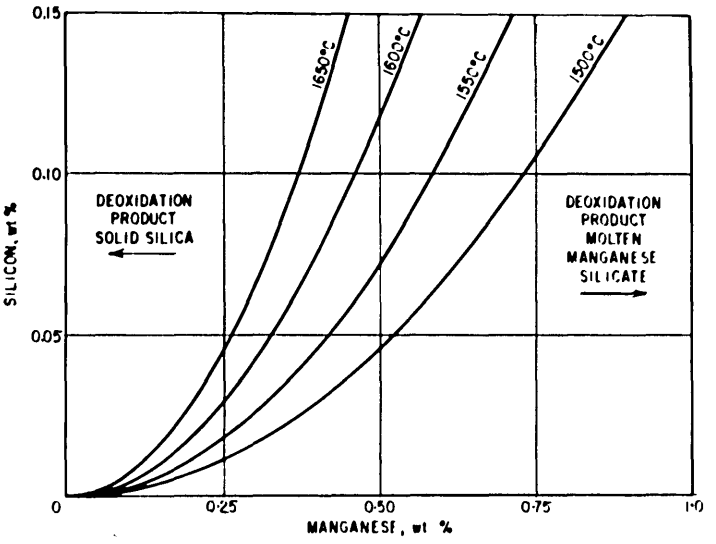

Fig. 2.9

Critical silicon and manganese contents of steel in equilibrium with silica-saturated deoxidation product, comprising almost pure manganese silicate, at various temperatures
(After Turkdogan, Ref. 20)

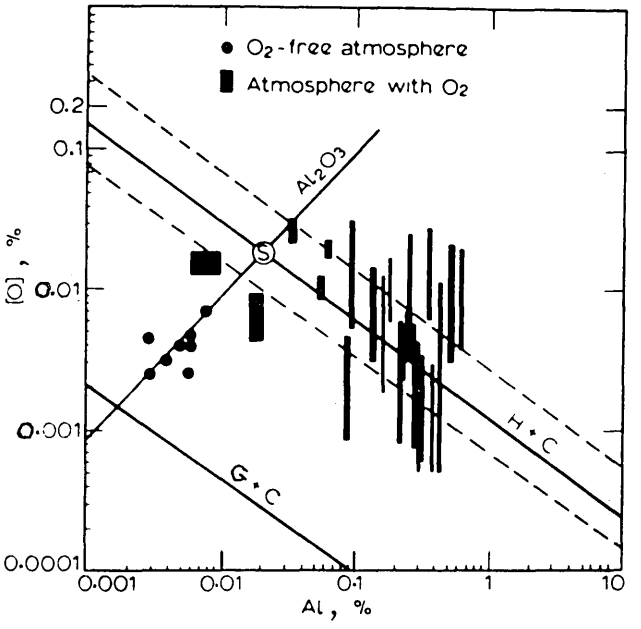

Fig. 2.10

Reactions between aluminium and dissolved oxygen in liquid iron at 1600°C in a stream of argon (kinetic tests) or in a stream of argon and oxygen (progressive deoxidation tests) G + C is the equilibrium curve of Gokcen and Chipman; H + C is the curve of Hilty and Crafts
(After Repetylo et al, Ref. 29)

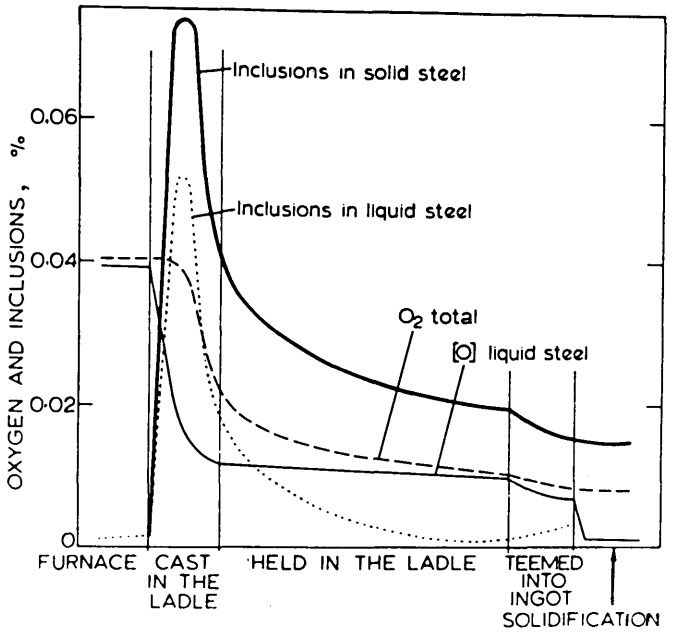

Fig. 2.11

Variation of oxygen and inclusion content during precipitation deoxidation (After Plöckinger and Wahlster, Refs. 32 and 33)

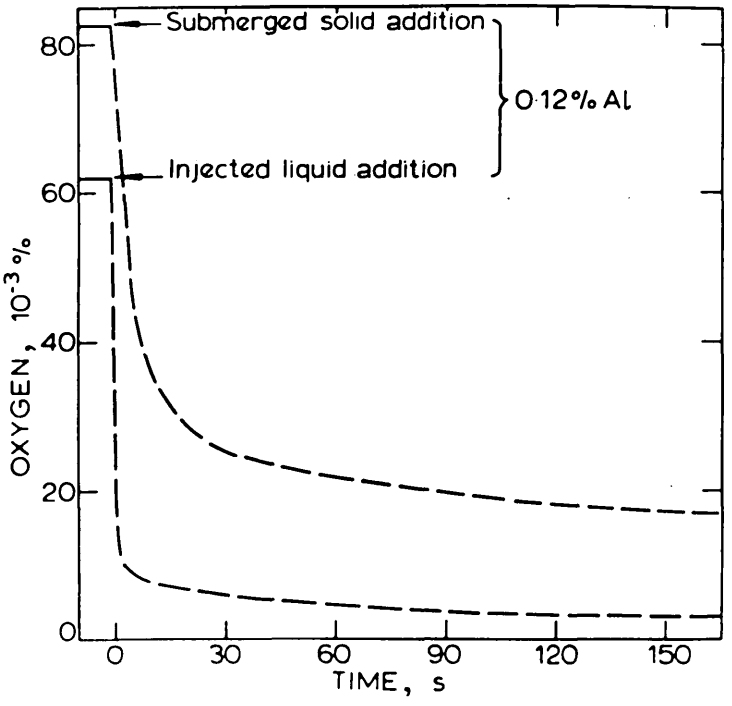

Fig. 2.12

Variation of dissolved oxygen with time for two methods of aluminium addition (After Olette, Gatellier and Torssell, Ref. 34)

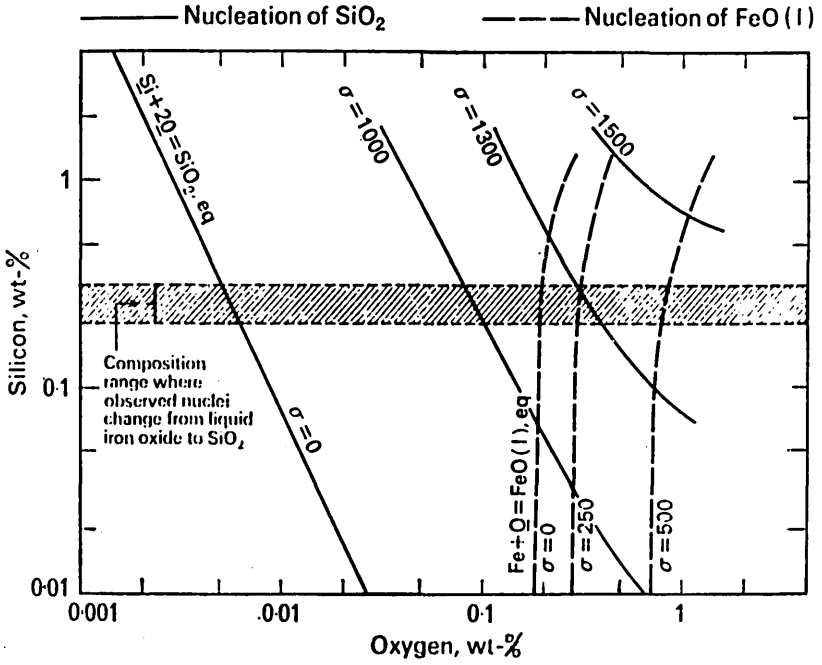

Fig. 2.13

Effect of interfacial energy, σ, on the degree of supersaturation required for nucleation of oxides in the Fe-O-Si system at 1536°C. σ in $J/m^2 \times 10^3$ (erg/cm^2)
(After Turpin and Elliott, Ref. 43)

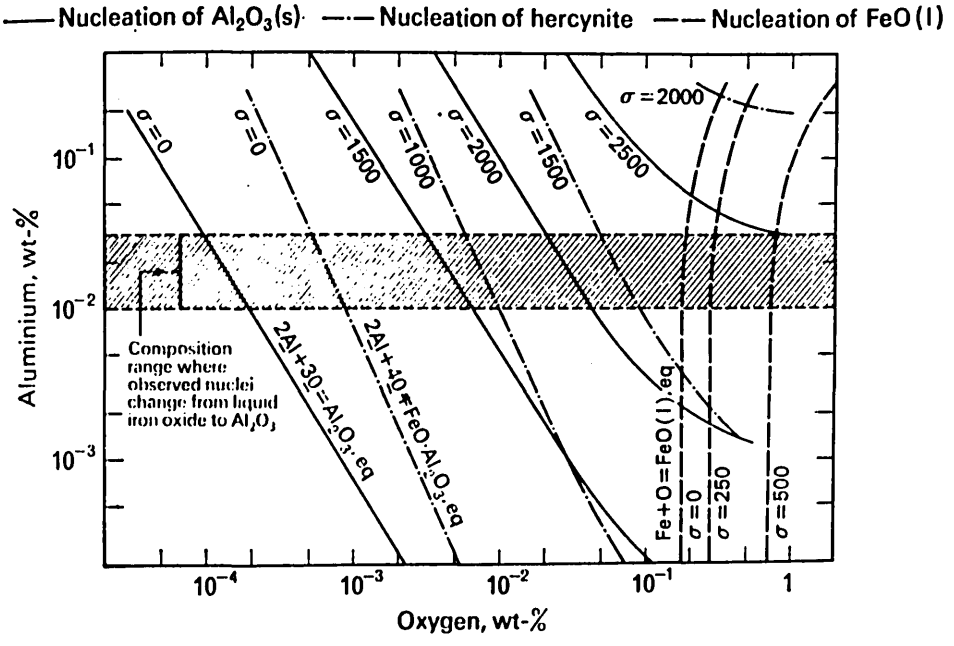

Fig. 2.14

Effect of interfacial energy, σ, on the degree of supersaturation required for nucleation of oxides in the Fe-O-Al system at 1536°C. σ in $J/m^2 \times 10^3$ (erg/cm^2)
(After Turpin and Elliott, Ref. 43)

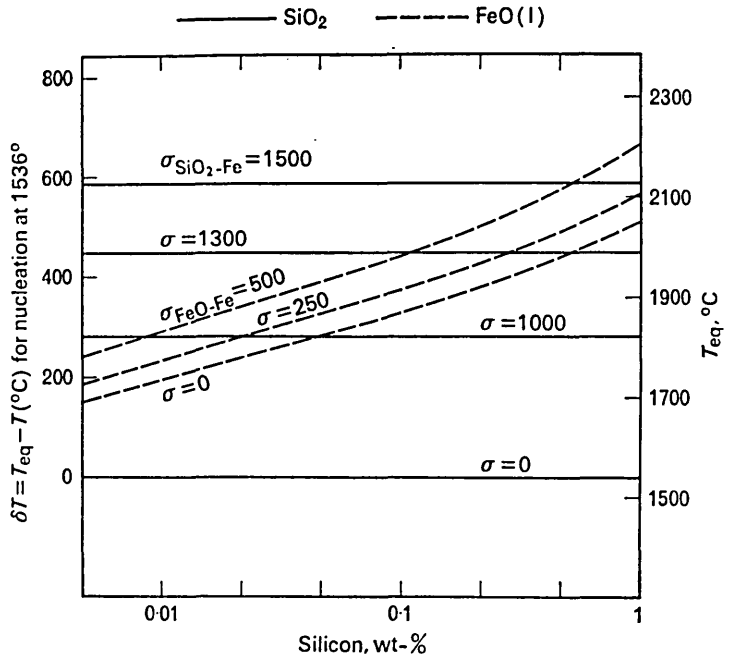

Fig. 2.15

Effect of interfacial energy, σ, on the degree of supercooling required for homogeneous nucleation of oxides in Fe-O-Si melts at 1536°C. σ in $J/m^2 \times 10^3$ (erg/cm^2)
(After Turpin and Elliott, Ref. 43)

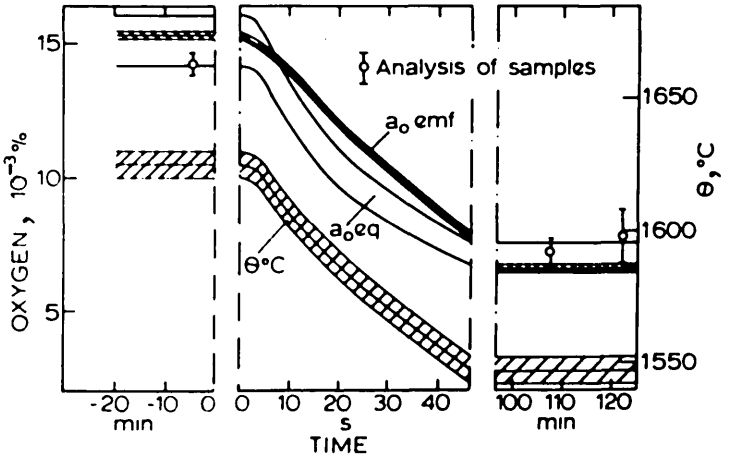

Fig. 2.16

Precipitation of oxide inclusions during cooling of a liquid Fe-O-Si alloy from 1625°C to 1550°C

a_O emf = oxygen activity determined electrochemically

a_O eq = oxygen activity determined from silicon content

(After Torsell, Gatellier and Olette, Ref. 45)

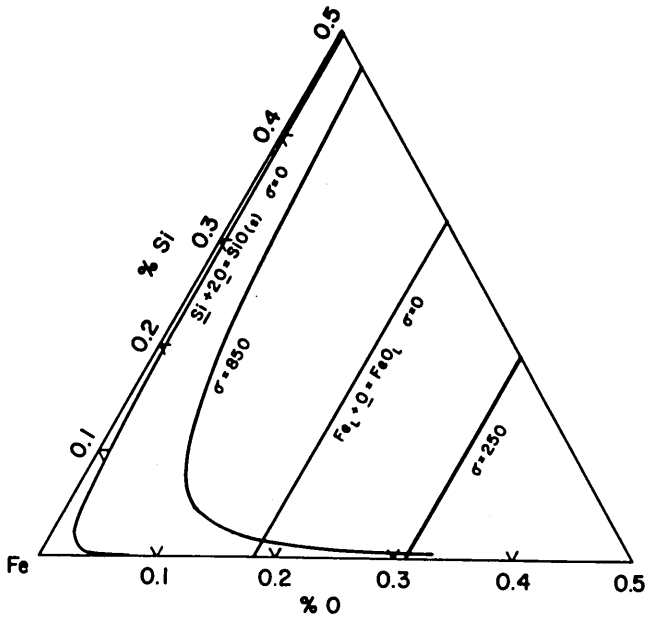

Fig. 2.17

Equilibrium compositions and compositions necessary for homogeneous nucleation of SiO_2 (S) and FeO (L) in Fe-O-Si alloys at 1550°C. Interfacial energy, σ in $J/m^2 \times 10^3$ (erg/cm^2)
(After Sigworth and Elliott, Ref. 44)

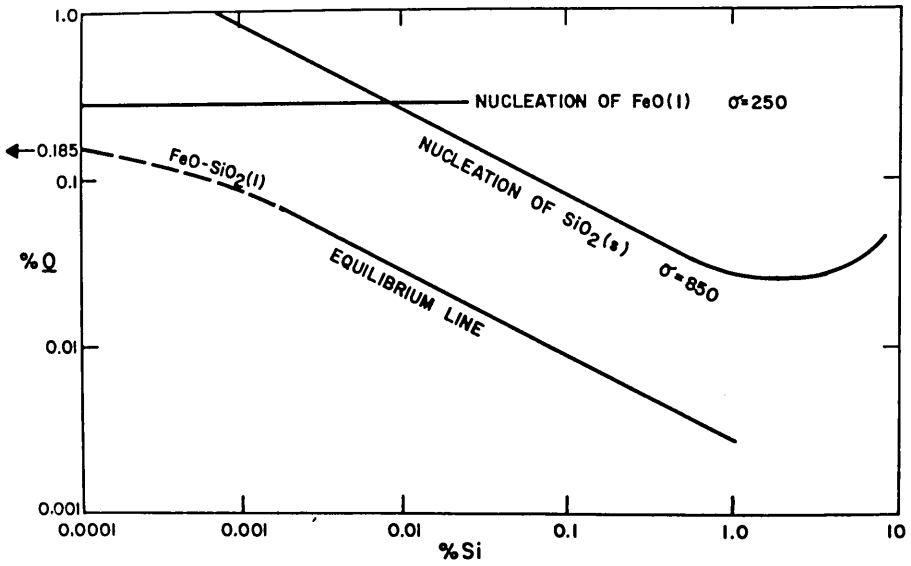

Fig. 2.18

Equilibrium and nucleation compositions for Fe-O-Si alloys at 1550°C
(After Sigworth and Elliott, Ref. 44)

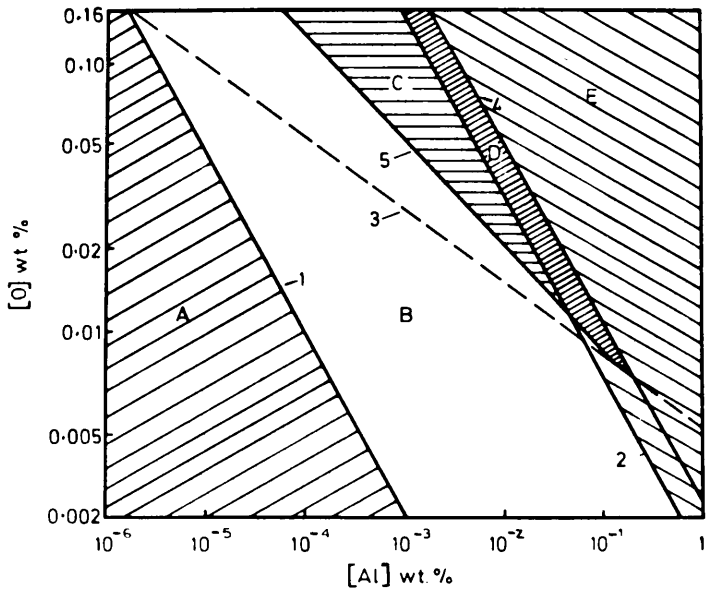

Fig. 2.19

Conditions for formation of nuclei in the Fe-O-Al system
(After Vorobnev and Levin, Ref. 47)

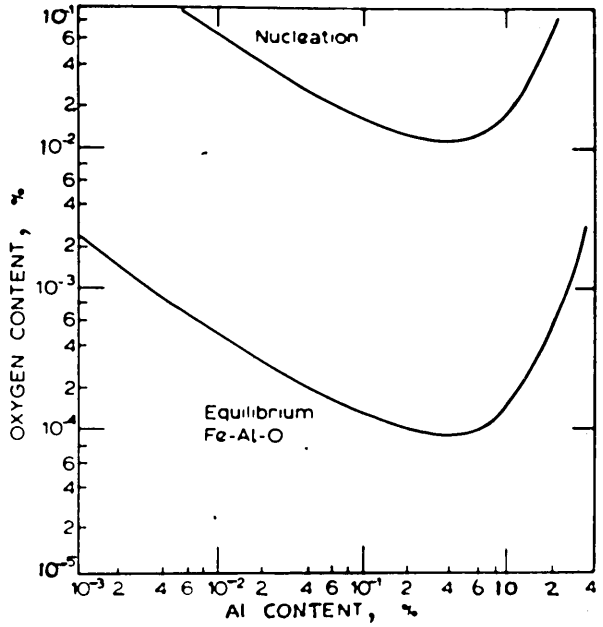

Fig. 2.20

Conditions for formation of alumina at 1600°C
(After Förster and Richter, Refs. 53 and 54)

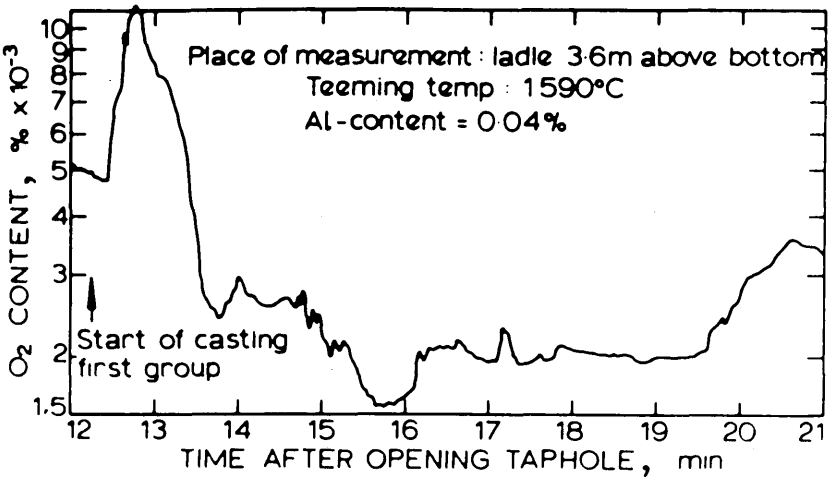

Fig. 2.21

Variation of dissolved oxygen in molten steel during teeming
(After Förster and Richter, Refs. 53 and 54)

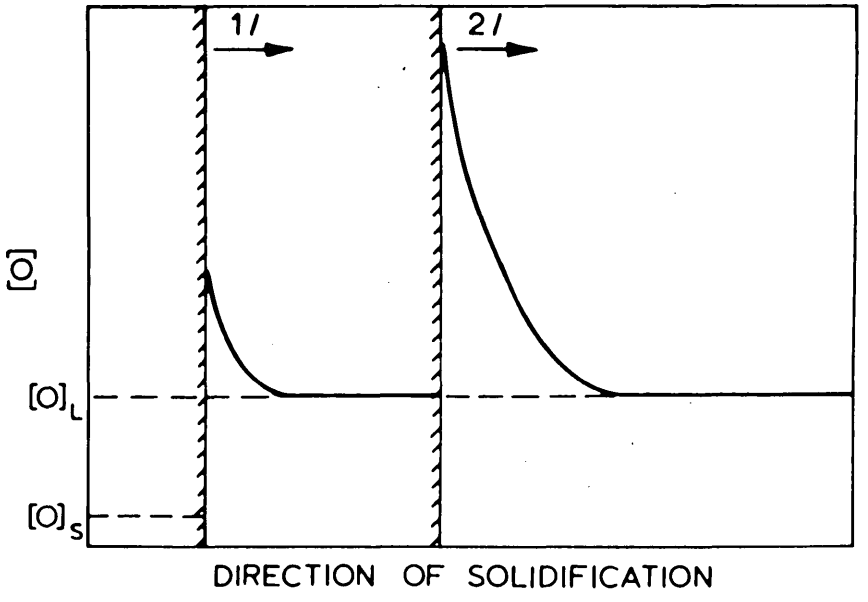

Fig. 2.22

Increase in oxygen ahead of the solidification front
(After Duckwitz et al, Ref. 56)

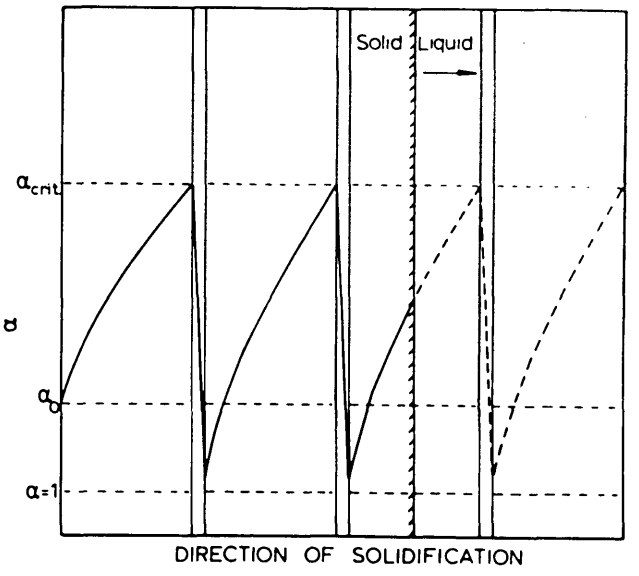

Fig. 2.23

Variation of oxide supersaturation ratio at the solid/liquid interface during solidification
α_o = oxide supersaturation ratio before solidification
α_{crit} = critical oxide supersaturation ratio
(After Duckwitz et al, Ref. 56)

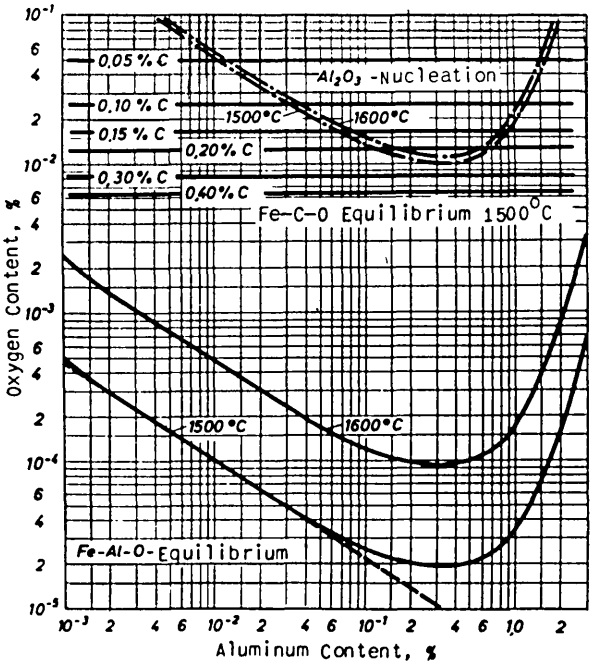

Fig. 2.24

Conditions for formation of alumina and carbon monoxide
(After Förster and Richter, Ref. 53)

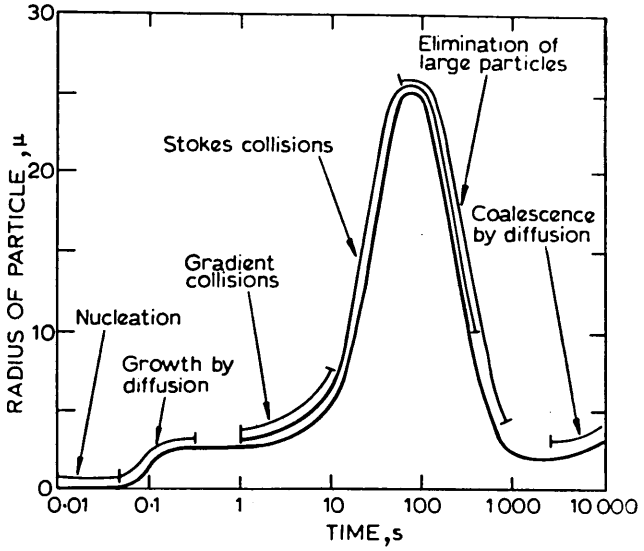

Fig. 2.25

Schematic diagram of inclusion growth
(After Lingborg and Torssell, Ref. 59)

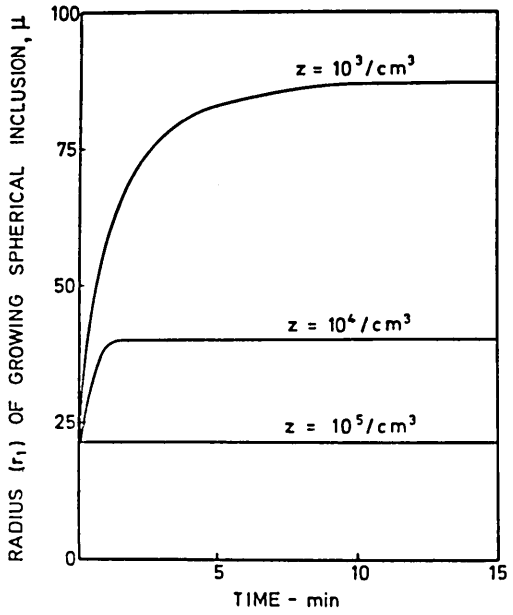

Fig. 2.26

Effect of number of nuclei on rate of inclusion growth
Z = number of growing inclusions per cm^3, initial equilibrium oxygen content, $[\%O]_i = 0.05$, final equilibrium oxygen content, $[\%O]_f = O$ and depth of liquid steel, $l_o = 2m$
(After Turkdogan, Ref. 60)

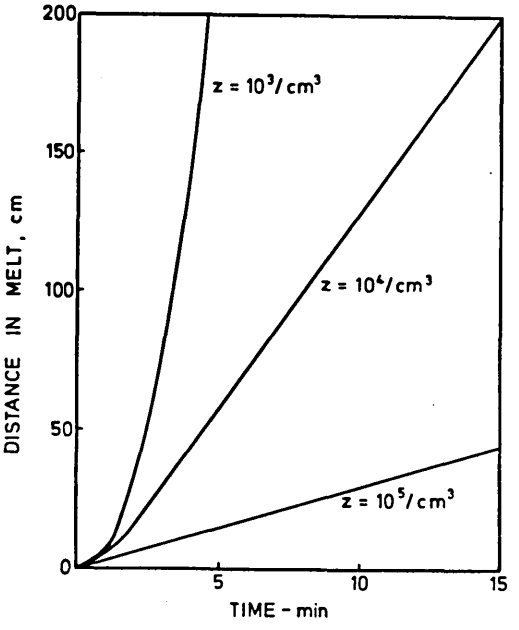

Fig. 2.27

Effect of number of nuclei, Z, on rate of ascent of inclusions
(After Turkdogan, Ref.60)

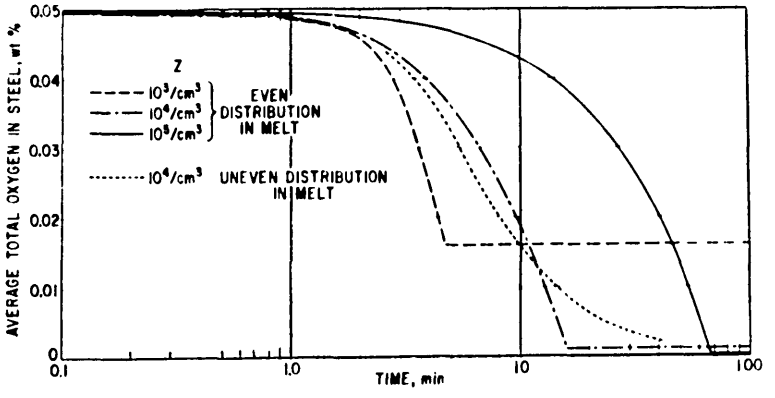

Fig. 2.28

Effect of number of nuclei, Z, and holding time on average total oxygen content of steel
(After Turkdogan, Ref. 60)

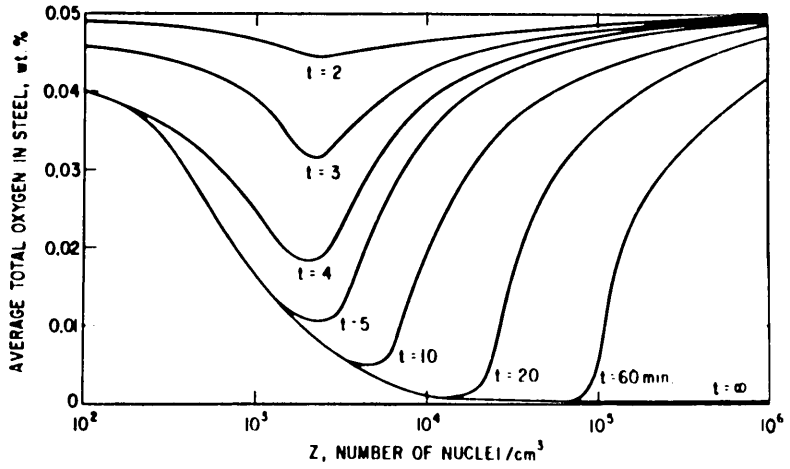

Fig. 2.29

Calculated data on average total oxygen content of steel as function of number of evenly-distributed nuclei/cm^3 in a quiescent melt and holding time after deoxidant additions.
$[\% O]_i = 0.05$, $[\% O]_f = 0$ and $l_o = 2$ m
(After Turkdogan, Refs. 10 and 60)

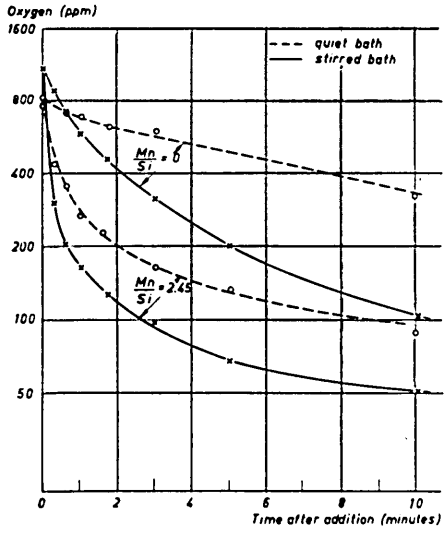

Fig. 2.30

Variation in oxygen content of liquid steel as a function of time after addition of 0.45% Si as pure silicon with Mn/Si = 0 or as silicon-manganese alloy with Mn/Si = 2.45 in a quiescent and stirred melt
(After Grevillius, Ref.61)

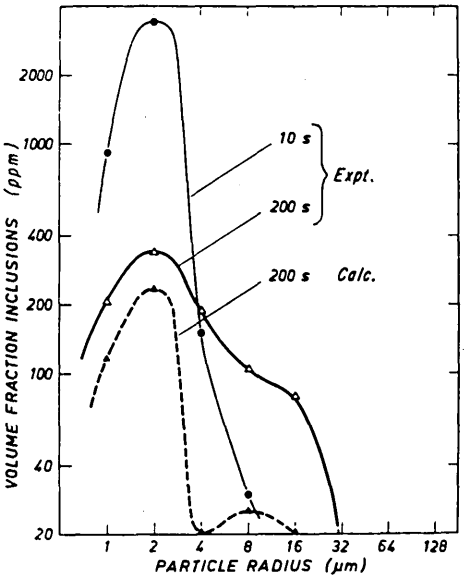

Fig. 2.31

Size distribution of SiO_2 inclusions after 10 s and 100 s of deoxidation time
(After Lindborg and Torssell, Ref. 59)

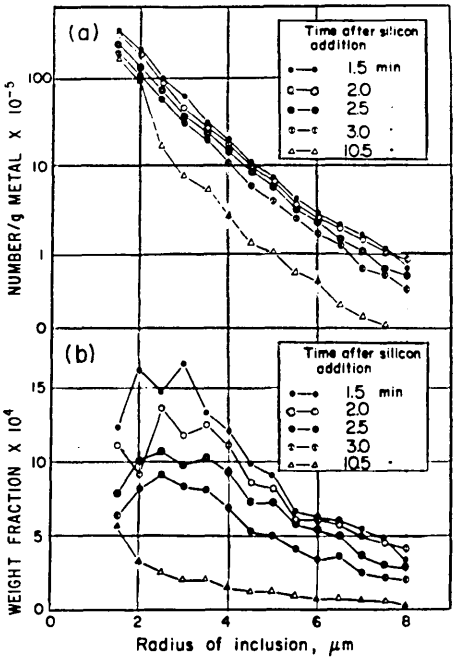

Fig. 2.32

Size distribution of SiO_2 inclusions produced by deoxidation with silicon
(After Miyashita, Ref.63)

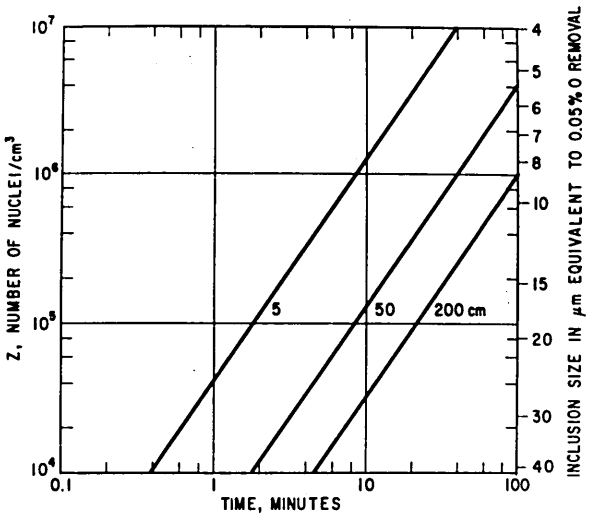

Fig. 2.33

Time for complete separation of oxide inclusions calculated for a stagnant melt 5, 50 and 200 cm deep with $[\% O]_i = 0.05$ as a function of number of evenly-distributed nuclei/cm^3

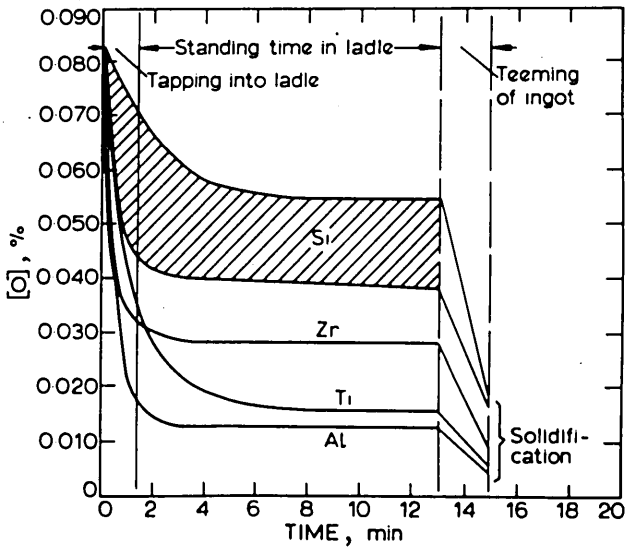

Fig. 2.34

Variation in total oxygen content after 3% addition of various deoxidants in the ladle (After Plöckinger and Wahlster, Ref.32)

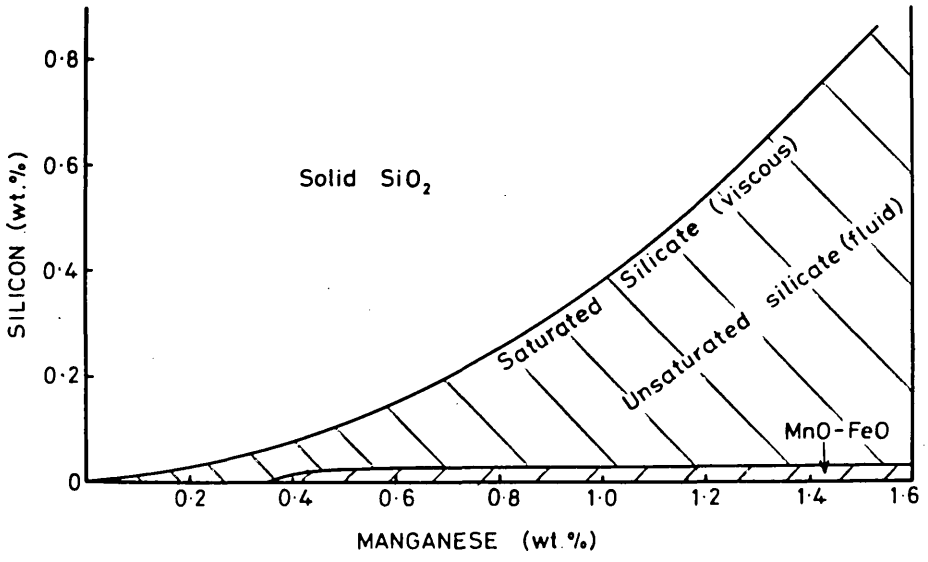

Fig. 2.35

Conditions for the formation of fluid manganese silicates at 1520°C
(After Korber and Oelsen, Ref. 14)

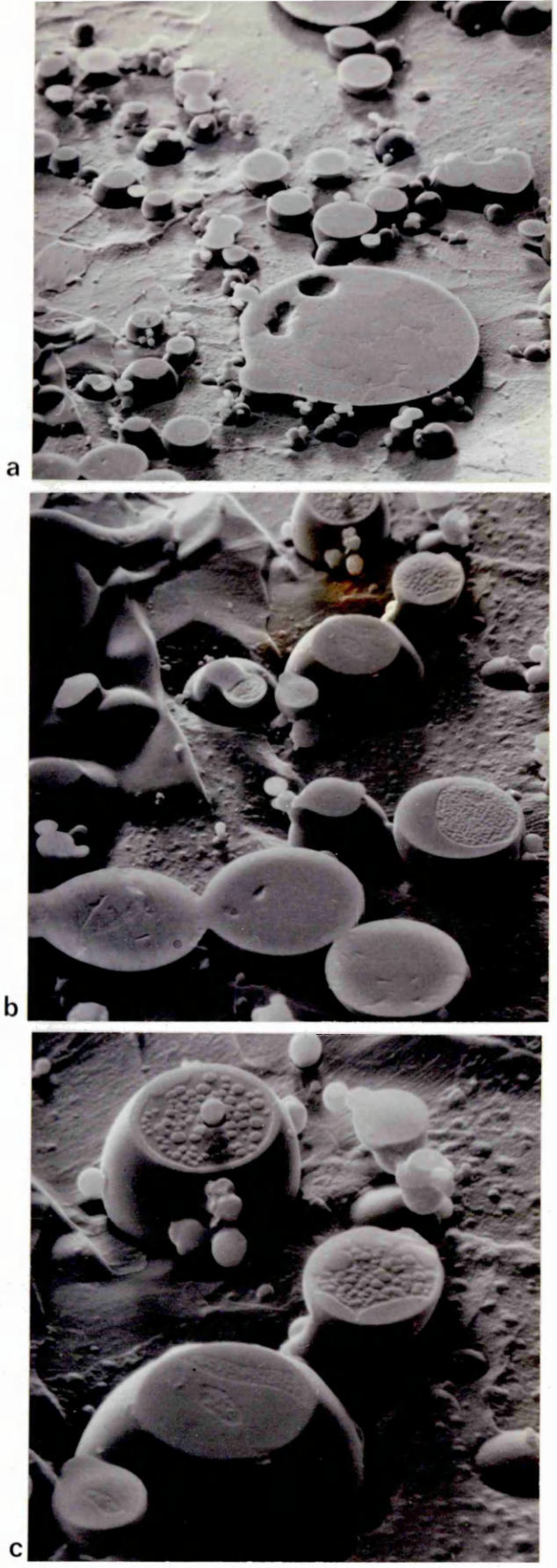

Fig. 2.36

Scanning electron micrographs of silicate inclusions in as-cast Fe-O-Si alloy after etching in bromine-methanol. Mag. (a) x 230, (b) x 575, (c) x 1150.

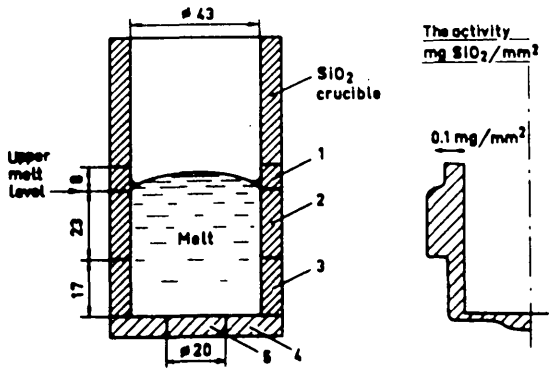

Silica Crucible			
Crucible Section	Surface Area, mm^2	Wt. of SiO_2	
		mg	%
1	1450	100	15
2	3110	380	85
3	2580	140	
4	1200	30	
5	250	10	

Fig. 2.37

Amount of SiO_2 on different parts of silica crucible
(After Lindskog, Ref. 84)

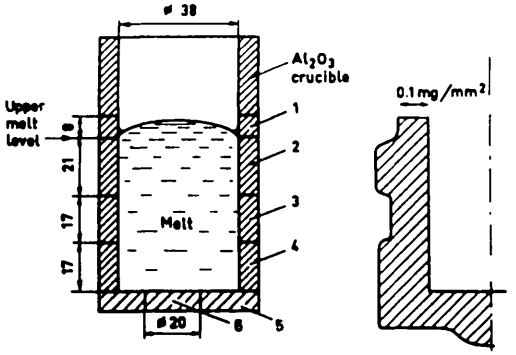

Alumina Crucible			
Crucible Section	Surface Area, mm^2	Wt. of SiO_2	
		mg	%
1	1200	140	10
2	2580	490	90
3	2100	300	
4	2100	390	
5	1150	120	
6	250	50	

Fig. 2.38

Amount of SiO_2 on different parts of alumina crucible
(After Lindskog, Ref. 84)

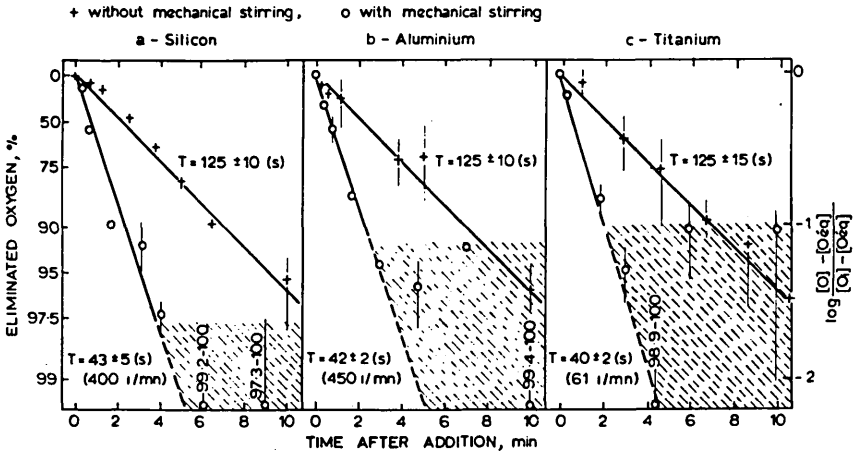

Fig. 2.39

Influence of mechanical stirring on the elimination of inclusions
(After Torssell, Gatellier and Olette, Ref. 45)

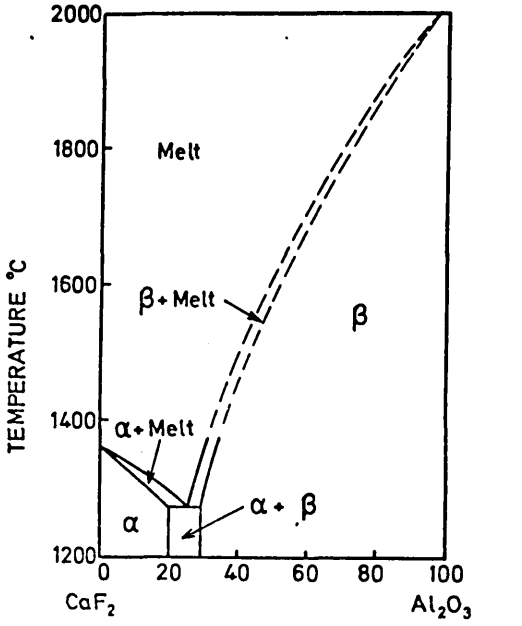

α = solid solution of Al_2O_3 in CaF_2
β = solid solution of CaF_2 in Al_2O_3

Fig. 2.40

Liquidus of CaF_2 - Al_2O_3 system
(After Choudhury and Wahlster, Ref. 91)

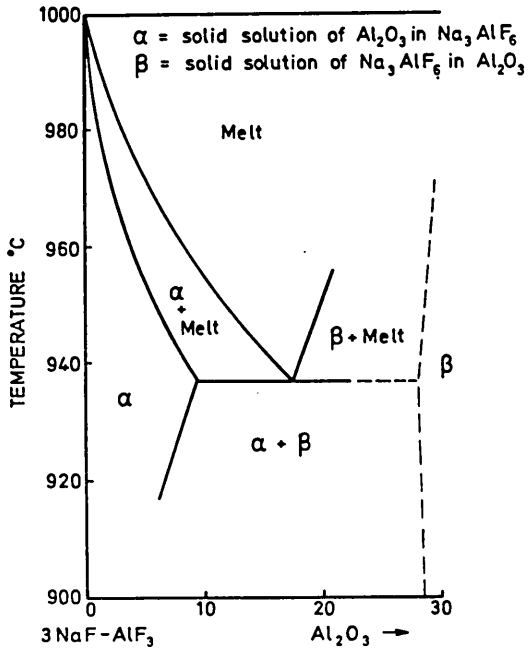

Fig. 2.41

Na_3AlF_6 - Al_2O_3 system
(After Choudhury and Wahlster, Ref. 91)

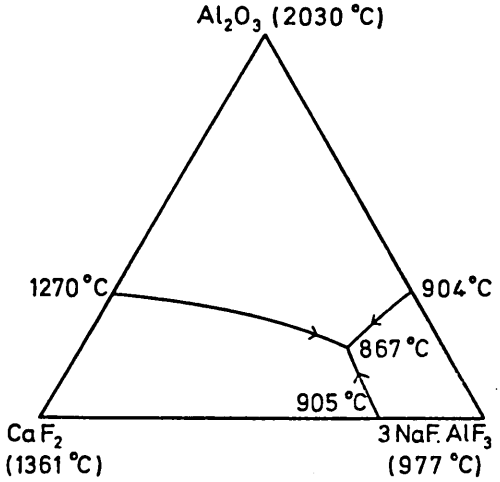

Fig. 2.42

Liquidus of Al_2O_3 - CaF_2 - Na_3AlF_6 system
(After Choudhury and Wahlster, Ref. 91)

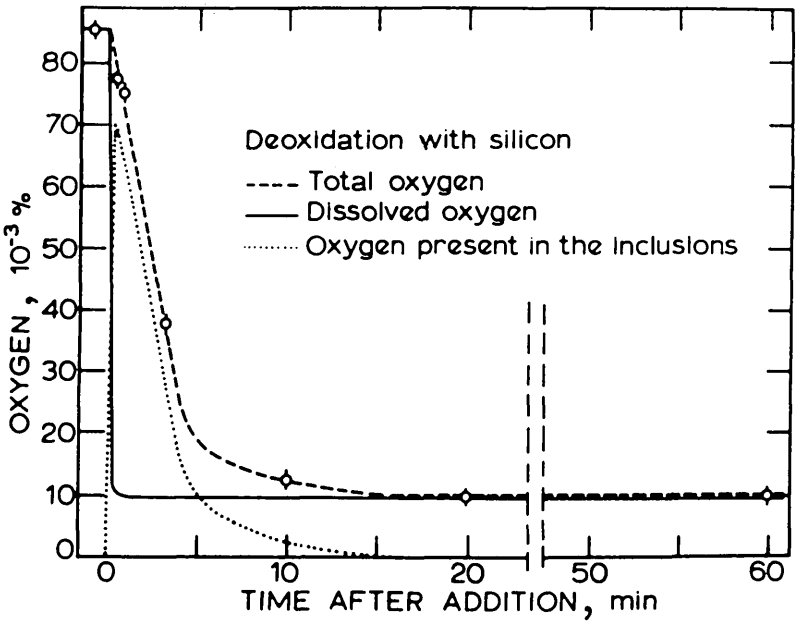

Fig. 2.43

Kinetics of reaction between silicon and dissolved oxygen in liquid iron at 1600°C
(After Gatellier, Torsell and Olette, Refs. 45 and 92)

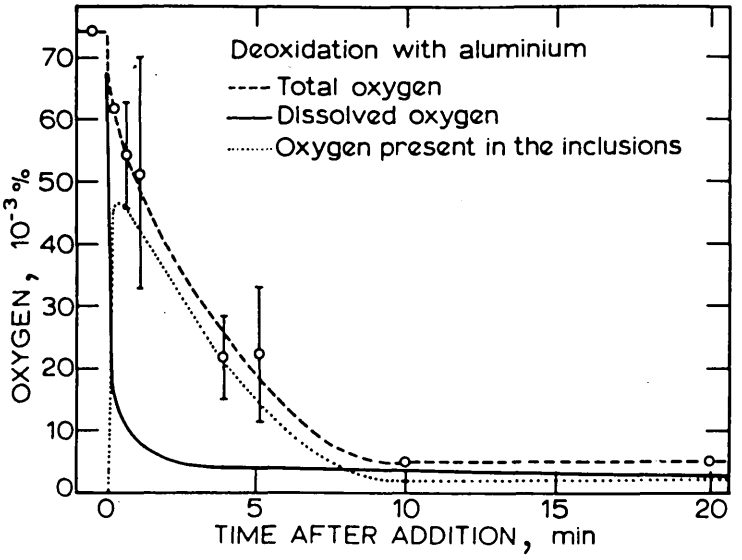

Fig. 2.44

Kinetics of reaction between aluminium and dissolved oxygen in liquid iron at 1600°C
(After Gatellier, Torssell and Olette, Refs. 45 and 92)

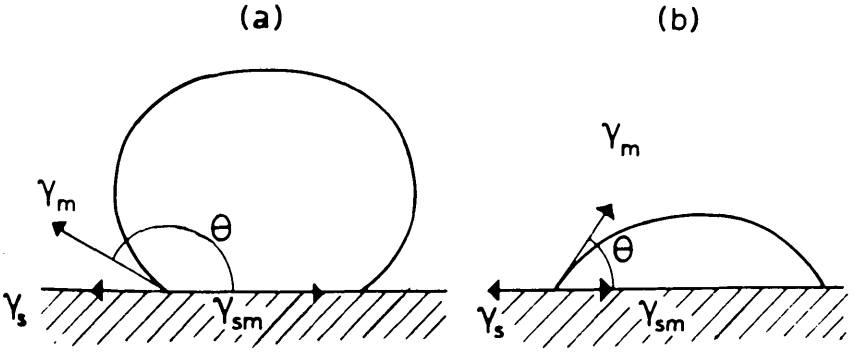

Fig. 2.45

Morphology of a droplet of metal resting on a solid support
(a) no wetting; (b) wetting tendency
(After Kozakevitch and Olette, Ref. 93)

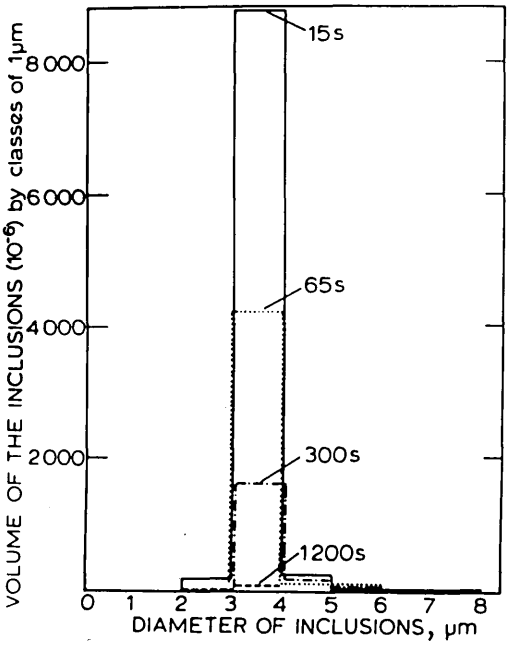

Fig. 2.46

Distribution of number and size of alumina inclusions
following deoxidation of an iron bath by aluminium
(After Gatellier, Torssell and Olette, Refs. 45 and 92)

Fig. 2.47

Scanning electron micrograph of alumina clusters
after etching in bromine-methanol
Mag. x 1600

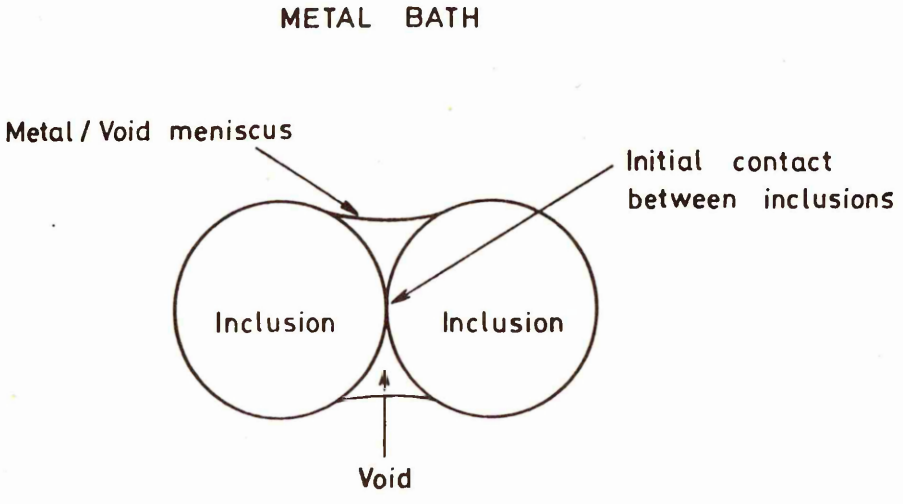

Fig. 2.48

Formation of inclusion agglomerates
(After Knüppel, Brotzmann and Förster, Ref. 58)

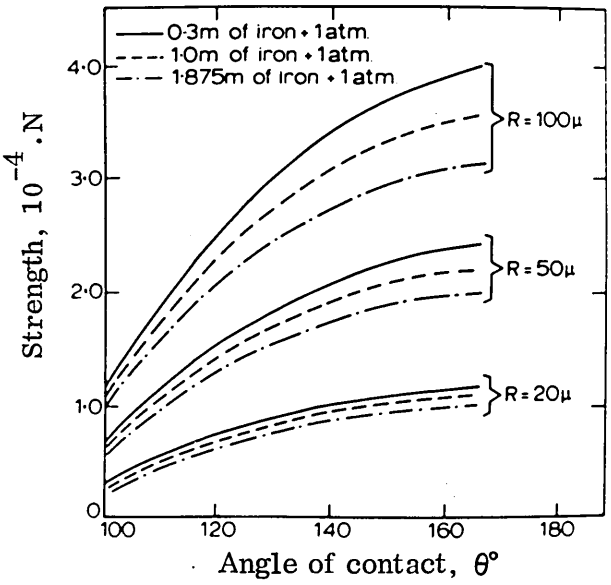

Fig. 2.49

Effect of angle of contact between metal and inclusion, the radius of the particles and the ferrostatic pressure on the strength of agglomeration of two solid particles immersed in liquid steel
(After Baptizmanskii et al, Ref. 99)

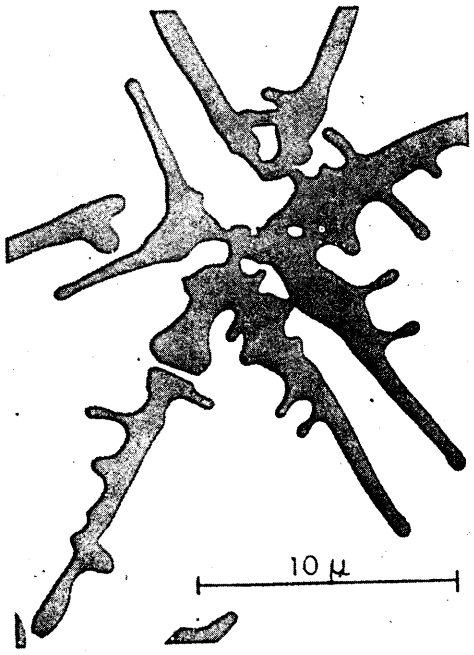

Fig. 2.50

Electron micrograph of a carbon replica of a dendritic alumina cluster
(After Torssell and Olette, Ref. 100)

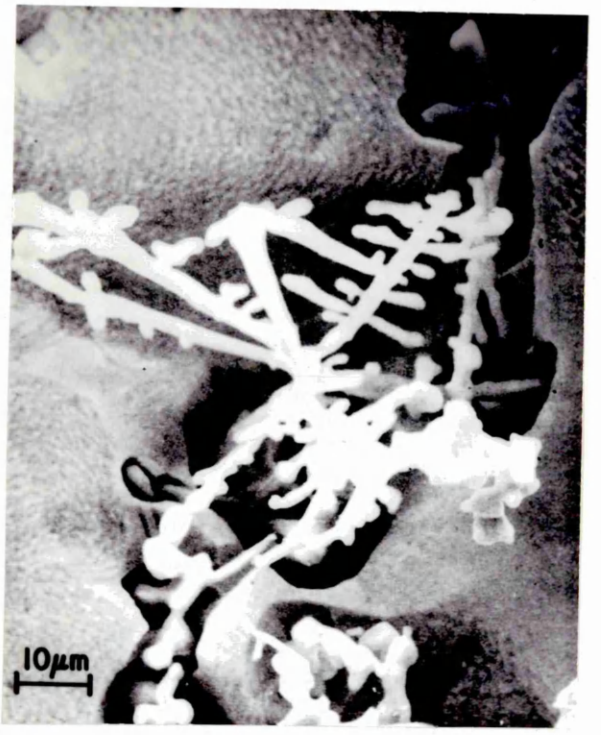

Fig. 2.51

Scanning electron micrograph of alumina clusters in as-cast steel containing 0.05% C, 0.30% Mn, 0.02% Si and 0.06% Al
(After Rege et al, Ref. 101)

Fig. 2.52

Scanning electron micrograph of alumina cluster after etching in bromine-methanol
Mag. x 3900

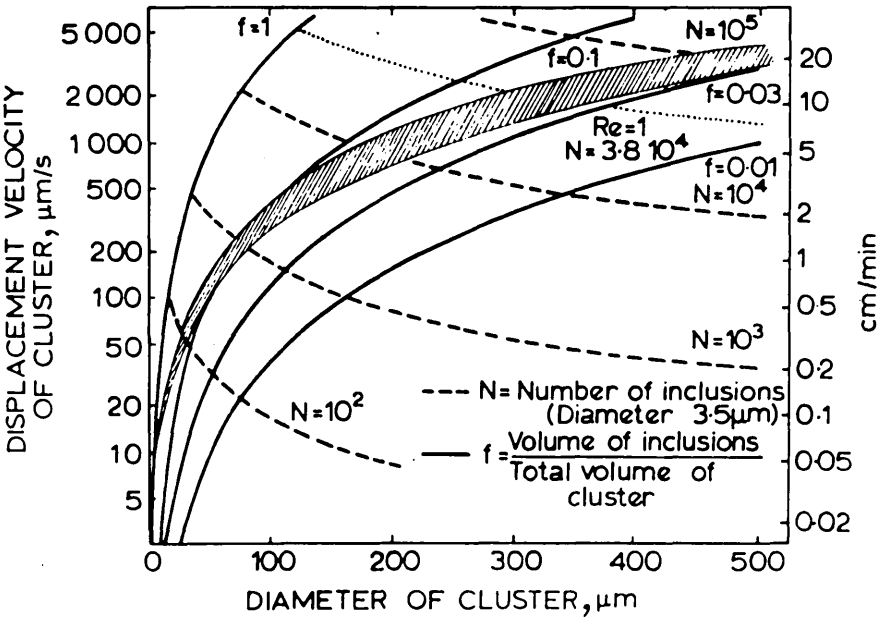

Fig. 2.53

Variation of rate of flotation of clusters of solid inclusions according to Stokes' law, as a function of their mean diameter, for clusters containing different proportions of inclusions
(After Kozakevitch et al, Ref. 93)

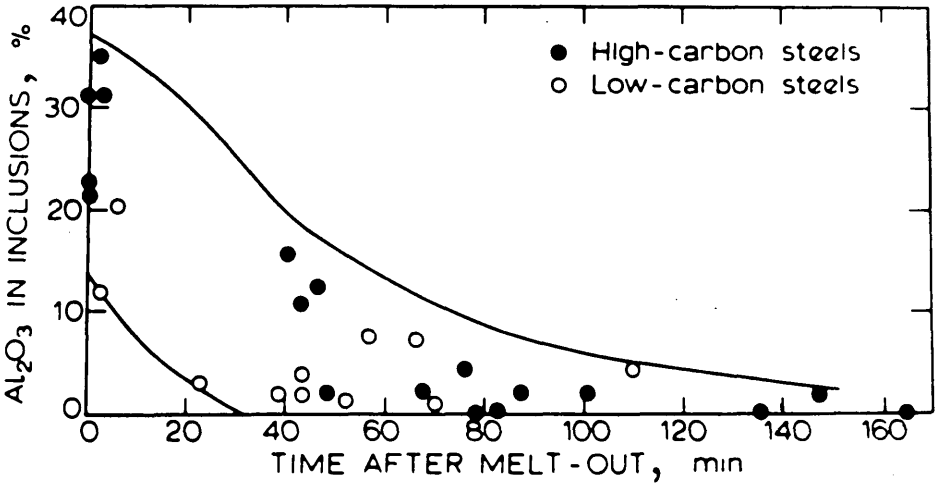

Fig. 2.54

Variation of Al_2O_3 content of inclusions during boil
(After Pickering, Ref. 102)

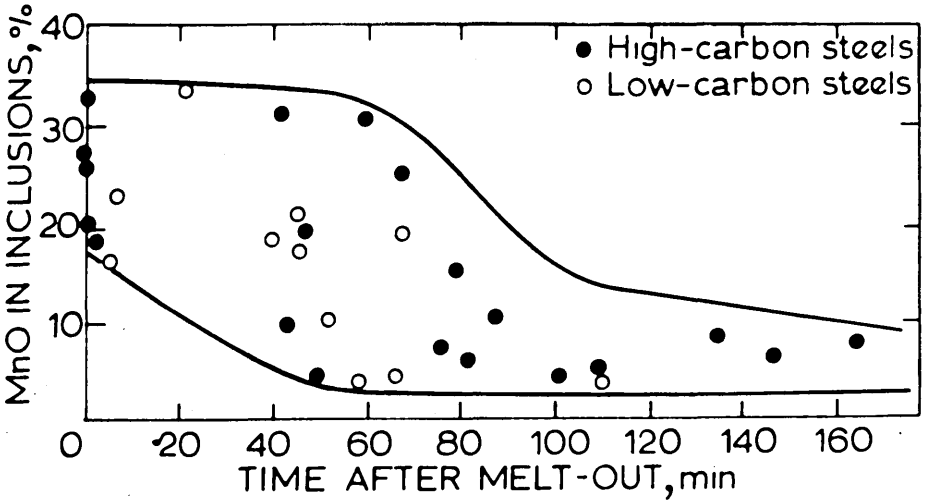

Fig. 2.55

Variation in MnO content of inclusions during boil
(After Pickering, Ref. 102)

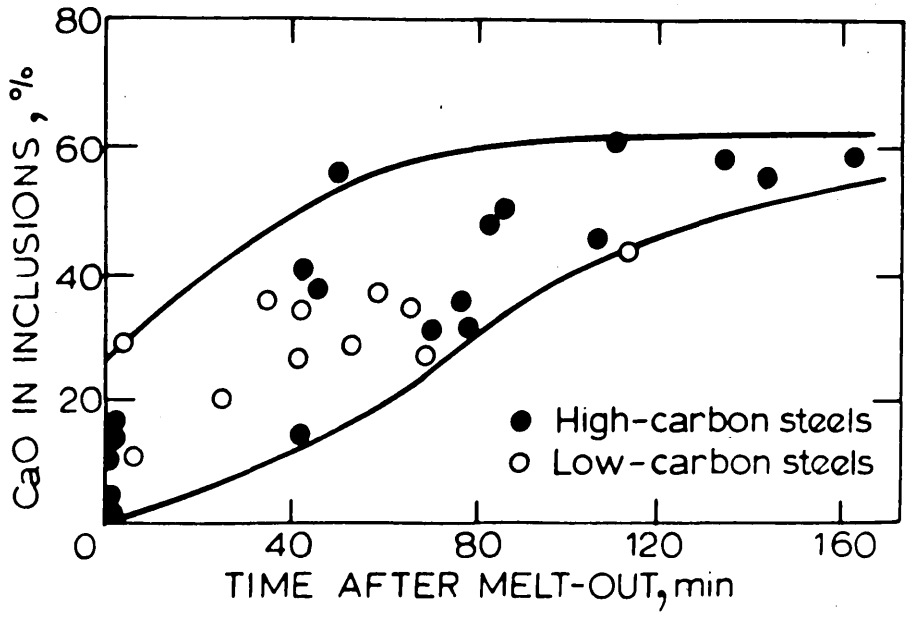

Fig. 2.56

Variation in CaO content of inclusions during boil
(After Pickering, Ref. 102)

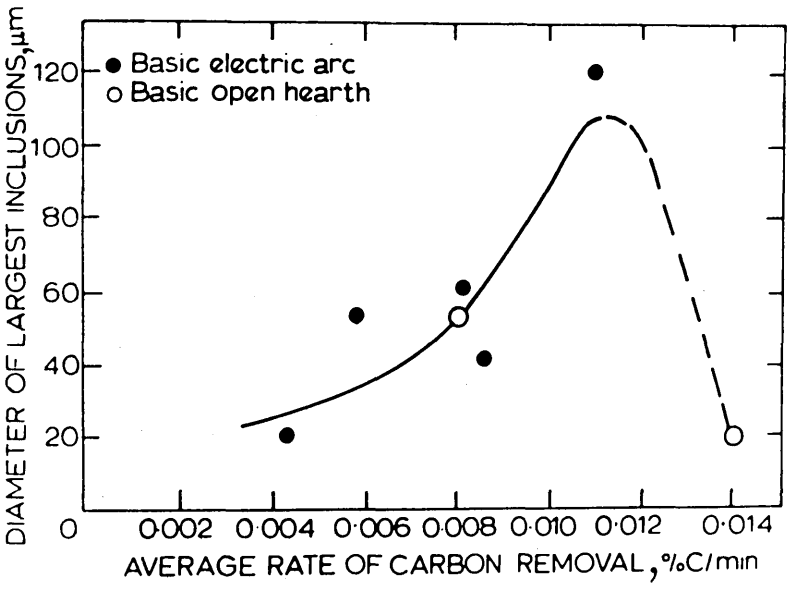

Fig. 2.57

Effect of rate of carbon oxidation on maximum size of inclusions picked up during the boil (After Pickering, Ref. 102)

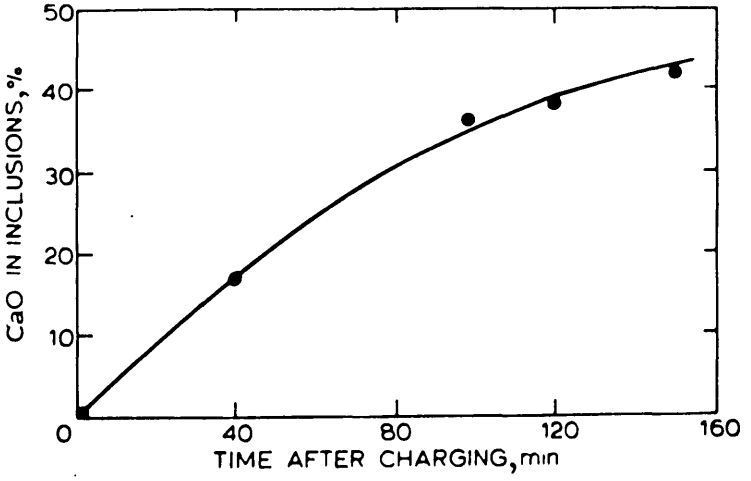

Fig. 2.58

Variation in CaO content of silicates during the boil in basic open-hearth process (After Pickering, Ref. 102)

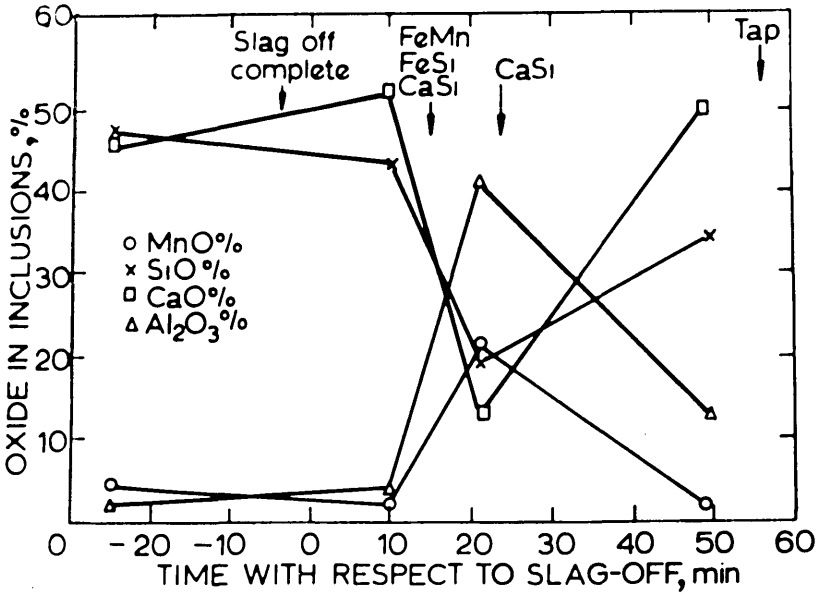

Fig. 2.59

Variation in inclusion composition during reducing period following CaSi additions (After Pickering, Ref. 102)

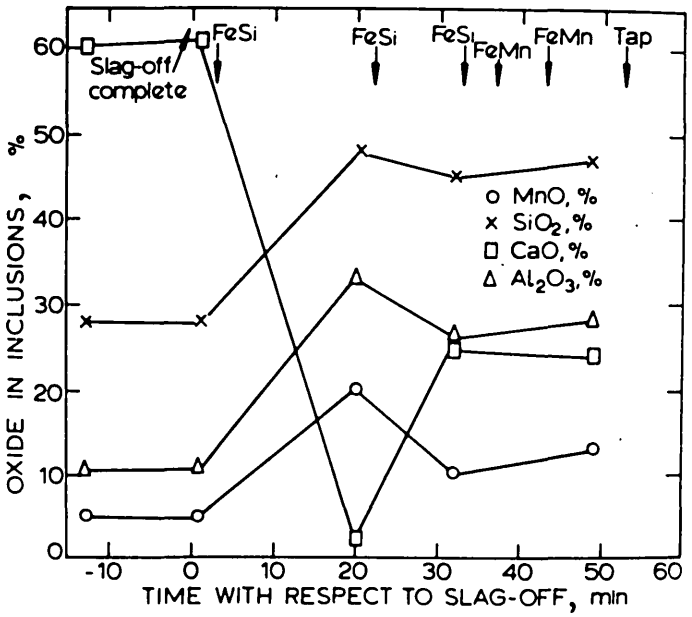

Fig. 2.60

Variation in inclusion composition during reducing period following FeSi additions (After Pickering, Ref. 102)

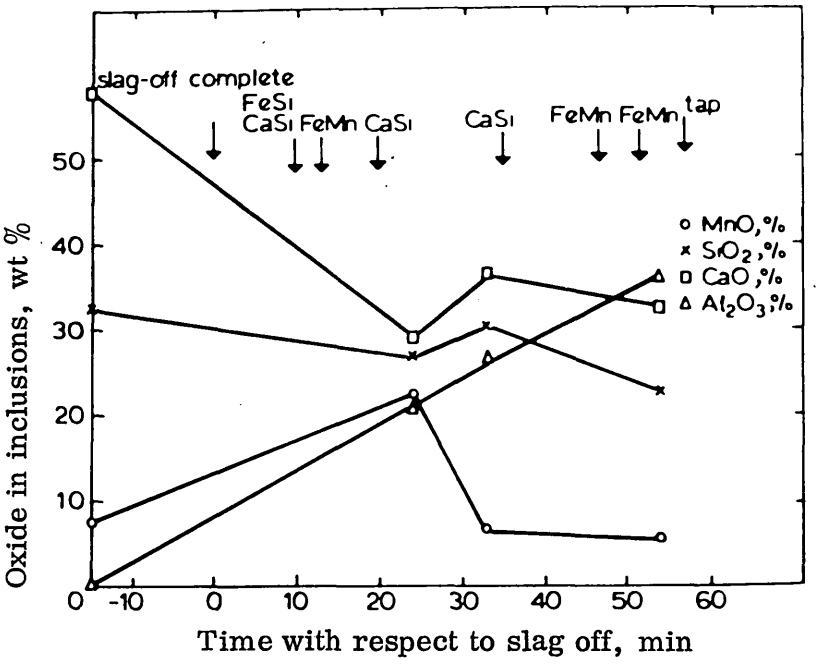

Fig. 2.61

Variation in inclusion composition during reducing period with progressive additions of aluminium-bearing ferro-alloys
(After Pickering, Ref. 102)

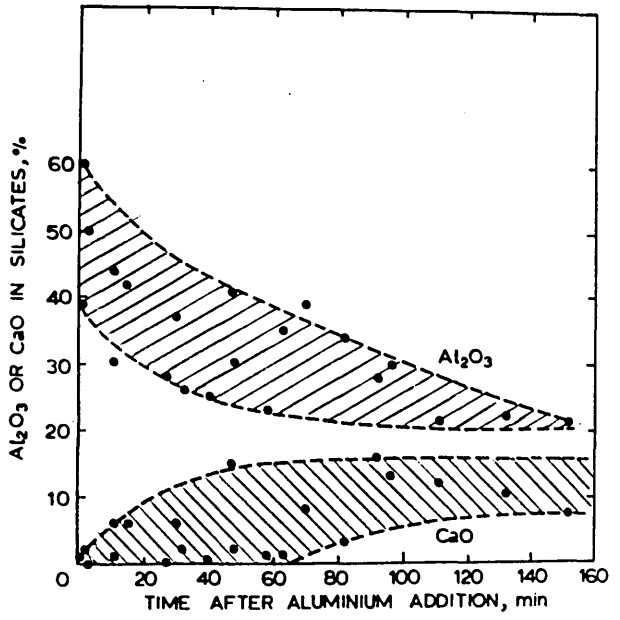

Fig. 2.62

Composition of silicate deoxidation products during refining following the simultaneous addition of aluminium and ferro-silicon
(After Pickering, Ref. 102)

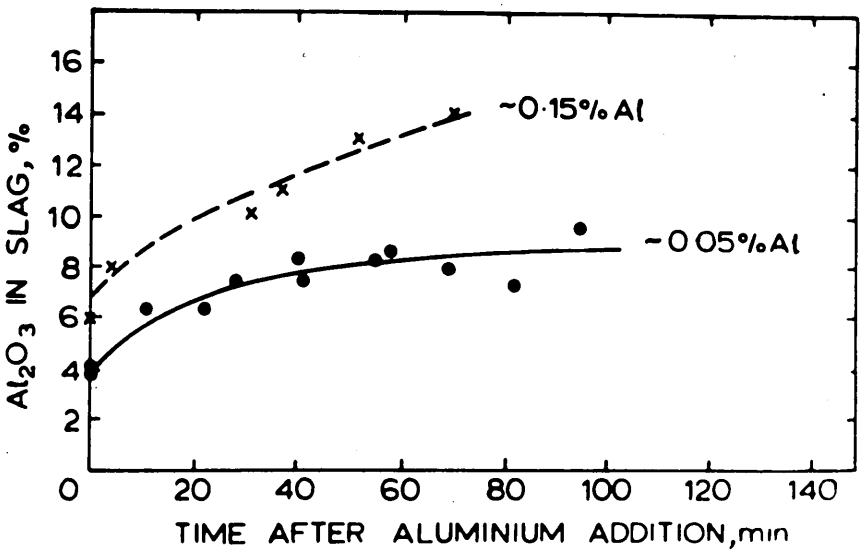

Fig. 2.63

Variation in Al_2O_3 content of slag during refining
(After Pickering, Ref. 102)

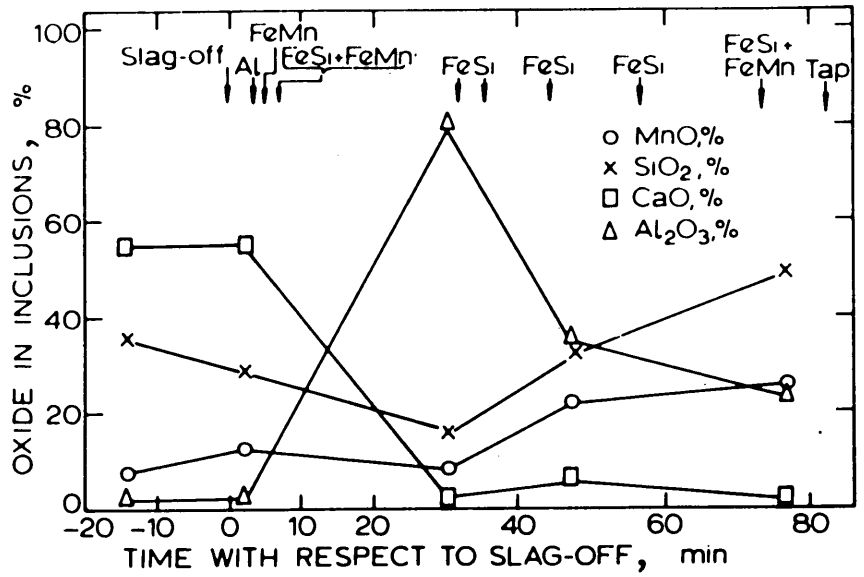

Fig. 2.64

Variation in inclusion composition during reducing period
following a primary aluminium addition
(After Pickering, Ref. 102)

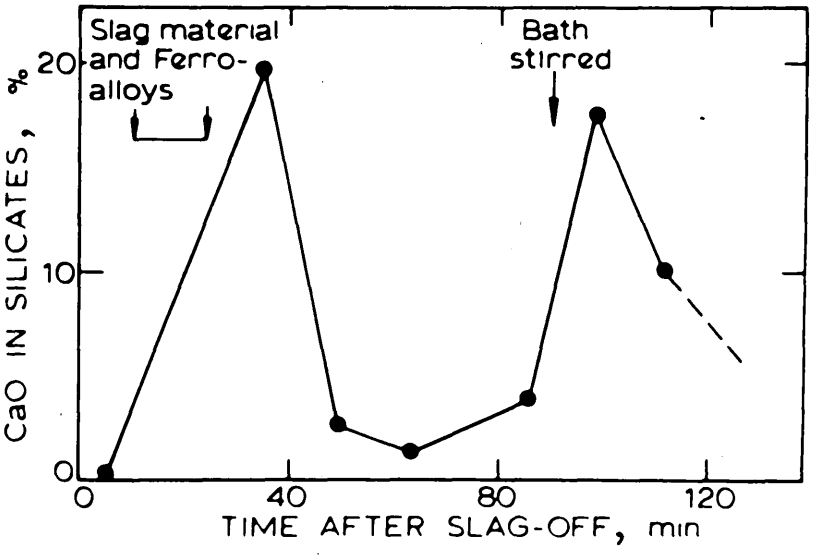

Fig. 2.65

Effect of turbulence during refining period
on CaO content of silicates
(After Pickering, Ref. 102)

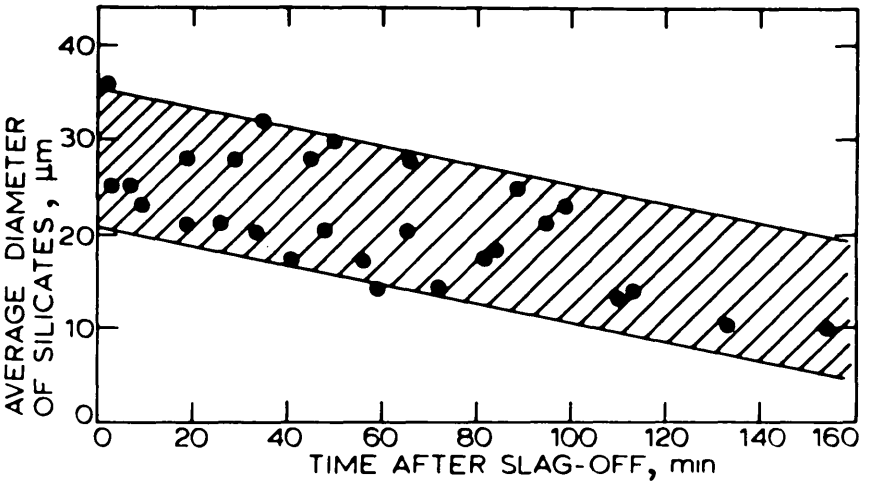

Fig. 2.66

Variation in size of silicate inclusions during refining
(After Pickering, Ref. 102)

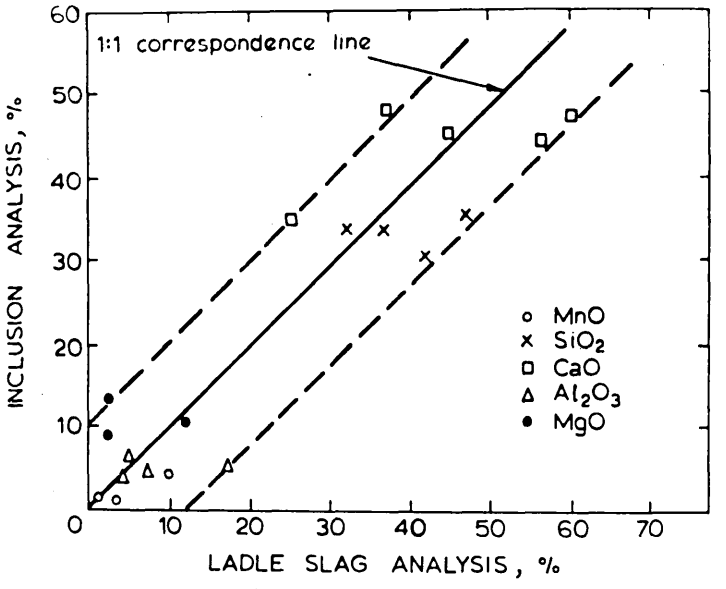

Fig. 2.67

Correspondence between analyses of inclusions in the ladle and the ladle slag analysis
(After Pickering, Ref. 102)

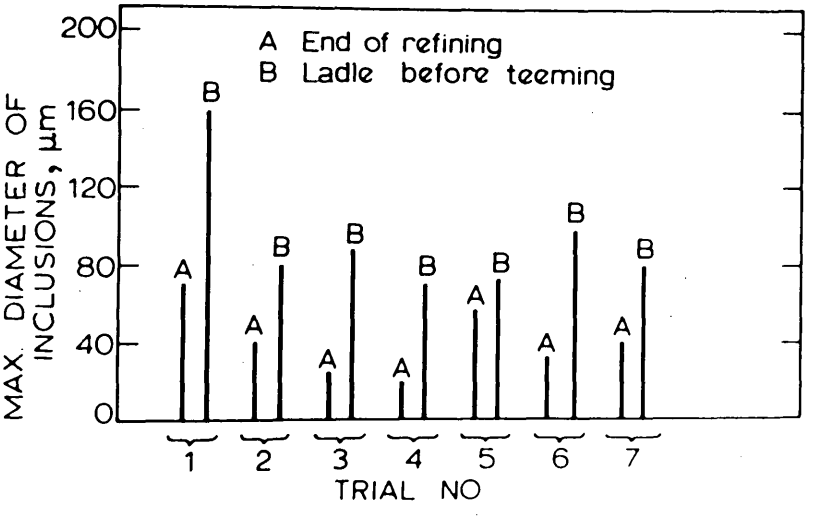

Fig. 2.68

Effect of tapping on maximum size of inclusions
(After Pickering, Ref. 102)

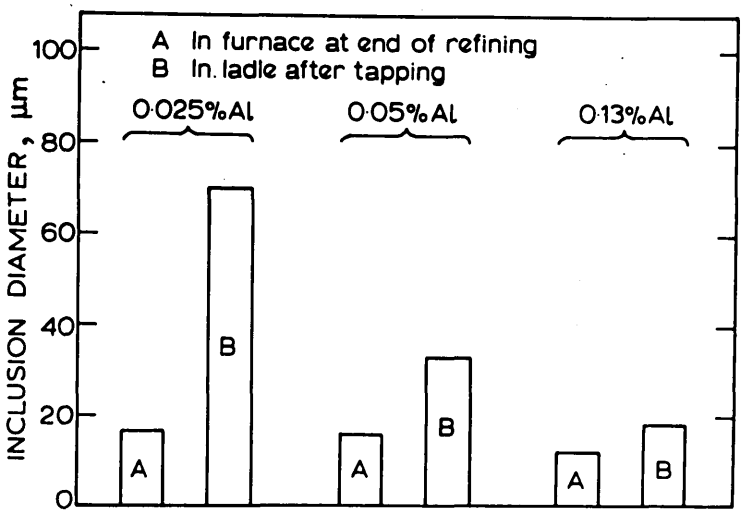

Fig. 2.69

Effect of tapping and of aluminium added to ladle on size of inclusions
(After Pickering, Ref. 102)

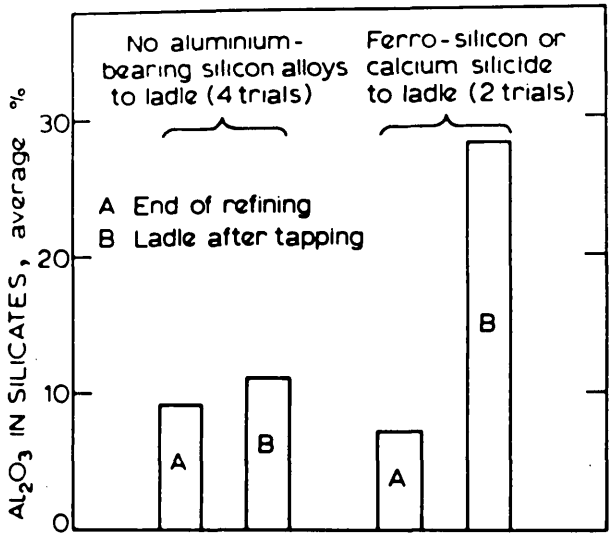

Fig. 2.70

Effect of aluminium-bearing silicon deoxidants added to the ladle on Al_2O_3 content of inclusions
(After Pickering, Ref. 102)

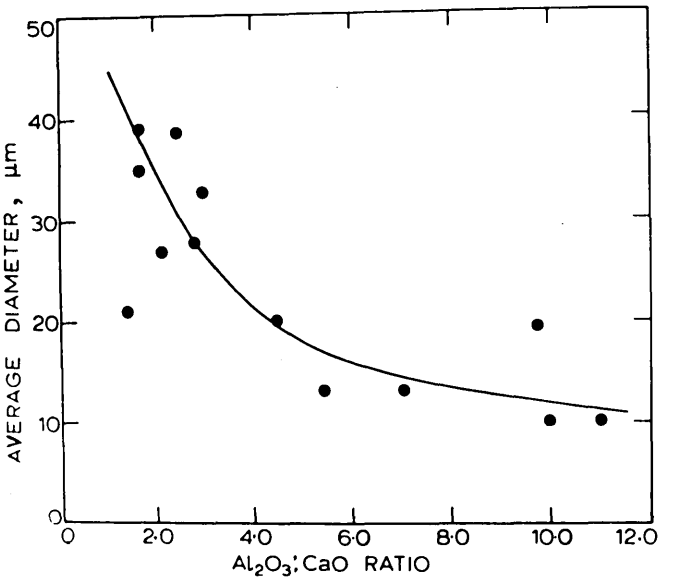

Fig. 2.71

Relationship between size and Al_2O_3 : CaO ratio of calcium aluminates during teeming (After Pickering, Ref. 102)

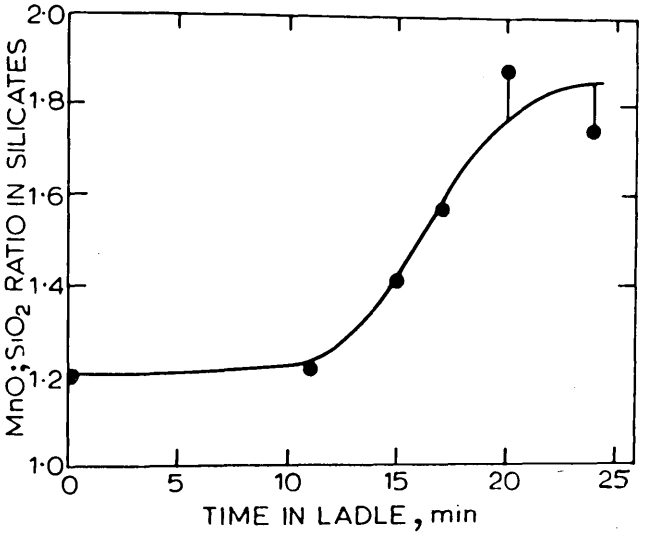

Fig. 2.72

Increase in MnO:SiO_2 ratio of silicates with increasing time in ladle for basic open-hearth steel (After Pickering, Ref. 102)

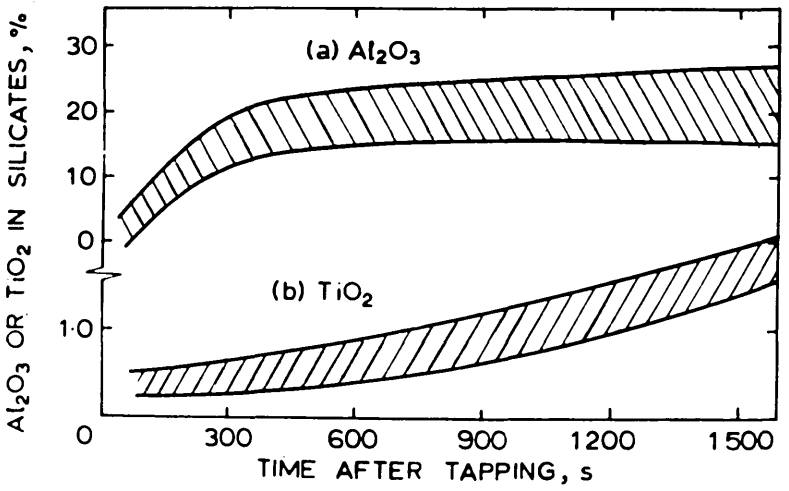

Fig. 2.73

Variation in Al_2O_3 and TiO_2 contents of silicates during teeming
(After Pickering, Ref. 102)

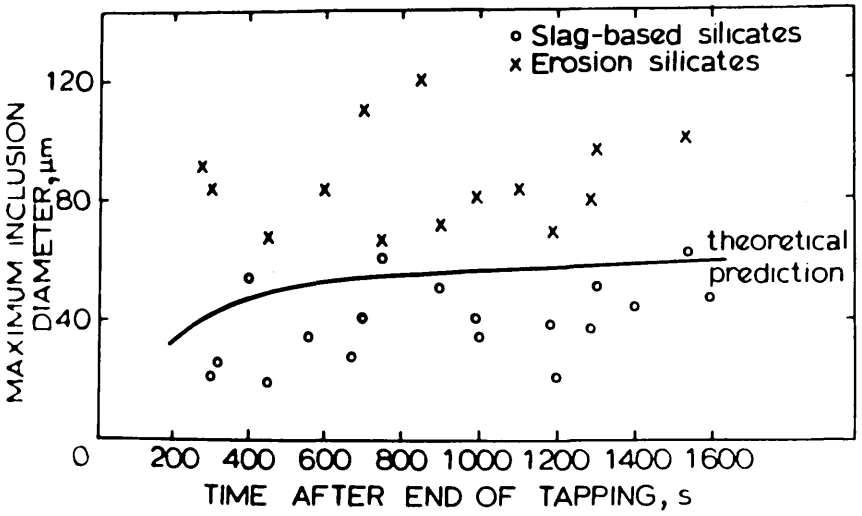

Fig. 2.74

Sizes of inclusions during teeming
(After Pickering, Ref. 102)

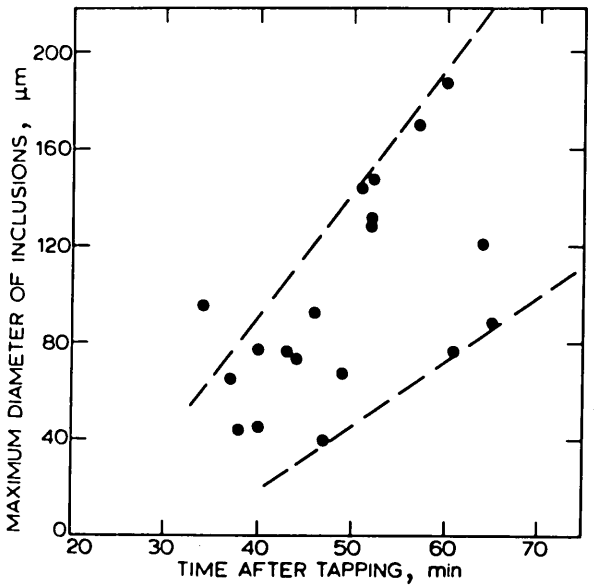

Fig. 2.75

Variation in maximum size of silicate erosion products during teeming
(After Pickering, Ref. 102)

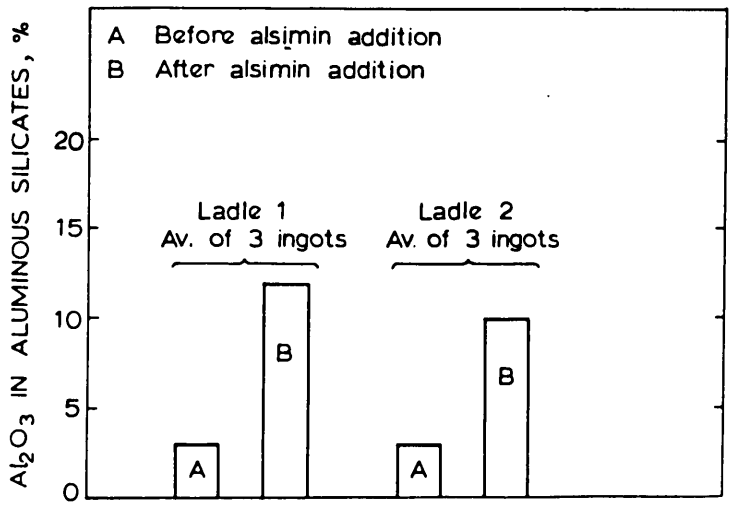

Fig. 2.76

Effect of aluminium-silicon deoxidant added to ingot mould
(After Pickering, Ref. 102)

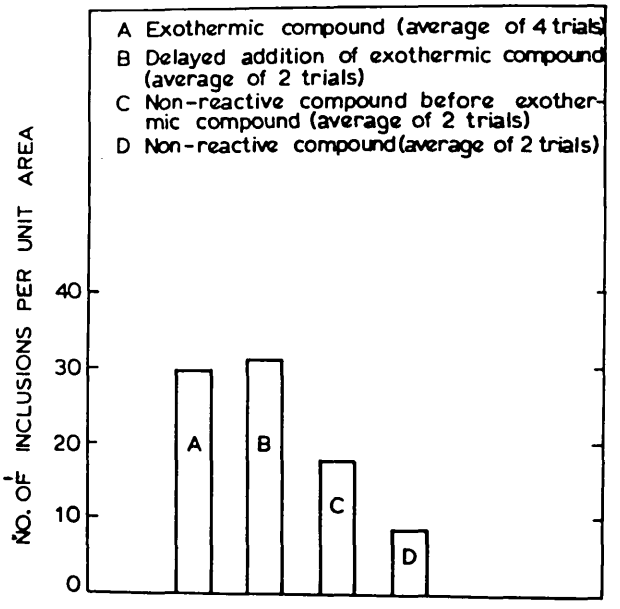

Fig. 2.77

Effect of feeder head compound on occurrence of calcium alumino-silicate inclusions
(After Pickering, Ref. 102)

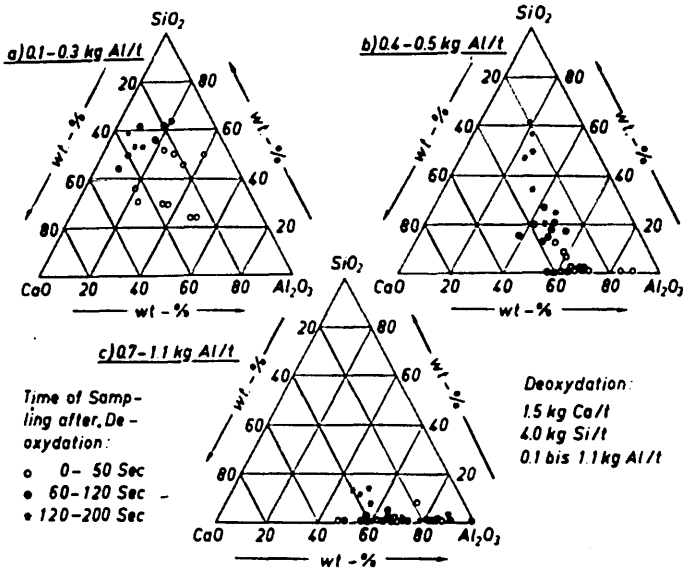

Fig. 2.78

Effect of deoxidation addition on the composition of the primary deoxidation products in the ladle
(After Wahlster et al, Ref. 116)

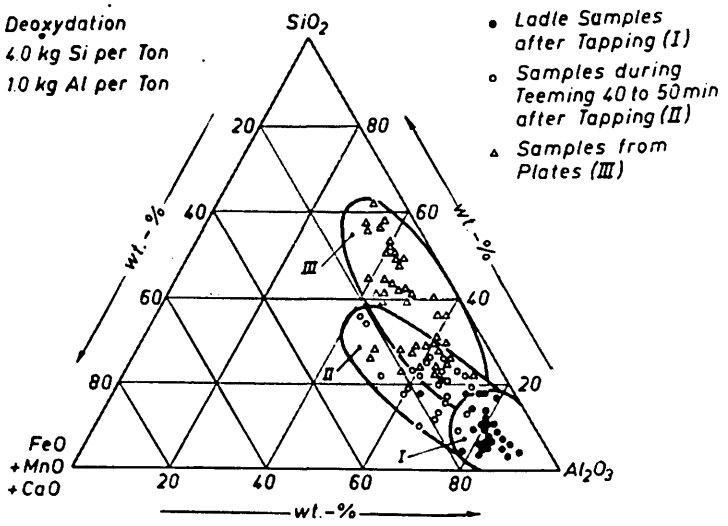

Fig. 2.79

Variation in composition of primary oxide inclusions during teeming
(After Wahlster et al, Ref. 116)

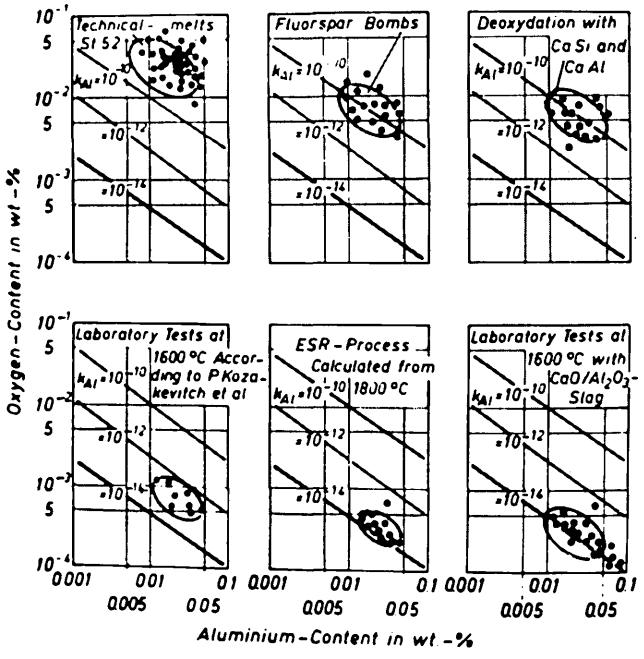

Fig. 2.80

Influence of deoxidation process on the solubility product of aluminium and oxygen, $[\%Al]^2[\%O]^3$
(After Wahlster et al, Ref. 116)

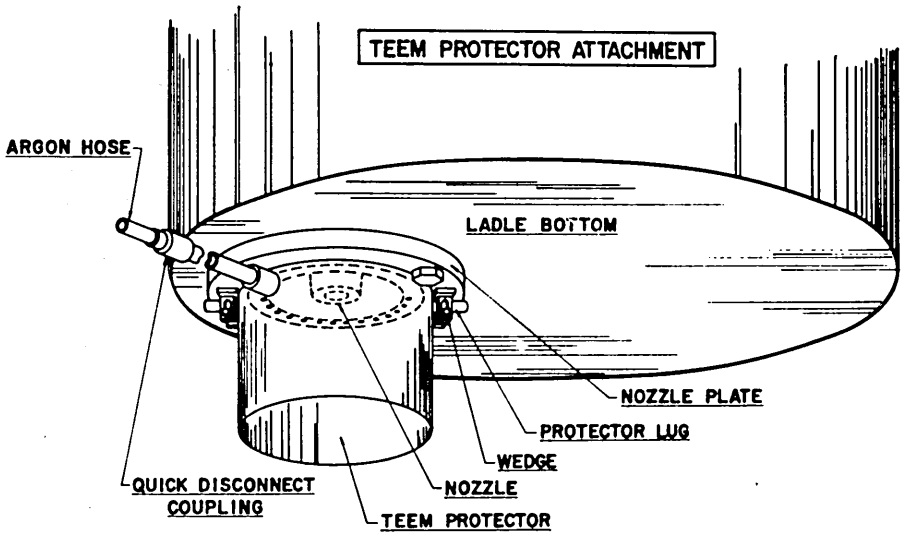

Fig. 2.81

Teeming stream protector for distributing argon around the teeming stream to prevent atmospheric reoxidation
(After Hoffman et al, Ref. 131)

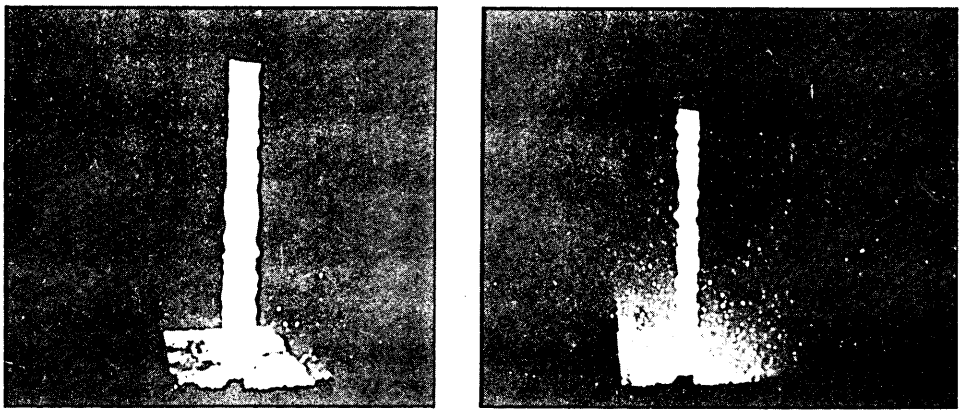

smooth rough

Fig. 2.82

Rough and smooth ladle stream entering a tundish
(After Little et al, Ref. 137)

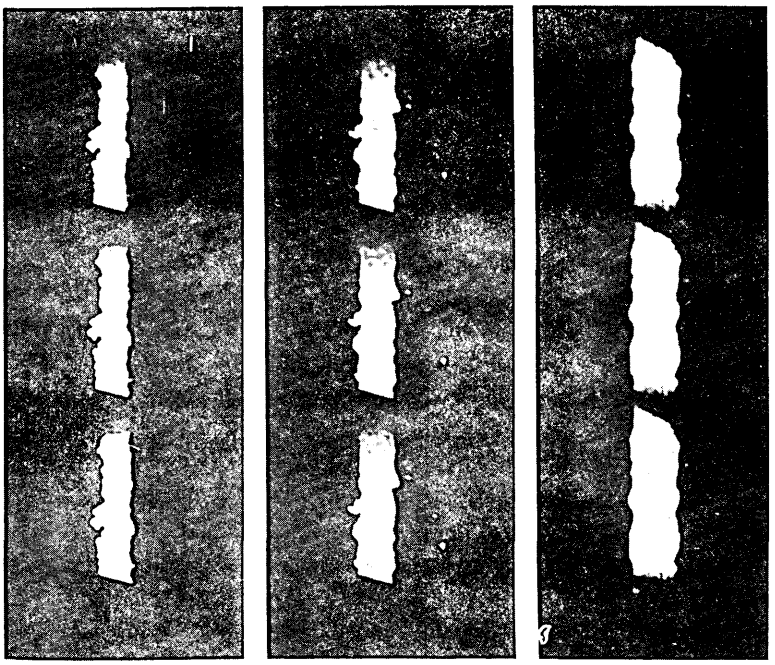

Fig. 2.83

Ladle stream appearance 5, 20 and 35 min (left to right) after start of teem.
Film speed 2000 frames per second
(After Little et al, Ref. 137)

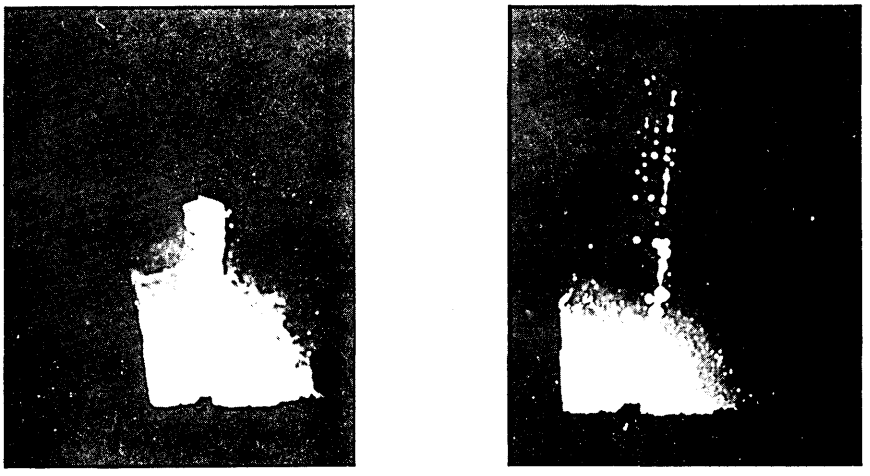

open closed

Fig. 2.84

Ladle stream appearance as stopper rod is lowered at end of a teeming cycle
(After Little et al, Ref. 137)

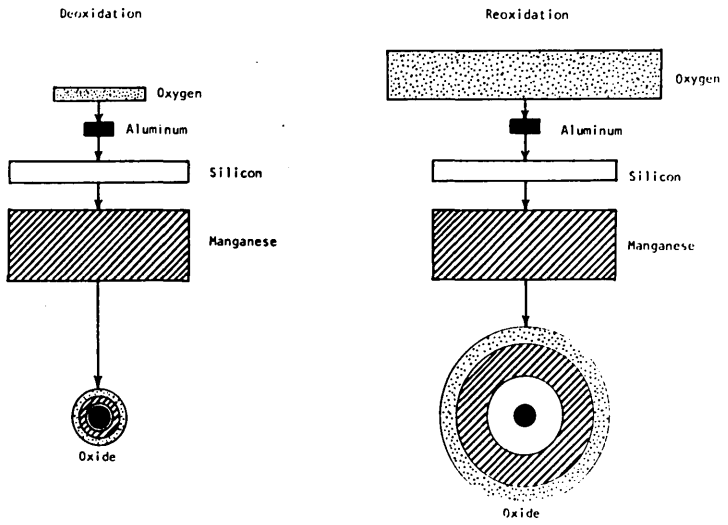

Fig. 2.85

Schematic formation of inclusions in as-cast steel deoxidised with silicon-manganese
(After Farrell et al, Ref. 139)

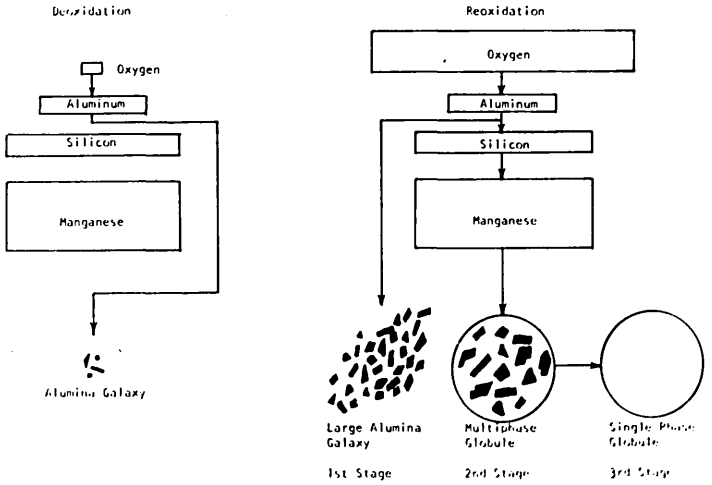

Fig. 2.86

Schematic formation of inclusions in as-cast steel deoxidised with aluminium
(After Farrell et al, Ref. 139)

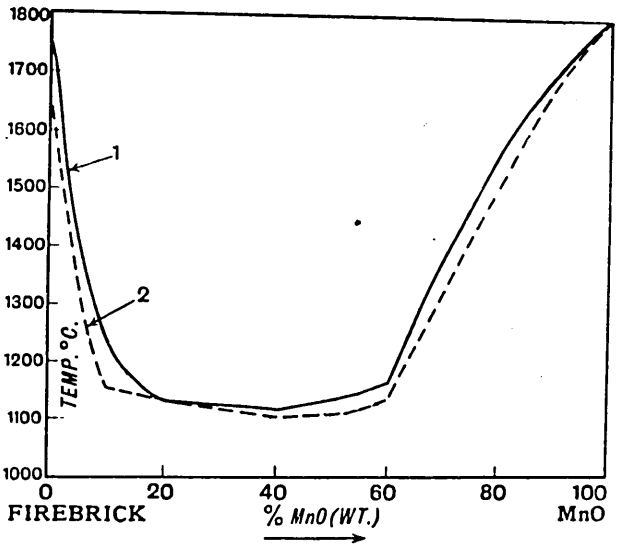

Fig. 2.87

Effect of increasing MnO content on the melting-point of firebrick
(After Rait, Ref. 149)

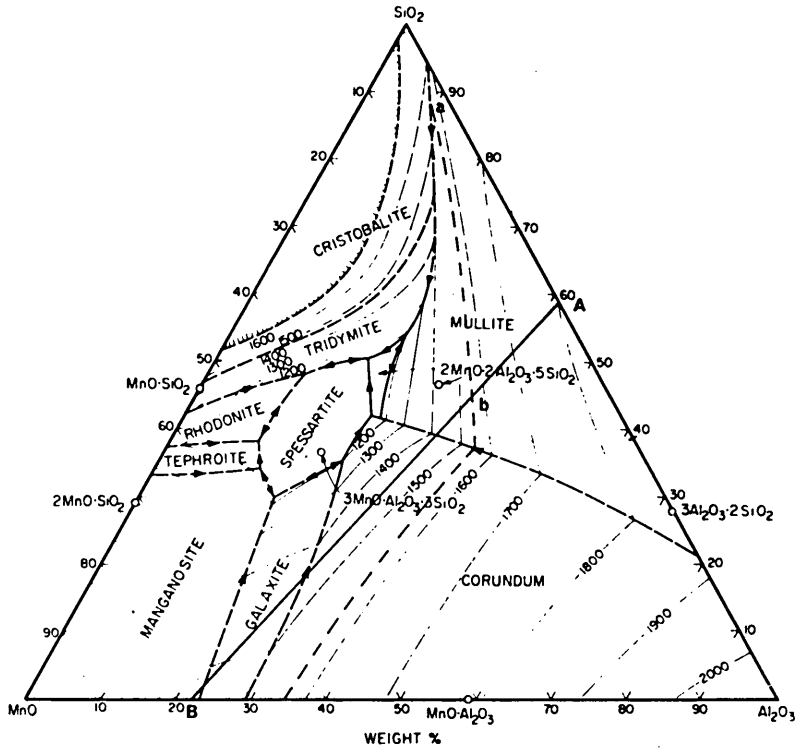

Fig. 2.88

Variation in composition of surface layer of firebrick. A represents initial brick composition, B represents complete conversion of SiO_2 to MnO
(After Stephenson et al, Ref. 156)

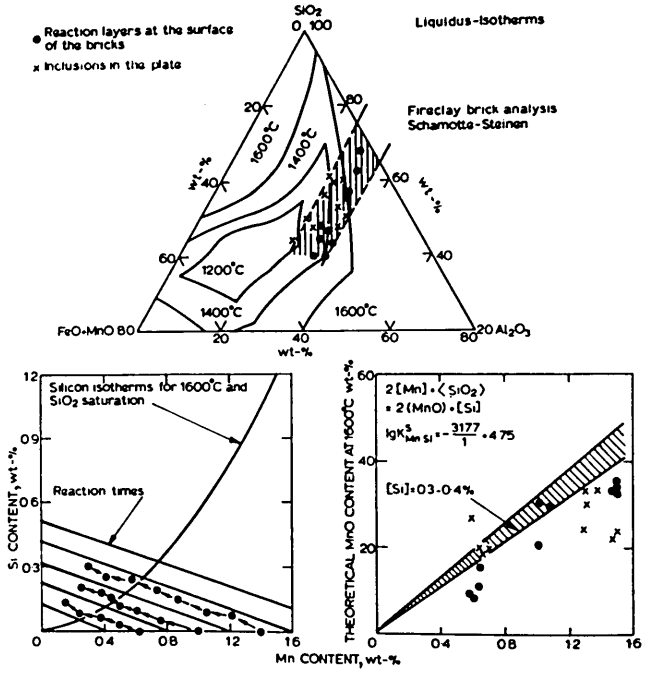

Fig. 2.89

Exogenous inclusion formation owing to manganese attack of fireclay bricks
(After Wahlster et al, Refs. 116, 117, 157)

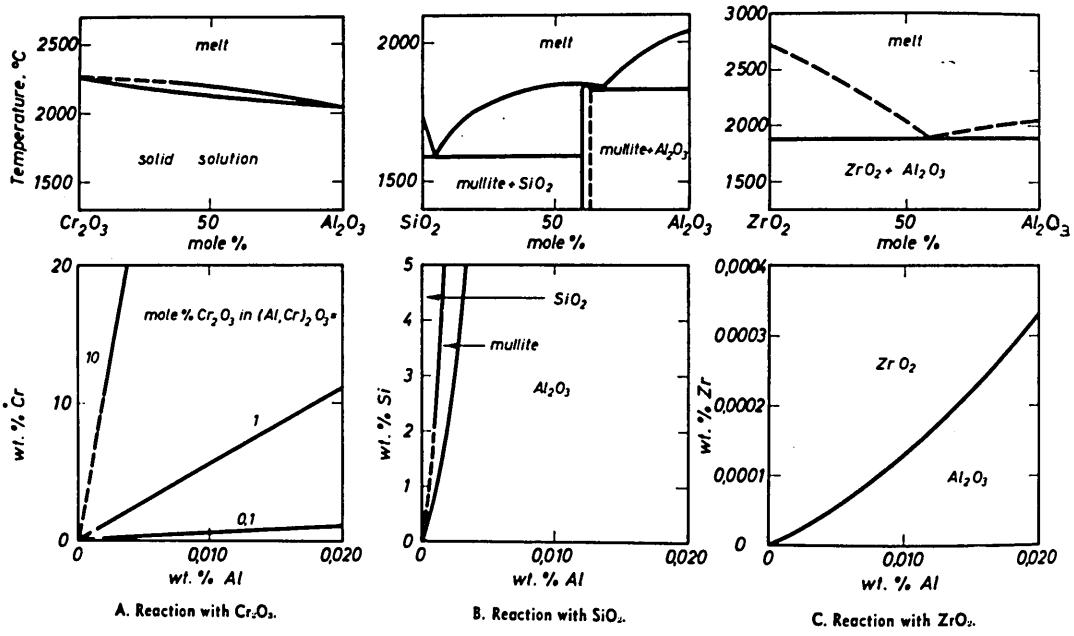

Fig. 2.90

Chemical equilibria between aluminium-deoxidised steel and refractory oxides at 1550°C
(After Schwerdtfeger and Schrewe, Ref. 159)

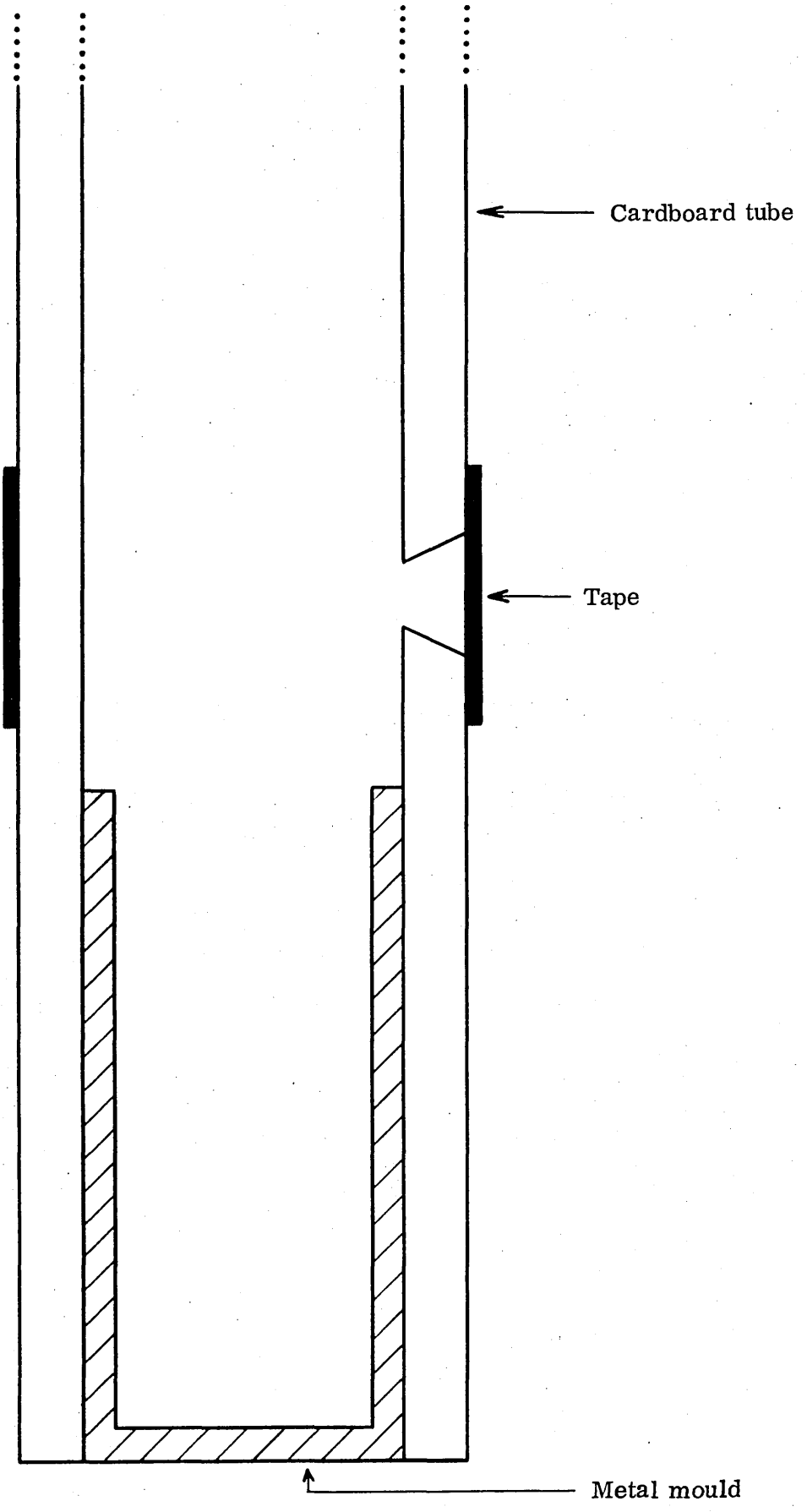

Fig. 3.1

Sampling device (not to scale)

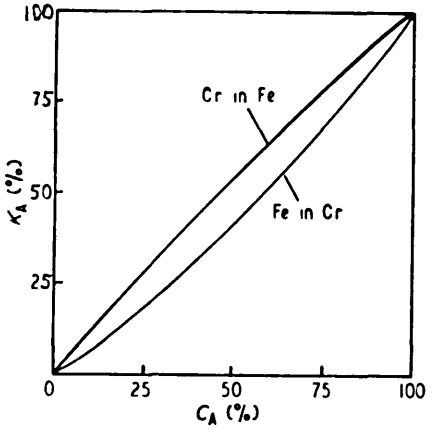

Fig. 3.2

The binary system Cr-Fe for a 20° take-off angle and a 25 kV operating voltage (After Salter, ref. 167)

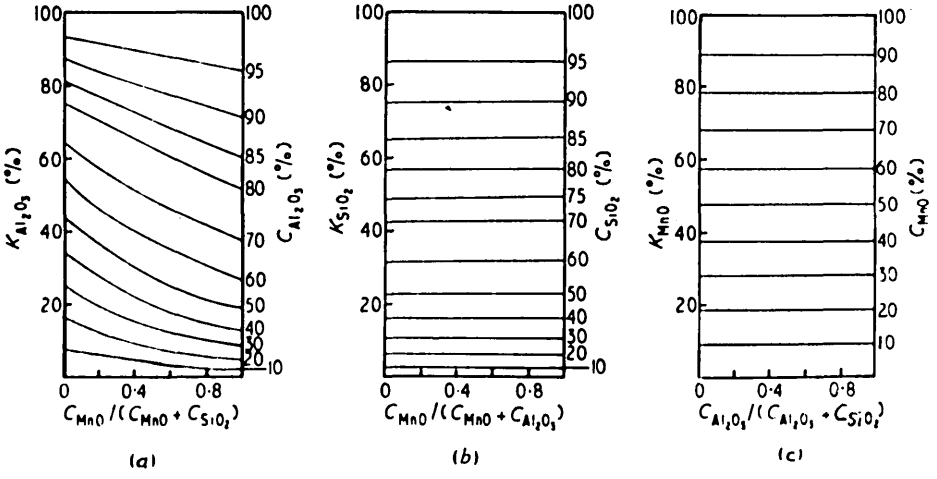

Fig. 3.3

Ternary correction curves for Al_2O_3-SiO_2-MnO
(a) Al_2O_3 in (MnO + SiO_2)
(b) SiO_2 in (MnO + Al_2O_3)
(c) MnO in (SiO_2 + Al_2O_3)
Take-off angle 20°; operating voltage 25 kV (After Salter, ref. 167)

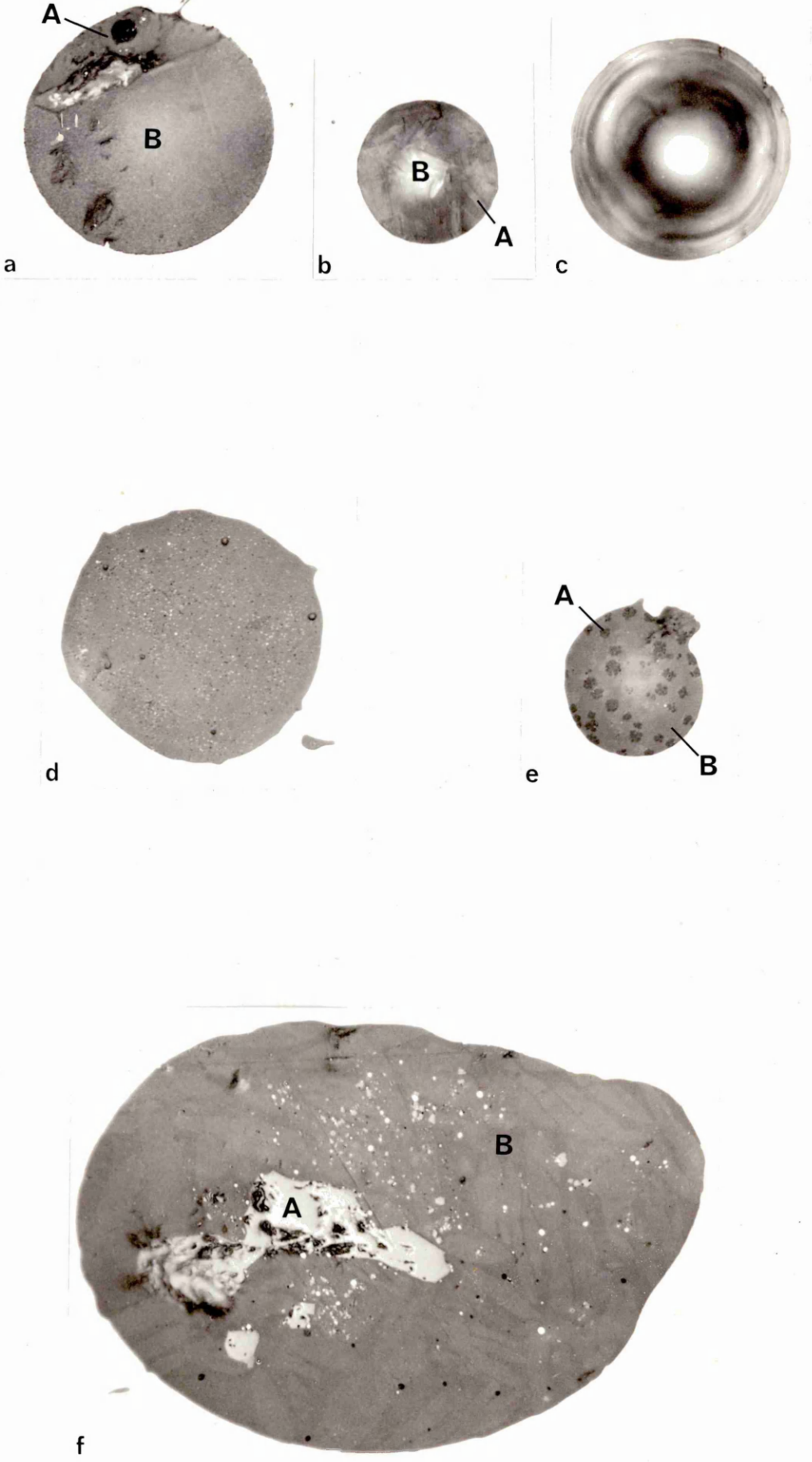

Fig. 4.3

Trial cast A.1 - Inclusions present in ladle during vacuum degassing x 750

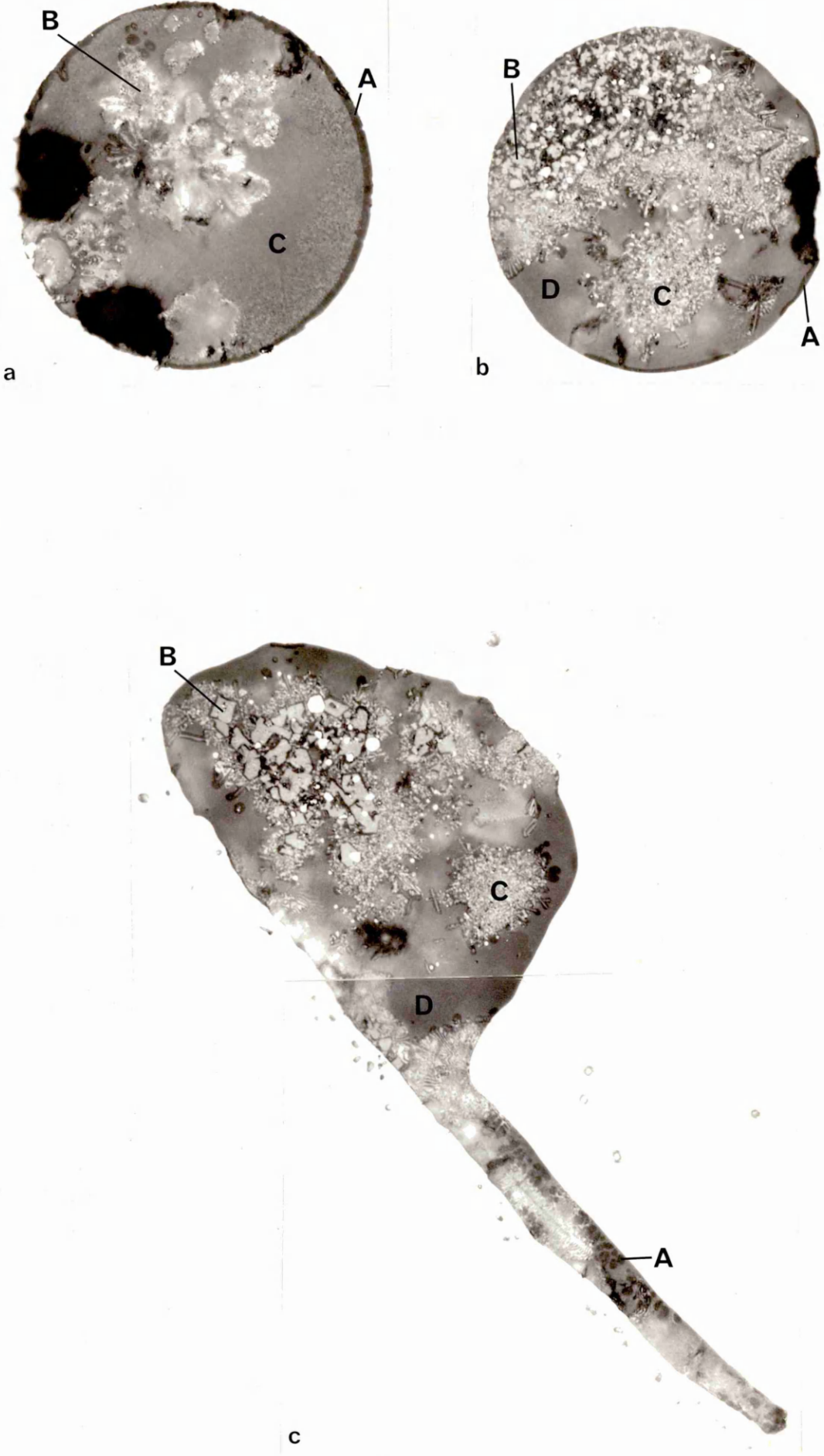

Fig. 4.4

Trial cast A.1 - Inclusions present in ladle stream during teeming x 750

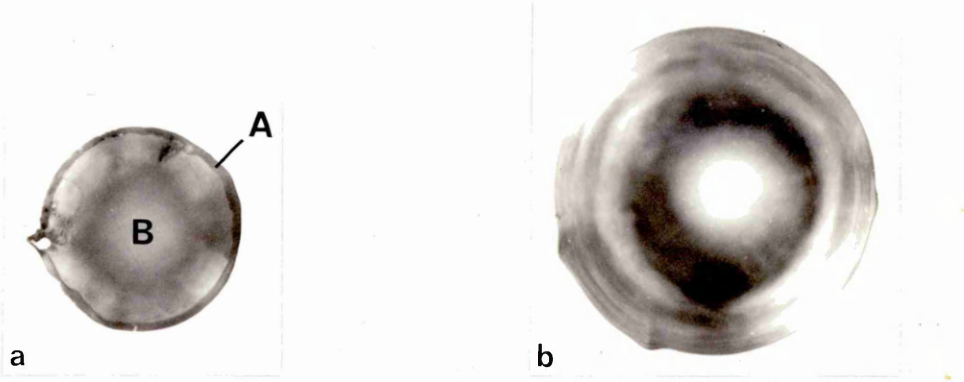

Fig. 4.5

Trial cast A.1 - Inclusions present in ladle stream during teeming x 750

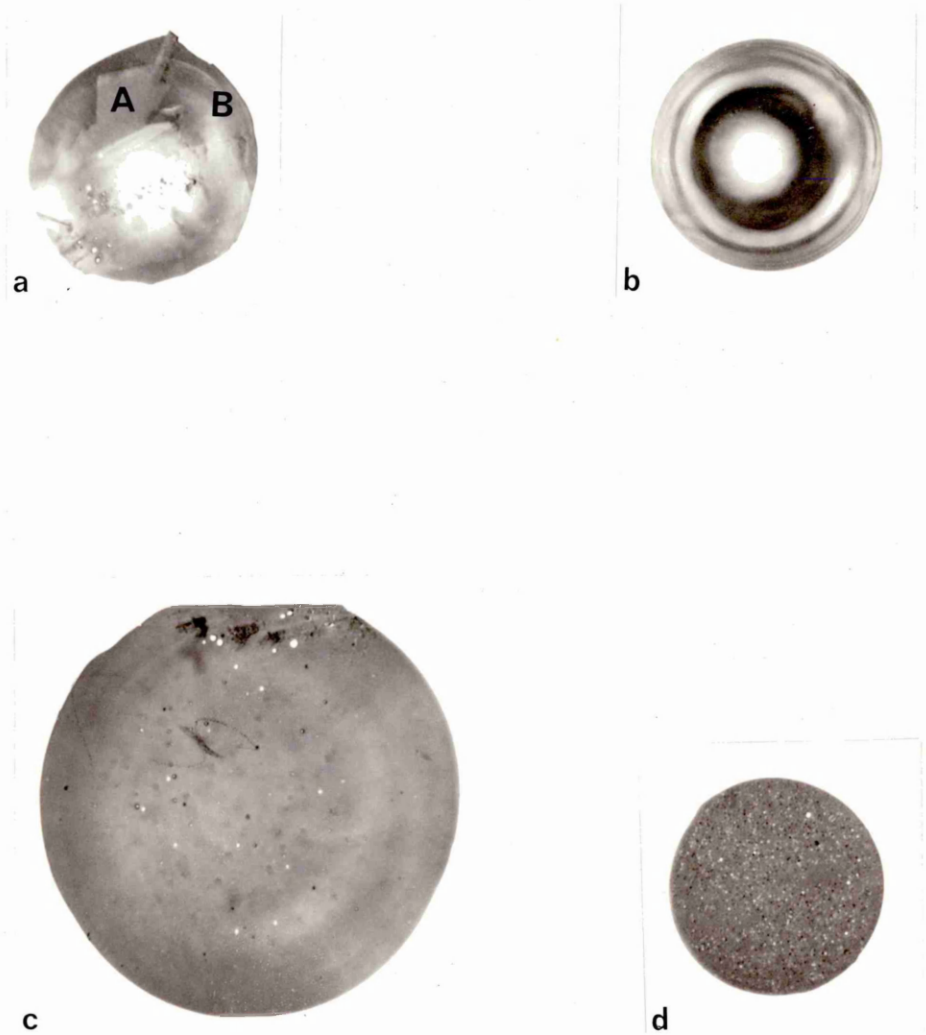

Fig. 4.6

Trial cast A.1 - Inclusions present in ingots during teeming x 750

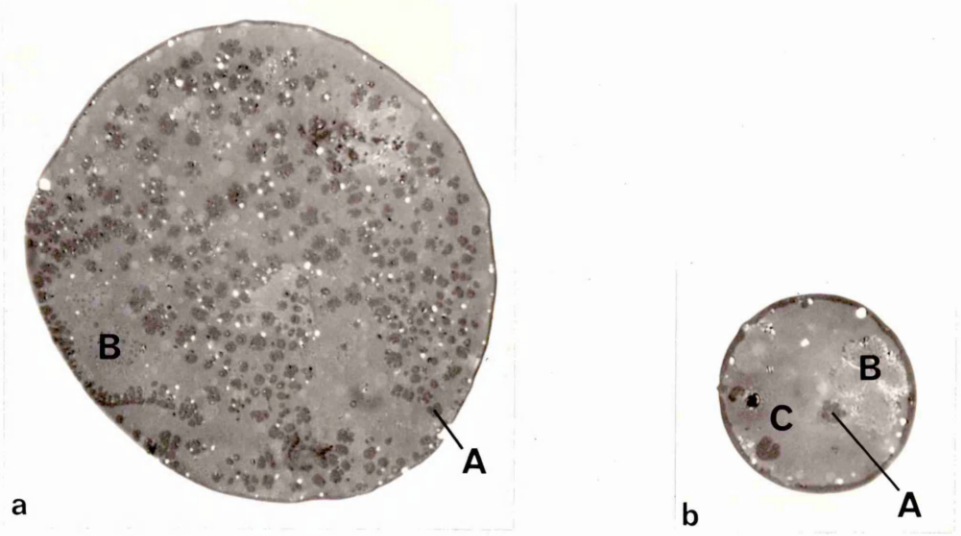

Fig. 4.7

Trial cast A.1 - Inclusions present in ingots during teeming x 750

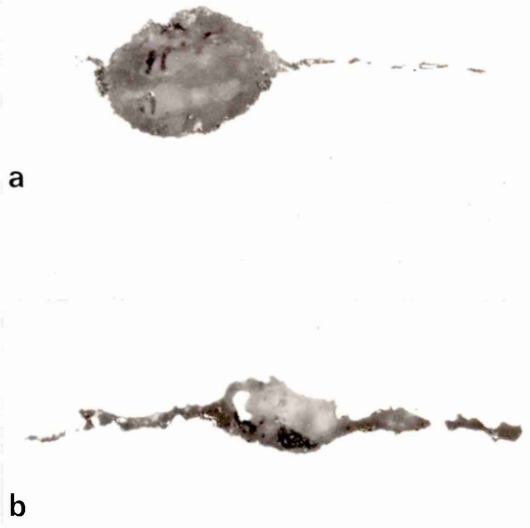

Fig. 4.8

Trial cast A.1 - Inclusions present in billets x 750

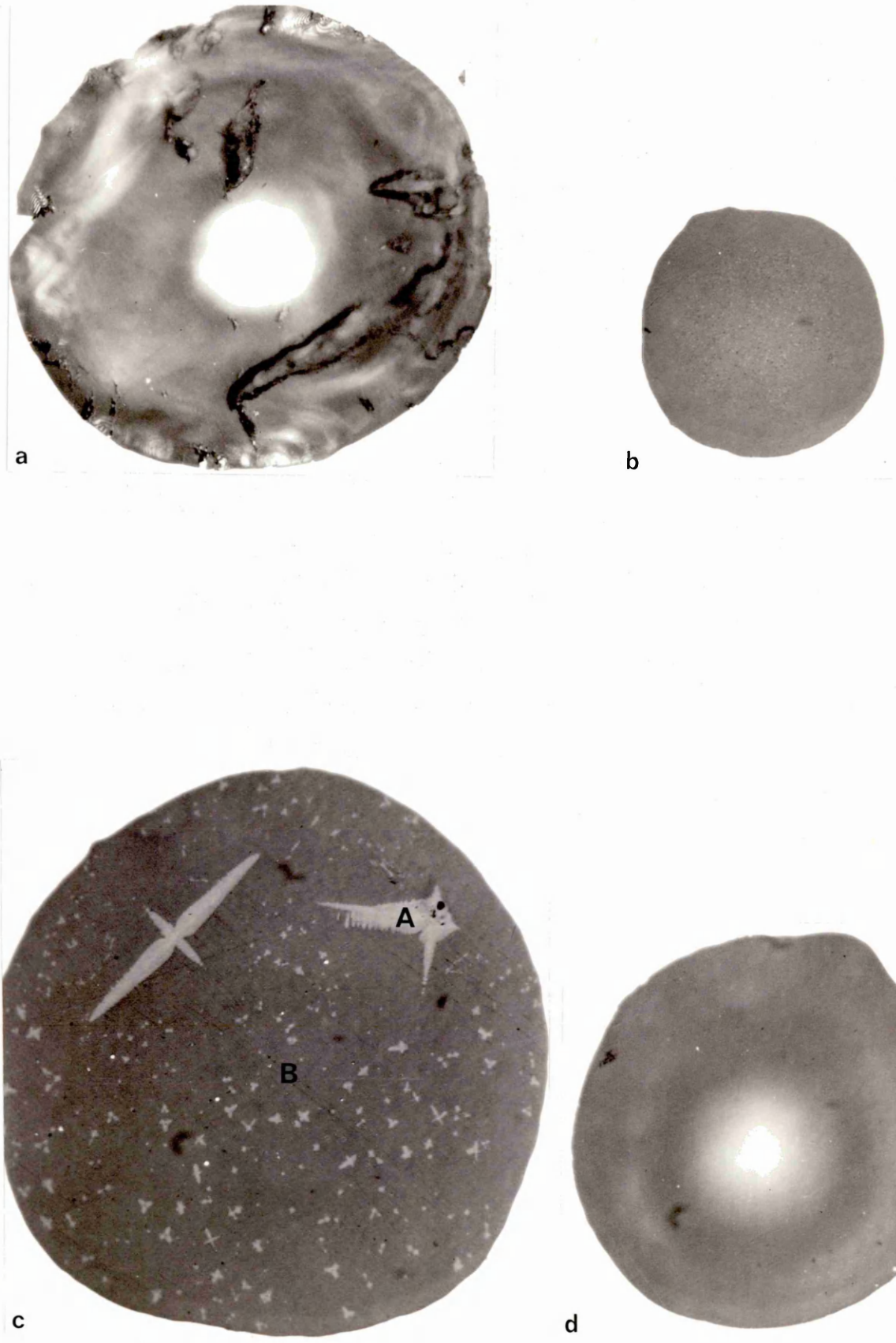

Fig. 4.9

Trial cast B.1 - Inclusions present in furnace during steelmaking x 750

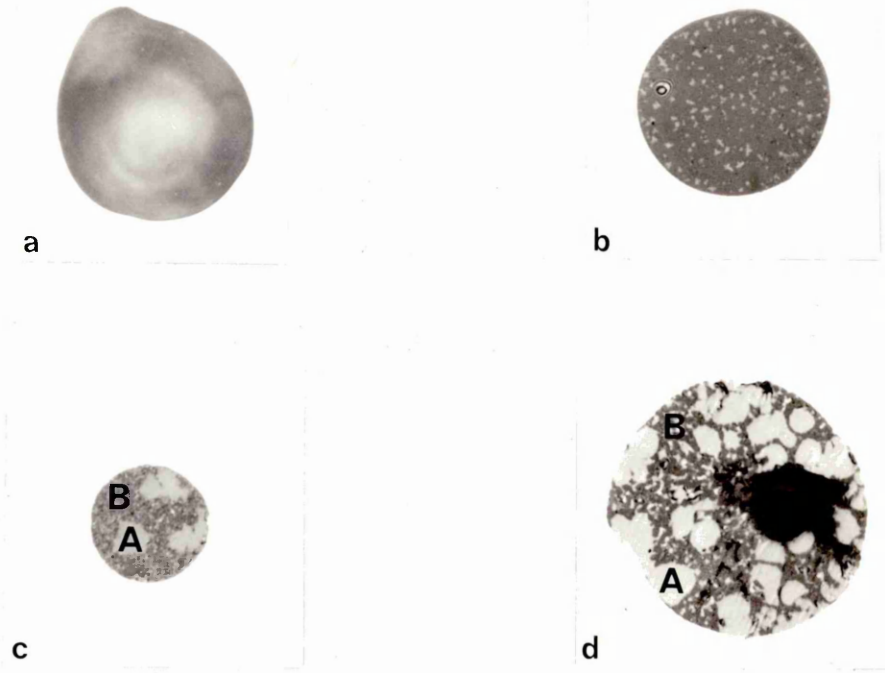

Fig. 4.10

Trial cast B.1 - Inclusions present in furnace during steelmaking x 750

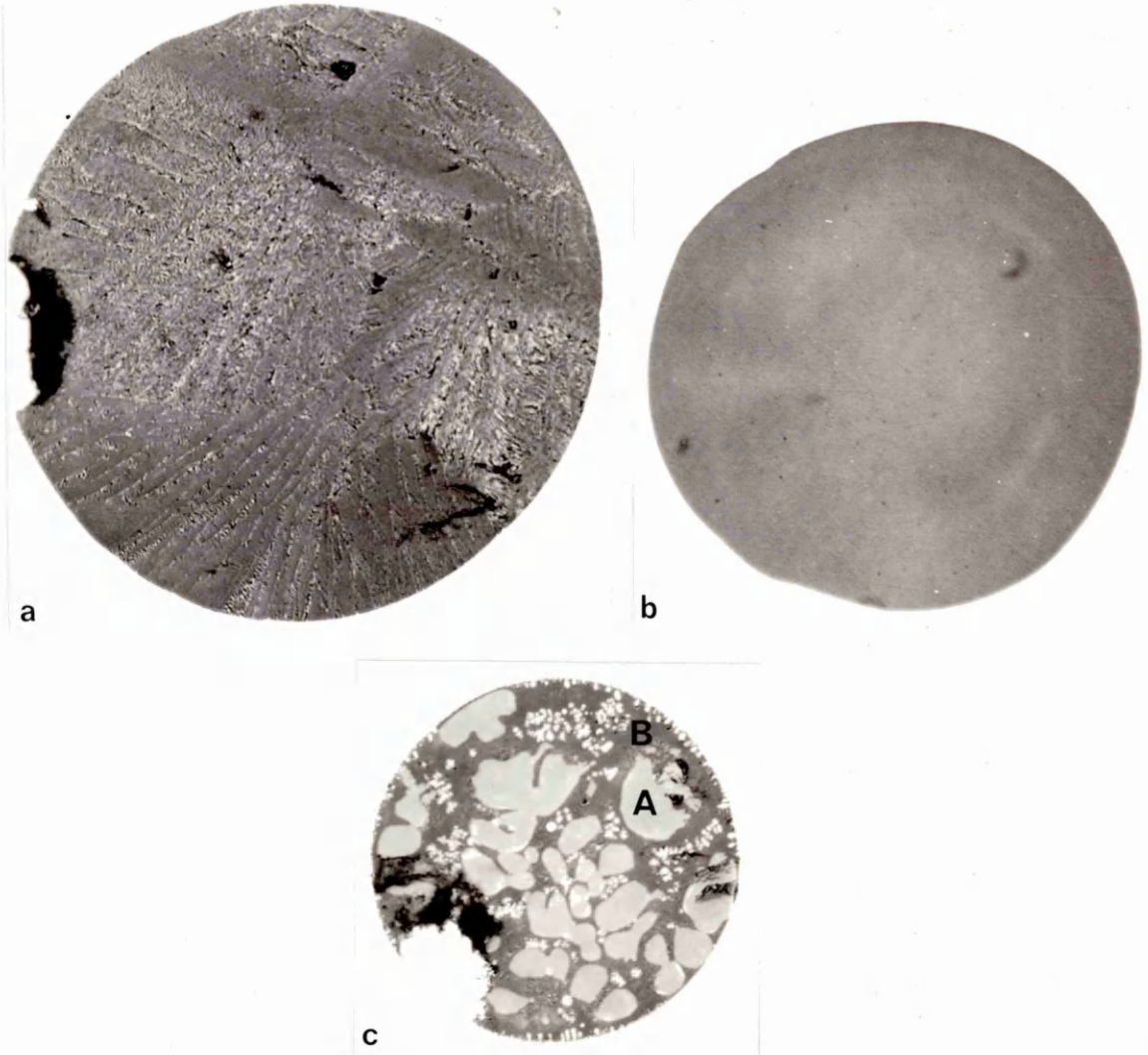

Fig. 4.11

Trial cast B.1 - Inclusions present in ladle after tapping x 750

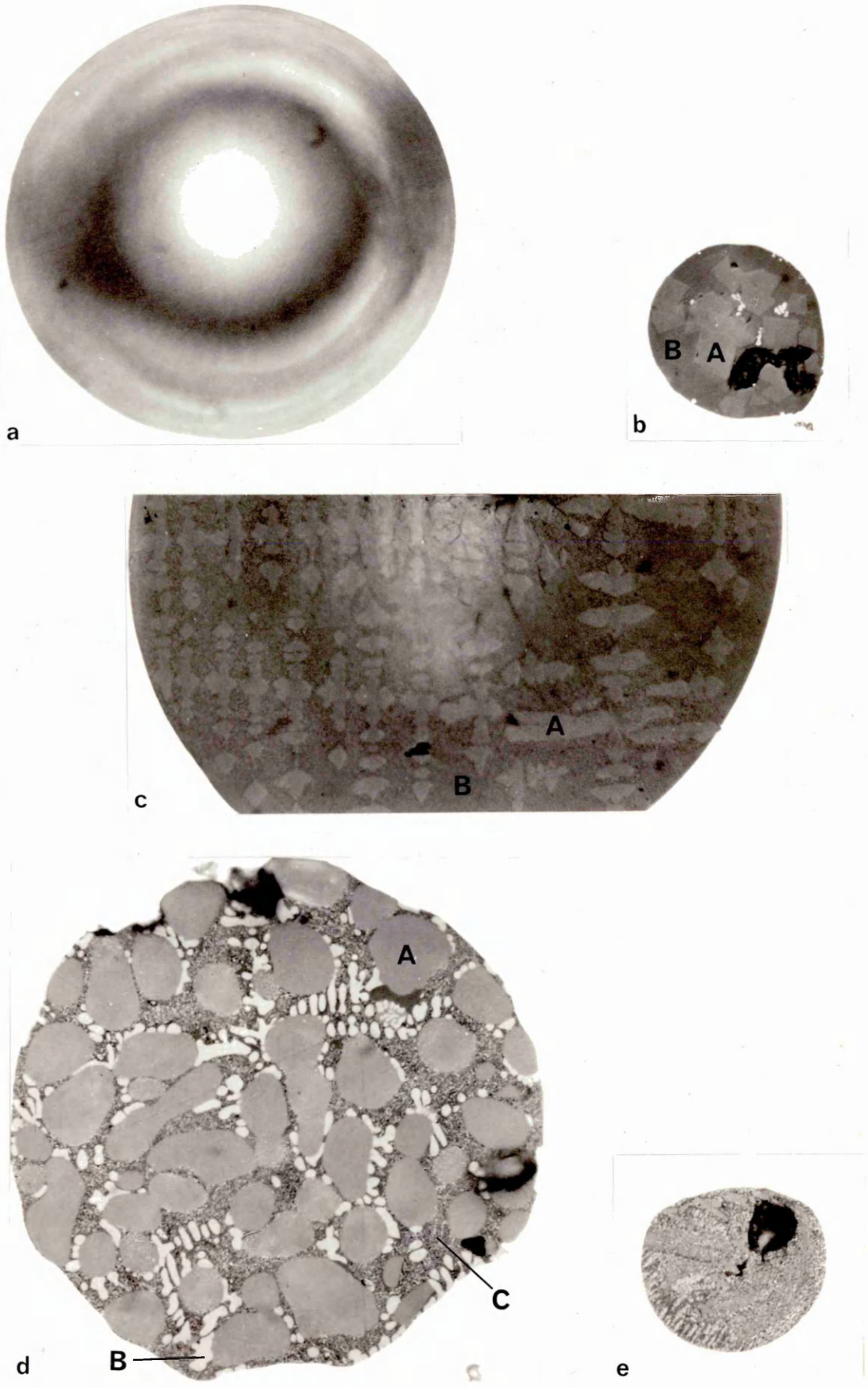

Fig. 4.12

Trial cast B.1 - Inclusions present in ladle stream during teeming x 750

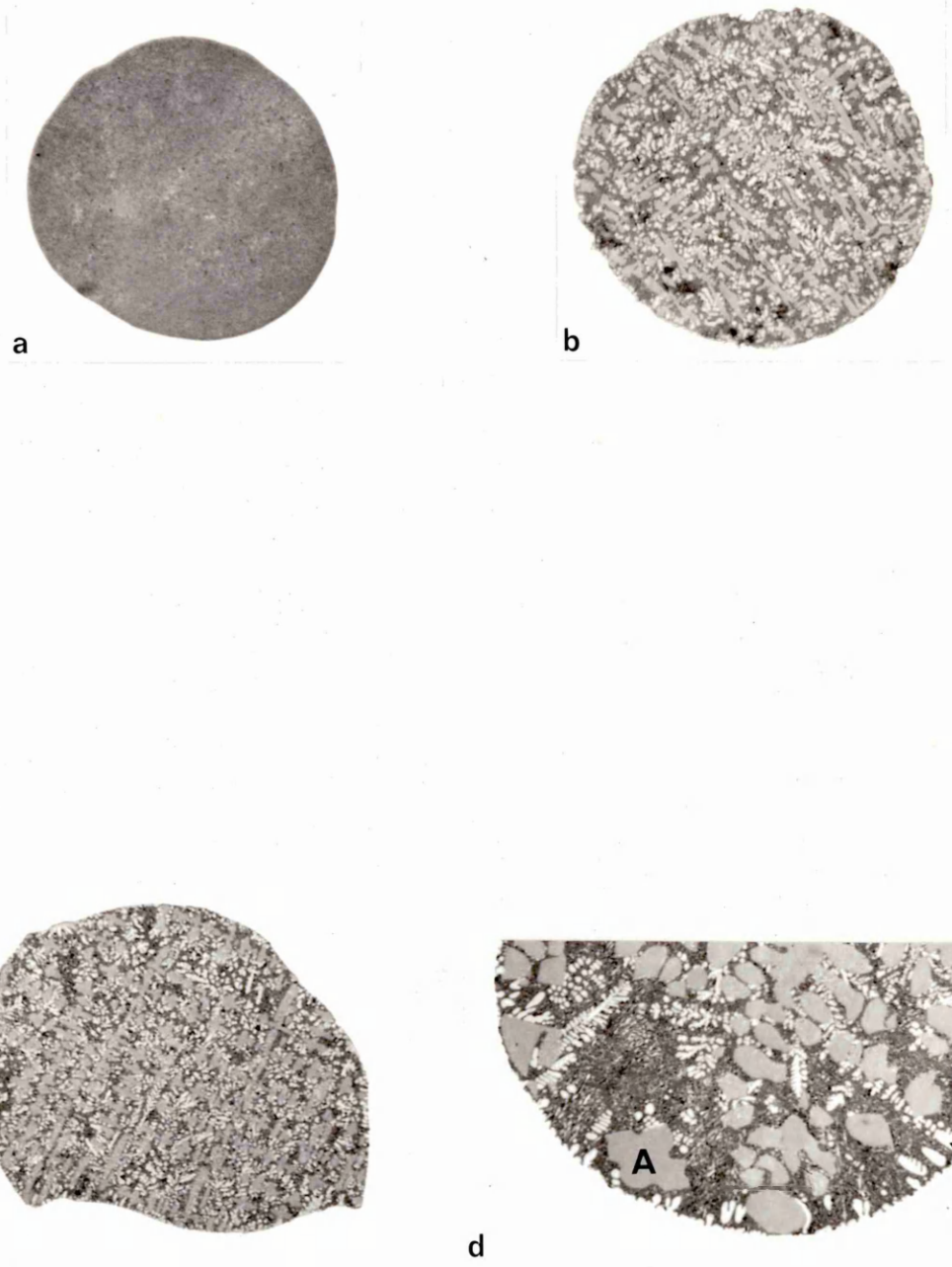

Fig. 4.13

Trial cast B.1 - Inclusions present in ingots during teeming x 750

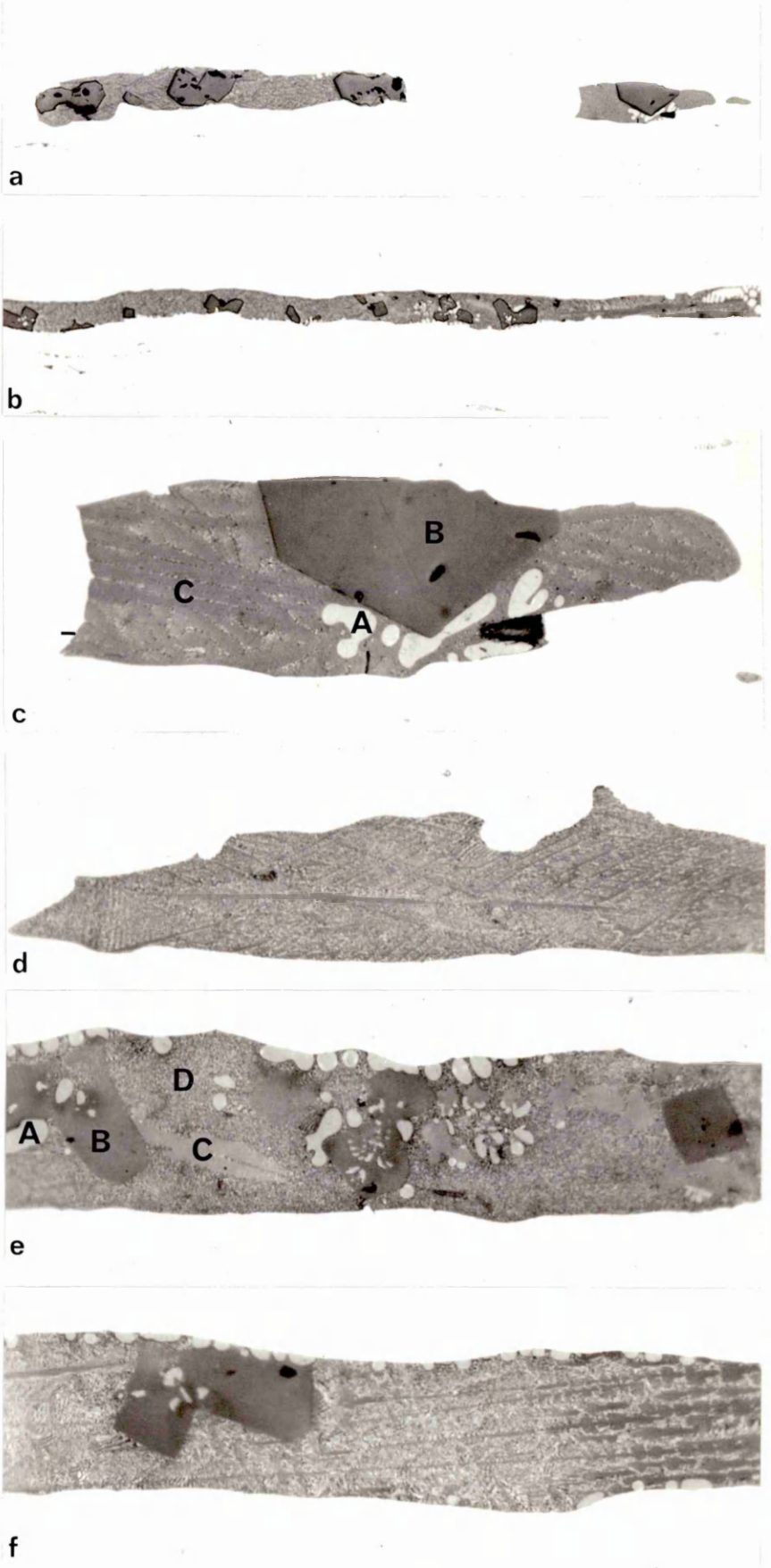

Fig. 4.14

Trial cast B.1 - Inclusions present in billets
(a) and (b) x 150; (c)-(f) x 750

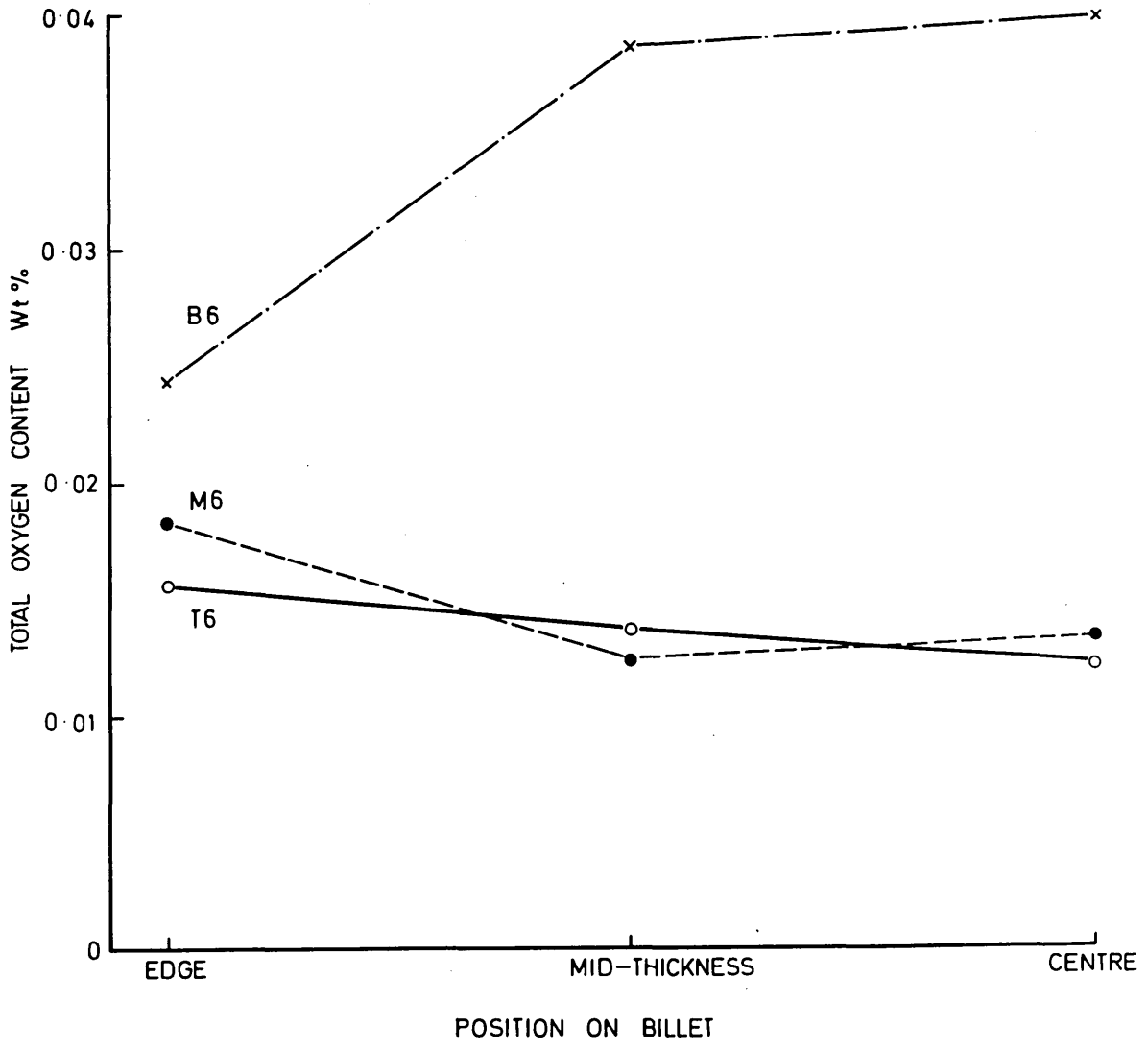

Ingot no. 6 (uphill-teemed)
B = bottom billet sample (98% down ingot)
M = middle billet sample (50% down ingot)
T = top billet sample (7% down ingot)

Fig. 4.15

Trial cast B.1 - Variation in total oxygen content of billet samples from ingot no. 6

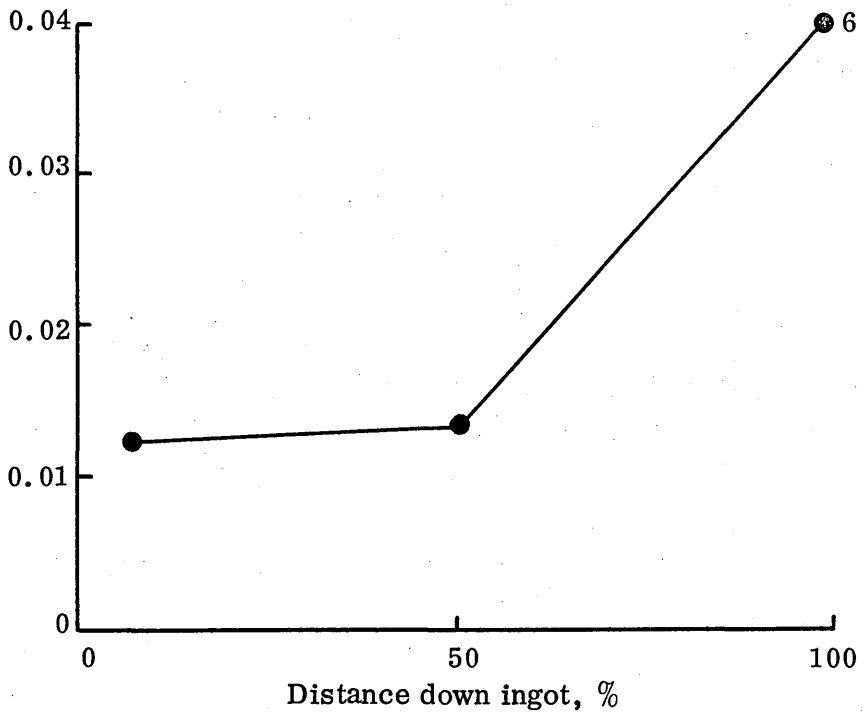

Fig. 4.16

Trial cast B.1 - Variation in total oxygen content down ingot 6

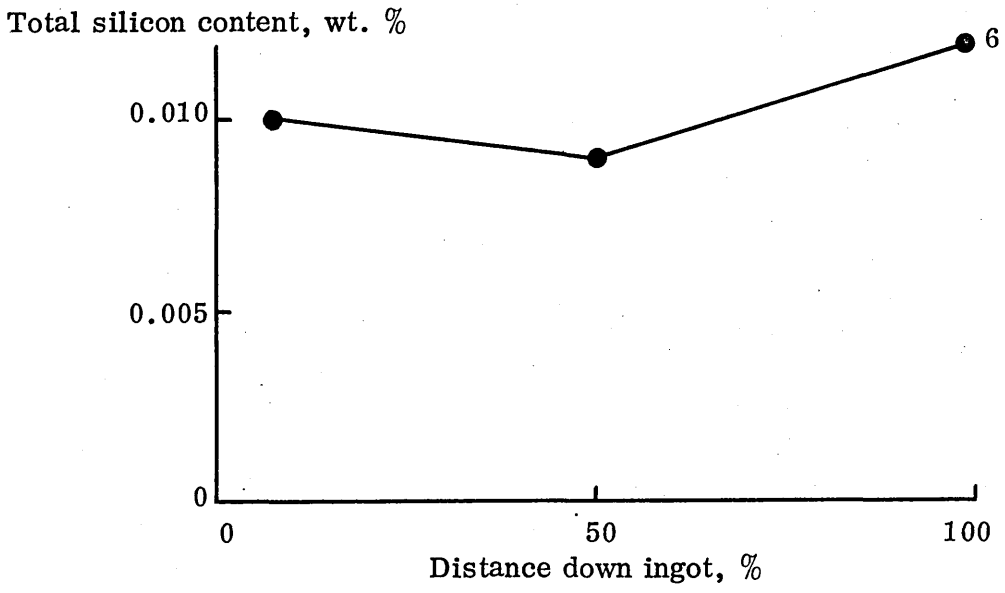

Fig. 4.17

Trial cast B.1 - Variation in total silicon content down ingot 6

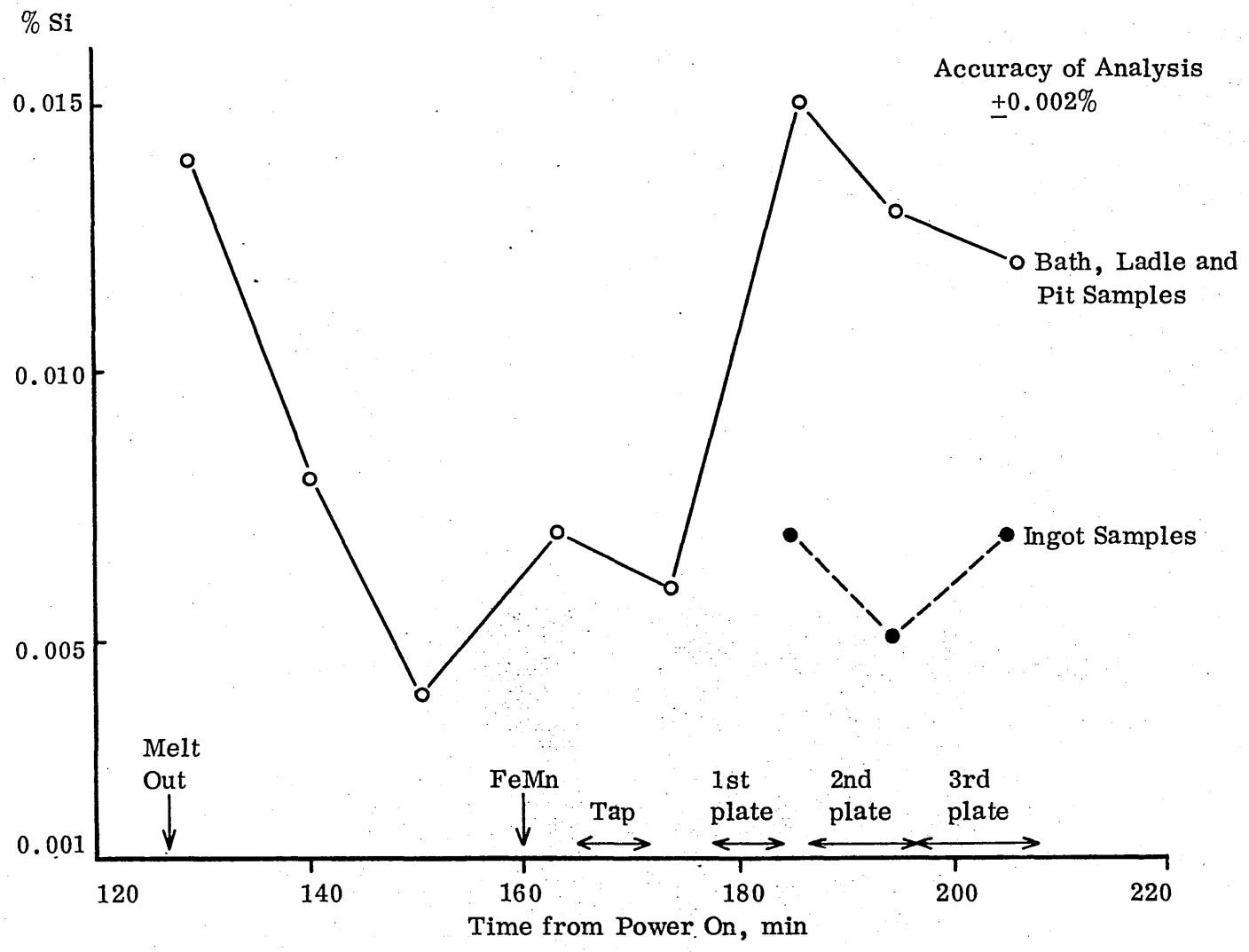

Fig. 4.18

Trial cast B.1 - Variation in silicon content during steelmaking, tapping and teeming

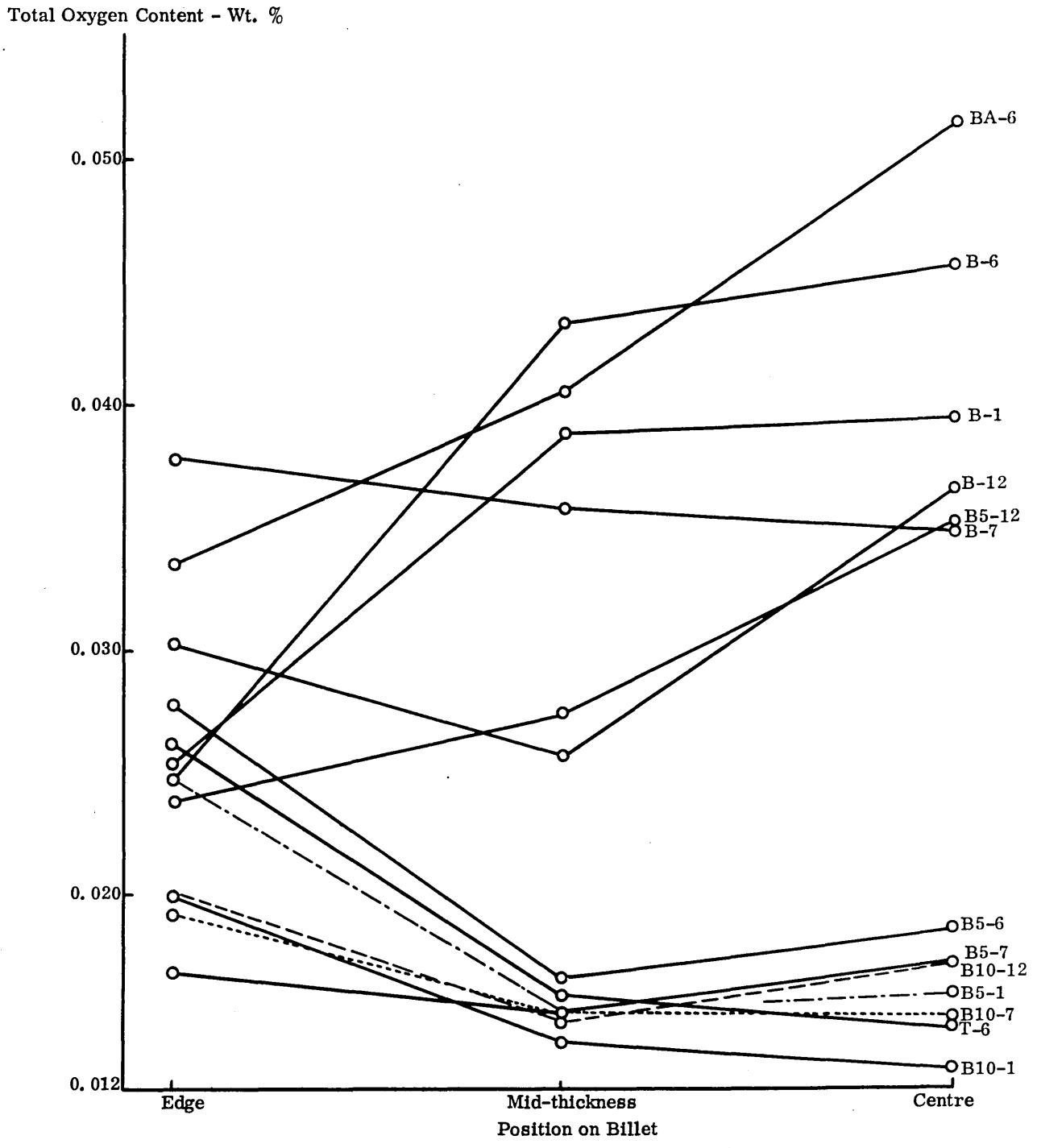

Ingots 1, 7 and 12 (uphill-teemed)
Ingot 6 (direct-teemed)
B = bottom billet sample (98% down ingot)
BA = bottom billet sample (95% down ingot)
B5 = middle billet sample (50% down ingot)
B10 = top billet sample (15% down ingot)
T = top billet sample (7% down ingot)

Fig. 4.19

Trial cast B.2 - Variation in total oxygen content of billet samples

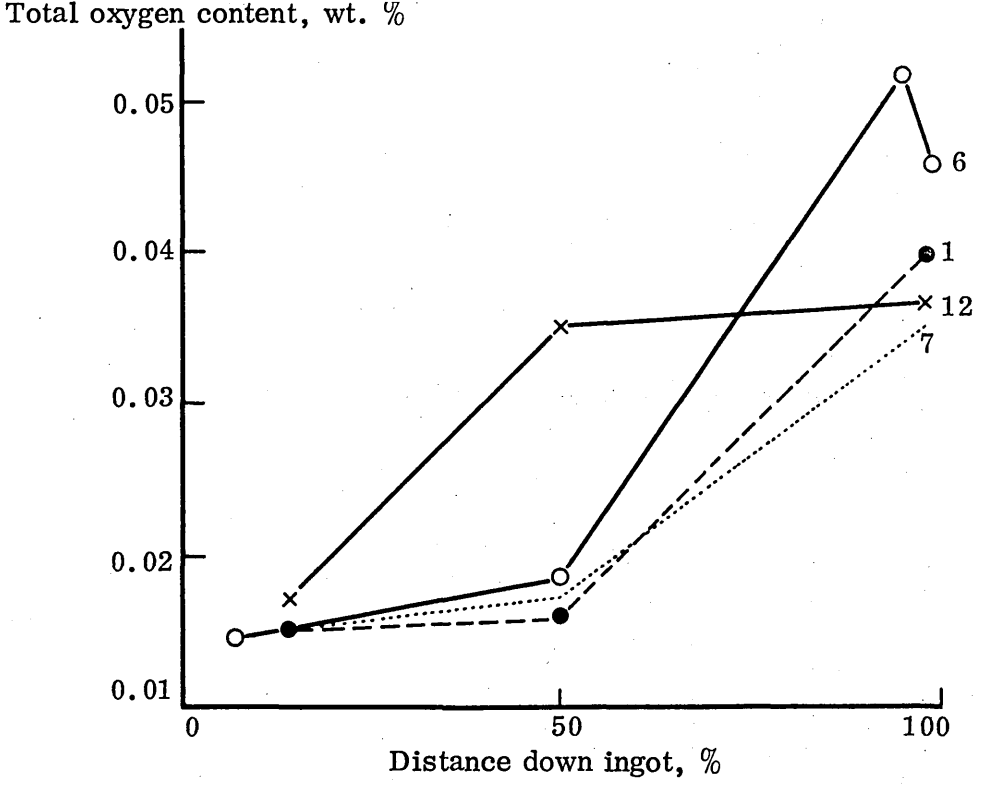

Fig. 4.20

Trial cast B.2 - Variation in total oxygen content down ingots 1, 6, 7 and 12

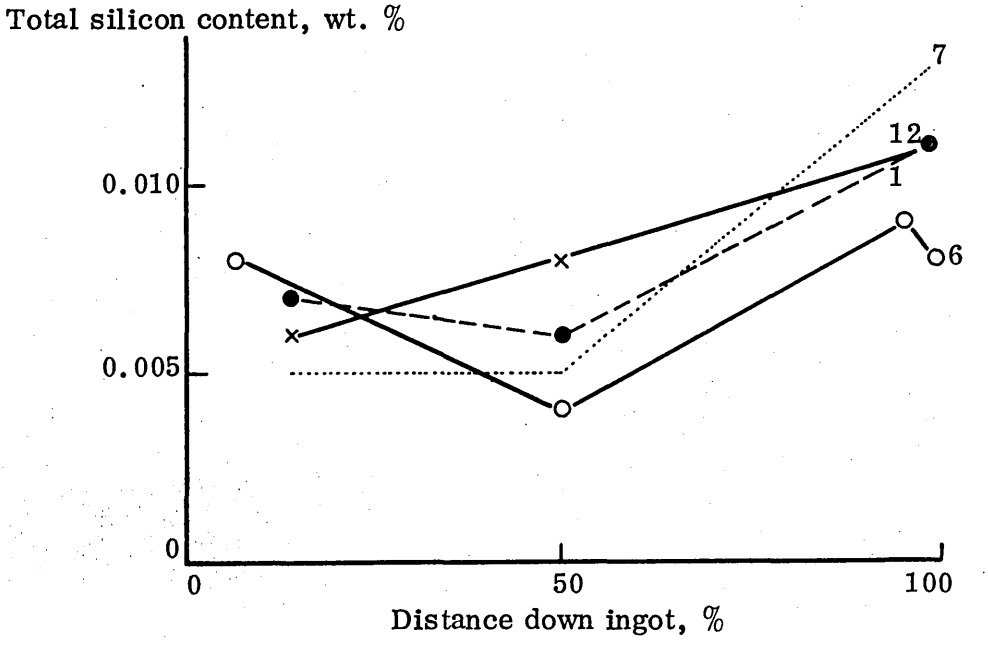

Fig. 4.21

Trial cast B.2 - Variation in total silicon content down ingots, 1, 6, 7 and 12

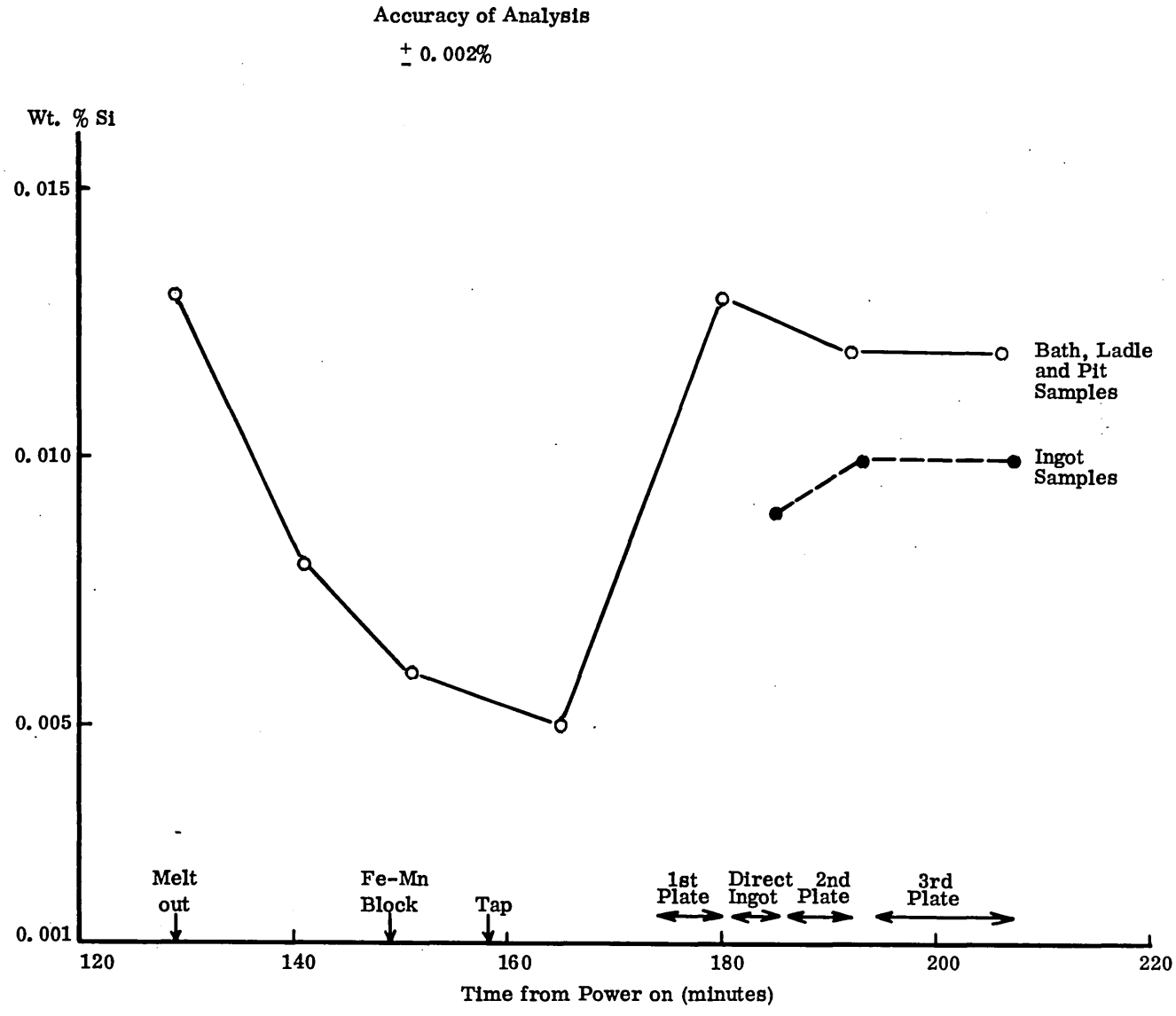

Fig. 4.22
Trial cast B.2 - variation
silicon content during steelma
tapping and teeming

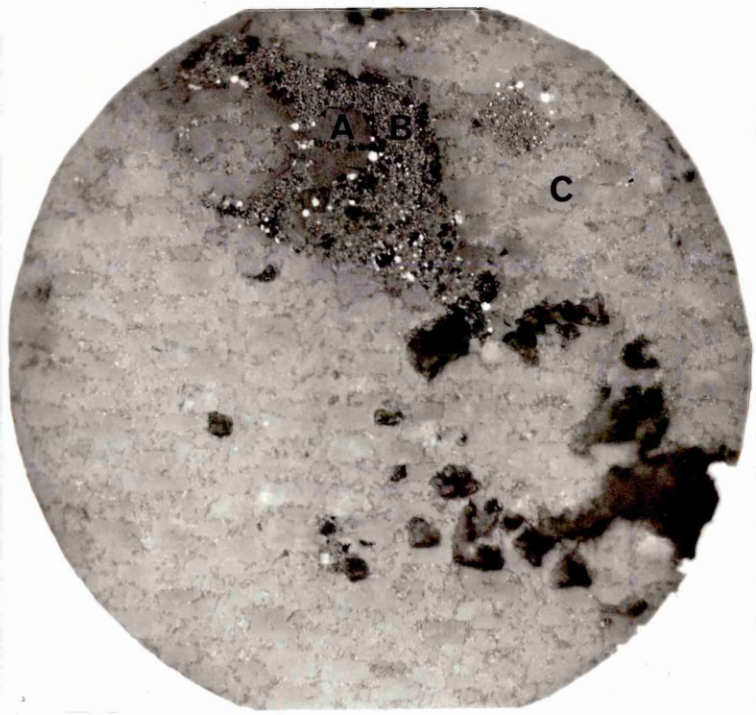

Fig. 4.23

Trial cast B.2 - Inclusion present in ingot during teeming x 750

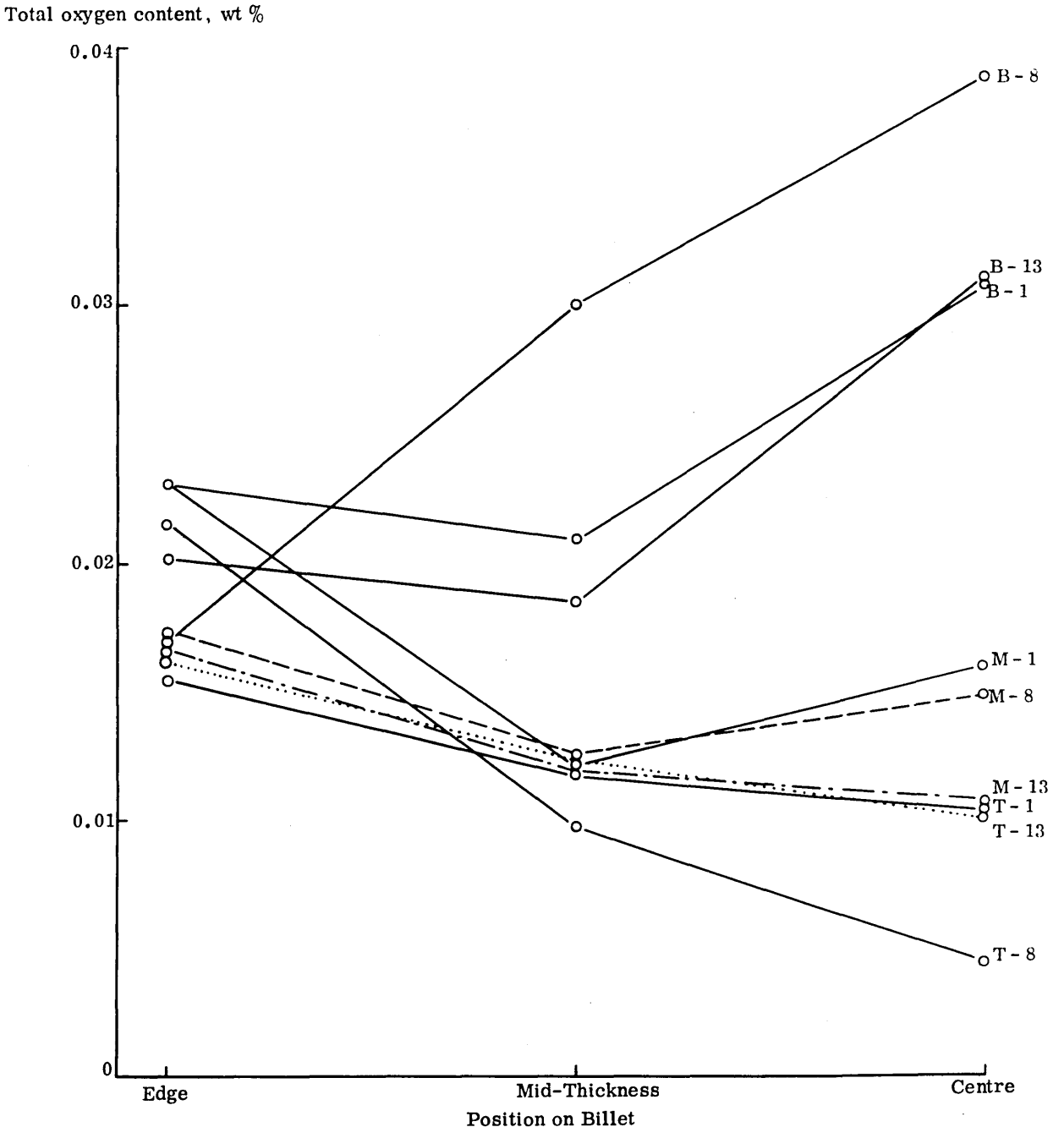

Ingots 1, 8 and 13 (uphill-teemed)
B = bottom billet sample (98% down ingot)
M = middle billet sample (60% down ingot)
T = top billet sample (7% down ingot)

Fig. 4.24

Trial cast B.3 - Variation in total oxygen content of billet samples

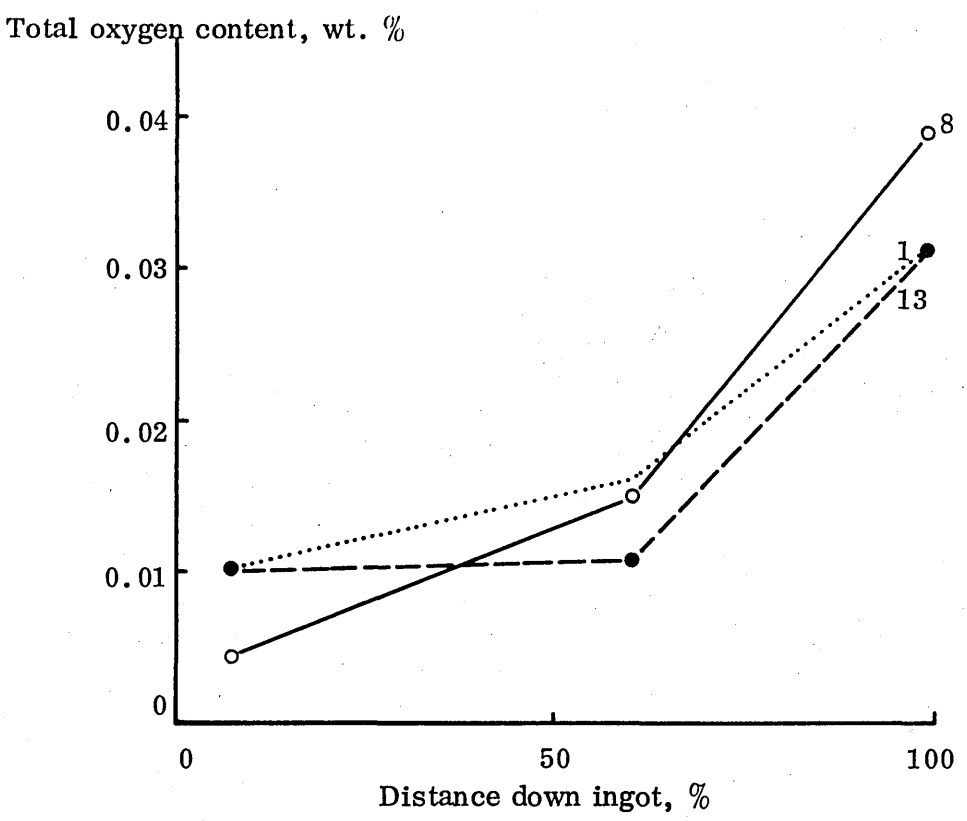

Fig. 4.25

Trial cast B.3 - Variation in total oxygen content down ingots 1, 8 and 13

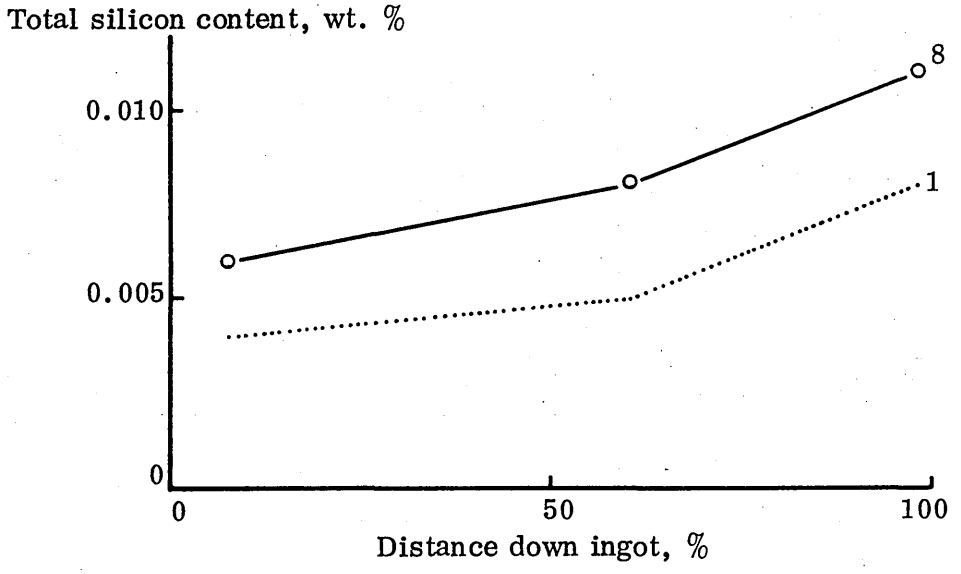

Fig. 4.26

Trial cast B.3 - Variation in total silicon content down ingots 1 and 8

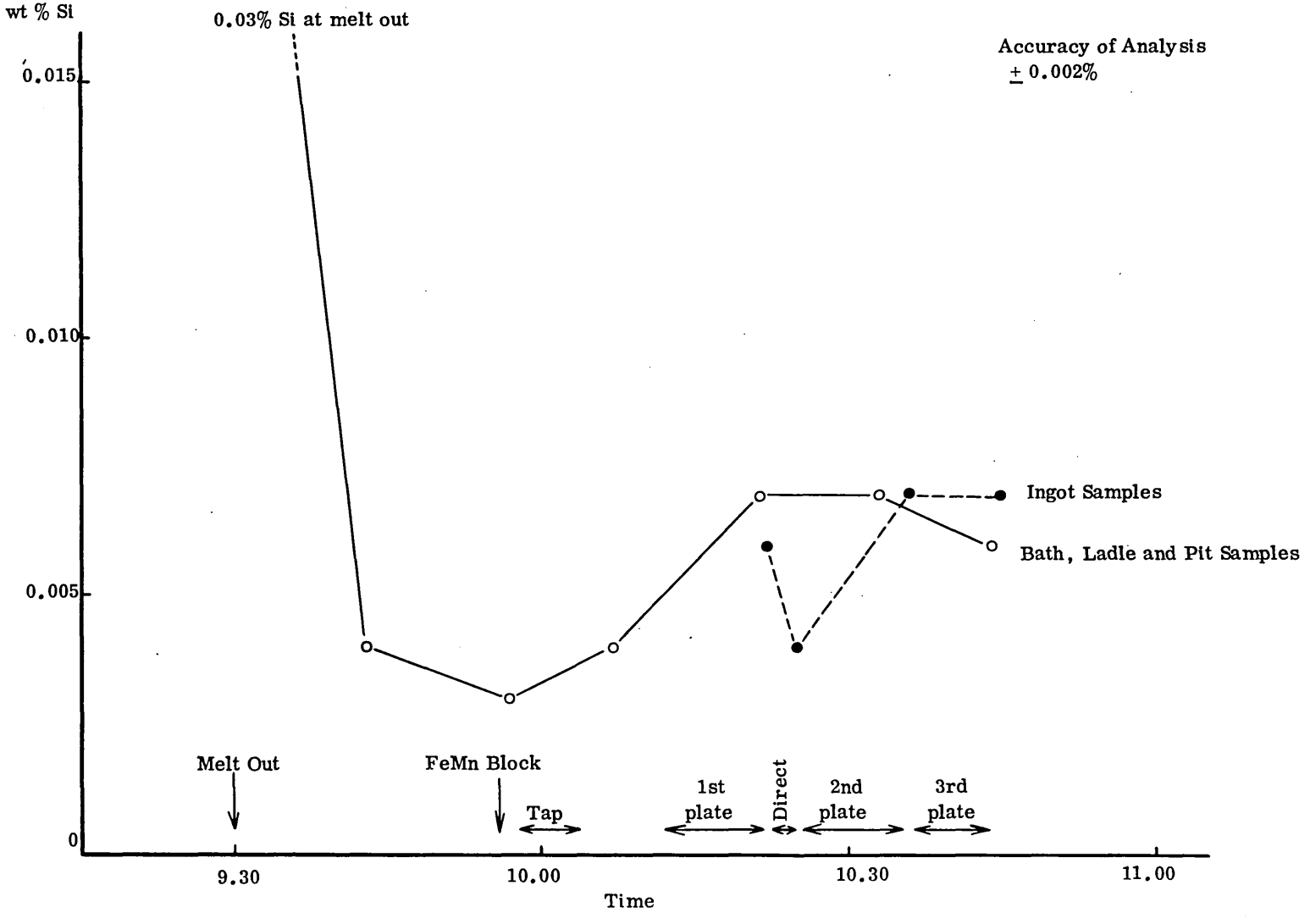

Fig. 4.27

Trial cast B.3 - Variation
silicon content during
steelmaking, tapping and teen

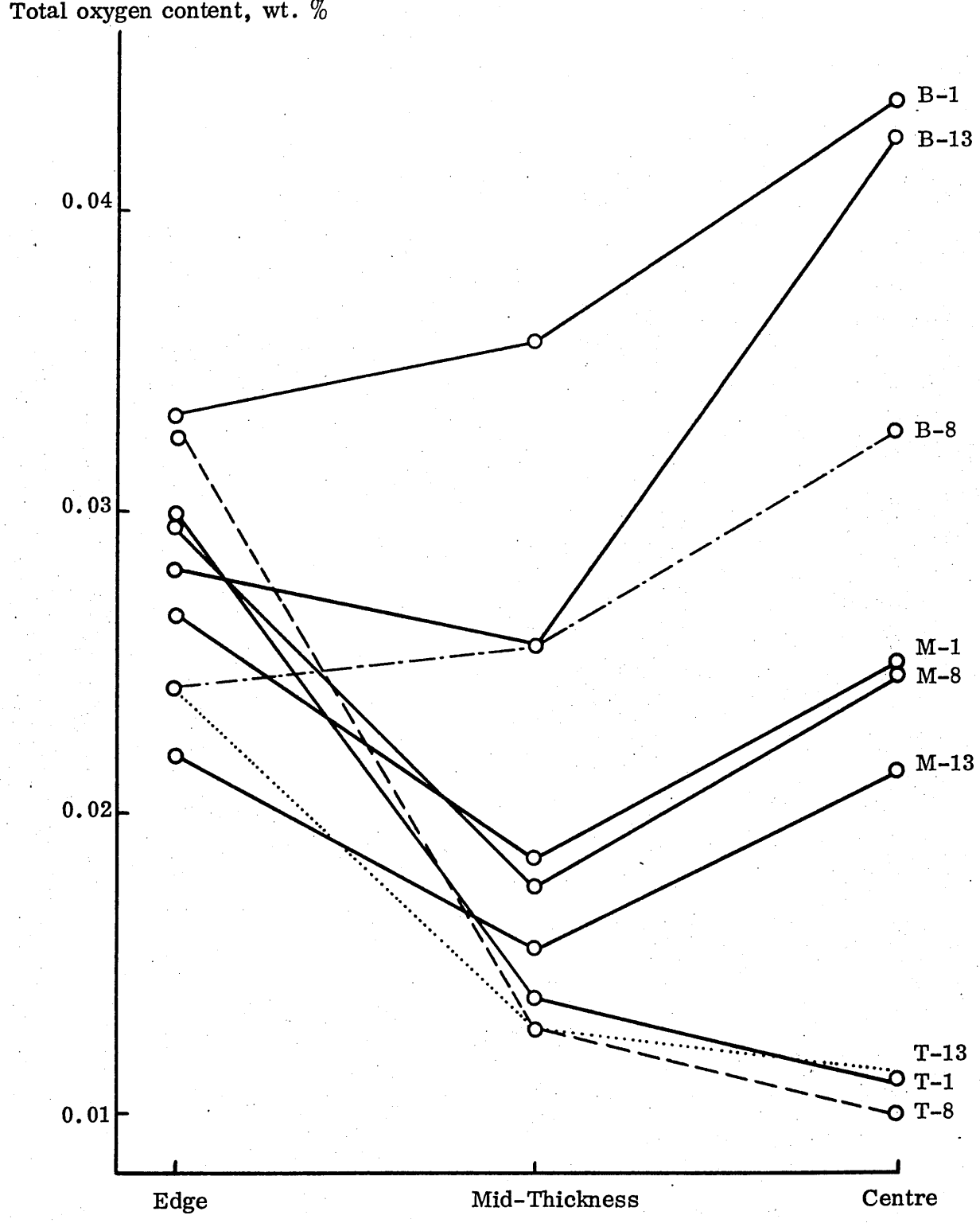

Ingots 1, 8 and 13 (uphill-teemed)
B = bottom billet sample (98% down ingot)
M = middle billet sample (68% down ingot)
T = top billet sample (7% down ingot)

Fig. 4.28

Trial cast B.4 - Variation in total oxygen content of billet samples

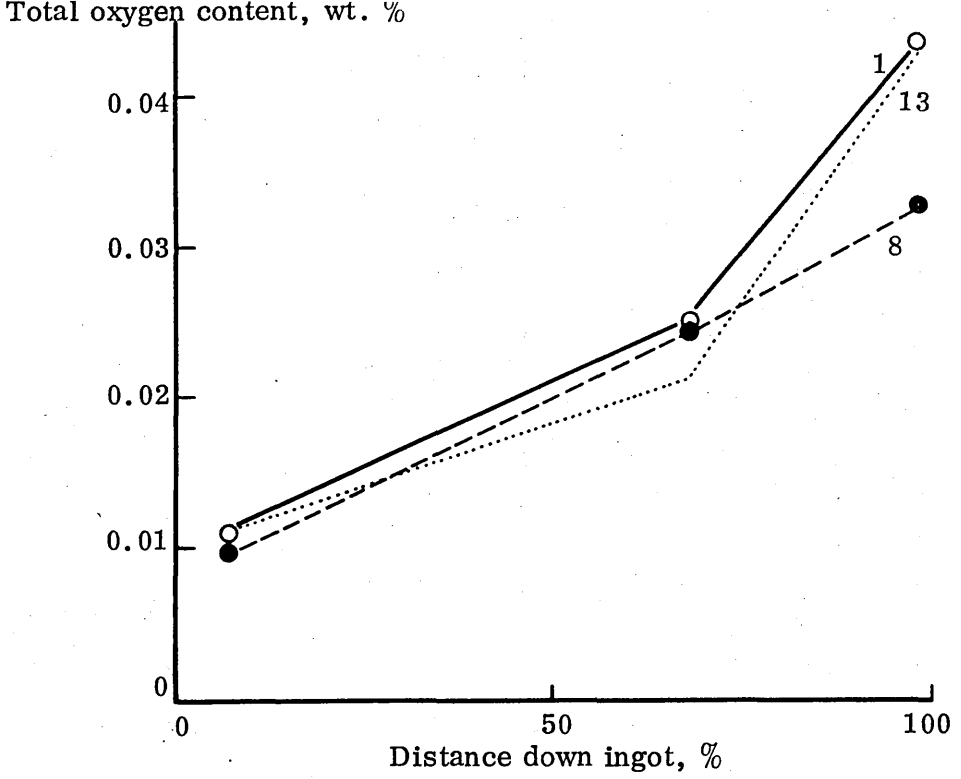

Fig. 4.29

Trial cast B.4 - Variation in total oxygen content down ingots 1, 8 and 13

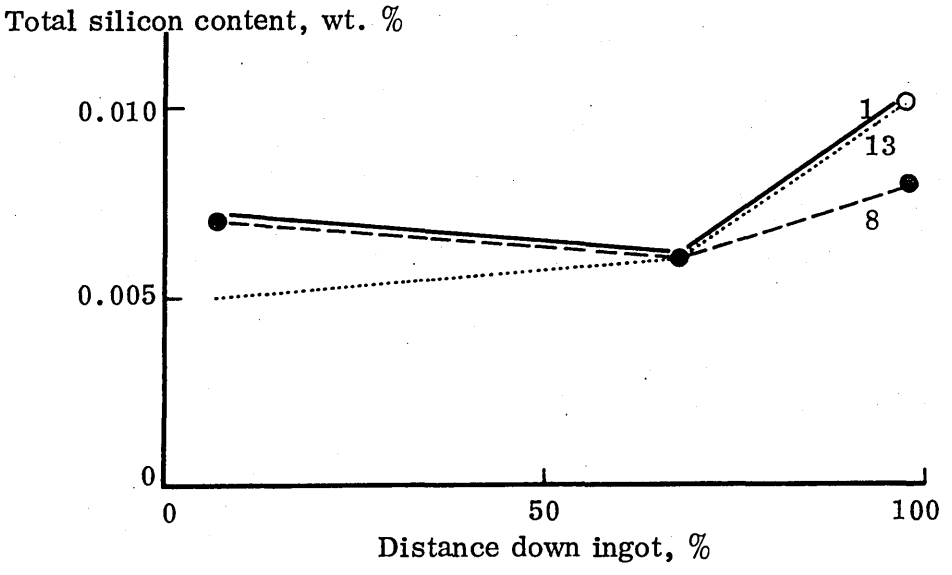

Fig. 4.30

Trial cast B.4 - Variation in total silicon content down ingots 1, 8 and 13

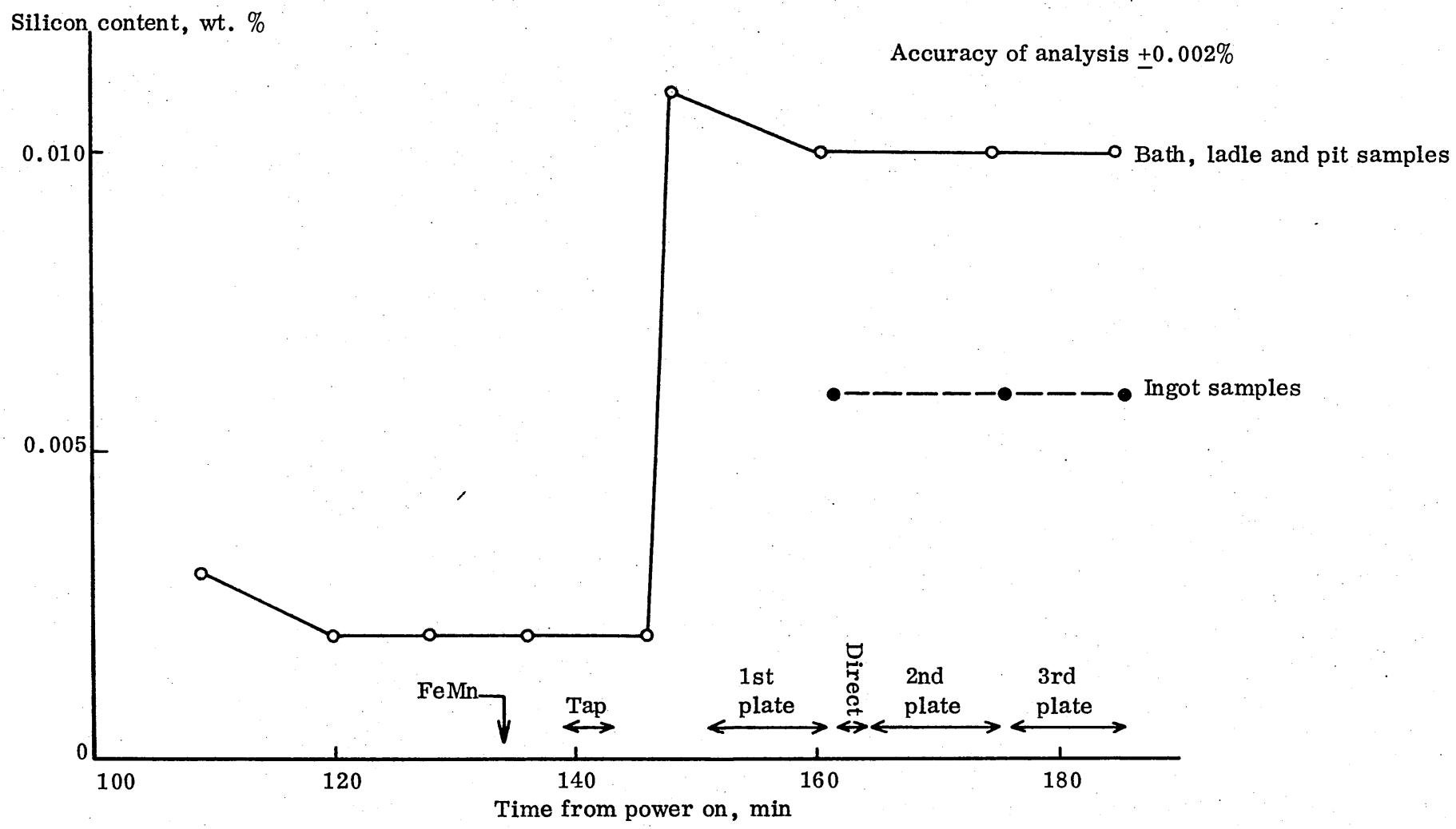

Fig. 4.31

Trial cast B.4 - Variation in silicon content during steelmaking, tapping and teeming

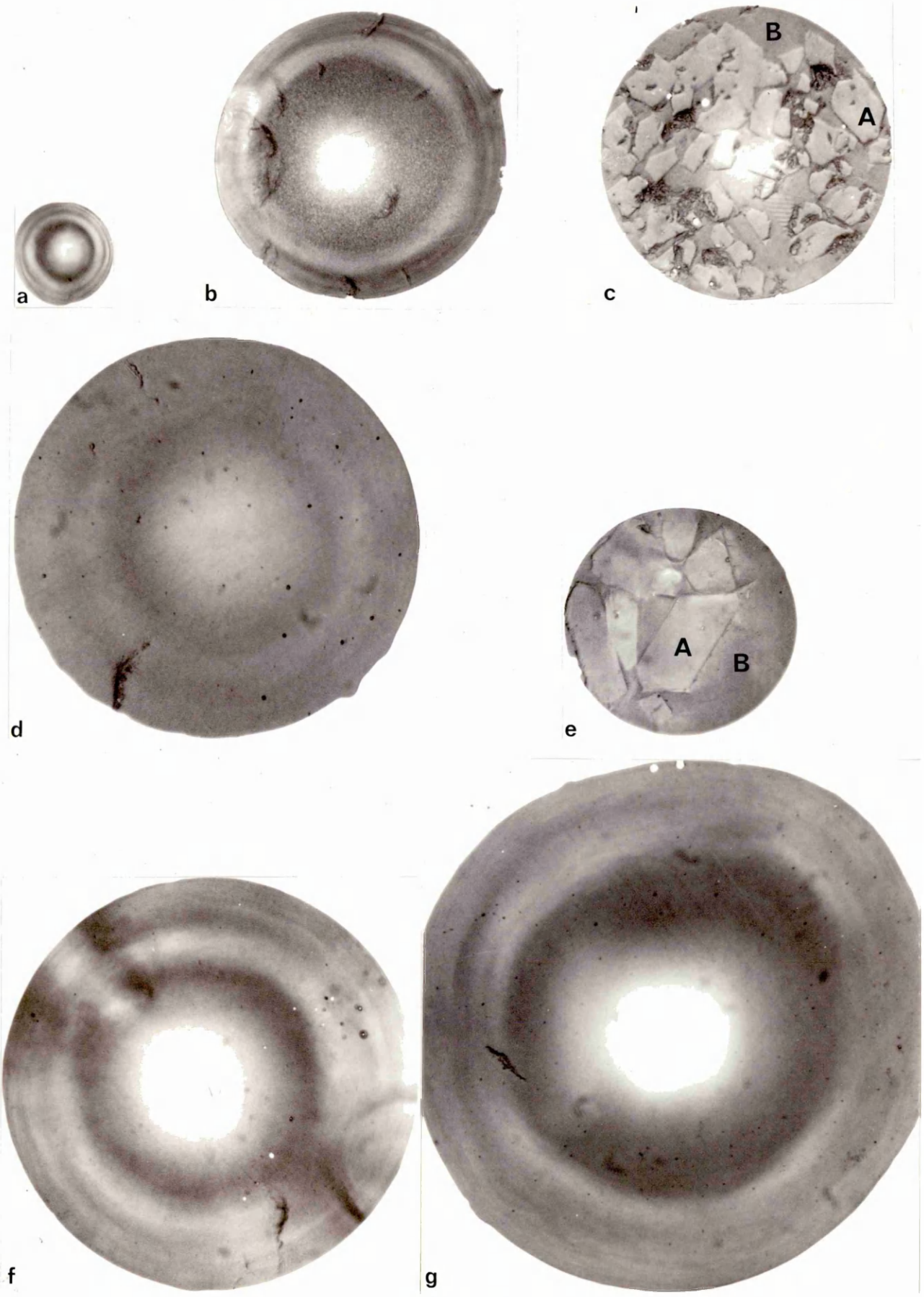

Fig. 4.32

Trial cast C.1 - Inclusions present in furnace during steelmaking x 750

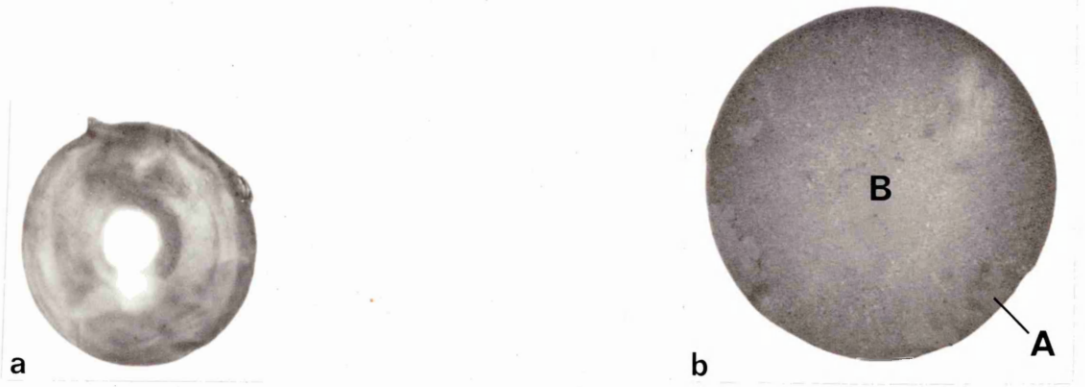

Fig. 4.33

Trial cast C.1 - Inclusions present in ladle after tapping x 750

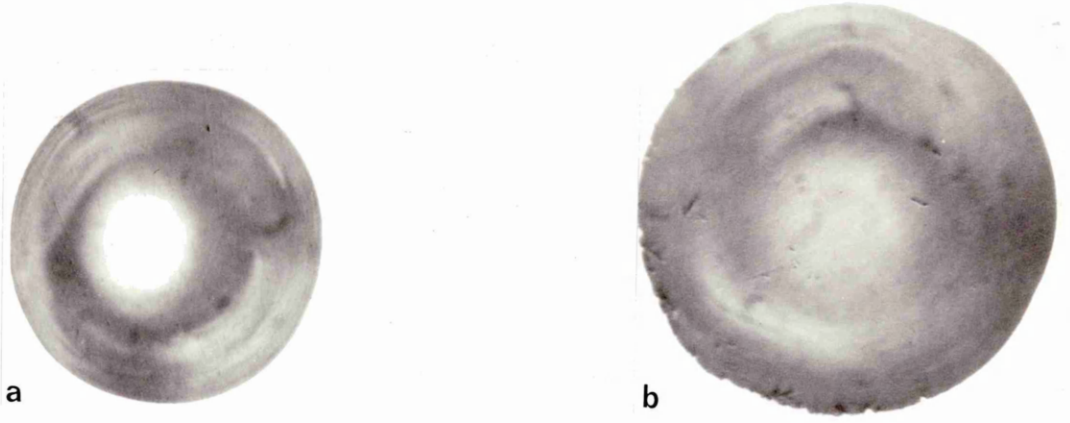

Fig. 4.34

Trial cast C.1 - Inclusions present in ladle stream during teeming x 750

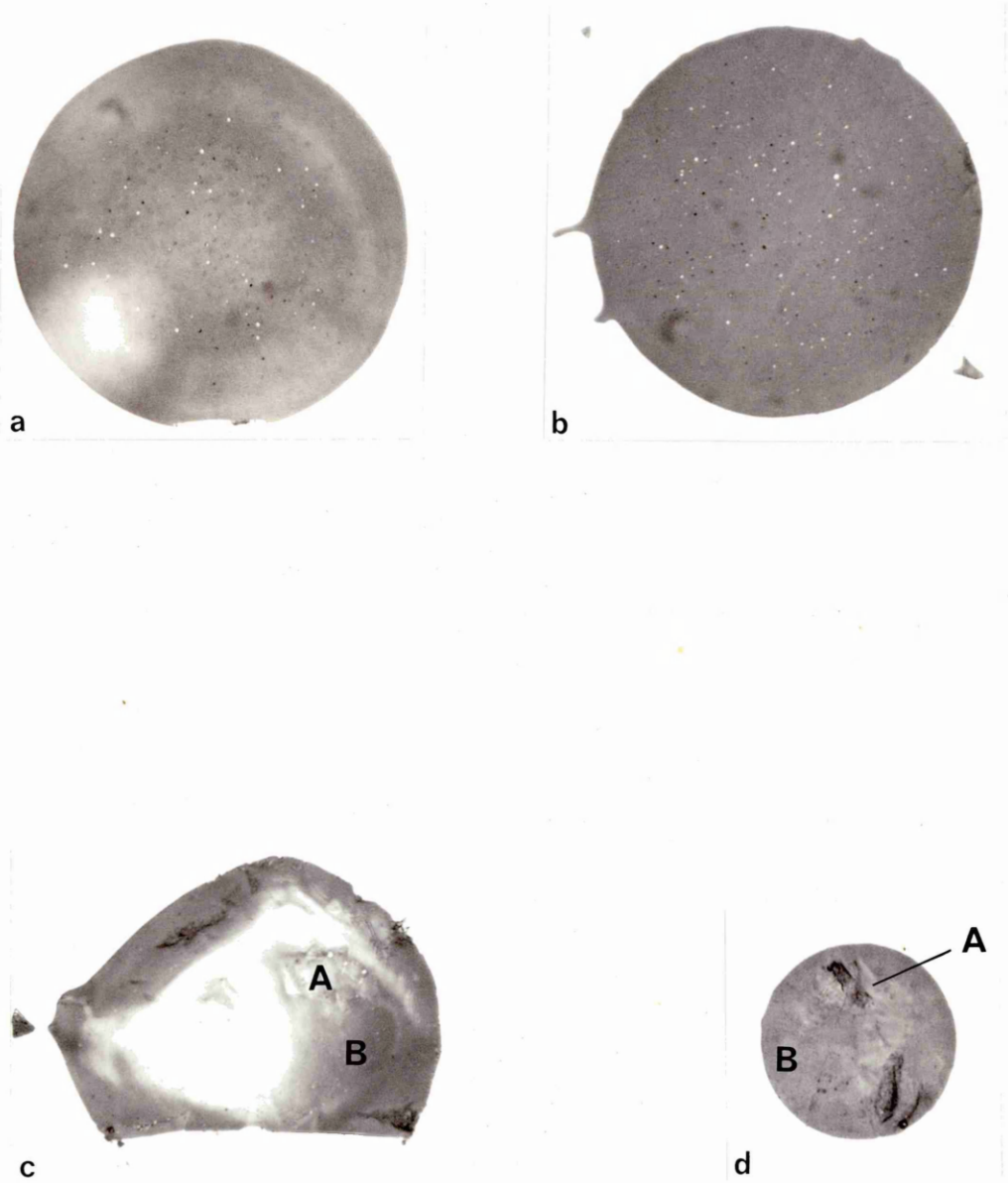

Fig. 4.35

Trial cast C.1 - Inclusions present in ingots during teeming x 750

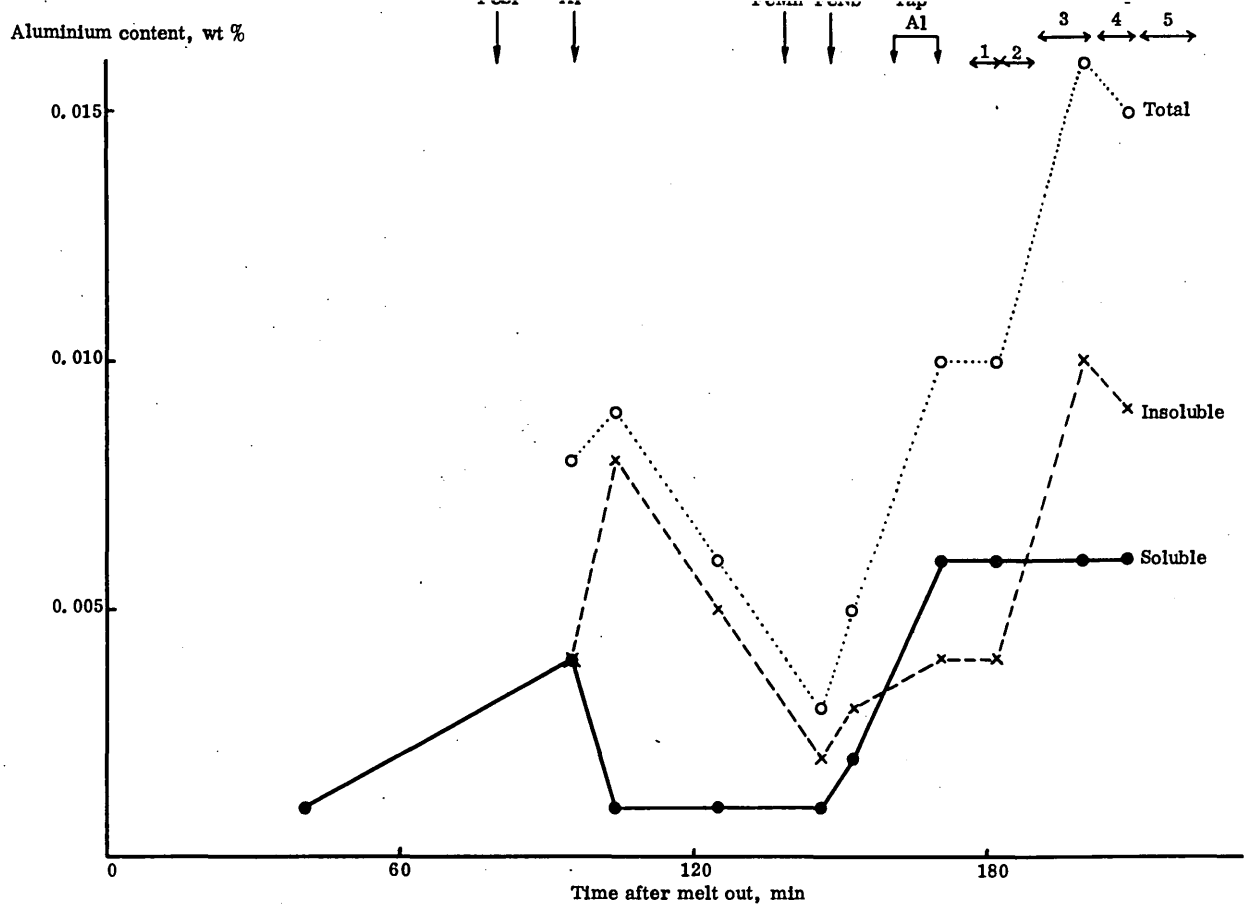

Fig. 4.36

Trial cast C.1 - Variation in aluminium content of bath, ladle and ingot samples with time

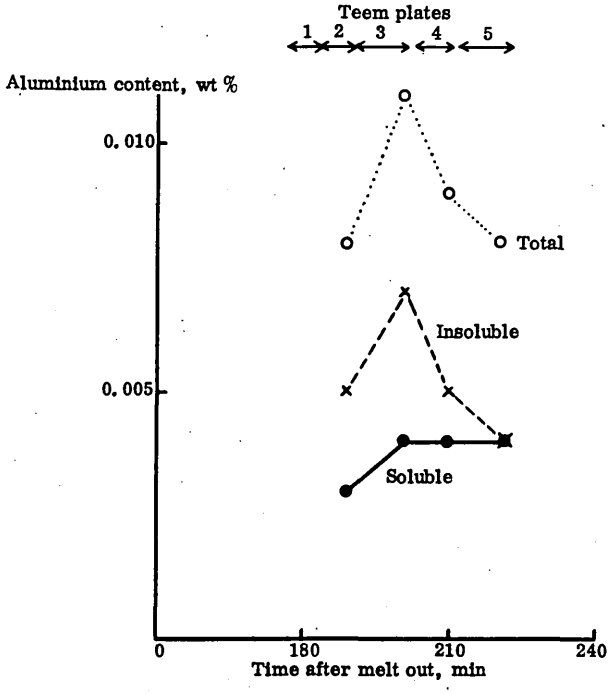

Fig. 4.37

Trial cast C.1 - Variation in aluminium content of ladle stream samples with time

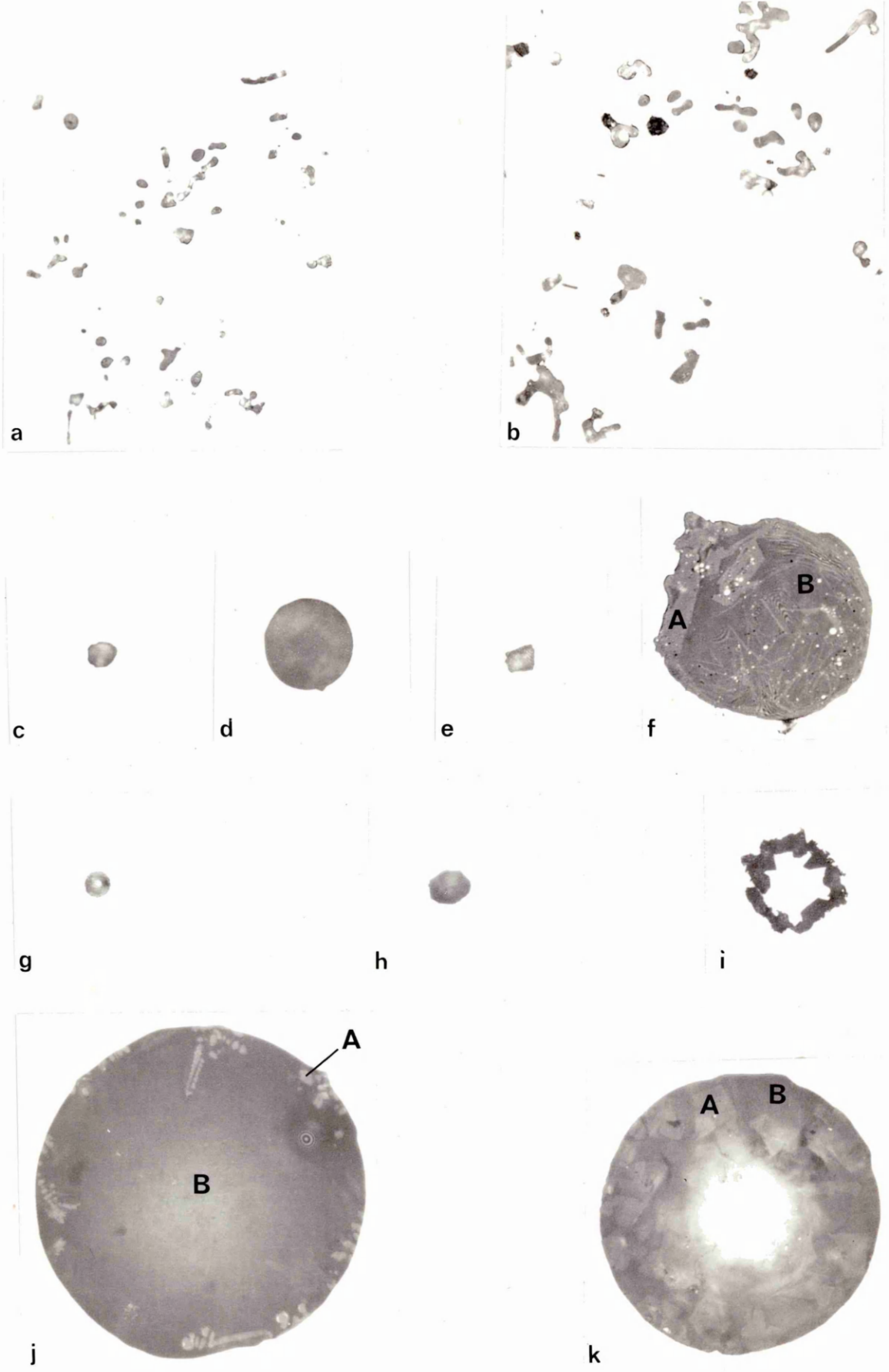

Fig. 4.38

Trial cast C.2 - Inclusions present in furnace during steelmaking x 750

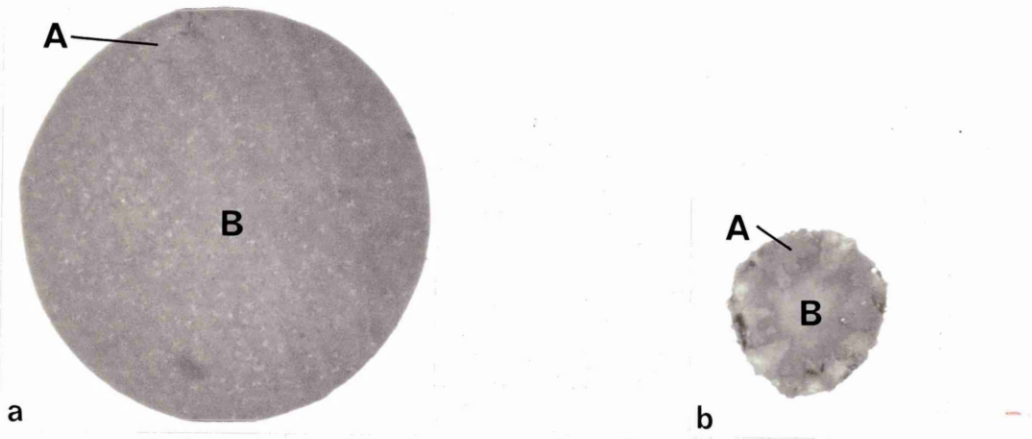

Fig. 4.39

Trial cast C.2 - Inclusions present in furnace during steelmaking x 750

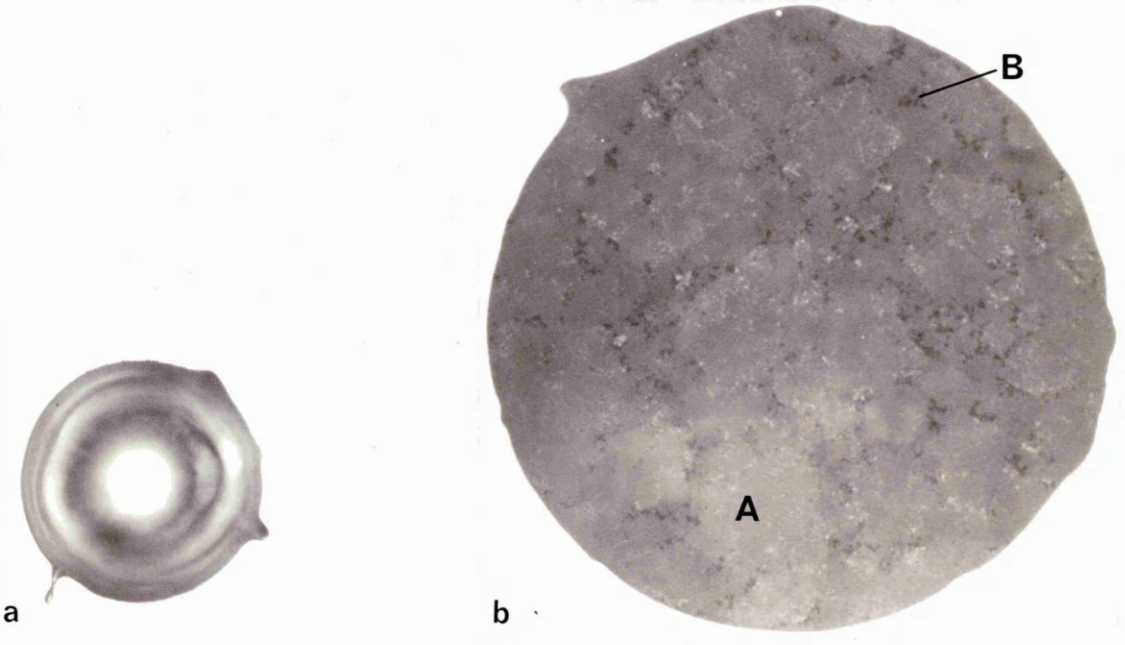

Fig. 4.40

Trial cast C.2 - Inclusions present in ladle after tapping x 750

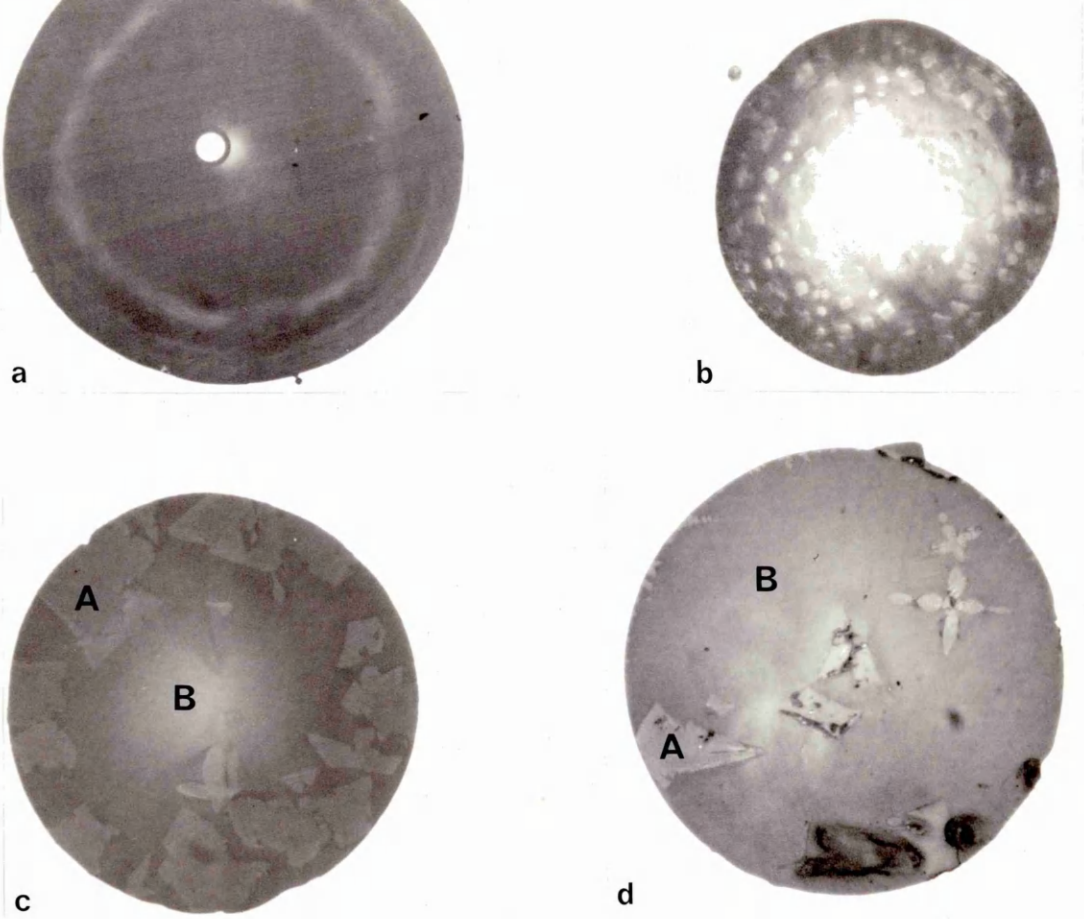

Fig. 4.41

Trial cast C.2 - Inclusions present in ladle stream during teeming x 750

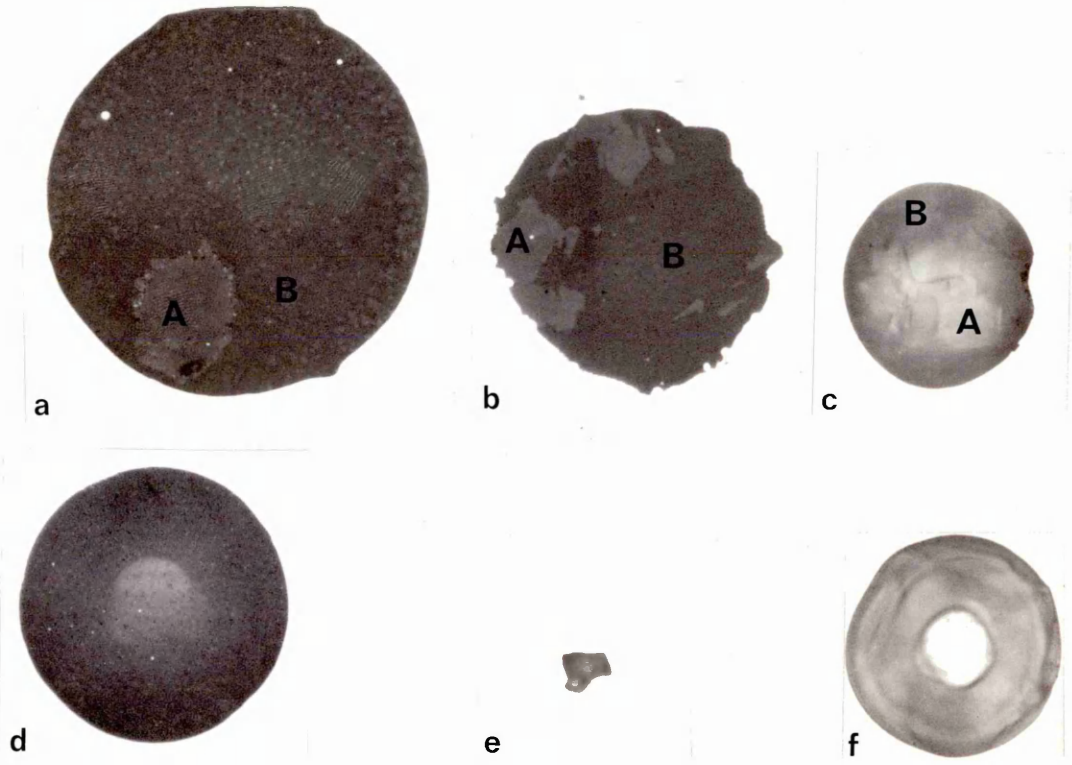

Fig. 4.42

Trial cast C.2 - Inclusions present in ingots during teeming x 750

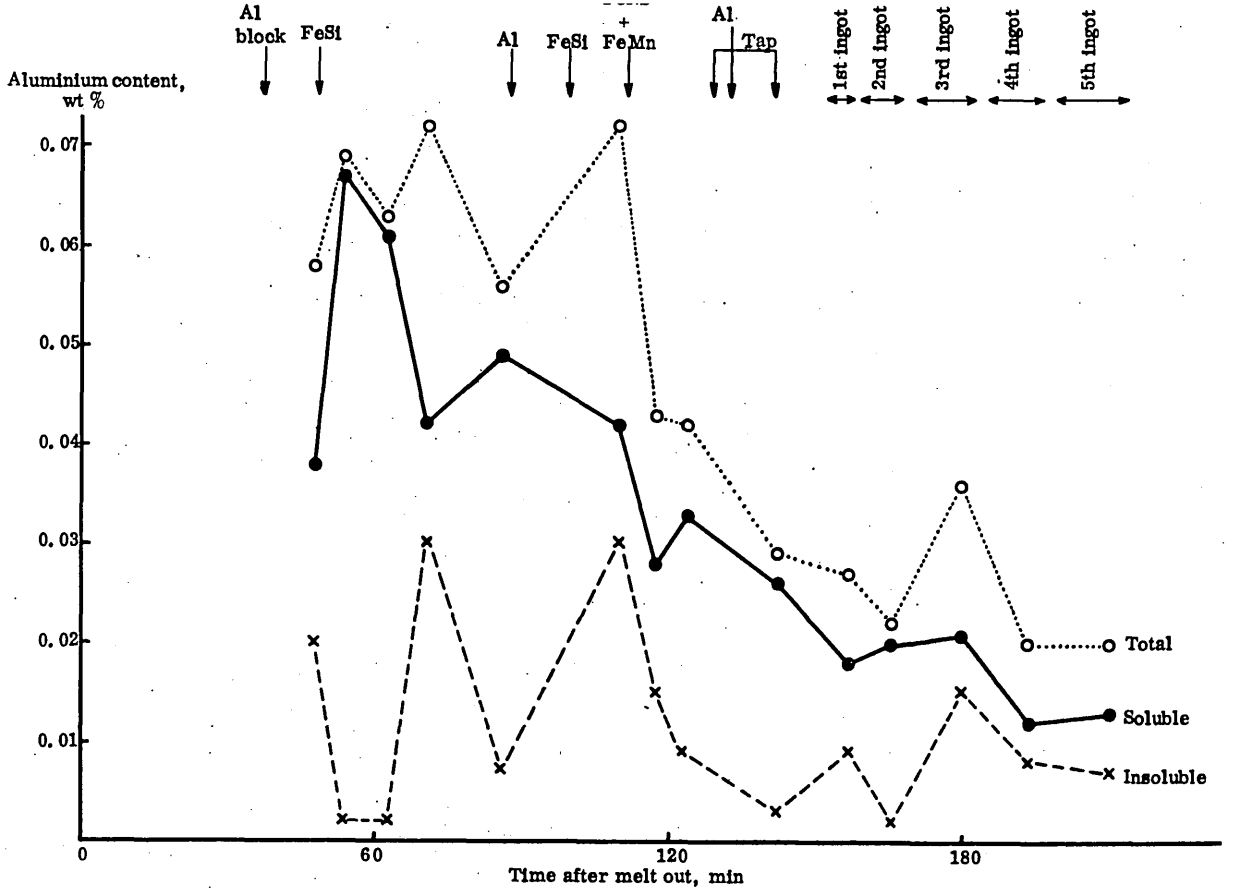

Fig. 4.43
Trial cast C.2 - variation in aluminium content of bath, ladle and ingot samples with time

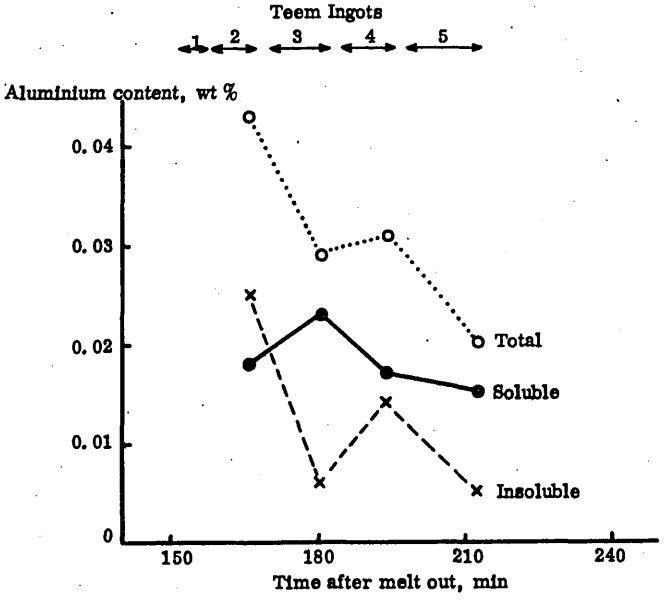

Fig. 4.44
Trial cast C.2 - variation in aluminium content of ladle stream samples with time

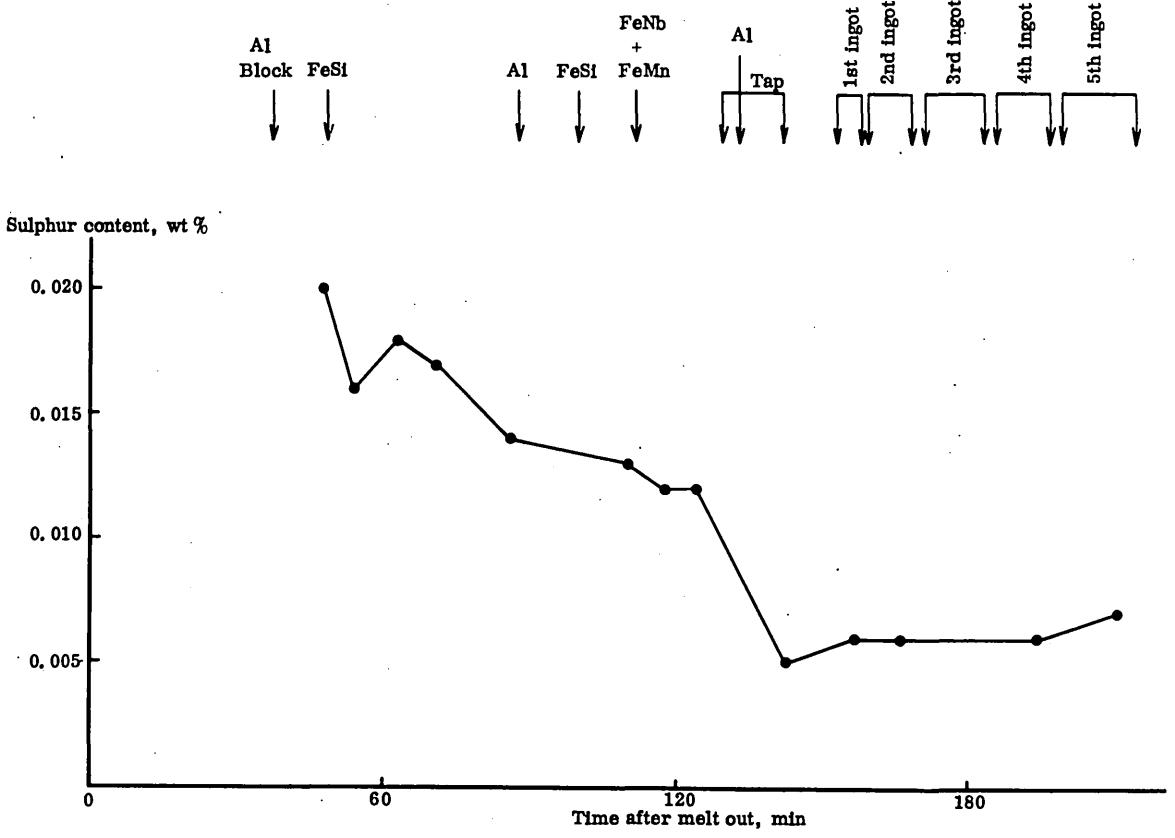

Fig. 4.45

Trial cast C.2 - Variation in sulphur content of bath, ladle and ingot samples with time

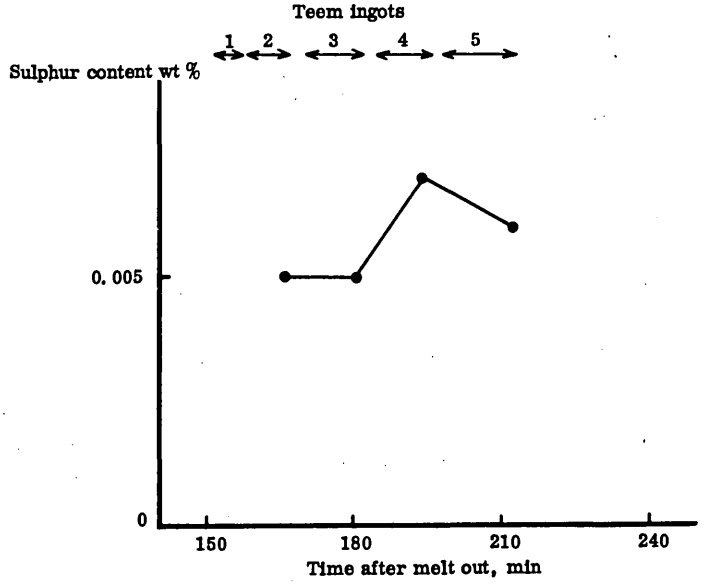

Fig. 4.46

Trial cast C.2 - Variation in sulphur content of ladle stream samples with time

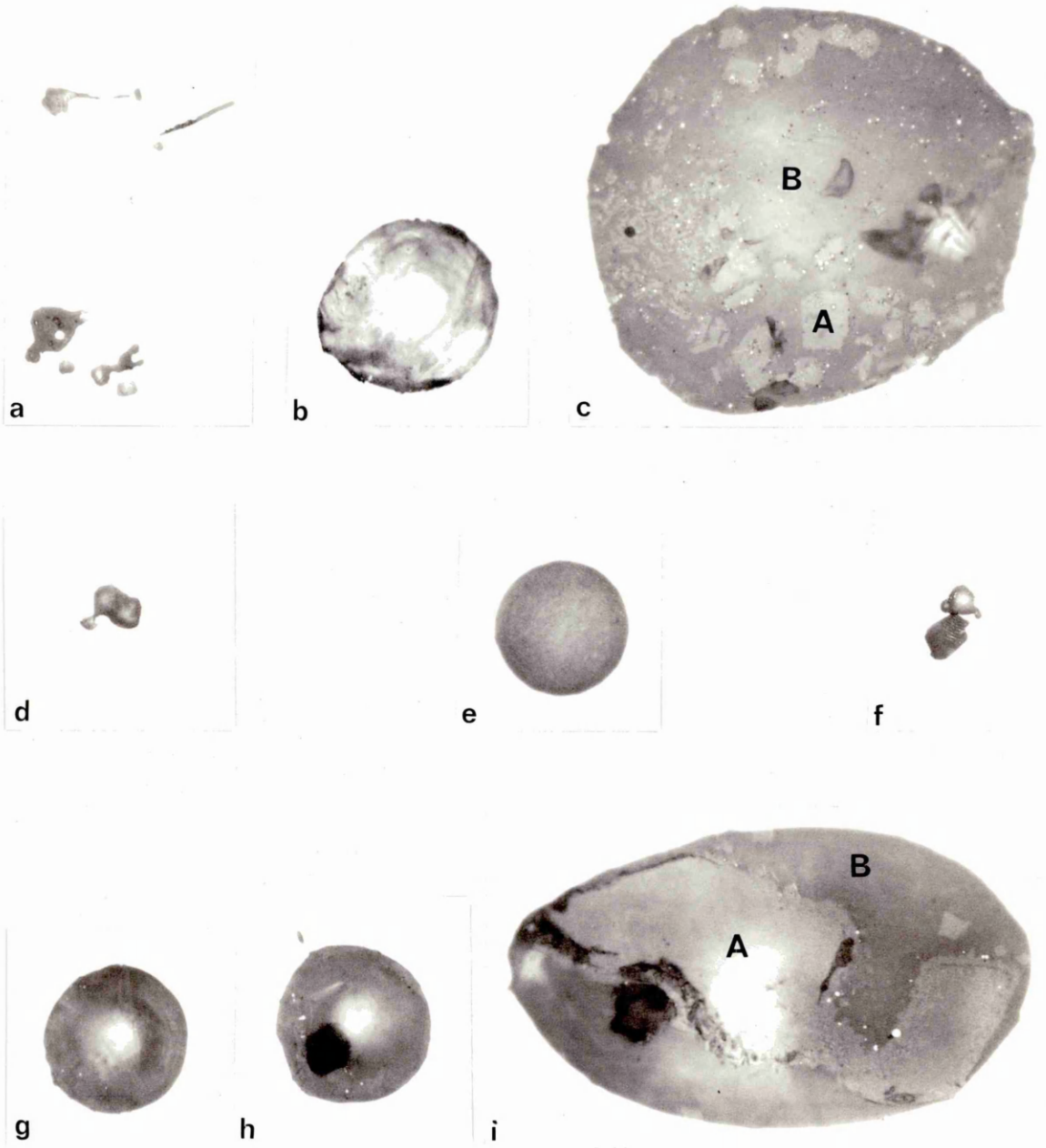

Fig. 4.47

Trial cast C.3 - Inclusions present in furnace during steelmaking x 750

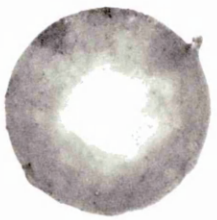

Fig. 4.48

Trial cast C.3 - Inclusion present in ladle after tapping x 750

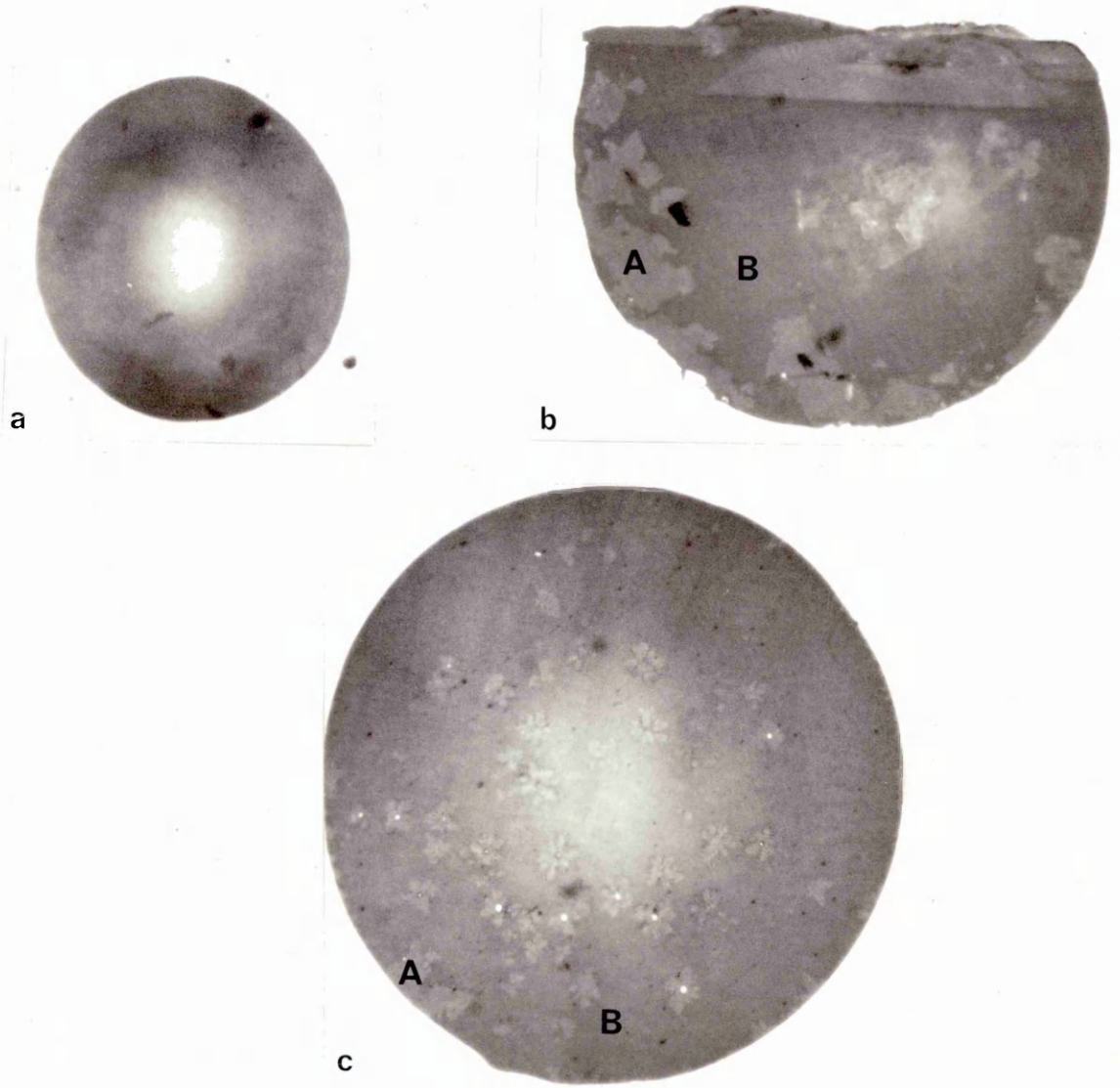

Fig. 4.49

Trial cast C.3 - Inclusions present in ladle stream during teeming x 750

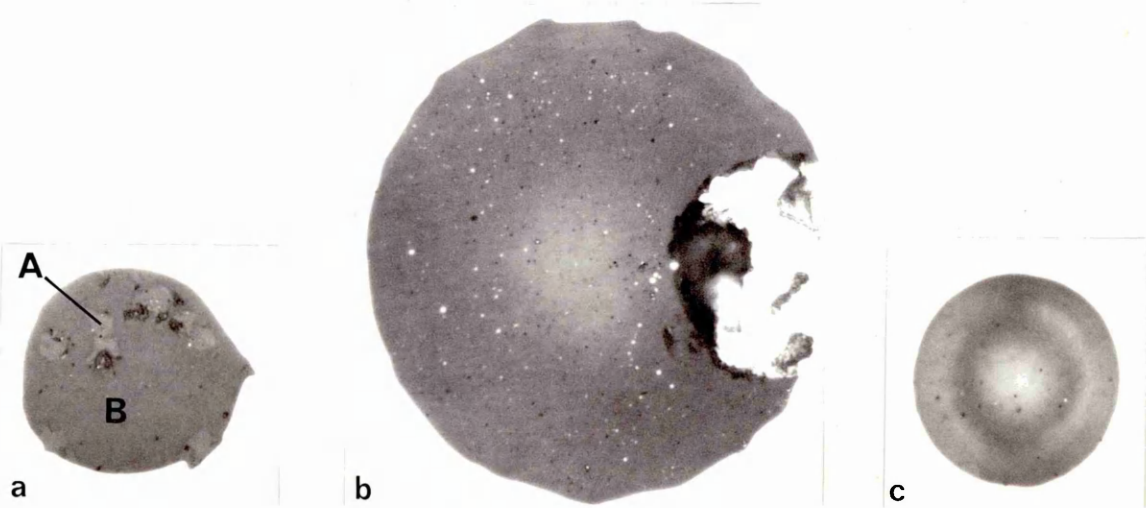

Fig. 4.50

Trial cast C.3 - Inclusions present in ingots during teeming x 750

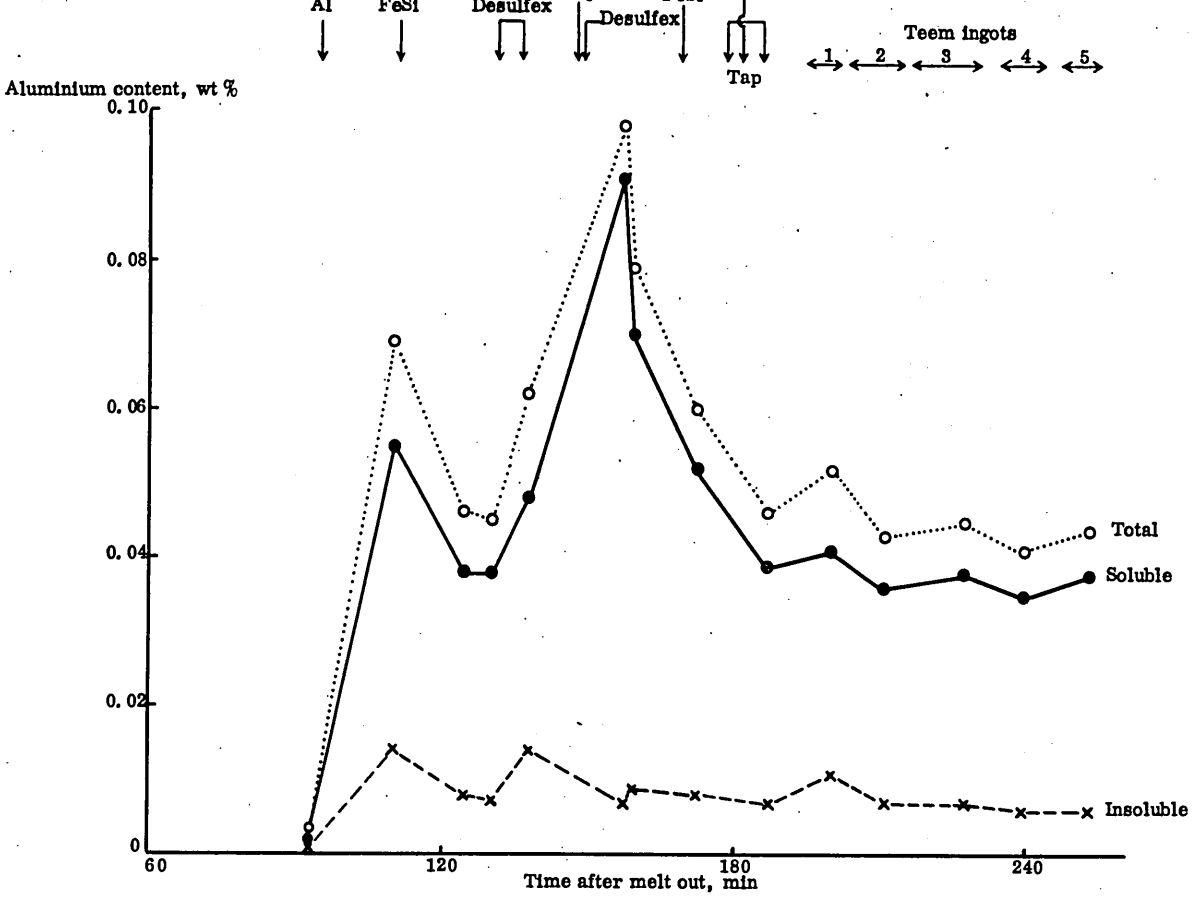

Fig. 4.51

Trial cast C.3 - variation in aluminium content of bath, ladle and ingot samples with time

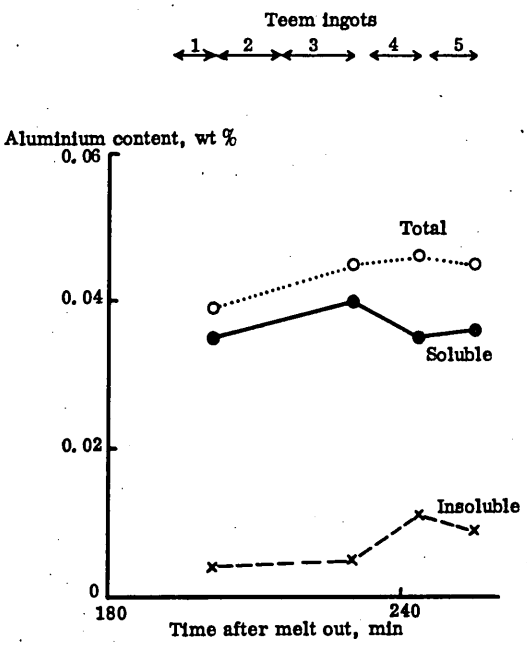

Fig. 4.52

Trial cast C.3 - variation in aluminium content of ladle stream samples with time

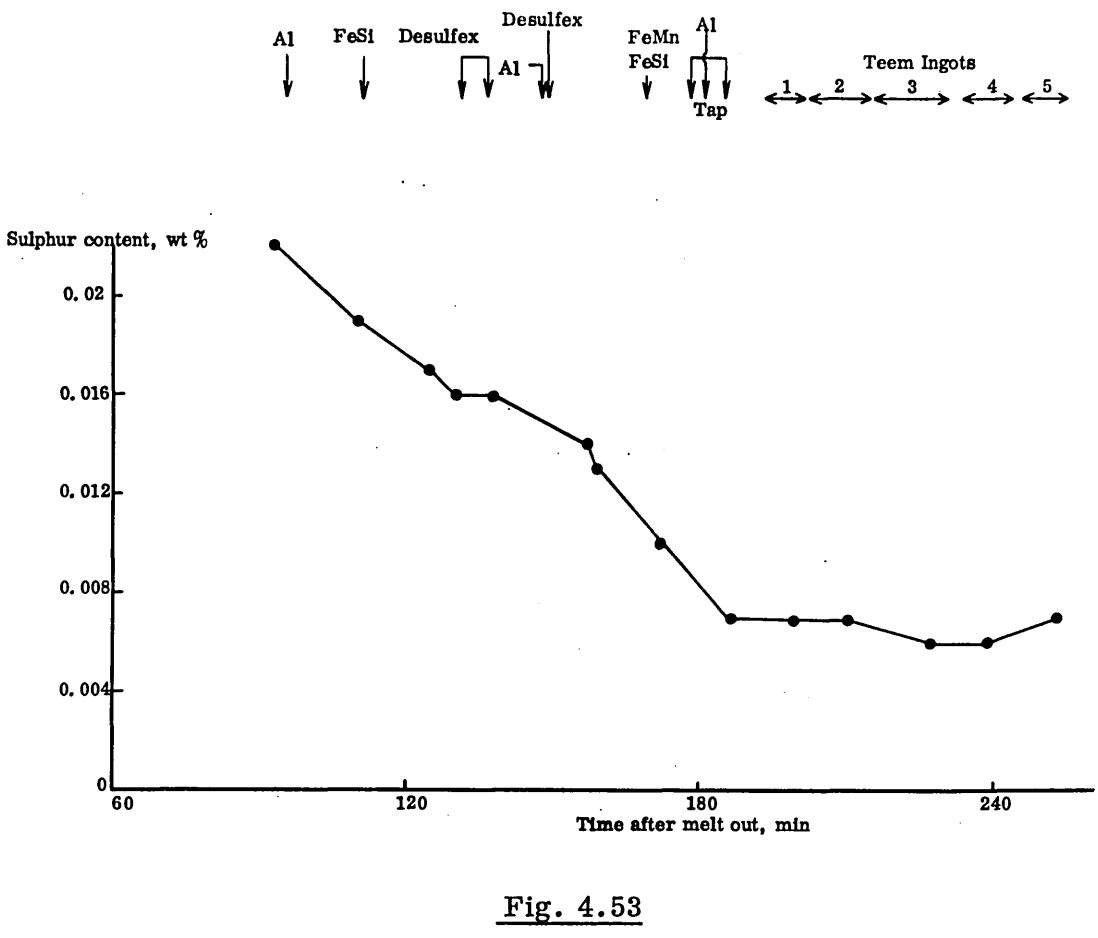

Fig. 4.53

Trial cast C.3 - Variation in sulphur content of bath, ladle and ingot samples with time

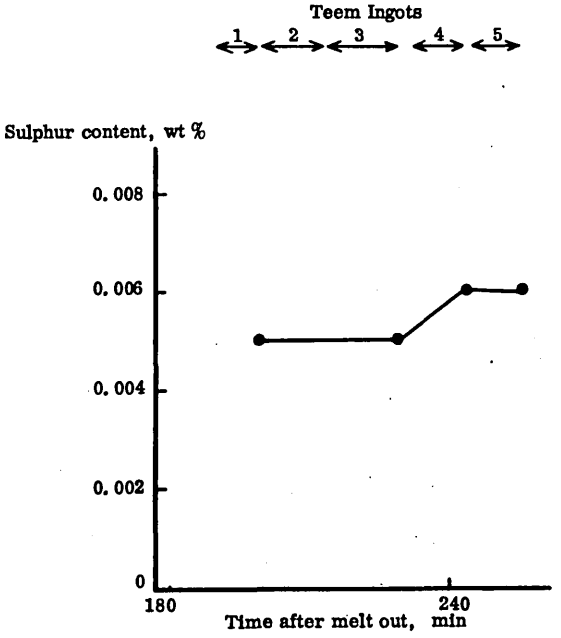

Fig. 4.54

Trial cast C.3 - Variation in sulphur content of ladle stream samples with time

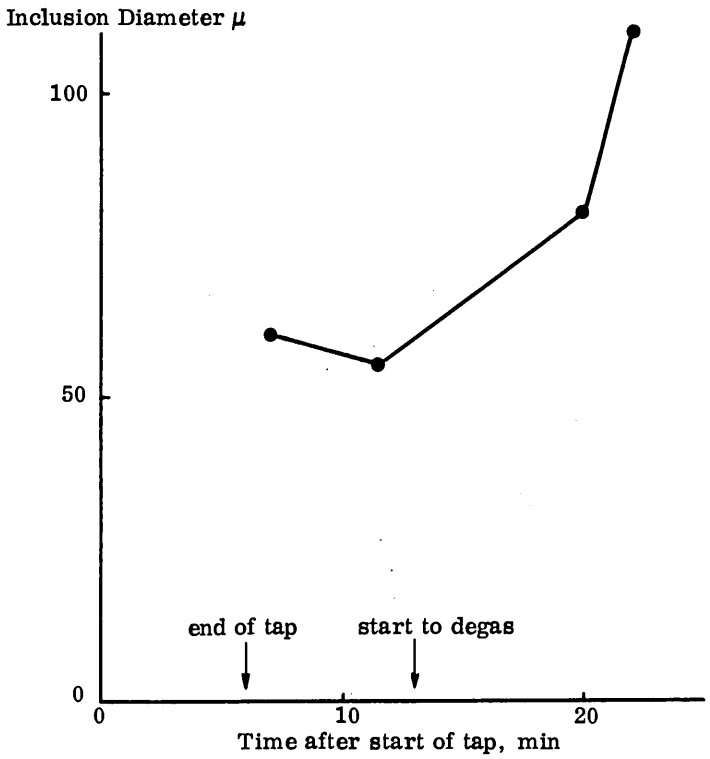

Fig. 5.1

Trial cast A.1 - Variation in average size of ladle deoxidation products with time

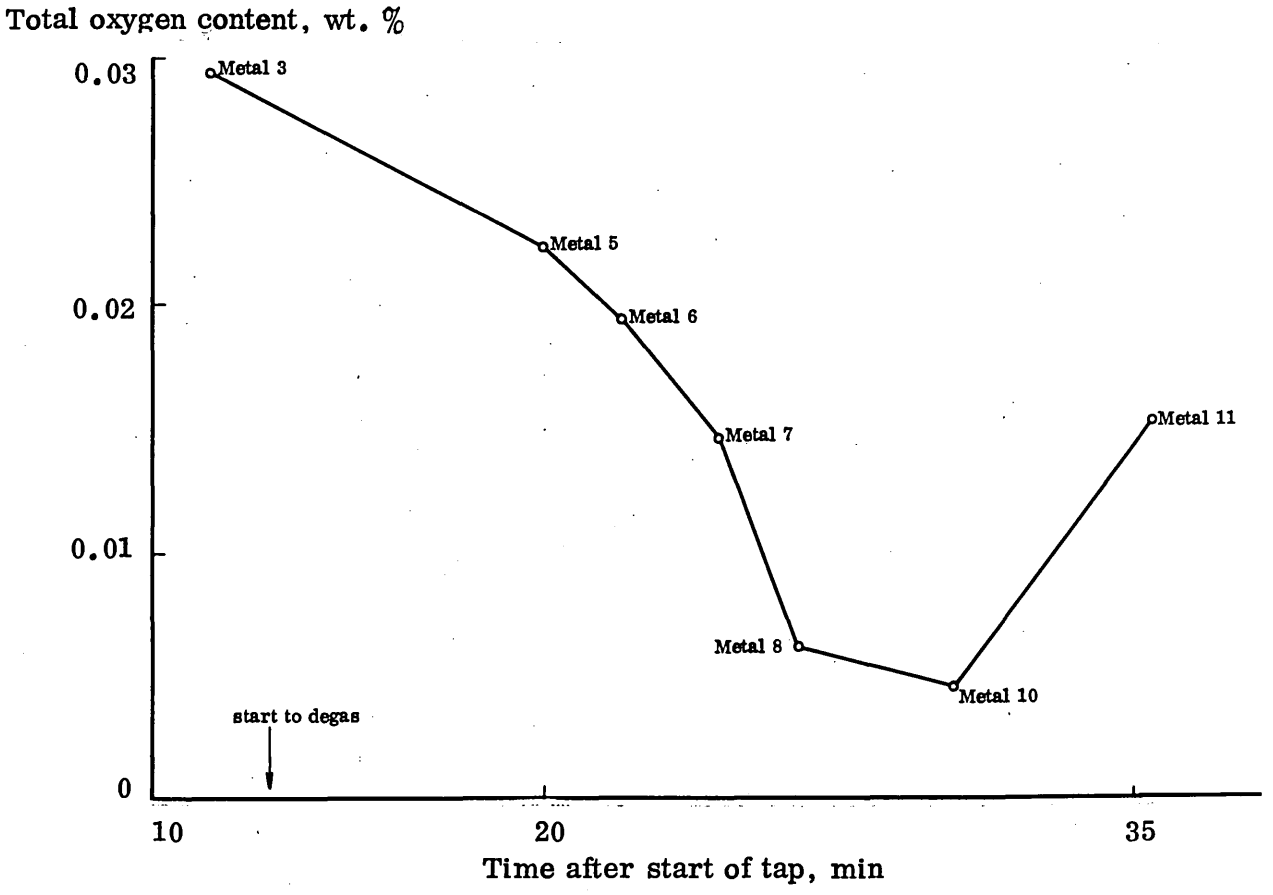

Fig. 5.2

Trial cast A.1 - Variation in total oxygen content during vacuum degassing

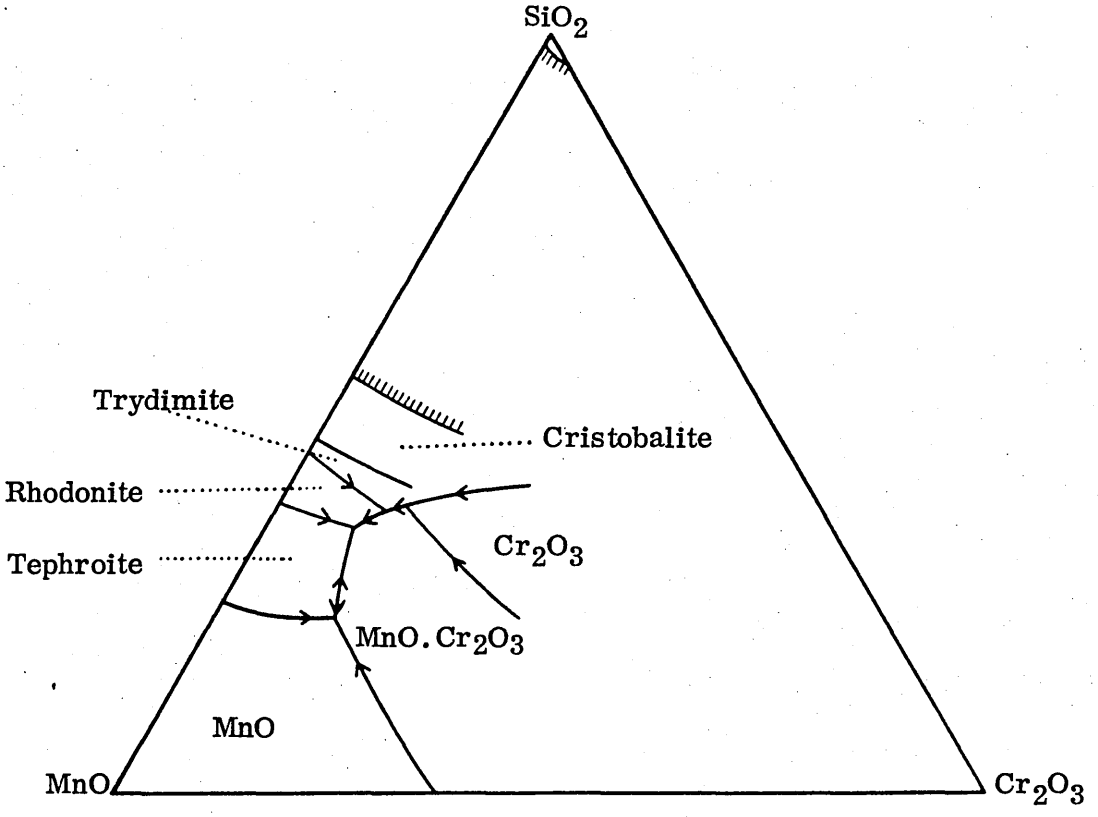

Fig. 5.3

Qualitative liquidus surface of the system $MnO-SiO_2-Cr_2O_3$

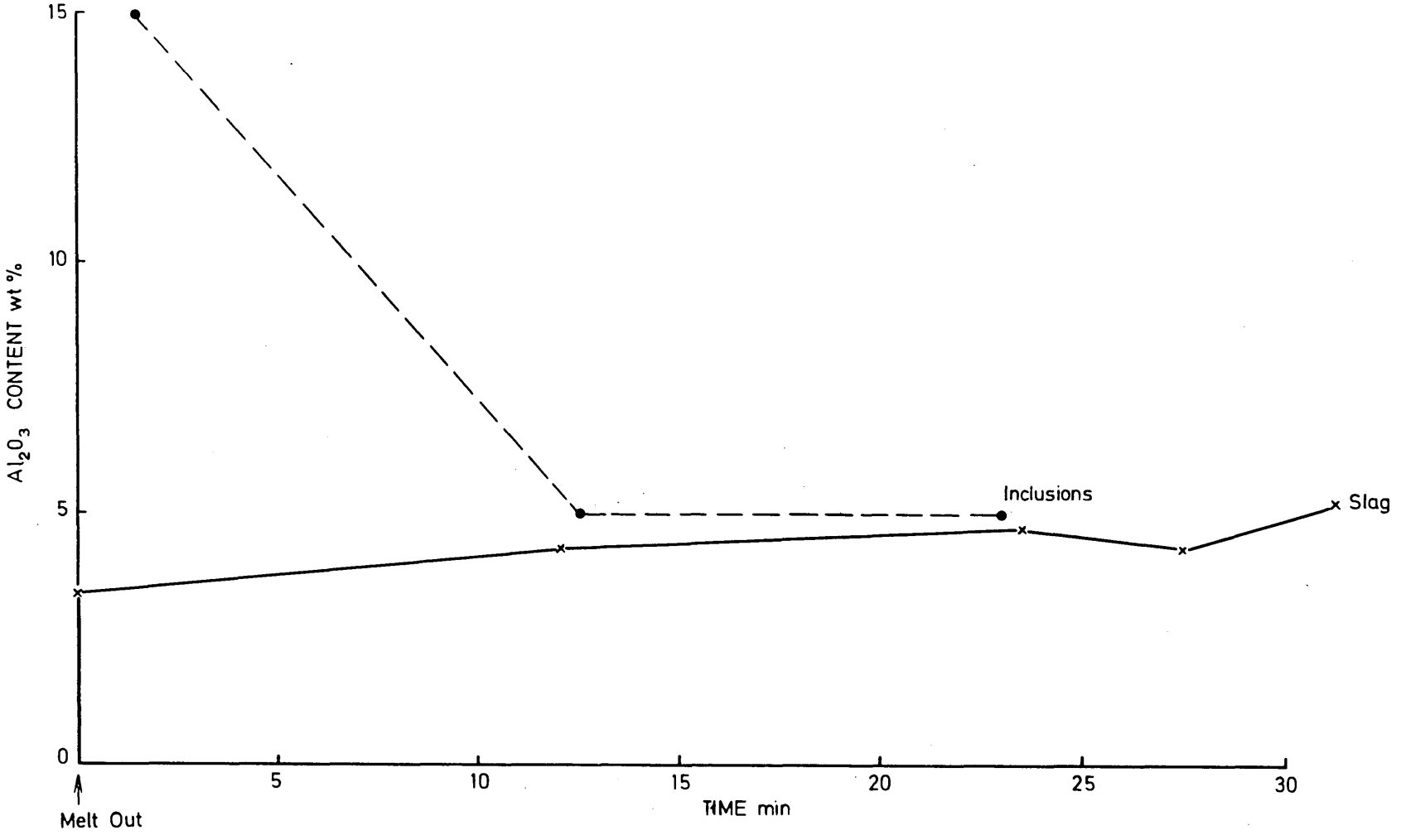

Fig. 5.4

Trial cast B.1 - Variation in Al_2O_3 content of slag and inclusions during oxidation period

a

b

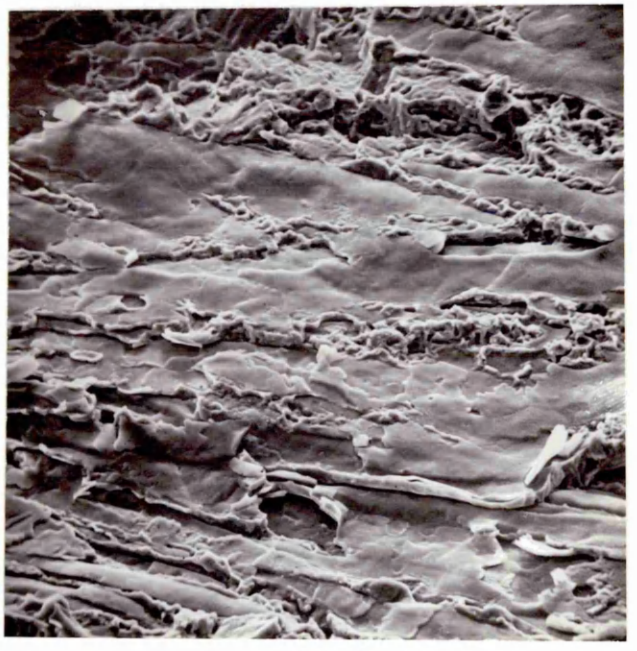

c

Fig. 5.5

Inclusions present in through-thickness tensile specimens
(a) Optical micrograph of aluminate stringer x 100
(b) Scanning electron micrograph of aluminate inclusions x 800
(c) Scanning electron micrograph of manganese sulphide x 400